MINNESOTA DEPARTMENT OF TRANSPORTATION

RESEARCH

2009-37

Developing a Resistance Factor for Mn/DOT's Pile Driving Formula

Take the steps... Research...Knowledge...Innovative Solutions!

Transportation Research

Technical Report Documentation Page

1. Report No.	2.	3. Recipients Accession No.
MN/RC 2009-37		

4. Title and Subtitle	5. Report Date
Developing a Resistance Factor for Mn/DOT's Pile Driving Formula	November 2009
	6.
7. Author(s) Samuel G. Paikowsky, Craig M. Marchionda, Colin M. O’Hearn, Mary C. Canniff and Aaron S. Budge	8. Performing Organization Report No.
9. Performing Organization Name and Address Geotechnical Engineering Research Laboratory University of Massachusetts Lowell, 1 University Ave., Lowell, MA 01824 Minnesota State University, Mankato Dept. of Mechanical and Civil Engineering 205 Trafton Science Center East Mankato, MN 56001	10. Project/Task/Work Unit No. 11. Contract (C) or Grant (G) No. (c)90707 (wo)
12. Sponsoring Organization Name and Address Minnesota Department of Transportation (Mn/DOT) 395 John Ireland Boulevard St. Paul, MN 55155-1899	13. Type of Report and Period Covered Final Report 14. Sponsoring Agency Code

15. Supplementary Notes
http://www.lrrb.org/pdf/200937.pdf

16. Abstract (Limit: 250 words)

Driven piles are the most common foundation solution used in bridge construction across the U.S. Their use is challenged by the ability to reliably verify the capacity and the integrity of the installed element in the ground. Dynamic analyses of driven piles are methods attempting to obtain the static capacity of a pile, utilizing its behavior during driving. Dynamic equations (a.k.a. pile driving formulas) are the earliest and simplest forms of dynamic analyses. Mn/DOT uses its own pile driving formula; however, its validity and accuracy has not been evaluated. With the implementation of Load Resistance Factor Design (LRFD) in Minnesota in 2005, and its mandated use by the Federal Highway Administration (FHWA) in 2007, the resistance factor associated with the use of the Mn/DOT driving formula needed to be calibrated and established.

The resistance factor was established via the following steps: (i) establishing the Mn/DOT foundation design and construction state of practice, (ii) assembling large datasets of tested deep foundations that match the state of practice established in the foregoing stage, (iii) establishing the uncertainty of the investigated equation utilizing the bias, being the ratio of the measured to calculated pile capacities for the database case histories, (v) calculating the LRFD resistance factor utilizing the method’s uncertainty established in step (iv) given load distribution and target reliability.

The research was expanded to include four additional dynamic formulas and the development of an alternative dynamic formula tailored for the Mn/DOT practices.

17. Document Analysis/Descriptors	18. Availability Statement
Pile, Pile driving, Formulas, Dynamic formula, Load Resistance Factor Design, LRFD, Resistance Factor, Bridge foundations	No restrictions. Document available from: National Technical Information Services, Springfield, Virginia 22161

19. Security Class (this report)	20. Security Class (this page)	21. No. of Pages	22. Price
Unclassified	Unclassified	294	

Developing a Resistance Factor for Mn/DOT's Pile Driving Formula

Final Report

Prepared by

Samuel G. Paikowsky
Craig M. Marchionda
Colin M. O'Hearn
Mary C. Canniff
Geotechnical Engineering Research Laboratory
University of Massachusetts – Lowell

Aaron S. Budge
Department of Mechanical and Civil Engineering
Minnesota State University, Mankato

November 2009

Published by

Minnesota Department of Transportation
Research Services Section
Transportation Bldg.
395 John Ireland Boulevard, Mail Stop 330
St. Paul, Minnesota 55155-1899

ACKNOWLEDGEMENTS

The presented research was supported by Minnesota Department of Transportation (Mn/DOT) via a grant to Minnesota State University at Mankato. The Technical Advisory Panel (TAP) is acknowledged for its support, interest, and comments. In particular we would like to mention, Mssrs. Gary Person, Richard Lamb, and Derrick Dasenbrock of the Foundations Unit, and Mssrs. Dave Dahlberg, Kevin Western, Bruce Iwen, and Paul Kivisto of the Bridge Office. The collaboration with Mn/DOT was an effective and rewarding experience. The research was carried out in collaboration with Professor Aaron S. Budge from Minnesota State University, Mankato. Prof. Budge facilitated the research and participated in establishing Mn/DOT design and construction practices described in Chapter 2 of this manuscript.

The research presented in this manuscript makes use of a large database specifically developed for Mn/DOT purposes. This database makes use of data originally developed for an Federal Highway Administration (FHWA) study described in publication no. FHWA-RD-94-042 (September, 1994) entitled *A Simplified Field Method for Capacity Evaluation of Driven Piles,* followed by an updated database denoted as PD/LT 2000 presented by Paikowsky and Stenersen (2000), which was also used for the LRFD development for deep foundations (presented in NCHRP Report 507). Sections 1.2 to 1.5 were copied from Paikowsky et al. (2009). Sections 1.2 and 1.3 are based originally on Paikowsky et al. (2004). The contributors for those databases are acknowledged for their support as detailed in the referenced publications. Mssrs. Carl Ealy and Albert DiMillio of the FHWA were constructive in support of the original research studies and facilitated data gathering via FHWA sources. Significant additional data were added to those databases, most of which were provided by six states: Illinois, Iowa, Tennessee, Connecticut, West Virginia, and Missouri. The data obtained from Mr. Leo Fontaine of the Connecticut DOT was extremely valuable to enlarge the Mn/DOT databases to the robust level presented in this study.

Previous students of the Geotechnical Engineering Research Laboratory at the University of Massachusetts Lowell are acknowledged for their contribution to the aforementioned databases, namely: John J. McDonell, John E. Regan, and Kirk Stenersen. Dr. Shailendra Amatya is acknowledged for his assistance in employing object oriented programming in the code S-PLUS for the development of the newly proposed Mn/DOT dynamic equation.

EXECUTIVE SUMMARY

Driven piles are the most common foundation solution used in bridge construction across the U.S. (Paikowsky et al., 2004). The major problem associated with the use of deep foundations is the ability to reliably verify the capacity and the integrity of the installed element in the ground. Dynamic analyses of driven piles are methods attempting to obtain the static capacity of a pile, utilizing its behavior during driving. The dynamic analyses are based on the premise that under each hammer blow, as the pile penetrates into the ground, a quick pile load test is being carried out. Dynamic equations (aka pile driving formulas) are the earliest and simplest forms of dynamic analyses. Mn/DOT uses its own pile driving formula; however, its validity and accuracy has never been thoroughly evaluated. With the implementation of Load Resistance Factor Design (LRFD) in Minnesota in 2005, and its mandated use by the Federal Highway Administration (FHWA) in 2007, the resistance factor associated with the use of the Mn/DOT driving formula needed to be calibrated and established.

Systematic probabilistic-based evaluation of a resistance factor requires quantifying the uncertainty of the investigated method. As the investigated analysis method (the model) contains large uncertainty itself (in addition to the parameters used for the calculation), doing so requires:

(i) Knowledge of the conditions in which the method is being applied, and
(ii) A database of case histories allowing comparison between the calculated value to one measured.

The presented research addresses these needs via:

(i) Establishing the Mn/DOT state of practice in pile design and construction, and
(ii) Compilation of a database of driven pile case histories (including field measurements and static load tests to failure) relevant to Minnesota design and construction practices.

The first goal was achieved by review of previously completed questionnaires, review of the Mn/DOT bridge construction manual, compilation and analysis of construction records of 28 bridges, and interviews with contractors, designers, and DOT personnel. The majority of the Minnesota recently constructed bridge foundations comprised of Closed-Ended Pipe (CEP) and H piles. The most common CEP piles are 12” x 0.25 and 16” x 0.3125, installed as 40% and 25% of the total foundation length. The most common H pile is 12 x 53 used in 7% of the driven length. The typical CEP is 12” x 0.25, 70 ft. long and carries 155 kips (average factored load). The typical H pile is 12 x 53, 40 ft. long and carries 157 kips. The piles are driven by Diesel hammers ranging in energy from 42 to 75 kip/ft. with 90% of the piles driven to or beyond 4 Blows Per Inch (BPI) and 50% of the piles driven to or beyond 8 BPI.

Large data sets were assembled, answering to the above practices. As no data of static load tests were available from Mn/DOT, the databases were obtained from the following:

(i) Relevant case histories from the dataset PD/LT 2000 used for the American Association of State Highway and Transportation Officials (AASHTO) specification LRFD calibration (Paikowsky and Stenersen, 2000, Paikowsky et al., 2004)
(ii) Collection of new relevant case histories from DOTs and other sources

In total, 166 H pile and 104 pipe pile case histories were assembled in Mn/DOT LT 2008 database. All cases contain static load test results as well as driving system and, driving resistance details. Fifty three percent (53%) of the H piles and 60% of the pipe piles in dataset Mn/DOT LT 2008 were driven by diesel hammers.

The static capacity of the piles was determined by Davisson’s failure criterion, established as the measured resistance. The calculated capacities were obtained using different dynamic

equations, namely, *Engineers News Record* (ENR), Gates, FHWA modified Gates, WSDOT, and Mn/DOT. The statistical performance of each method was evaluated via the bias of each case, expressed as the ratio of the measured capacity over the calculated capacity. The mean, standard deviation, and coefficient of variation of the bias established the distribution of each method's resistance.

The distribution of the resistance along with the distribution of the load and established target reliability (presented by Paikowsky et al. 2004 for the calibration of the AASHTO specifications) was utilized to calculate the resistance factor associated with the calibration method under the given condition. Two methods of calibration were used: MCS (Monte Carlo Simulation), using iterative numerical process, and FOSM (First Order Second Moment), using a closed form solution.

The Mn/DOT equation generally tends to over-predict the measured capacity with a large scatter. The performance of the equation was examined by detailed subset databases for each pile type: H and pipe. The datasets started from the generic cases of all piles under all driving conditions (258 pile cases) and ended with the more restrictive set of piles driven with diesel hammers within the energy range commonly used by Mn/DOT practice and driving resistance of 4 or more BPI. The 52 data sub-categorizations (26 for all driving conditions and 26 for EOD alone) were presented in the form of a flow chart along all statistical data and resulting resistance factors. Further detailed investigations were conducted on specific subsets along with examination of the obtained resistance distribution using numerical method (Goodness of Fit tests) and graphical comparisons of the data vs. the theoretical distributions.

Due to the Mn/DOT dynamic equation over-prediction and large scatter, the obtained resistance factors were consistently low, and a resistance factor of $\phi = 0.25$ is recommended to be used with this equation, for both H and pipe piles. The reduction in the resistance factor from $\phi = 0.40$ currently in use, to $\phi = 0.25$, reflects a significant economical loss for a gain in a consistent level of reliability. Alternatively, one can explore the use of other pile field capacity evaluation methods that perform better than the currently used Mn/DOT dynamic equation, hence allowing for higher efficiency and cost reduction.

Two approaches for remediation are presented. In one, a subset containing dynamic measurements during driving is analyzed, demonstrating the increase in reliability when using dynamic measurements along with a simplified field method known as the Energy Approach. Such a method requires field measurements that can be accomplished in several ways.

An additional approach was taken by developing independently a dynamic equation to match Mn/DOT practices. A linear regression analysis of the data was performed using a commercial software product featuring object oriented programming. The simple obtained equation (in its structure) was calibrated and examined. A separate control dataset was used to examine both equations, demonstrating the capabilities of the proposed new Mn/DOT equation. In addition, the database containing dynamic measurements was used for detailed statistical evaluations of existing and proposed Mn/DOT dynamic equations, allowing comparison on the same basis of the field measurement-based methods and the dynamic equations.

Finally, an example was constructed based on typical piles and hammers used by Mn/DOT. The example demonstrated that the use of the proposed new equation may result at times with savings and at others with additional cost, when compared to the existing resistance factor currently used by the Mn/DOT. The proposed new equation resulted in consistent savings when compared to the Mn/DOT current equation used with the recommended resistance factor developed in this study for its use ($\phi = 0.25$).

It is recommended to establish a transition period in the field practices of pile monitoring. The use of the existing Mn/DOT equation with both resistance factors ($\phi = 0.40$ and $\phi = 0.25$) should be examined against the use of the new equation and the associated resistance factors ($\phi = 0.60$ for H piles and $\phi = 0.45$ for pipe piles). The accepted factored resistance should consider all values. While collecting such data for a period of time, a longer-term testing program of dynamic and when possible static load testing should be developed in order to evaluate and review the proposed methodologies.

TABLE OF CONTENTS

LIST OF TABLES

LIST OF FIGURES

CHAPTER 1 BACKGROUND

1.1 RESEARCH OBJECTIVES

1.1.1 Overview

The Mn/DOT pile driving formula is currently used for evaluating the capacity of driven piles during construction. This formula was not examined thoroughly either for its validity (theoretical basis) or for its performance (prediction vs. outcome). With the international and national design methodologies moving towards Probability Based Design (PBD) and the FHWA requirement to implement the AASHTO Specifications based on Load and Resistance Factor Design (LRFD) methodology, a need arises to develop reliable resistance factors for the use of Mn/DOT pile driving formula. In doing so, the research scope calls for the buildup of a database to evaluate statistically the uncertainty of the Mn/DOT dynamic equation. In addition, this effort enables the examination of other dynamic pile driving formulae, and possible modifications and/or alternative formulations applicable to Minnesota practices as well.

The developed resistance factor(s) need to be compatible with the LRFD development of the AASHTO specifications, and enable the reliable (quantified) use of the dynamic equation in the field, hence mitigating risk and providing cost saving.

1.1.2 Concise Objective

Developing a resistance factor for Mn/DOT's pile driving formula.

1.1.3 Specific Tasks

Meeting the concise objective requires the following specific tasks:

1. Establish Mn/DOT state of practice in pile design and construction
2. Compile databases relevant to Mn/DOT practices
3. Databases analysis for trend and uncertainty evaluation
4. LRFD calibration based on the obtained uncertainty
5. Methodology evaluation
6. Recommendations and final reporting

1.2 ENGINEERING DESIGN METHODOLOGIES

[Section 1.2 was copied from Paikowsky et al. (2009) and is based originally on Paikowsky et al. (2004).]

1.2.1 Working Stress Design

The working Stress Design (WSD) method, also called Allowable Stress Design (ASD), has been used in Civil Engineering since the early 1800s. Under WSD, the design loads (Q), which consist of the actual forces estimated to be applied to the structure (or a particular element of the structure), are compared to the nominal resistance, or strength (R_n) through a factor of safety (FS):

$$Q \le Q_{all} = \frac{R_n}{FS} = \frac{Q_{ult}}{FS} \quad (1.1)$$

where Q = design load; Q_{all} = allowable design load; R_n = nominal resistance of the element or the structure, and Q_{ult} = ultimate geotechnical foundation resistance.

The *Standard Specifications for Highway Bridges* (AASHTO, 1997), based on common practice, presents the traditional factors of safety used in conjunction with different levels of control in analysis and construction. Though engineering experience over a lengthy period of time resulted with adequate factors of safety, their source, reliability and performance had remained mostly unknown. The factors of safety do not necessarily consider the bias, in particular, the conservatism (i.e., underprediction) of the analysis methods; hence, the validity of their assumed effect on the economics of design is questionable.

1.2.2 Limit State Design

Demand for more economical design and attempts to improve structural safety have resulted in the re-examination of the entire design process over the past 50 years. A design of a structure needs to ensure that while being economically viable, it will suit the intended purpose during its working life. Limit State (LS) is a condition beyond which the structure (i.e. bridge in the relevant case), or a component, fails to fulfill in some way the intended purpose for which it was designed. Limit State Design (LSD) comes to meet the requirements for safety, serviceability, and economy. LSD most often refers, therefore, to two types of limit states: Ultimate Limit State (ULS), which deals with the strength (maximum loading capacity) of the structure, and Serviceability Limit State (SLS), which deals with the functionality and service requirements of a structure to ensure adequate performance under expected conditions (these can be for example under normal expected loads or extreme events, e.g. impact, earthquake, etc.).

The ULS design of a structure and its components (e.g. column, foundation) depends upon the predicted loads and the capacity of the component to resist them (i.e. resistance). Both loads and resistance have various sources and levels of uncertainty. Engineering design has historically compensated for these uncertainties by using experience and subjective judgment. The new approach that has evolved aims to quantify these uncertainties and achieve more rational engineering designs with consistent levels of reliability. These uncertainties can be quantified using probability-based methods resulting for example with the Load and Resistance Factor Design (LRFD) format allowing the separation of uncertainties in loading from uncertainties in resistance, and the use of procedures from probability theory to assure a prescribed margin of safety.

The same principles used in the LRFD for ULS can be applied to the SLS, substituting the capacity resistance of the component with a serviceability limit, may it be a quantified displacement, crack, deflection or vibration. Since failure under the SLS will not lead to collapse, the prescribed margin of safety can be smaller, i.e. the SLS can tolerate a higher probability of "failure" (i.e. exceedance of the criterion) compared with that for the ULS.

1.2.3 Geotechnical and AASHTO Perspective

The LSD and LRFD methods are becoming the standard methods for modern-day geotechnical design codes. In Europe (CEN, 2004 and e.g. for Germany DIN EN 1997-1, 2008 including the National Annex, 1 draft 2009), Canada (Becker, 2003), China (Zhang, 2003), Japan (Honjo et al., 2000; Okahara et al., 2003), the US (Kulhawy and Phoon, 2002; Withiam, 2003; Paikowsky et al., 2004), and elsewhere, major geotechnical design codes are switching from the Allowable Stress Design (ASD) or equivalently the Working Stress Design (WSD) to LSD and LRFD.

A variation of LRFD was first adopted by AASHTO for the design of certain types of bridge superstructures in 1977 under a design procedure known as Load Factor Design (LFD). The AASHTO LRFD Bridge Design and Construction Specifications were published in 1994 based on NCHRP project 12-33. Since 1994 (16^{th} edition, 1^{st} LRFD addition) to 2006, the AASHTO LRFD Specifications applied to Geotechnical Engineering utilized the work performed by Barker et al., (1991). This code was mostly based on adaptation of Working Stress Design (WSD) to LRFD and only marginally addresses the SLS. A continuous attempt has been made since to improve upon the scientific basis on which the specifications were developed, including NCHRP 20-7 Task 88, NCHRP 12-35 and 12-55 for earth pressures and retaining walls, NCHRP 12-24 for soil-nailing, and NCHRP 24-17 that calibrated for the first time the LRFD parameters for deep foundations based on extensive databases of deep foundation testing (Paikowsky et al., 2004). NCHRP 12-66 (headed by Samuel Paikowsky) is a major effort addressing the needs of SLS in design of bridge foundations. The project's complete approach required developing serviceability criteria for bridges based on foundation performance, defining methods for the evaluation of foundation displacements and establishing their uncertainty, and calibrating the resistance factors assigned for the use of these methods based on the established SLS and target reliability. The backbone of the study was the development of databases to establish the uncertainty of the methods used to evaluate the horizontal and vertical displacements of foundations.

1.3 LOAD AND RESISTANCE FACTOR DESIGN

[Section 1.3 was copied from Paikowsky et al. (2009) and is based originally on Paikowsky et al. (2004).]

1.3.1 Principles

The intent of LRFD is to separate uncertainties in loading from uncertainties in resistance, and then to use procedures from probability theory to assure a prescribed margin of safety. Sections 1.3 and 1.4 outline the principles of the methodology and present the common techniques used for its implementation.

Figure 1.1 shows Probability Density Functions (PDFs) for load effect (Q) and resistance (R). "Load effect" is the load calculated to act on a particular element (e.g. a specific shallow foundation) and the resistance is its bearing load capacity. As in geotechnical engineering problems, loads are usually better known than are resistances, the Q typically has smaller variability than R; that is, it has a smaller coefficient of variation (COV), hence a narrower PDF.

In LRFD, partial safety factors are applied separately to the load effect and to the resistance. Load effects are increased by multiplying characteristic (or nominal) values by load factors (γ); resistance (strength) is reduced by multiplying nominal values by resistance factors (ϕ). Using this approach the factored (i.e., reduced) resistance of a component must be larger than a linear combination of the factored (i.e. increased) load effects. The nominal values (e.g. the nominal resistance, R_n) are those calculated by the specific calibrated design method and are not necessarily the means (i.e. the mean loads, m_Q, or mean resistance, m_R of Figure 1.1). For example, R_n is the predicted value for a specific analyzed foundation, obtained say using Vesić's bearing capacity calculation, while m_R is the mean possible predictions for that foundation considering the various uncertainties associated with that calculation.

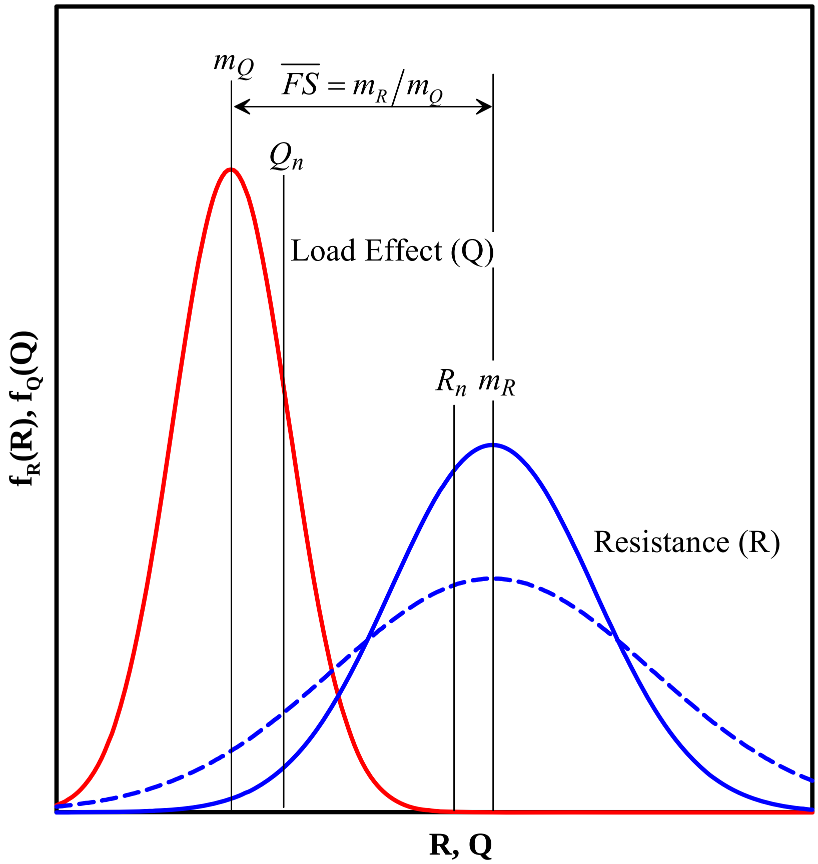

Figure 1.1 An illustration of probability density functions for load effect and resistance.

This principle for the strength limit state is expressed in the AASHTO LRFD Bridge Design Specifications (e.g. AASHTO 1994 to 2008) in the following way;

$$R_r = \phi R_n \geq \sum \eta_i \gamma_i Q_i \tag{1.2}$$

where the nominal (ultimate) resistance (R_n) multiplied by a resistance factor (ϕ) becomes the factored resistance (R_r), which must be greater than or equal to the summation of loads (Q_i) multiplied by corresponding load factors (γ_i) and a modifier (η_i).

$$\eta_i = \eta_D \eta_R \eta_I \geq 0.95 \tag{1.3}$$

where η_i = factors to account for effects of ductility (η_D), redundancy (η_R), and operational importance (η_I).

Based on considerations ranging from case histories to existing design practice, a prescribed value is chosen for probability of failure. Then, for a given component design (when applying resistance and load factors), the actual probability for a failure (the probability that the factored loads exceed the factored resistances) should be equal or smaller than the prescribed value. In foundation practice, the factors applied to load effects are typically transferred from structural codes, and then resistance factors are specifically calculated to provide the prescribed probability of failure.

The importance of uncertainty consideration regarding the resistance and the design process is illustrated in Figure 1.1. In this figure, the central factor of safety is $\overline{FS} = m_R / m_Q$, whereas the nominal factor of safety is $FS_n = R_n / Q_n$. The mean factor of safety is the mean of the ratio R/Q and is not equal to the ratio of the means. Consider what happens if the uncertainty in resistance is increased, and thus the PDF broadened, as suggested by the dashed curve. The mean resistance for this curve (which may represent the result of another predictive method) remains unchanged, but the variation (i.e. uncertainty) is increased. Both distributions have the same mean factor of safety (one uses in WSD), but utilizing the distribution with the higher variation will require the application of a smaller resistance factor in order to achieve the same prescribed probability of failure to both methods.

The limit state function g corresponds to the margin of safety, i.e. the subtraction of the load from the resistance such that (referring to Figure 1.2a);

$$g = R - Q \tag{1.4}$$

For areas in which $g < 0$, the designed element or structure is unsafe as the load exceeds the resistance. The probability of failure, therefore, is expressed as the probability for that condition;

$$p_f = P(g < 0) \tag{1.5}$$

In calculating the prescribed probability of failure (p_f), a derived probability density function is calculated for the margin of safety g(R,Q) (refer to Figure 1.2a), and reliability is expressed using the "reliability index", β. Referring to Figure 1.2b, the reliability index is the number of standard deviations of the derived PDF of *g*, separating the mean safety margin from the nominal failure value of g being zero;

$$\beta = m_g / \sigma_g = (m_R - m_Q) \Big/ \sqrt{\sigma_Q^2 + \sigma_R^2} \tag{1.6}$$

where m_g, σ_g are the mean and standard deviation of the safety margin defined in the limit state function Eq. (1.4), respectively.

The relationship between the reliability index (β) and the probability of failure (p_f) for the case in which both R and Q follow normal distributions can be obtained based on Eq. (1.6) as:

$$p_f = \Phi(-\beta) \tag{1.7}$$

where Φ is the error function defined as $\Phi(z) = \int_{-\infty}^{z} \frac{1}{\sqrt{2\pi}} \exp\left[-\frac{u^2}{2}\right] du$. The relationship between β and p_f are provided in Table 1.1. The relationships in Table 1.1 remain valid as long as the assumption that the reliability index β follows a normal distribution.

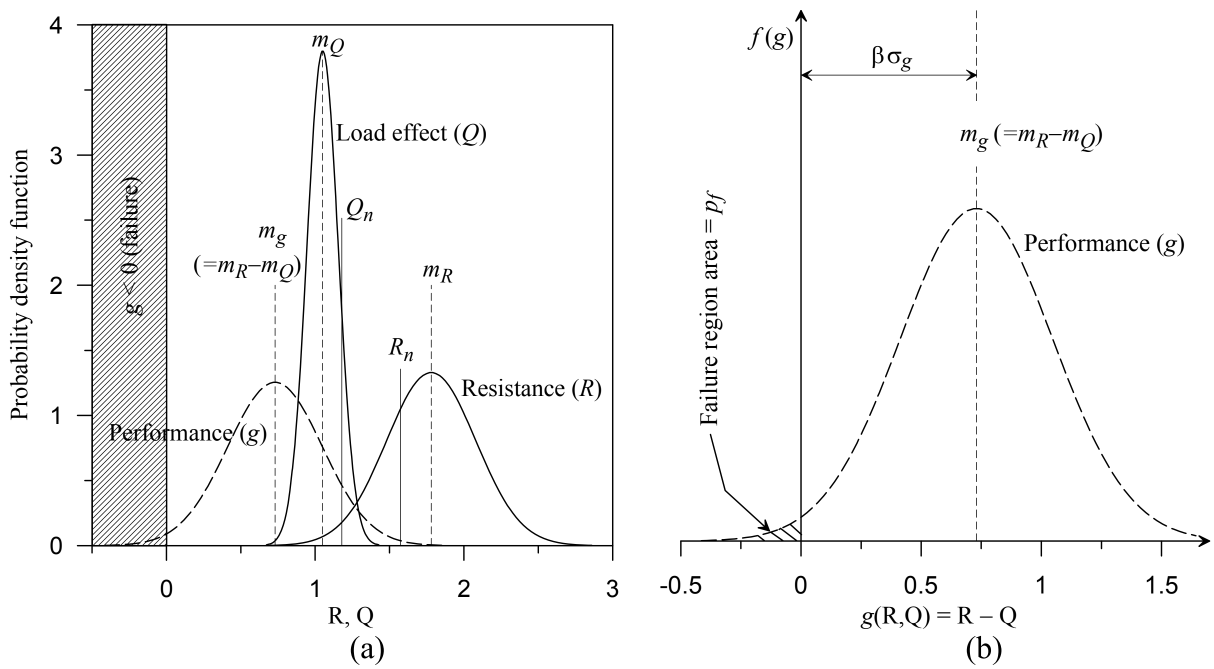

Figure 1.2 An illustration of probability density function for (a) load, resistance and performance function, and (b) the performance function (g(R,Q)) demonstrating the margin of safety (p_f) and its relation to the reliability index β (σ_g = standard deviation of g).

Table 1.1 Relationship Between Reliability Index and Target Reliability

Reliability Index β	Probability of Failure p_f
1.0	0.159
1.2	0.115
1.4	0.0808
1.6	0.0548
1.8	0.0359
2.0	0.0228
2.2	0.0139
2.4	0.00820
2.6	0.00466
2.8	0.00256
3.0	0.00135
3.2	6.87 E^{-4}
3.4	3.37 E^{-4}
3.6	1.59 E^{-4}
3.8	7.23 E^{-5}
4.0	3.16 E^{-5}

As the performance of the physical behavior of engineering systems usually cannot obtain negative values (load and resistance), it is better described by a lognormal distribution. The margin of safety is taken as log R – log Q, when the resistances and load effects follow lognormal distributions. Thus, the limit state function becomes:

$$g = \ln(R) - \ln(Q) = \ln(R/Q) \tag{1.8}$$

If R and Q follow log-normal distributions, log R and log Q follows normal distributions, thus the safety margin g follows a normal distribution. As such, the relationship obtained in Eq. (1.7) is still valid to calculate the failure probability. Figure 1.2b illustrates the limit state function g for normal distributed resistance and load, the defined reliability index, β (also termed target reliability), and the probability of failure, p_f. For lognormal distributions, these relations will relate to the function g = ln(R/Q).

The values provided in Table 1.1 are based on series expansion and can be obtained by a spreadsheet (e.g. NORMSDIST in Excel), or standard mathematical tables related to the standard normal probability distribution function. It should be noted, however, that previous AASHTO LRFD calibrations and publications for Geotechnical engineering, notably Barker et al. (1991), and Withiam et al. (1998) have used an approximation relationship proposed by Rosenbluth and Estava (1972), which greatly errs for $\beta < 2.5$, the typical zone of interest in ULS design calibration ($\beta = 2$ to 3) and more so in the zone of interest for SLS calibrations ($\beta<2.0$).

For lognormal distributions of load and resistance one can show (e.g. Phoon et al., 1995) that Eq. (1.6) becomes:

$$\beta = \frac{m_{RN} - m_{QN}}{\sqrt{\sigma_{QN}^2 + \sigma_{RN}^2}} = \frac{\ln\left[(m_R/m_Q)\sqrt{(1+COV_Q^2)/(1+COV_R^2)}\right]}{\sqrt{\ln\left[(1+COV_R^2)(1+COV_Q^2)\right]}} \tag{1.9}$$

in which:

m_{QN}, m_{RN} the mean of the natural logarithm of the load and the resistance

σ_{QN}, σ_{RN} the standard deviations of the natural logarithm of the load and the resistance.

m_Q, m_R, COV_Q, COV_R the simple means and the coefficient of variations for the load and the resistance of the normal distributions. These values can be transformed from the lognormal distribution using the following expressions for the load and similar ones for the resistance:

$$\sigma_{QN}^2 = \ln\left(1 + COV_Q^2\right) \tag{1.10}$$

and

$$m_{QN} = \ln\left(m_Q\right) - 0.5\sigma_{QN}^2 \tag{1.11}$$

1.3.2 The Calibration Process

The problem facing the LRFD analysis in the calibration process is to determine the load factor (γ) and the resistance factor (ϕ) such that the distributions of R and Q will answer to the requirements of a specified β. In other words, the γ and ϕ described in Figure 1.3 need to answer to the prescribed target reliability (i.e. a predetermined probability of failure) described in Eq. (1.9). Several solutions are available and are described below, including the recommended procedure for the current research (part 1.3.5)

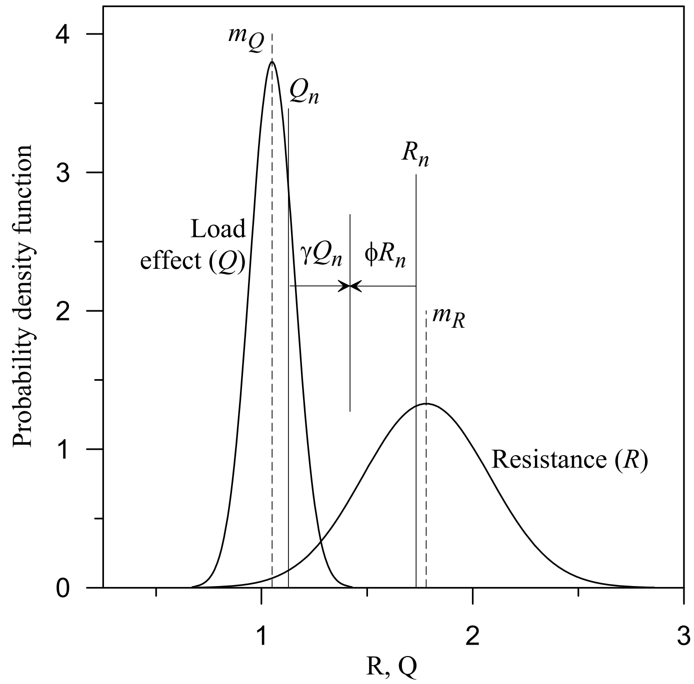

Figure 1.3 An illustration of the LRFD factors determination and application (typically $\gamma \geq 1$, $\phi \leq 1$) relevant to the zone in which load is greater than resistance ($Q > R$).

1.3.3 Methods of Calibration – FOSM

The First Order Second Moment (FOSM) was proposed originally by Cornell (1969) and is based on the following. For a limit state function g(•):

mean $$m_g \approx g(m_1, m_2, m_3, \cdots, m_n) \tag{1.12}$$

variance $$\sigma_g^2 \approx \sum_{i=1}^{n} \left(\frac{\partial_g}{\partial_{xi}} \right)^2 \bullet \sigma_i^2 \tag{1.13}$$

or $$\approx \sum_{i=1}^{n} \left(\frac{g_i^+ - g_i^-}{\Delta x_i} \right)^2 \bullet \sigma_i^2$$

where m_l and σ_i are the means and standard deviations of the basic variables (design parameters), χ_i, i=1,2,…,n, $g_i^+ = m_i + \Delta m_i$ and $g_i^- = m_i - \Delta m_i$ for small increments Δm_i, and Δx_i is a small change in the basic variable value x_i.

Practically, the FOSM method was used by Barker et al. (1991) to develop closed form solutions for the calibration of the Geotechnical resistance factors (ϕ) that appear in the previous AASHTO LRFD specifications.

$$\phi = \frac{\lambda_R(\sum \gamma_i Q_i)\sqrt{\frac{1+COV_Q^2}{1+COV_R^2}}}{m_Q \exp\{\beta\sqrt{\ln[(1+COV_R^2)(1+COV_Q^2)]}\}} \tag{1.14}$$

where: λ_R = resistance bias factor, mean ratio of measured resistance over predicted resistance
COV_Q = coefficient of variation of the load
COV_R = coefficient of variation of the resistance
β = target reliability index

When just dead and live loads are considered Eq. (1.14) can be rewritten as:

$$\phi = \frac{\lambda_R\left(\gamma_D \frac{Q_D}{Q_L} + \gamma_L\right)\sqrt{\frac{1+COV_{QD}^2+COV_{QL}^2}{1+COV_R^2}}}{\left(\lambda_{QD}\frac{Q_D}{Q_L}+\lambda_{QL}\right)\exp\left\{\beta_T\sqrt{\ln[(1+COV_R^2)(1+COV_{QD}^2+COV_{QL}^2)]}\right\}} \tag{1.15}$$

where: γ_D, γ_L = dead and live load factors
Q_D/Q_L = dead to live load ratio
λ_{QD}, λ_{QL} = dead and live load bias factors

The probabilistic characteristics of the foundation loads are assumed to be those used by AASHTO for the superstructure (Nowak, 1999), thus γ_D, γ_L, λ_{QD} and λ_{QL} are fixed and a resistance factor can be calculated for a resistance distribution (λ_R, COV_R) for a range of dead load to live load ratios.

1.3.4 Methods of Calibration – FORM

LRFD for structural design has evolved beyond FOSM to the more invariant First Order Reliability Method (FORM) approach (e.g. Ellingwood et al., 1980, Galambas and Ravindra, 1978), while Geotechnical applications have lagged behind (Meyerhof, 1994). In order to be consistent with the previous structural code calibration and the load factors to which it leads, the calibration of resistance factors for deep foundations in NCHRP project 24-17 used the same methodology (Paikowsky et al., 2004). The LRFD partial safety factors were calibrated using FORM as developed by Hasofer and Lind (1974). FORM can be used to assess the reliability of a component with respect to specified limit states, and provides a means for calculating partial safety factors ϕ and γ_i for resistance and loads, respectively, against a target reliability level, β. FORM requires only first and second moment information on resistances and loads (i.e. means and variances), and an assumption of distribution shape (e.g. Normal, lognormal, etc.). The calibration process is presented in Figure 1.4 and detailed by Paikowsky (2004).

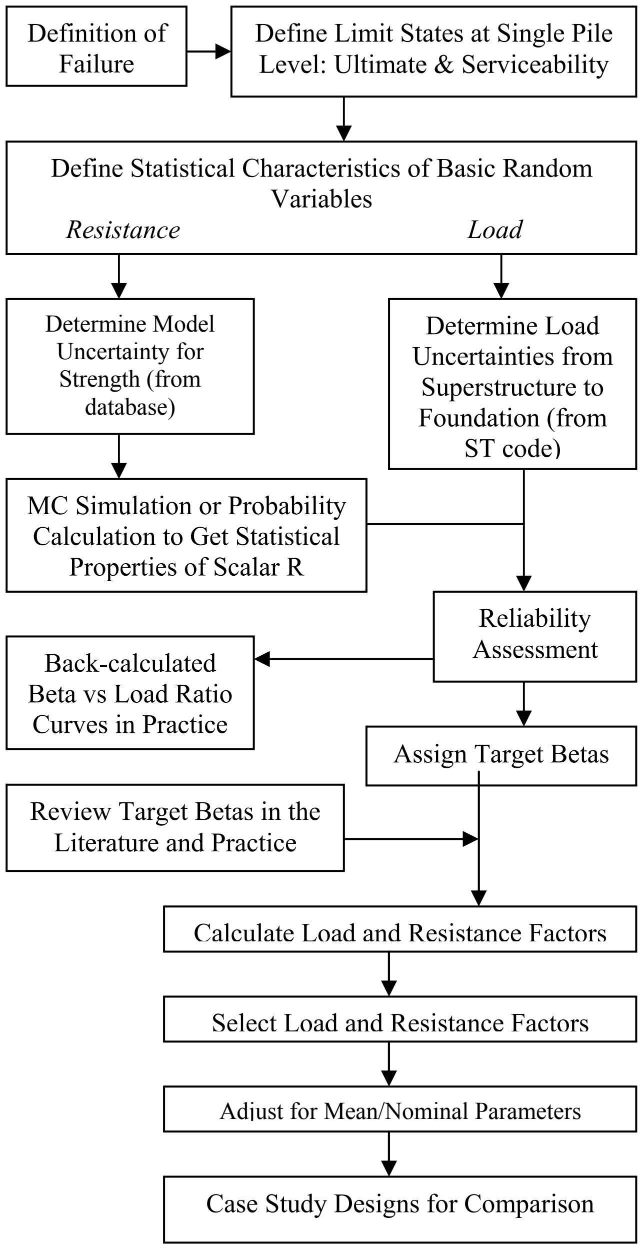

Notes: ST = Structural
MC = Monte Carlo
μ = mean
G(x) = performance function of the limit state = limit state function
G(x) = 0 = limit defining failure for G(x) < 0
$G_L(x)$ = linearized performance function

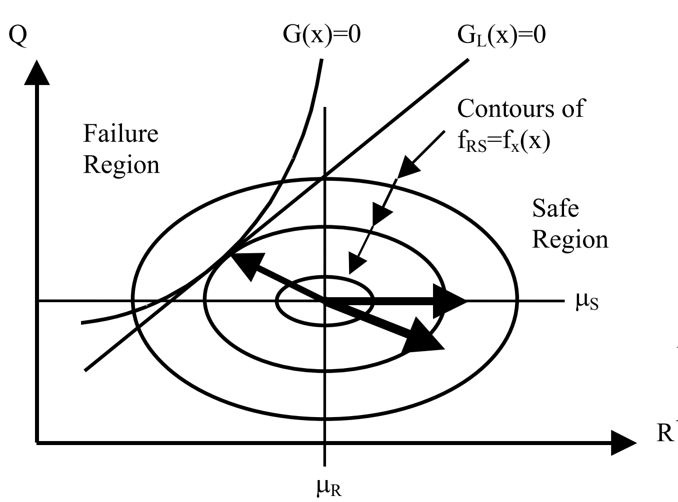

Figure 1.4 Resistance factor analysis flow chart (after Ayyub and Assakkaf, 1999 and Ayyub et al., 2000, using FORM - Hasofer and Lind 1974).

Each limit state (ultimate or serviceability) can be represented by a performance function of the form:

$$g(X) = g(X_1, X_2, \cdots, X_n) \tag{1.16}$$

in which $X = (X_1, X_2, \ldots, X_n)$ is a vector of basic random variables of strengths and loads. The performance function g(X), often called the limit state function, relates random variables to either the strength or serviceability limit-state. The limit is defined as g(X) = 0, implying failure when g(X) ≤ 0 (but strictly $g(X) < 0$) (Figures 1.2 and 1.4). Referring to Figure 1.4, the reliability index β is the distance from the origin (in standard normal space transformed from the space of the basic random variables) to the failure surface (at the most probable point on that surface), at the point on g(X)=0 at which the joint probability density function of X is greatest. This is sometimes called the *design point*, and is found by an iterative solution procedure (Thoft-Christensen and Baker, 1982). This relationship can also be used to back calculate representative values of the reliability index β from current design practice. The computational steps for determining β using FORM are provided by Paikowsky et al. (2004).

In developing code provisions, it is necessary to follow current design practice to ensure consistent levels of reliability over different evaluation methods (e.g. pile resistance or displacement). Calibrations of existing design codes are needed to make the new design formats as simple as possible and to put them in a form that is familiar to designers. For a given reliability index β and probability distributions for resistance and load effects, the partial safety factors determined by the FORM approach may differ with failure mode. For this reason, calibration of the calculated partial safety factors (PSF's) is important in order to maintain the same values for all loads at different failure modes. In the case of geotechnical codes, the calibration of resistance factors is performed for a set of load factors already specific in the structural code. Thus, the load factors are fixed. In this case, a simplified algorithm was used for project NCHRP 24-17 to determine resistance factors:

1. For a given value of the reliability index β, probability distributions and moments of the load variables, and the coefficient of variation for the resistance, compute mean resistance R using FORM.
2. With the mean value for R computed in step 1, the partial safety factor ϕ is revised as:

$$\phi = \frac{\sum_{i=1}^{n} \gamma_i m_{Li}}{m_R} \tag{1.17}$$

where m_{Li} and m_R are the mean values of the loads and strength variables, respectively and γ_i, $i = 1, 2, \ldots, n$, are the given set of load factors.

A comparison between resistance factors obtained using FORM and those using FOSM for 160 calibrations of axial pile capacity prediction methods are presented in Figure 1.5. The data in Figure 1.5 suggest that FORM results in resistance factors consistently higher than those obtained by FOSM. As a rule of thumb, FORM provided resistance factors for deep foundations approximately 10% higher than those obtained by FOSM. The practical conclusions that can be obtained from the observed data is that first evaluation of data can be done by the simplified closed form FOSM approach and the obtained resistance factors are on the low side (safe) for the resistance distributions obtained in the NCHRP 24-17 project (Paikowsky et al., 2004).

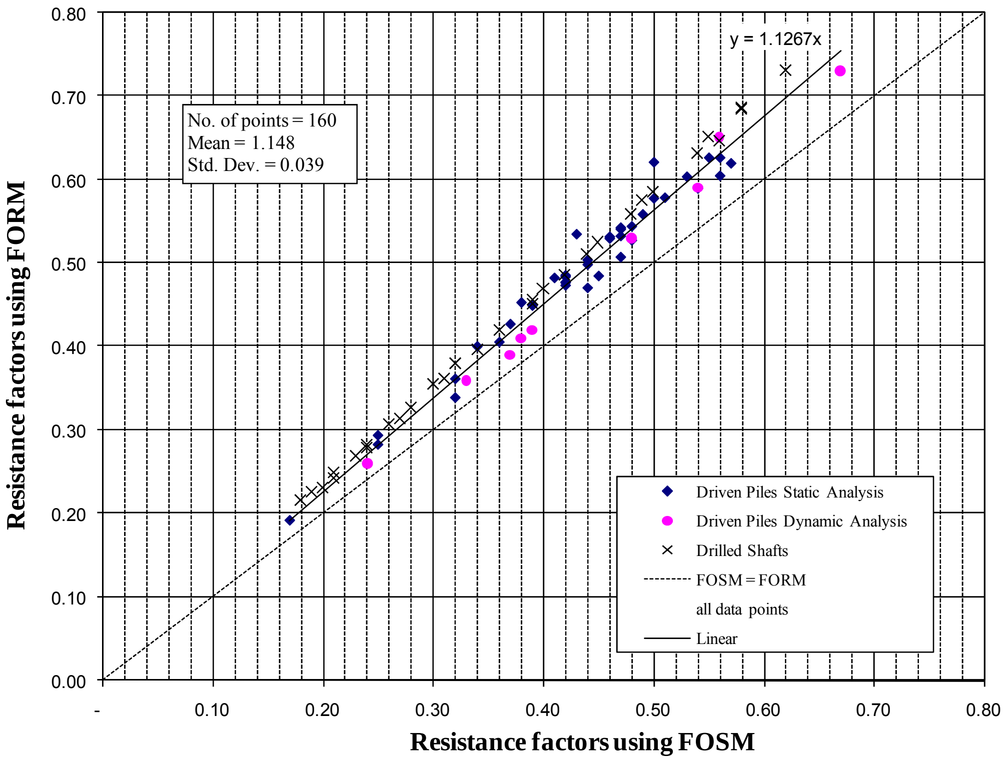

Figure 1.5 Comparison between resistance factors obtained using the First Order Second Moment (FOSM) vs. those obtained by using First Order Reliability Method (FORM) for a target reliability of β = 2.33 (Paikowsky et al., 2004).

1.3.5 Methods of Calibration – MCS

Monte Carlo Simulation (MCS) became the preferable calibration tool by AASHTO and is recommended for all AASHTO related calibrations. MCS is a powerful tool for determining the failure probability numerically, without the use of closed form solutions as those given by Equations 1.14 or 1.15. The objective of MCS is the numerical integration of the expression for failure probability, as given by the following equation.

$$p_f = P(g \leq 0) = \frac{1}{N}\sum_{i=1}^{N} I[g_i \leq 0] \tag{1.18}$$

where I is an indicator function which is equal to 1 for $g_i \leq 0$, i.e., when the resulting limit state is in the failure region, and equal to 0 for $g_i > 0$ when the resulting limit state is in the safe region; N is the number of simulations carried out. As $N \rightarrow \infty$, the mean of the estimated failure probability using the above equation can be shown to be equal to the actual failure probability (Rubinstein, 1981).

Code calibration in its ideal format is accomplished in an iterative process by assuming agreeable load and resistance factors, γ's and ϕ's, and determining the resultant reliability index, β. When the desired target reliability index, β_T, is achieved, an acceptable set of load and resistance factors has been determined. One unique set of load and resistance factors does not exist; different sets of factors can achieve the same target reliability index (Kulicki et al., 2007).

The MCS process is simple and can be carried out as follows:

- Identify basic design variables and their distributions. Load is assumed to be normally distributed.
- Generate N number of random samples for each design variable based on their distributions, i.e. using the reported statistics of load and resistance and computer-generated random numbers.
- Evaluate the limit state function N times by taking a set of the design variables generated above, and count the number for which the indicator function is equal to 1
- If the sum of the indicator function is N_f, i.e., the limit state function was $g_i \leq 0$ (in the failure region) for N_f number of times out of the total of N simulations carried out, then the failure probability p_f can be directly obtained as the ratio N_f/N.

The resistance factor based on the MCS process can be calculated utilizing the fact that to attain a target failure probability of p_{fT}, N_{fT} samples of the limit state must fall in the failure region. Since in the present geotechnical engineering LRFD only one resistance factor is used, while keeping the load factors constant, a suitable choice of the resistance factor would shift the limit state function so that N_{fT} samples fall in the failure region. The resistance factor derived in this study using MCS is based on this concept.

Kulicki et.al (2007) made several observations regarding the above outlined process:

1. The solution is only as good as the modeling of the distribution of load and resistance. For example, if the load is not correctly modeled or the actual resistance varies from the modeled distribution, the solution is not accurate, i.e. if the statistical parameters are not well defined, the solution is equally inaccurate.
2. If both the distribution of load and resistance are assumed to be normally or lognormally distributed, Monte Carlo simulation using these assumptions should theoretically produce the same results as the closed-form solutions.
3. The power of the Monte Carlo simulation is its ability to use varying distributions for load and resistance.

In summary, refinement in the calibration should be pursued not in refining the process used to calculate the reliability index; the Monte Carlo simulation as discussed above is quite adequate and understandable to the practicing engineer. Refinement should be sought in the determination of the statistical parameters of the various components of force effect and resistance and using the load distributions available for the structural analysis, means focusing on the statistical parameters of the resistance.

1.4 FORMAT FOR DESIGN FACTORS DEVELOPMENT

[Section 1.4 was copied from Paikowsky et al. (2009).]

1.4.1 General

AASHTO development and implementation of LSD and LRFD have been driven primarily by the objectives of achieving a uniform design philosophy for bridge structural and geotechnical engineering; hence, obtaining a more consistent and rational framework of risk management in geotechnical engineering.

The previous section (1.3) detailed the principles of LRFD and described the calibration process. The philosophy of attaining this calibration, however, varies widely between choosing values based on range of already available parameters, expert opinion, comprehensive resistance calibration, or material factor approach. Previous effort to calibrate the ULS of deep foundations had concentrated on comprehensive calibration of the resistance models as an integral entity (Paikowsky et al., 2004). This philosophy was based on the fact that in contrast to other engineering disciplines (e.g. structural analysis), the model uncertainty in Geotechnical Engineering is dominant. The specifications provide an existing ideal framework for prescribed comprehensive methodology and, hence, its direct calibration when possible results with highly accurate LRFD as demonstrated in the following sub-sections. This approach was followed by and large in the development of the SLS (NCHRP 12-66) and is followed (when possible) in this study as well. The calibration of shallow foundations for ULS has, however, more complex aspects not attainable (at present time) to be calibrated directly. Hence, the following section (based primarily on Honjo and Amatya, 2005) is provided as a background to the diverse approach comprising the current research.

1.4.2 Material and Resistance Factor Approach

It is identified by many that some of the key issues in developing sound geotechnical design codes based on LSD and LRFD are definition of characteristic values and determination of partial factors together with the formats of design verification (Simpson and Driscoll, 1998; Orr, 2002; Honjo and Kusakabe, 2002; Kulhawy and Phoon, 2002 etc.). The characteristic values of the design parameters are conveniently defined as their mean values.

The approach concerning design factors development formats can be summarized as whether one should take a material factor approach (MFA) or a resistance factor approach (RFA). In MFA, partial factors are directly applied to characteristic values of materials in design calculation, whereas in RFA, a resistance factor is applied to the resulting resistance calculated using the characteristic values of materials. One of the modifications of RFA is a multiple resistance factor approach (MRFA) where several resistance factors are employed to be applied to relatively large masses of calculated resistances. The advantage of MRFA is claimed to ensure more consistent safety margin in design compared to RFA (Phoon et al. 1995, 2000; Kulhawy and Phoon, 2002). In general, MFA originated in Europe, whereas, RFA originated in North America. However, they are now used mixedly worldwide, e.g. the “German approach” to EC7 coincides with RFA while Eurocode7 allows several design approaches, both MFA and RFA and the member state can define their presence in their National Annex to the EC7.

1.4.3 Code Calibrations

A procedure to rationally determine partial factors in the design verification formulas based on reliability analysis is termed code calibration. Section 1.3.2 and the details in sections 1.3.3, 1.3.4 and 1.3.5 presented the analytical meaning of the calibration in the LRFD methodology. One of the best known monumental works in this area is by Ellingwood et al. (1982) where load and resistance factors were determined based on a reliability analysis using FORM. Since then, a reasonable number of code calibration studies have been carried out in structural engineering (e.g. Nowak, 1999). However, rational code calibration studies in geotechnical engineering codes started only in the past decade or so (Barker et al. 1991; Phoon et al., 1995; Honjo et al., 2002; Paikowsky et al., 2004; etc.).

Barker et al. (1991) proposed resistance factors for the AASHTO bridge foundation code published in 1994 (AASHTO, 1994). The calibration was based on FOSM but used back-calculation from factors of safety and introduced a significant amount of engineering judgments in determining the factors along a not so clearly described process. Based on the difficulties encountered in using their work, the revision of the partial factors for deep foundations in the AASHTO specification was carried out by Paikowsky et al. (2004), in which a large database was developed and used in a directly calibrated model (RFA approach together with reliability analysis by FORM) to determine the resistance factors. The SLS calibration (NCHRP 12-66) was also developed in a similar approach using MCS to determine the factors. Examples from both are provided below. Phoon et al. (1995, 2000) carried out calibration of the factors for transmission line structure foundations based on MRFA by reliability analysis. Some simplified design formats were employed, and factors were adjusted until the target reliability index was reached. Kobayashi et al. (2003) have calibrated resistance factors for building foundations for the Architectural Institute of Japan (AIJ) limit state design building code (AIJ, 2002). This code provides a set of load and resistance factors for all aspects of building design in a unified format. FORM was used for the reliability analysis and MRFA was the adopted format of design verification as far as the foundation design is concerned.

1.4.4 Example of Code Calibrations – ULS

The capacity of the comprehensive direct model calibration resistance factor approach is demonstrated. Large databases of pile static load tests were compiled and static and dynamic pile capacities of various design methods were compared to the nominal strength obtained from the static load test. The geotechnical parameter variability was minimized (indirectly) by adhering to a given consistent procedure in soil parameters selection (e.g. NSPT correction and friction angle correlations), as well as load test interpretation (e.g. establishing the uncertainty in Davisson's criterion for capacity determination and then using it consistently). Two examples for such large calibrations are presented in Figures 1.6 and 1.7 for given specific dynamic and static pile capacity prediction methods, respectively (Paikowsky et al., 2004).

Further sub-categorization of the analyses led to detailed resistance factor recommendations based on pile type, soil type and analyses method combinations. Adherence to the uncertainty of each combination as developed from the database and consistent calibrations led to a range of resistance factors (see for example Table 25 of NCHRP 507 Report, Paikowsky et al., 2004). The latest version of the specifications (AASHTO, 2006) avoided the detailed calibrations and presented one "simplified" resistance factor (ϕ = 0.45) for static analysis of piles along with one design method (Nordlund/Thurman).

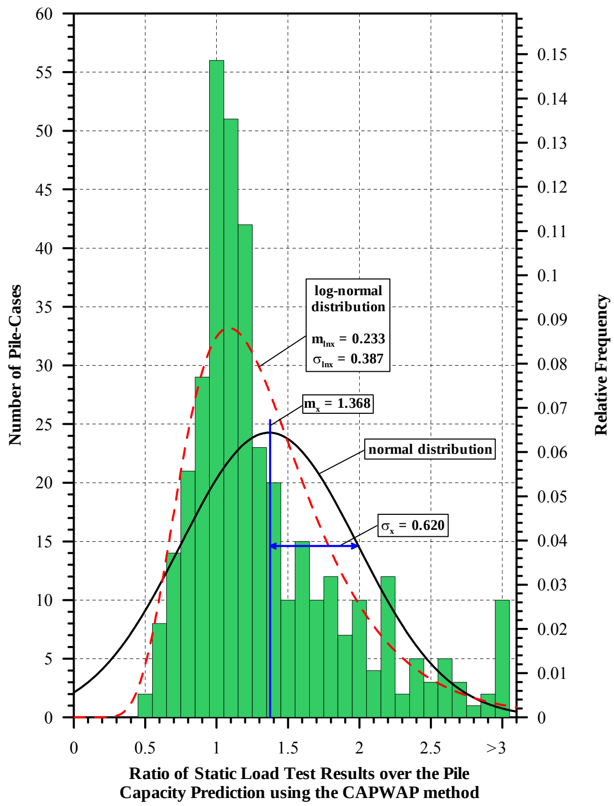

Figure 1.6 Histogram and frequency distributions for all (377 cases) measured over dynamically (CAPWAP) calculated pile-capacities in PD/LT2000 (Paikowsky et al., 2004).

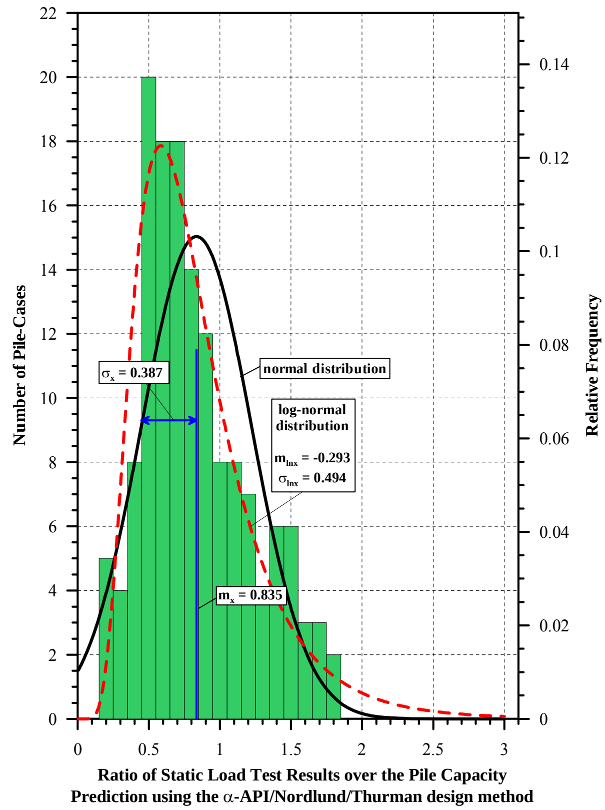

Figure 1.7 Histogram and frequency distribution of measured over statically calculated pile capacities for 146 cases of all pile types (concrete, pipe, H) in mixed soil (Paikowsky et al., 2004).

The first large LRFD bridge design project in New England (including superstructure and substructure) based on AASHTO 2006 specifications is currently being carried out. A large static load test program preceded the design. Identifiable details are not provided, but Tables 1.2 and 1.3 present the capacity evaluation for two dynamically and statically tested piles (class A prediction, submitted by the PI about one month before testing) using the calibrated resistance factors for the specific pile/soil/analysis method combination vs. the "simplified" AASHTO version of the resistance factor. In both cases, the calculated factored capacity using the "simplified" resistance factor exceeded the unfactored and factored measured resistance (by the load test) in a dangerous way, while the use of the calibrated resistance factors lead to consistent and prudent design. The anticipated substructure additional cost has increased by 100% (in comparison to its original estimate based on the AASHTO specifications) and exceeded $100 million (at the time of the load test program) and one year in project delay. The power of the comprehensive direct RFA calibration based on databases vs. arbitrary assignments of resistance factors is clearly demonstrated in the first case of its significant use in New England.

Table 1.2 H Pile – Summary (14x177, Penetration = 112ft)

Static:

Static Pile Capacity Combinations:

Analysis Combination	Estimated Capacity (R_n) (kips)	NCHRP 507 Resistance Factor for H Piles in sand (ϕ)	Factored Resistance (R_r)	NCHRP 507 Resistance Factor for H Piles in Mixed Soils (ϕ)	Factored Resistance (R_r)	AASHTO LRFD Specifications 2006 Resistance Factor (ϕ)	Factored Resistance (R_r)
β-Method/Thurman (Steel Only)	894	0.30	268	0.20	179	Not Specified	
β-Method/Thurman (Box Area)	1,076		323		215		
Nordlund/Thurman (Steel Only)	841	0.45	379	0.35	252	0.45	379
Nordlund/Thurman (Box Area)	1,023		460		307		460
FHWA Driven Ver. 1.2 (Steel Only)	845						
FHWA Driven Ver. 1.2 (Box Area)	1,032						

Notes:

1. Resistance Factors taken from NCHRP Report 507 Table 25 for a Redundant Structure.

[shaded box] Recommended range for preliminary design

Reference: *Static Pile Capacity and Resistance Factors for Pile Load Test Program*, GTR report submitted to Haley and Aldrich, Inc. (H&A) dated June 21, 2006 (Paikowsky, Thibodeau and Griffin).

Note: Above DRIVEN values were obtained by inserting the friction values and unit weights directly into DRIVEN, limiting the friction angle to 36°.

Dynamic:

Sakonnet River Bridge Test Pile Program Portsmouth, RI - Summary of Dynamic Measurement Predictions and Factored Resistance (H Piles)

Pile Type	Time of Driving	Energy Approach			CAPWAP		
		EA[1] (kips)	ϕ[2]	R_r (kips)	CAP[1] (kips)	ϕ[2]	R_r (kips)
H	EOD	481	0.55	265	310	0.65	202
	BOR	606	0.40	242	434	0.65	282[3]

[1]Values represent EOD predictions and average of all BOR predictions.

[2]All ϕ factors taken from NCHRP 507 (Paikowsky et al., 2004)

[3]Only ϕ factors for BOR CAPWAP appear in AASHTO (2006) specifications and are marked by shaded cells

Reference: *Pile Capacity Based on Dynamic Testing and Resistance Factors for Pile Load Test Program,* GTR report submitted to H&A dated July 17, 2006 (based on earlier submittals of data and analyses) (Paikowsky, Chernauskas, and Hart).

Static Load Test

Load Test Capacity (Davisson's Criterion):

Q_u = 378kips at 0.68inch

Resistance Factors NCHRP 507 and AASHTO Specifications:

ϕ = 0.55 (1 test pile large site variability)

ϕ = 0.70 (1 pile medium site variability)

Factored Resistance: R_r = 208 to 265kips

Reference: Load Test Results presented and analyzed by H&A.

Table 1.3 42" Pipe Pile – Summary (ϕ = 42", w.t. = 1", 2" Tip, Penetration = 64ft)

Static:

Static Pile Capacity Combinations: Assumed Displaced Soil Volume Based on Uniform Wall Thickness (1.0 inches)

Analysis Combination	Estimated Capacity (R_n) (kips)	NCHRP 507 Resistance Factor for Pipe Piles in sand (ϕ)	Factored Resistance (R_r)	NCHRP 507 Resistance Factor for Pipe Piles in Mixed Soils (ϕ)	Factored Resistance (R_r)	AASHTO LRFD Specifications 2006 Resistance Factor (ϕ)	Factored Resistance (R_r)
β-Method/Thurman (Steel Only)	924	0.35	324	0.25	231	Not Specified	-
β-Method/Thurman (30% Tip Area)	984		345		246		-
β-Method/Thurman (50% Tip Area)	1,084		380		271		-
β-Method/Thurman (70% Tip Area)	1,184		415		296		-
β-Method/Thurman (100% Tip Area, plugged)	1,335		467		334		-
Nordlund/Thurman (Steel Only)	690	0.55	379	0.35	241	0.45	310
Nordlund/Thurman (30% Tip Area)	750		412		262		337
Nordlund/Thurman (50% Tip Area)	850		467		297		382
Nordlund/Thurman (70% Tip Area)	950		522		332		427
Nordlund/Thurman (100% Tip Area, plugged)	1,101		605		385		495

Notes:

1. Resistance Factors taken from NCHRP Report 507 Table 25 for a Redundant Structure.
2. Tip resistance for steel only included 2-inch wall thickness accounting for the driving shoe.

Recommended range for preliminary design soil plug only

Reference: *Static Pile Capacity and Resistance Factors for Pile Load Test Program*, GTR report submitted to Haley and Aldrich, Inc. (H&A) dated June 21, 2006 (Paikowsky, Thibodeau and Griffin).

Static Load Test (Open Pipe Pile)

Load Test Capacity (Davisson's Criterion):

Q_u = 320kips at 0.52 inch

Resistance Factors NCHRP 507 and AASHTO Specifications:

ϕ = 0.55 (1 pile large site variability)

ϕ = 0.70 (1 pile medium site variability)

Factored Resistance: R_r = 176 to 224kips

Reference: Load Test Results presented and analyzed by H&A.

1.4.5 Example of Code Calibrations – SLS

The factors associated with the Serviceability Limit State were evaluated under project NCHRP 12-66. Following the development of serviceability criteria for bridges (Paikowsky, 2005; Paikowsky and Lu, 2006), large databases of foundation performance were accumulated and analyzed for direct RFA calibrations (Paikowsky et al., 2009). Examples of databases examining the performance of displacement analyses of shallow foundations are presented in Figures 1.8 and 1.9 for AASHTO (2008) and Schmertmann et al. (1978) settlement analysis methods, respectively. These robust analysis results allow direct calibration of resistance factors for applied loads for a given SLS criterion (displacement). The data in Figures 1.8 and 1.9 are related to: 1ft (0.30m) ≤ B ≤ 28ft (8.53m), B_{avg} = 8ft (2.44m), 1.0 ≤ L/B ≤ 6.79, L/B_{avg} = 1.55, 25.2ksf (1205kPa) ≤ q_{max} ≤ 177.9ksf (8520kPa) for which B and L are the smaller and larger footing size, respectively and q_{max} is the maximum stress applied to the foundations under the measured displacement.

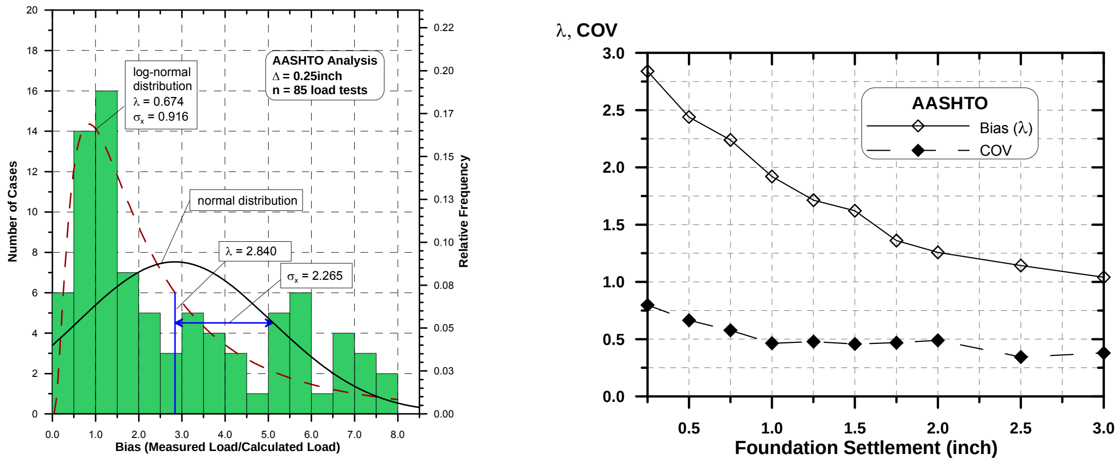

(a) (b)

Figure 1.8 (a) Histogram and frequency distributions of measured over calculated loads for 0.25" settlement using AASHTO's analysis method for 85 shallow foundation cases, and (b) variation of the bias and uncertainty in the ratio between measured to calculated loads for shallow foundations on granular soils under displacements ranging from 0.25 to 3.00in.

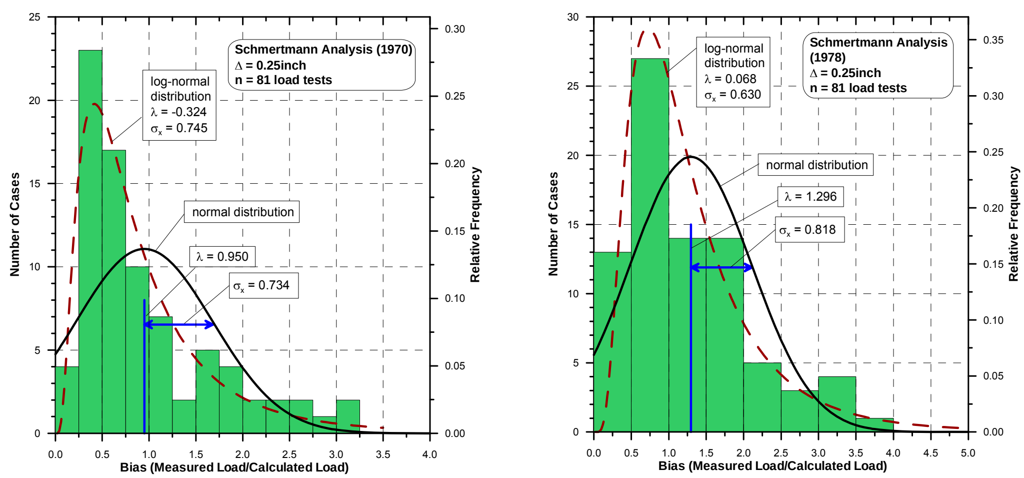

(a)

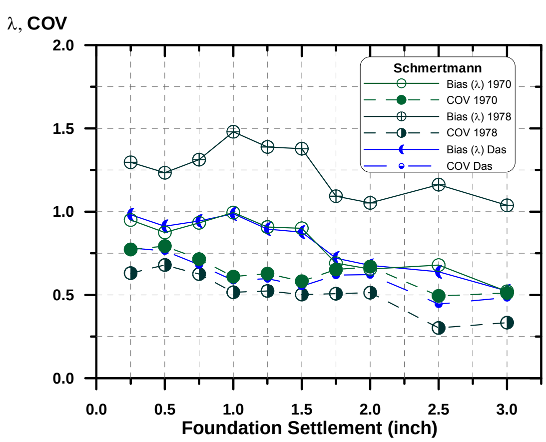

(b)

Figure 1.9 (a) Histogram and frequency distributions of measured over calculated loads for 0.25" settlement using Schmertmann (1970) and Schmertmann et al. (1978) analysis methods for 81 shallow foundation cases, and (b) variation of the bias and uncertainty in the ratio between measured to calculated loads for shallow foundations on granular soils under displacements ranging from 0.25 to 3.00in.

1.5 METHODOLOGY FOR CALIBRATION

[Section 1.5 was copied from Paikowsky et al. (2009).]

1.5.1 Principles

Section 1.4 reviewed the format for the design factors. The resistance factor approach (RFA) was adopted in this study following previous NCHRP deep foundations LRFD database calibrations (Paikowsky et al., 2004). Figures 1.10 and 1.11 illustrate the sources of uncertainty and principal differences between Probability Based Design (PBD) application to the design of a structural element of the superstructure and to a geotechnical design of a foundation in the substructure. Considering a bridge girder as a simple supported beam under the assumption of homogenous cross-section, horizontal symmetry line and beam height, h, one can accurately calculate moments (hence, stresses) and deflections in the beam. The major source of uncertainty remains the loading (especially the live and extreme event loading on the bridge) while the material properties and physical dimensions present relatively a smaller uncertainty. Figure 1.11 (borrowing from the concept presented by Ovesen, 1989) demonstrates the higher degree of uncertainty associated with the design of a foundation. The material properties are based on subsurface investigation and direct or indirect parameter evaluation. The loading arriving to the foundation and its distribution is greatly unknown as only limited information was ever gathered on loading at the foundation level. As such, the loading uncertainty is assumed as that attributed to the design of the structural element. The main difficulty associated with the design of a foundation in comparison with a structural element, remains with the analysis model. While the calculation model in the structural element is explicit (though becoming extremely complex and less definite as the element evolves in geometry and composition and requires the interaction with other units), the analysis model for the evaluation of the soil resistance (i.e. bearing capacity) is extremely uncertain due to the assumptions and empirical data made during its establishment.

As such, the uncertainty of the geotechnical resistance model controls the resistance evaluation of the foundation. The concept adopted in this research (similar to that adopted by Paikowsky et al., 2004 for deep foundations) focused, therefore, on the calibration of selected bearing capacity (resistance) models as a complete unit while reducing other associated sources of uncertainty by following specific procedures, e.g. soil parameter establishment. This approach is discussed in section 1.4, and demonstrated in the examples presented in sections 1.4.4 and 1.4.5. The systematic analysis of many case histories via a selected resistance model and their comparison to measured resistance provided the uncertainty of the model application, but includes in it the influence of the different sites from which the data are obtained as well as the uncertainty associated with the 'measured' resistance.

The assumption made that the obtained uncertainty represents the variability of the model application for a specific foundation analysis, i.e. the resistance variability as depicted in Figures 1 and 3, is reasonable and proven successful though it may contain some conservatism, depending on the quality and reliability of the database cases. More so, the calibration of soil type, specific model and pile type combination as applied previously to deep foundations, has proven extremely effective compared to arbitrary selection of parameters or WSD back-calculated values that defeat the PBD principles as demonstrated in section 1.4.4. The present calibration is comprised mostly of adopting the vertical load statistics established in NCHRP 24-17 (Paikowsky et al., 2004), and resistance for design methodologies based on the state of practice established as outline above.

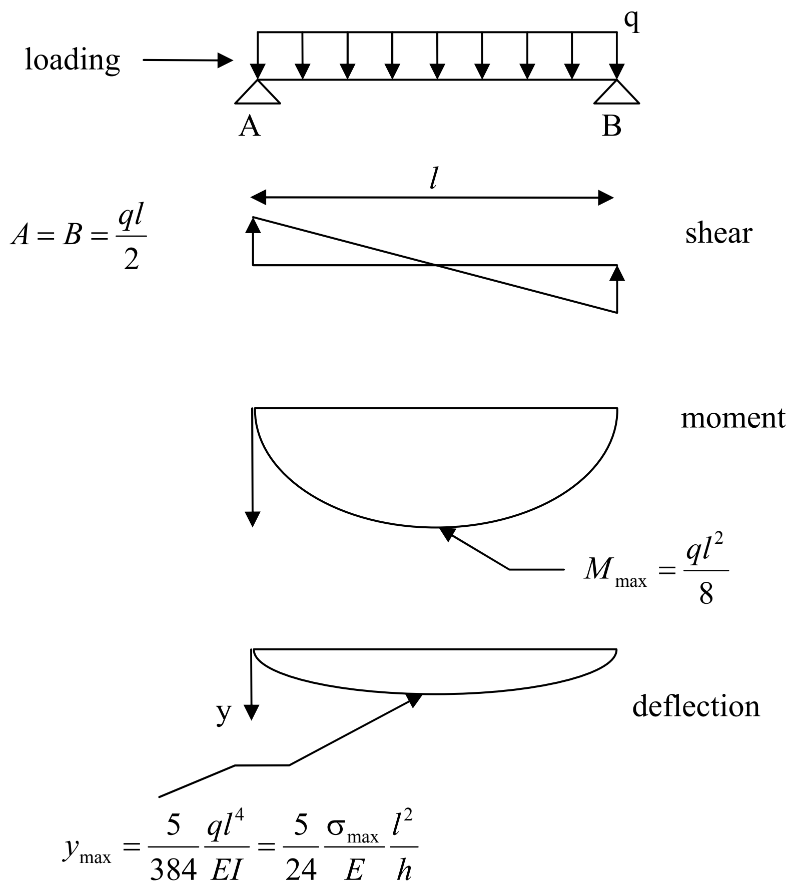

Sources of Uncertainty

- Loading
- Dimensions/Geometry
- Material Properties

Most Noticeable:

1. No uncertainty in the model – under given loading conditions the uncertainty in the material properties dictates the uncertainty in strength and deflection
2. Largest uncertainty in the loading, source, magnitude, distribution (in case of bridges)

(Assuming homogenous cross-section, horizontal symmetry line and beam height, h)

Figure 1.10 Simplified example of a beam design and associated sources of uncertainty.

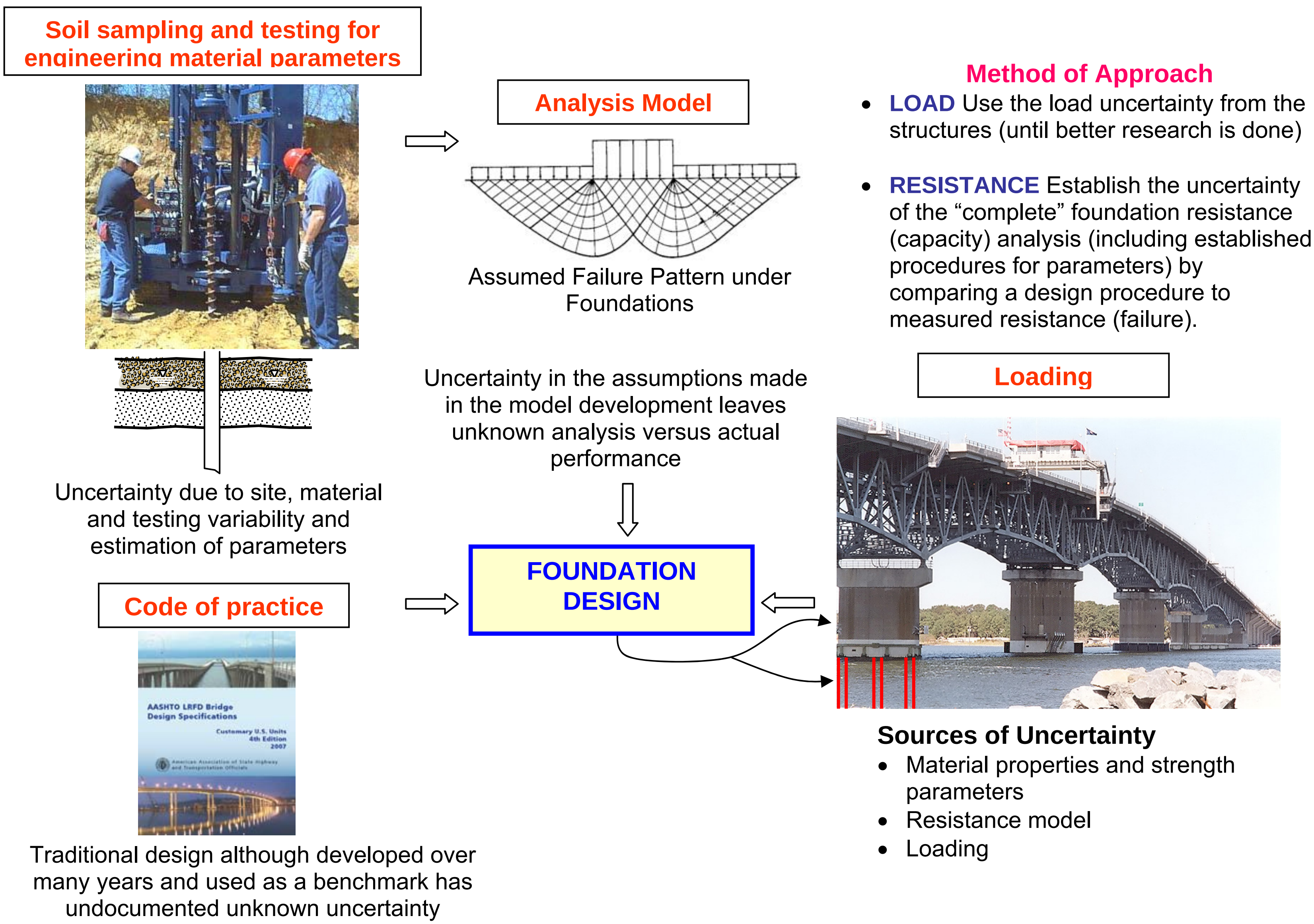

Figure 1.11 Components of foundation design and sources of uncertainty.

1.5.2 Overview of the Calibration Procedure

The probability-based limit state designs are presently carried out using methods categorized in three levels (Thoft-Christensen and Baker, 1982):

- Level 3: methods of reliability analyses utilizing full probabilistic descriptions of design variables and the true nature of the failure domains (limit states) to calculate the exact failure probability, for example, Monte Carlo Simulation (MCS) techniques; safety is expressed in terms of failure probability
- Level 2: simplification of Level 3 methods by expressing uncertainties of the design variables in terms of mean, standard deviation and/or coefficient of variation and may involve either closed form or approximate iterative procedures (e.g. FOSM, FORM and SORM analyses) or more accurate techniques like MCS to evaluate the limit states; safety is expressed in terms of reliability index
- Level 1: more of a limit state design than a reliability analysis; partial safety factors are applied to the pre-defined nominal values of the design variables (namely the loads and resistance(s) in LRFD), however, the partial safety factors are derived using Level 2 or Level 3 methods; safety is measured in terms of safety factors

Irrespective of the probabilistic design levels described above, the following steps are involved in the LRFD calibration process.

1. Establish limit state equation to be evaluated
2. Define statistical parameters of basic random variables, or the related distribution functions
3. Select a target failure probability or reliability value
4. Determine load and resistance factors consistent with the target value using reliability theory. More applicable to AASHTO LRFD geotechnical application is a variation where structural selected load factors are utilized to determine resistance factors for a given target value.

The following section outlines the work done to achieve the above steps and the way it is presented in the following chapters.

1.6 DYNAMIC EQUATIONS

1.6.1 Dynamic Analysis of Piles – Overview

Dynamic analyses of piles are methods which predict pile capacity based on the behavior of the hammer-pile-soil system during driving. Such methods are based on the idea that the driving operation induces failure in the pile-soil system. In other words, pile driving is analogous to a very fast load test under each hammer blow. The pile must, however, experience a minimum permanent displacement, or set (approximately 0.1 inch), during each hammer blow to fully mobilize the resistance of the pile-soil system. If there is very little or no permanent downward displacement of the pile tip, then the pile-soil system experiences mostly elastic deformation. As a result, capacity predictions based on measurements taken at this time may not be indicative of the full resistance of the pile-soil system. There are basically two methods of estimating the capacity of driven piles based on dynamic driving resistance: pile driving formulae (i.e. dynamic equations) and wave equation analysis.

1.6.2 Dynamic Equations – Review

For centuries quantitative analyses of pile capacity have been performed using dynamic equations, (Cummings, 1940). These equations can be categorized into three groups: theoretical equations, empirical equations, and those which consist of a combination of the two. It is important to mention that forty-five (45) of the state highway departments in the United States include a dynamic formula in their foundation specifications for the determination of bearing value for single acting steam/air hammers. Thirty (30) of these 45 states use the Engineering News Record (ENR) formula and nine (9) states use other variations of the rational pile formula, (Paikowsky, 1994). In general, all the pile formulae, with the exception of Gates formula, are derived from the rational pile formula (Bowles, 1988). With the exception of Gates and FHWA Modified Gates equations, a reference will be made here only to theoretical equations because empirical and semi-empirical equations are restricted to the conditions and assumptions of their original data set.

1.6.3 The Basic Principle of the Theoretical Dynamic Equations

The theoretical equations have been formulated around analyses which evaluate the total resistance of the pile, based on the work done by the pile during penetration. Observations of the hammer's ram stroke and the pile set are used in determining this work done by the hammer and the pile. These theoretical equation formulations assume elasto-plastic force-displacement relations as detailed in Figure 1.12.

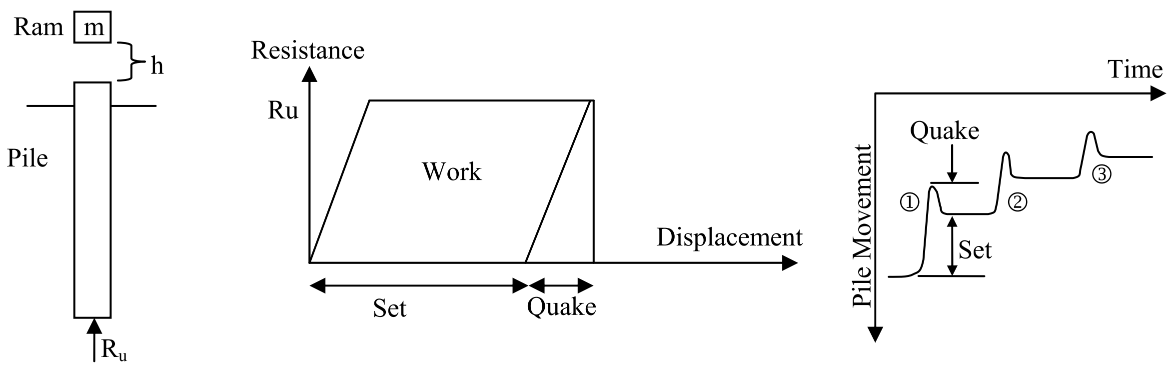

(a) (b) (c)

Figure 1.12 The principle of the dynamic equation: (a) ram-pile mechanics, (b) elasto-plastic relations assumed between the load acting on the pile and its displacement under a single hammer impact, and (c) pile top displacement under a sequence of hammer blows.

Refering to Figure 1.12(a), the energy of a ram falling a free fall, a stroke h, is the nominal hammer energy: E_n = mgh = W_rh assuming pile driving (including hammer) efficiency η, the energy transferred by the impact is:

$$E_i = E_h\eta = W_r h\eta \tag{1.19}$$

Assuming elasto-plastic pile movement force relations as depicted in Figure 1.12(b), the total work done by the pile during penetration can be computed as:

$$W = R_u \left(S + \frac{Q}{2} \right) \tag{1.20}$$

where: R_u - the yield resistance = ultimate carrying pile capacity,
S - the pile set, denoting the permanent displacement of the pile under each hammer blow, equivalent to the soil's plastic deformation.
Q - quake, denoting the elastic deformation of the pile-soil system.

The set and the quake can be measured directly from the pile movement under the impact of the hammer as depicted in Figure 1.12(c) for a sequence of three blows. The image in Figure 1.12(c) refers to a tracing of pile movement obtained by passing a pen on the pile from left to right while the pile moves under the three blows.

Equating the energy delivered by the hammer to the work done by the pile in penetration,

$$E_i = W$$

$$W_r \cdot h \cdot \eta = R_u(s+Q/2)$$

$$R_u = \frac{W_r h \eta}{\left(s + Q/2 \right)} \tag{1.21}$$

This energy equilibrium equation is the valid basis of all the theoretical equations.

A theoretical expansion of equation 1.21 is presented in the form of the General (a.k.a. Rational) Pile Driving Formula (Chellis, 1961).

$$R_u = \frac{e_f E_n}{s + 1/2 (C_1 + C_2 + C_3)} X \frac{W_r + e^2 W_p}{W_r + W_p} \tag{1.22a}$$

where: Ru – ultimate carrying pile capacity
e_f = hammer efficiency
E_n = nominal hammer energy
W_r = weight of falling ram
W_p = weight of pile
s = set
C_1, = elastic (temporary) compression of pile head and cap
C_2, = elastic (temporary) compression of pile
C_3 = elastic (temporary) compression of the soil
e = coefficient of restitution

For drop hammers or single acting steam hammers, Chellis proposed to use the nominal energy $E_n = W_r \cdot h$, hence, falls back to Hiley (1930) formula (marked as equation 1.22b in Table 1.4).

Many of the 'theoretical' equations possess the shape of the general (rational) equation in one form or another (including the Mn/DOT dynamic formula). The general equation is clearly made of two parts; the term on the left expands on the energy equilibrium format of Equation 1.20 by attempting to evaluate the quake as the combined elastic compression of the driving system, pile and the soil. The term on the right side of Equation 1.22a is an attempt to evaluate the energy loss in the impact between the ram, the assembly and the pile. For detailed development of this term and/or the rational equation see Hiley (1930), Cummings (1940), Taylor (1948) or Bowles (1977). Cummings (1940) notes that the originator of this equation may be Redtenbacher (ca. 1859). This term is based on Newton's conservation of momentum theory, what is commonly known as Newtonian impact. However, this theorem is applicable to a collision between extremely rigid (stiff) bodies (e.g. billiard balls) and is theoretically invalid for an elastic impact as is the case in pile driving (noted so by Sir Newton himself).

The Gates equation (Gates, 1957), while empirical was found to provide reasonable results (e.g. Olsen and Flaate, 1967, Long et al., 1999, Paikowsky et al., 2004). The equation was further enhanced by the FHWA (FHWA, 1988, see also Fragaszy et al., 1985) based on statistical correlation with static load test data.

1.6.4 Summary of Various Dynamic Equations

A list of known dynamic equations developed over the years is presented in Table 1.4.

1.6.5 The Reliability of the Dynamic Equations

In general, dynamic equations are of limited accuracy (see for example Housel, 1965, 1966, Flaate, 1964 and Olsen and Flaate, 1967) and a high factor of safety is therefore required when using their un-calibrated estimated capacity (e.g. F.S.=6 for the ENR equation). Dynamic equations are largely inaccurate because: (a) their parameters, such as the efficiency of energy transfer and the pile/soil quake, are crudely approximated, (b) some of the theoretical developments of the rational pile formula, especially those relating the energy transfer mechanism to a Newtonian analysis of ram-pile impact, are theoretically invalid (see aforementioned discussion), and (c) There is no differentiation between static and dynamic soil resistances where it is known that such differences exist, especially in cohesive soils (Taylor, 1948).

1.6.6 LRFD Calibration of Dynamic Equations

Paikowsky et al., (2004) checked the prediction accuracy of the ENR equation, Gates and FHWA modified Gates equation for 384 cases. These cases included all pile types, all hammer types and all time of driving, i.e. end of driving and restrikes, hence, related at times to multiple records of the same pile. The equations investigated, in contrast with the Mn/DOT pile driving equation, do not require field observations other than the blow count at the end of driving. Data PD/LT 2000 was therefore directly utilized for the evaluation of the uncertainty of the methods as presented in Table 1.5.

Table 1.5 also presents the resistance factors calculated for the established uncertainty using three reliability indices. Further details of the findings and comparisons to those obtained in the present study are presented in Chapter 7.

Table 1.4 Dynamic Equations

No.	Equation	Description	Reference
1.22a	$R_u = \dfrac{e_f W_r h}{s + \frac{1}{2}(C_1 + C_2 + C_3)} X \dfrac{W_r + e^2 W_p}{W_r + W_p}$	Drop Hammers, Single-Acting Steam Hammers	Hiley (1930)
1.22b	$R_u = \dfrac{12 e_f E_n}{s + \frac{1}{2}(C_1 + C_2 + C_3)} X \dfrac{W_r + e^2 W_p}{W_r + W_p}$	Double-Acting, Differential-Acting Steam & Diesel Hammers	Chellis (1961)
1.23	$R_u = \dfrac{W_r * h}{S + 1.0}$	Drop Hammer	Engineering News-Record (1888)
1.24	$R_u = \dfrac{W_r * h}{S + 0.1}$	Steam Hammer	Engineering News-Record (1888)
1.25	$R_u = 27.11\sqrt{E_n * e_h}(1 - \log s)$		Gates (1957)
1.26	$R_u = 1.75\sqrt{E_n} * \log(10 * N) - 100$		FHWA (1988)
1.27	$R_u = \dfrac{WH}{S} * \dfrac{W}{W + W_p}$		Eytelwein (see Chellis, 1961)
1.28	$R_u = -\dfrac{SAE_p}{L} + \sqrt{\left(\dfrac{2WHAE_p}{L}\right) + \left(\dfrac{SAE_p}{L}\right)^2}$		Weisbach
1.29	$R_u = \dfrac{e_f WH}{S + (2e_f WHL / AE_p)^{1/2}}$		Danish (Olsen & Flaate, 1967)
1.30	$R_u = 7.2\sqrt{e_f WH} * \log(10/S) - 17$	Timber Piles	Olsen & Flaate (1967)
1.31	$R_u = 9.0\sqrt{e_f WH} * \log(10/S) - 27$	Precast Concrete Piles	Olsen & Flaate (1967)
1.32	$R_u = 13.0\sqrt{e_f WH} * \log(10/S) - 83$	Steel Piles	Olsen & Flaate (1967)
1.33	$R_u = \dfrac{e_h E_h C_1^1}{s + C_2^1 C_3^1}$		Canadian Building Code (1975), see Bowles (1977)
1.34	$R_u = \dfrac{e_h E_h}{s + C_1^2}$		Olsen & Flaate (1967)
1.35	$R_u = \dfrac{e_h E_h}{k_u s}$	Janbu	Olsen & Flaate (1967), Mansur & Hunter (1970)
1.36	$R_u = \left[\dfrac{1.25 e_h E_h}{s + C}\right]\left[\dfrac{W_r + n^2 W_p}{W_r + W_p}\right]$	using F.S. = 6 and impact energy calculation	Engineering News-Record (1965)
1.37	$R_u = \dfrac{e_h h(W_r + A_r p)}{s + C}$		AASHTO (1973-1976)
1.38	$R_u = \dfrac{e_h E_h}{s(1 + 0.3C_1^3)}$		Navy McKay (see Bowles, 1977)
1.39	$R_u = \dfrac{e_h E_h C_1^4}{s + C_2^4}$		Pacific Coast (see Uniform Building Code and Bowles, 1977)

Notes:
R_u= ultimate carrying capacity of pile, in pounds (1.22a, 1.22b)
R_u= ultimate carrying capacity of pile, in kips
R_u= ultimate carrying capacity of pile, in tons (1.30, 1.31, 1.32)
W_r= weight of falling ram, in pounds (1.22a, 1.22b)
W_r= weight of falling mass, in tons (1.30, 1.31, 1.32)
W_r= weight of falling mass, in kips
E_n= rated energy of hammer per blow, in foot-pounds (1.22a, 1.22b)
h= height of free fall of ram, in inches (1.22a, 1.22b, 1.30, 1.31, 1.32)
e_f= efficiency
W_p= weight of pile, in pounds (1.22a, 1.22b)
e= coefficient of restitution
s= final set of pile, in inches (1.22a,1.22b, 1.30, 1.31, 1.32)
C_1 = temporary compression allowance for pile head and cap, in inches (PL/AE)
C_2 = temporary compression of pile, in inches (PL/AE)
C_3 = quake, in inches
h= height of free fall of ram, in feet
E_n= rated energy of hammer per blow, in kips-foot
s= set of pile, in inches
N= blows per inch (BPI)
A= cross-section of pile
E_p= modulus of elasticity of pile
L= pile length
C= 2.5mm = 0.1 inches
p= steam pressure
k= 0.25 for steel piles = 0.10 for all other piles

$$C_1^1 = \frac{W_r + n^2(0.5W_p)}{W_r + W_p}$$

$$C_2^1 = \frac{3R_u}{2A}$$

$$C_3^1 = \frac{L}{E} + C_4^1$$

C_4^1 = 0.0001 in^3/k = 3.7 X 10^{-10} m^3/kN

$$C_1^2 = \sqrt{\frac{e_h E_h L}{2AE}}$$

$$k_u = C_d\left(1 + \sqrt{1 + \frac{\lambda}{C_d}}\right)$$

$$C_d = 0.75 + 0.15\frac{W_p}{W_r}$$

$$\lambda = \frac{e_h E_h L}{AEs^2}$$

$$C_1^3 = \frac{W_p}{W_r}$$

$$C_1^4 = \frac{W_r + kW_p}{W_r + W_p}$$

$$C_2^4 = \frac{P_u L}{AE}$$

Table 1.5 Statistical Summary and Resistance Factors of the Dynamic Equations (Paikowsky et al., 2004)

Method		Time of Driving	No. of Cases	Mean	Standard Deviation	COV	Resistance Factors for a given Reliability Index, β		
							2.0	2.5	3.0
Dynamic Equations	ENR	General	384	1.602	1.458	0.910	0.33	0.22	0.15
	Gates	*General*	384	1.787	0.848	0.475	0.85	0.67	0.53
	FHWA Modified Gates	General	384	0.940	0.472	0.502	0.42	0.33	0.26
		EOD	135	1.073	0.573	0.534	0.45	0.35	0.27
		EOD Bl. Ct. < 4BPI	62	1.306	0.643	0.492	0.60	0.47	0.37
WEAP		*EOD*	99	1.656	1.199	0.724	0.48	0.34	0.25

Notes: EOD = End of Driving; BOR = Beginning of Restrike; Bl. Ct. = Blow Count;
ENR = Engineering News Record Equation; BPI = Blows Per Inch; COV = Coefficient of Variation;
Mean = ratio of the static load test results (Davisson's Criterion) to the predicted capacity = $K_{SX} = \lambda$ =bias

1.7 DYNAMIC METHODS OF ANALYSIS USING DYNAMIC MEASUREMENTS

1.7.1 Overview

Dynamic measurements allow to obtain stresses and strains at the pile top following the hammer impact. Processing the obtained data allows to calculate the force and velocity signals with time and, hence, calculate the energy delivered to the pile's top and other relevant parameters (e.g. maximum and final pile top displacement).

Methods of analysis that require dynamic measurements can be broadly categorized as those that utilize a simplified analysis of instantaneous pile capacity evaluation for each hammer blow and those that require elaborate calculations (e.g. signal matching) traditionally carried out in the office. One relevant method of each category is described below and evaluated as part of this research study.

1.7.2 The Energy Approach

The Energy Approach uses basic energy relations (presented in section 1.6.3, equation 1.20) in conjunction with dynamic measurements to determine pile capacity. The concept was first presented by Paikowsky (1982) and was examined on a limited scale by Paikowsky and Chernauskas (1992). Extensive studies of the Energy Approach method were carried out by Paikowsky et al. (1994), Paikowsky and LaBelle (1994), and Paikowsky and Stenersen (2000). The underlying assumption of this approach is the balance of energy between the total energy delivered to the pile and the work done by the pile/soil system with the utilization of measured data. The basic Energy Approach equation is:

$$R_u = \frac{E_{\max}}{Set + \frac{(D_{\max} - Set)}{2}} \qquad (1.40)$$

where R_u = maximum pile resistance, E_{max} = measured maximum energy delivered to the pile, D_{max} = measured maximum pile top displacement, and Set = permanent displacement of the pile at the end of the analyzed blow, or 1/measured blow count. For further details regarding the Energy Approach method see Paikowsky et al. (1994) and Paikowsky (1995).

1.7.3 Signal Matching Analysis

The signal matching technique is often referred to as postdriving analysis or the office method. With the availability of faster, portable computers, it became reasonably simple to conduct the analysis in the field, though it is not a field method analysis as it cannot be carried out for each blow during driving. The response of the modeled pile-soil system (e.g., force at the pile top) under a given boundary condition (e.g., measured velocity at the pile top) is compared to the measured response (force measured). The modeled pile-soil system or, more accurately, the modeled soil that brings about the best match (visual graphical match) between the calculated and measured responses, is assumed to represent the actual soil resistance. The static component of that resistance is assumed to be the pile's capacity and reflects that time of driving. The signal matching procedure was first suggested by Goble et al. (1970), utilizing the computer program CAPWAP. Others developed similar analyses, (e.g., Paikowsky 1982; Paikowsky and Whitman 1990) utilizing the computer code TEPWAP. The TNO program was developed by Middendorp and van Weel (1986), which led to improvements and to the CAPWAPC program, which in its modified forms, is used to date.

1.8 RESEARCH STRUCTURE AND EXECUTION

1.8.1 Summary of Research Structure

The research is centered on the development of databases containing case histories of driven piles, statically load tested to failure, relevant to Mn/DOT practices. The databases are used to investigate Mn/DOT dynamic pile formula, as well as others, and establish the statistical parameters of the methods' uncertainty. The obtained results along with established target reliability, load distributions and load factors are then used for developing resistance factors to be used with the dynamic equations. Independent development of Mn/DOT alternative dynamic formula is presented and proposed.

1.8.2 Task Outline for the Research Execution

Task 1 – Establish Mn/DOT State of Practice Data relevant to the subsurface conditions and practices of substructure design and construction in Minnesota are collected and summarized. This ensures the relevance of the pile performance database (see Task 2) to the needs of Mn/DOT. In developing the state of design and practice use is made of the following: (1) a detailed questionnaire distributed as part of NCHRP project 12-66 (Paikowsky and Canniff, 2004) and completed by Mr. Dave Dahlberg of the Mn/DOT, and (2) review of local construction records, interviews of contractors, designers and DOT personnel.

Task 2 – Database Compilation A database compiled at UML (PD/LT 2000) is modified to a new database (Mn/DOT/LT 2008) in order to address the specific needs of MN. The required actions include: (1) review of all cases and eliminating unrelated data, (e.g pile types, sizes, soil conditions etc. not relevant to Mn/DOT practices) (2) searching original reports for the construction details required for the proposed research (3) updating database Mn/DOT/LT 2008.

Task 3 – Database Analyses All relevant cases are analyzed using at least four different dynamic equations, including: (1) Mn/DOT equation, (2) FHWA modified Gates (3) ENR and, (4) WA DOT. All results related to the piles' static capacity based on Davisson's failure criterion and statistical parameters of mean and bias of the ratios are evaluated for each method. In addition, (a) in depth evaluation of the Mn/DOT equation is carried out as to uncertainty and possible improvements, and (b) independent analysis of the data including sub categorization based on driving resistance, End of Driving vs. Beginning of Restrike, pile and soil types, etc. are performed.

Task 4 – LRFD Calibration The statistical parameters calculated in Task 3 are used along with the target reliability, load distribution and load factors used in NCHRP 24-17 (for the AASHTO deep foundations, Paikowsky et al., 2004) to calculate the appropriate resistance factors using MC method of analysis.

Task 5 – Methodology Evaluation Provided that Task 3 yields a significant database for statistical analysis, an independent control group can be assembled from additional case histories not included in Mn/DOT/LT 2008. These cases are used for independent evaluation of the factors recommended in Task 4. This task may include work on possible load test program carried out by the Mn/DOT.

Task 6 – Final Report

A final report and a presentation of results, including the details of the analyses and recommended resistance factors, is prepared. Presentation of results in the Mn/DOT is expected as part of the scope of the project included in the final report.

1.9 MANUSCRIPT OUTLINE

Background information dealing with the project, LRFD calibration and dynamic analyses is presented in Chapter 1. Chapter 2 establishes the Mn/DOT state of practice, being in line with Task 1. The developed databases and their investigations are presented in Chapter 3 being in line with Task 2. Chapter 3 follows the various stages of databases developments and their relevance to Mn/DOT practices. Chapter 4 presents the first stage analysis of the databases aimed at investigating the uncertainty of the different dynamic equations. The second stage of the analysis of the databases involves sub-categorization based on hammer type and energy level and is presented in Chapter 5. Both Chapters 4 and 5 relate to Tasks 3 and 4 as the analyses presented followed by LRFD calibrations. Chapter 6 presents the development of an independent Mn/DOT dynamic equation and its evaluation. Chapter 7 compares different methods' performance including those based on dynamic measurements. Chapter 8 summarizes the findings and presents the recommendations of this research study.

CHAPTER 2 ESTABLISH MN/DOT STATE OF PRACTICE

2.1 OBJECTIVES AND METHOD OF APPROACH

Data relevant to the subsurface conditions and practices of substructure design and construction in Minnesota were collected and summarized. This compilation of data ensures the relevance of the pile performance database to the needs of the Mn/DOT. The following steps were used in developing the state of design and practice: (1) a detailed questionnaire distributed as part of NCHRP project 12-66 (Paikowsky, 2004) and completed by Mr. Dave Dahlberg of the Mn/DOT, (2) review of Mn/DOT bridge construction manual, and (3) review of local construction records of 28 bridges, interviews of contractors, designers and DOT personnel.

2.2 SUMMARY OF PREVIOUS SURVEY

The following major findings are summarized based on the survey conducted as part of project NCHRP 12-66 and completed by Engineer David Dahlberg in August 2004.

1. In 2003: 33 bridges built, and 66 bridges rehabilitated.
   In 1999-2003, 66 bridges built, 269 bridges rehabilitated
2. Bridge types: 50% multi-span simple supported (mostly prestressed girders), 17% multi-span continuous, 24% single-span simple supported, 9% integral abutment (simple and multi-span).
3. Most abutments are semi-stub and most piers are column bent.
4. Mn/DOT is using driven piles as 85% of the bridge foundations.
5. Batter piles are the preferable choices for withstanding lateral loads with batter between 1H:6V to 1H:4V.
6. Most piers (95%) are supported by 5 or more driven piles.

2.3 INFORMATION GATHERED FROM THE MN/DOT BRIDGE CONSTRUCTION MANUAL (2005)

2.3.1 Piles and Equipment

1. Steel piles are most often used as driven piles, H piles, most commonly HP 10x42 and HP 12x53 are mentioned.
2. Precast Presstressed Concrete Piles (PPC) are rarely used.
3. Drop hammers and S/A steam/air hammers are rarely used. D/A hammers are also used with unknown frequency. Guidelines for ram weight and drop heights are provided.
4. Diesel hammers are the pile driving hammers of choice with the common types being MKT, ICE and Delmag.
5. Swinging leads are the most common crane set-up for pile driving.

2.3.2 Inspection and Forms

1. Clear guidelines for pile driving inspection are provided including the need to obtain the mill shipping papers and the material tests required if those are missing.
2. A detailed list of inspection requirements is provided in the manual under "MAKE CERTAIN", p. 5-393.162(2) calling for high quality detailed inspection and data gathering.
3. A pile and driving equipment data form is provided in the manual (Figure A J-393, 161) for the information collection as used in the WE analysis.
4. A detailed overview of ASD and LRFD principles is provided along with:
   a. Examples of load calculations and determination of required nominal pile bearing resistance (R_n)
   b. A practical suggestion to review the "Construction Notes" on the first sheet of the bridge plans (see p. 5-393.160(2)) and if the foundations were designed using LRFD methodology, the following note will appear "The pile load shown in the plans and the corresponding bearing capacity (R_n) was compiled using LRFD methodology."

2.3.3 Testing and Calculations

1. Indicator piles (termed Test Piles) are required with clear guidelines for high quality supervisions.
2. Test pile reports are completed on standardized forms with completed examples provided in the manual (Figures A, B, E, and F on p. 5-393-105).
3. Pile redriving (restriking) is clearly explained and outlined. Examples of test pile and pile driving reports that incorporate pile redrives are provided (Figures M, N, and O on p. 5-393.165).
4. Evaluation of safe pile capacity (safety margins included) is provided via pile driving formulas (section 5-393.160), formulated for both ASD and LRFD.
5. Pile load tests – Though general practice suggests relying on dynamic formulas, detailed guidelines of static pile load tests are provided including:
   a. Form for a pile load test data (Figure A p.5-393.167)
   b. Examples of presentation and analyses of pile load test data (Figures B, and C p. 5-393.167).

2.4 REQUIRED ADDITIONAL INFORMATION FOR CURRENT STUDY

1. Type and frequency of piles and driving equipment used in Mn/DOT projects.
2. Typical soil profiles.
3. Preferable combinations of typical soil profile, pile type, design load, driving equipment, end of driving, restrike and redrive criteria.

2.5 METHOD OF APPROACH

2.5.1 Contractors

1. Identify all major pile driving contractors performing pile driving for the Mn/DOT projects.
2. Meet the major contractors, phone interview the smaller contractors and review with them using a questionnaire:
   a. Details of equipment and construction methods used; specifically:
      i. hammers used (manufacturer, year, size, typical setting)
      ii. driving systems (cushions, capblocks, etc.)
      iii. are vibratory hammers being used? If so, to what stage prior to driving? What equipment do they use?
      iv. how often do they use preboring and their experience with it, especially to what depth do they typically prebore relative to final tip penetration
      v. how often to they use jetting and their experience with it, especially to what depth do they typically jett relative to final tip penetration.
   b. Their preferable driving practices assuming they determine the piles and equipment (i.e. assuming value engineering is allowed and proposed by them) considering hammer/pile combination including, if possible, range of loads.

2.5.2 DOT

1. Review with DOT senior Geotechnical personnel the following: (i) best ways to go about achieving our goals, and (ii) what projects do they suggest us to look at. Make sure to include (i) projects with most recent practices (on the order of a 1-year period), and (ii) projects containing most valuable and detailed data (dynamic measurements, static load tests, etc.).
2. Compile a project and pile case list, the more cases we have, the better, but not less than say 40 piles and at least 20 piles for each pile type (e.g. H Piles, Pipe piles--differentiating between open and closed ended, etc.) on at least 10 different project sites.
3. Once a list of projects is compiled; identify for each project:
   a. Original design pile type, size, design load
   b. Subsurface conditions, typical boring logs, subsurface cross-sections
   c. As built pile type size, design load
   d. Equipment used in construction
   e. Construction details, jetting, predrilling, vibrating depths, etc.
   f. Criteria for stop driving (penetration, blow count, refusal, etc.), specify restrike and redrive cases.
   g. Monitoring type and quality: observation of resistance (blow counting), saximeter data, dynamic measurements, static load tests, etc.
   h. Frequency of damage identification and type (pile breakage).
   i. For completeness of the above, gather the aforementioned Mn/DOT Bridge Construction Manual forms as much as possible; e.g. pile and driving equipment

data forms, test pile reports, pile capacity evaluation, WEAP submittal, geotechnical reports, etc.

4. In case of difficulties, best to consult the DOT's Project Engineer for the specific site.

2.6 FINDINGS

2.6.1 Mn/DOT – Details of Selected Representative Bridges

Table 2.1 provides details of bridge names, locations, bridge type, number of spans, total length and width of the bridge, type of construction, and the year the bridge was completed. The 28 projects were selected by Mn/DOT personnel and represent the most typical design and practices over the past four years. Table 2.1A provides the bridge construction classification used for the categorization of Table 2.1.

Table 2.2 provides the soil conditions and pile type with pile size details of the selected representative bridges.

Appendix A provides the foundation construction details of the selected representative bridges including indicator piles driving resistance, etc.

Table 2.3 provides a summary of the side and tip soil strata for each of the different pile types for each bridge, final energy of the pile driving hammer, final set of the pile, and evaluation of capacity using the Mn/DOT formula.

Table 2.4 provides a summary for each project including pile type, number of piles, average and total pile length, design load and total load. In developing the loading per pile for projects designed in the Allowable Stress Design Methodology (ASD), the ratio of the factor of safety to resistance factor, F.S.=1.4167/ϕ was implemented (Paikowsky, 2004). As such, the design load was substituted by its LRFD factored load in the following way:

$$\text{Factored Load (LRFD)} = 1.4167 \times \text{Design Load (ASD)} \quad (2.1)$$

For example, Bridge #34027 (Case #5, Table 2.3), design load per pile was calculated as the total load divided by the number of piles. In this case, the total ASD load was 1800 + 1800 + 2688 + 2688 = 8,976kips carried by 96 CEP 12x0.25 inch piles. This results in an average pile load of 93.5kips (ASD) = 132.5kips (LRFD). The value 132.5kips appears in Table 2.4, third entry.

2.6.2 Contractors Survey

Appendix B presents three surveys completed by various pile driving contractors from the State of Minnesota, providing detailed answers of available equipment and pile driving practices and preferences.

2.7 SUMMARY OF DATA

2.7.1 Summary Tables

Tables 2.5 to 2.8 present a summary and statistical analyses of the 28 selected bridge projects. Table 2.5 summarizes the range of pile length, average pile length, total load and average load per pile categorized according to pile type. For example, the data of Table 2.5

suggests that the most commonly used pile (40%) was a CEP 12” x 0.25” with an average length of 70 ft and an average design (factored) load of 155 kips.

Table 2.1 Mn/DOT - Details of Selected Representative Bridges

Case No.	Bridge Name	MN Bridge Number	Bridge Type	Notation	# of Spans	Span Lengths (ft)	Total Length (ft)	Width (ft)	Construction Type	Year Built
1	Ramp 35W to TH 62	27V66	Continuous, multi-span	MS-C	3	150,200,150	509	34	Precast segmental box	2007
2	TH 121 to TH 62	27V69	Simple, multi-span	MS-S	2	65,80	145	25-33	Prestressed concrete beams	2007
3	Ramp 35W to TH 62	27V73	Continuous, multi-span	MS-C	3	120,170,120	419	33	Precast segmental box	2007
4	Ramp Over Nicollet Ave.	27V75	Continuous, multi-span	MS-C	6	120,200,200, 200,200,120	1089	43	Precast segmental box	2007
5	TH 62 Over Nicollet Ave.	27V78	Simple, single-span	SS-S	1	85	85	55	Prestressed concrete beams	2007
6	Ramp over 35W / TH 62	27V79	Continuous, multi-span	MS-C	7	110,180(x5),110	1159	45	Precast segmental box	2007
7	Diamond Lake Road	27V84	Continuous, multi-span	MS-C	2	103,103	208	70	Steel plate girders	2007
8	TH 59 over CPRR	03009	Simple, multi-span	MS-S	5	43,73,50,73,55	298	89	Prestressed concrete beams	2007?
9	Zumbro River	25027	Continuous, multi-span	MS-C	3	55,66,66	187	53	Prestressed rect. concrete beams	2004
10	TH 23 over TH 71	34027	Simple, multi-span	MS-S	3	51,103,51	215	45	Prestressed concrete beams	2005
11	CSAH 9 over TH 23	34028	Simple, multi-span	MS-S	2	113,113	230	61	Prestressed concrete beams	2003
12	TH 23 over Nest Lake	34013	Simple, multi-span	MS-S	2	78,78	160	108	Prestressed concrete beams	2003
13	TH 171 over Red River	35010	Continuous, multi-span	MS-C	7	65,78(x5),65	520	43	Steel beams	2006
14	TH 75 over Two Rivers	35012	Simple, multi-span	MS-S	2	72,72	149	48	Prestressed concrete beams	2006
15	TH 15 over Crow River	43016	Simple, multi-span	MS-S	3	52,80,52	188	101	Prestressed concrete beams	2005
16	TH 371 over CSAH 46	49037	Simple, multi-span	MS-S	3	55,88,55	199	46	Prestressed concrete beams	2005
17	TH 371 over CSAH 46	49038	Simple, multi-span	MS-S	3	55,88,55	199	46	Prestressed concrete beams	2005
18	TH 371 over CSAH 47	49039	Simple, multi-span	MS-S	3	55,90,55	202	46	Prestressed concrete beams	2005
19	TH 371 over CSAH 47	49040	Simple, multi-span	MS-S	3	55,90,55	202	46	Prestressed concrete beams	2005
20	48th Street over TH 63	55068	Simple, multi-span	MS-S	2	115,115	236	104	Prestressed concrete beams	2003
21	TH 63 over Willow Creek	55073	Continuous, multi-span	MS-C	3	36.5,44.0,36.5	120	~80	Concrete Slab	2004
22	Woodlake Dr. over Willow Creek	55075	Continuous, multi-span	MS-C	3	36.5,44.0,36.5	120	57	Concrete Slab	2003
23	35E Ramp over TH 694	62902	Continuous, multi-span	MS-C	9	125.5,155,270, 258,219,219, 219,260,192.5	1928	52	Steel plate girders	2006
24	TH 22 over Horseshoe Lake	73035	Simple, multi-span	MS-S	4	56,57,57,56	229	43	Prestressed concrete beams	2006
25	TH 14 over CSAH 60	81003	Simple, multi-span	MS-S	2	145,145	297	46	Prestressed concrete beams	2004
26	TH 14 over CSAH 60	81004	Simple, multi-span	MS-S	2	145,145	297	46	Prestressed concrete beams	2004
27	CSAH 3 over TH 14	81005	Simple, multi-span	MS-S	2	107,107	220	65	Prestressed concrete beams	2004
28	TH 74 over Whitewater River	85024	Simple, multi-span	MS-S	2	84,84	169	43	Prestressed concrete beams	2006

Table 2.1A MN Bridge Construction Classification of Details

Bridge Type	Superstructure Type	
1	**2**	3
Multispan Simple Supported	**Steel Girders**	Multiple Beam/Girders
		Box Girders
	Concrete	Prestressed Girders
		CIP Box Girders
		Concrete Slab
Multispan Continuous	**Steel Girders**	Multiple Beam/Girders
		Box Girders
	Concrete	Prestressed Girders
		CIP Box Girders
		Concrete Slab
Single Span Simple 1.1.1.1.1.1	**Steel Girders**	Multiple Beam/Girders
		Box Girders
	Concrete	Prestressed Girders
		CIP Box Girders
		Concrete Slab

Bridge Type	Superstructure Type	
1	2	3
Integral Abutment Simple Span	**Steel Girders**	Multiple Beam/Girders
		Box Girders
	Concrete	Prestressed Girders
		CIP Box Girders
		Concrete Slab
Integral Abutment Multispan	**Steel Girders**	Multiple Beam/Girders
		Box Girders
	Concrete	Prestressed Girders
		CIP Box Girders
		Concrete Slab
Specify Others if Relevant to New Design		

Typical Mn/DOT construction practice:

1. Multi-span simple supported prestressed concrete girders bridge with a typical span of 100ft semi-stub abutment and column bent pier.
2. Single-span simple supported prestressed concrete girders bridge with a typical span of 100ft (up to 150ft) semi-stub abutment.
3. Multi-span continuous steel girders with a typical span of 120ft semi-stub abutment and column bent pier.
4. Multi-span integral abutment bridges steel girders with a typical span of 100ft and prestressed concrete girders with a typical span of 50ft, pile supported integral abutment and pile bent with encasement wall piers

Notes:

2

A. Abutment Type	
A1	Gravity
A2	U
A3	Cantilever
A4	Full Height
A5	Stub
A6	Semi Stub
A7	Counter Fort
A8	Pile Bent
A9	Reinforced Earth System
A10	Spill-through
A11	Pile Supported Integral
A12	Others, please specify

B. Bearing Type	
B1	Elastomeric Bearings
B2	Seismic Isolaters
B3	Rocker Bearings
B4	Roller Bearings
B8	Siding Plate Bearing
B6	Pot Bearing
B7	Spherical Bearing
B8	Lead Rubber
B9	Others, please specify

1	C. Bearing Function
C1	Fixed Allows Rotation only
C2	Expansion Allows Rotation and Horizontal Translation
C3	Expansion allows Rotation and Vertical + Horizontal Translation

D. Pier Type	
D1	Hammerhead S/M
D2	Column Bent
D3	Pile Bent
D4	Solid Wall
D5	Integral Pier
D6	Others, please specify

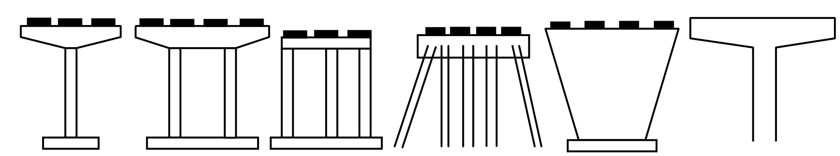

D1S (single column) D1M (multi column) D2 D3 D4 D5

Table 2.2 Mn/DOT Foundation Details of Selected Representative Bridges

Case No	Bridge Name	MN Bridge No.	General Soil Condition									Foundation Type		Foundation Size						
			Abutments				Piers					Abut-ments	Piers	Abutments		Piers				
			Desig-nation	Soil	Desig-nation	Soil	1	2	3	4	5					1	2	3	4	5
1	Ramp 35W to TH 62	27V66	North Abut	Sand	South Abut	Sand	Sand	Sand	-	-	-	CIPC Pipe	CIPC Pipe	North 16" CIPC 5/16" Wall 30 piles 70 ft long	South 16" CIPC 5/16" Wall 34 piles 80 ft long	16" CIPC 5/16" Wall 30 piles 80 ft long	16" CIPC 5/16" Wall 30 piles 70 ft long	-	-	-
2	TH 121 to TH 62	27V69	West Abut	Loose Sand	East Abut	Loose Sand, Clay	Peat, Sand	-	-	-	-	CIPC Pipe	CIPC Pipe	West 12" CIPC 1/4" Wall 12 piles (+5 wingwall) 70 ft long	East 12" CIPC 1/4" Wall 11 piles (+4 wingwall) 80 ft long	12" CIPC 1/4" Wall 18 piles 80 ft long	-	-	-	-
3	Ramp 35W to TH 62	27V73	West Abut	Loose Sand	East Abut	Fine Sand, Gravel	Loose Sand	Fine Sand, Gravel	-	-	-	H-Pile	H-Pile	West HP 14x73 23 piles 55 ft long	East HP 14x73 33 piles 50 ft long	HP 14x73 20 piles 50 ft long	HP 14x73 20 piles 50 ft long	-	-	-
4	Ramp Over Nicollet Ave.	27V75	West Abut	Fine Sand, Org.	East Abut	Fine Sand, Org.	Fine Sand, Gravel	Fine Sand, Gravel	Fine Sand, Gravel	Fine Sand, Gravel	Fine Sand, Gravel	CIPC Pipe	CIPC Pipe	West 16" CIPC 5/16" Wall 56 piles 65 ft long	East 16" CIPC 5/16" Wall 42 piles 70 ft long	16" CIPC 5/16" Wall 36 piles 65 ft long	16" CIPC 5/16" Wall 40 piles 65 ft long	16" CIPC 5/16" Wall 45 piles 70 ft long	16" CIPC 5/16" Wall 40 piles 70 ft long	16" CIPC 5/16" Wall 40 piles 70 ft long
5	TH 62 Over Nicollet Ave.	27V78	West Abut	Fine Sand, Gravel	East Abut	Fine Sand, Gravel	-	-	-	-	-	CIPC Pipe	CIPC Pipe	West 16" CIPC 1/4" Wall 34 piles 60 ft long	East 16" CIPC 1/4" Wall 34 piles 60 ft long	-	-	-	-	-
6	Ramp over 35W / TH 62	27V79	East Abut	Loose Sand, Fine Sand, some Clay	West Abut	Fine Sand, Gravel	Loose Sand, Fine Sand	Loose Sand, Fine Sand	Loose Sand, Fine Sand	Loose Sand, Fine Sand, Gravel	Loose Sand, Fine Sand, Gravel	CIPC Pipe	CIPC Pipe	East 16" CIPC 5/16" Wall 24 piles 40 ft long	West 16" CIPC 5/16" Wall 43 piles 70 ft long	16" CIPC 5/16" Wall 36 piles 30 ft long	16" CIPC 5/16" Wall 36 piles 30 ft long	16" CIPC 5/16" Wall 45 piles 75 ft long	16" CIPC 5/16" Wall 38 piles 65 ft long	16" CIPC 5/16" Wall 36/36 piles 60/60 ft long
7	Diamond Lake Road	27V84	West Abut	Loose Sand, Sand and Gravel, some Clay	East Abut	Loose Sand, Sand and Gravel, some Clay	Loose Sand, Sand and Gravel, some Clay	-	-	-	-	CIPC Pipe	CIPC Pipe	West 12" CIPC 1/4" Wall 64 piles 60 ft long	East 12" CIPC 1/4" Wall 44 piles 60 ft long	12" CIPC 1/4" Wall 36 piles 65 ft long	-	-	-	-
8	TH 59 over CPRR	03009	West Abut	Clay, Sand and Gravel	East Abut	Sand and Gravel, Loose Sand	Sand and Gravel, Sand, Clay	Sand and Gravel, Sand, Clay	Sand and Gravel, Sand, Clay	Sand and Gravel, Sand, Clay	-	CIPC Pipe	CIPC Pipe	West 12" CIPC 1/4" Wall 15 piles 80 ft long	East 12" CIPC 1/4" Wall 25 piles 50 ft long	12" CIPC 1/4" Wall 34 piles 100 ft long	12" CIPC 1/4" Wall 34 piles 120 ft long	12" CIPC 1/4" Wall 34 piles 120 ft long	12" CIPC 1/4" Wall 34 piles 120 ft long	-

Table 2.2 Mn/DOT Foundation Details of Selected Representative Bridges (Cont. page 2/4)

Case No	Bridge Name	MA Bridge No.	General Soil Condition									Foundation Type		Foundation Size						
			Abutments				Piers					Abut-ments	Piers	Abutments		Piers				
			Desig-nation	Soil	Desig-nation	Soil	1	2	3	4	5/6					1	2	3	4	5/6
9	Zumbro River	25027	South Abut	Sand and Gravel, Sand-stone	North Abut	Loamy Sand, Loam, Sand-stone	Sand and Gravel, Sand-stone	Sand and Gravel, Sand-stone	-	-	-	H-pile	H-Pile	South HP 10x42 19 piles 55 ft long	North HP 10x42 21 piles 30 ft long	HP 10x42 11 piles 55 ft long	HP 10x42 11 piles 55 ft long	-	-	-
10	TH 23 over TH 71	34027	West Abut	Sand and Gravel, Sand	East Abut	Sand and Gravel, Sand, Loamy Sand	Sand, Sand and Gravel, Sandy Loam	Sand and Gravel, Sand, Loamy Sand	-	-	-	CIPC Pipe	CIPC Pipe	West 12" CIPC 1/4" Wall 20 piles 60 ft long	East 12" CIPC 1/4" Wall 20 piles 65 ft long	12" CIPC 1/4" Wall 32 piles 40 ft long	12" CIPC 1/4" Wall 32 piles 40 ft long	-	-	-
11	CSAH 9 over TH 23	34028	South Abut	Sand and Gravel, Sand	North Abut	Sand and Gravel, Sand	-	-	-	-	-	CIPC Pipe	-	South 12" CIPC 1/4" Wall 29 piles 20 ft long	North 12" CIPC 1/4" Wall 29 piles 20 ft long	-	-	-	-	-
12	TH 23 over Nest Lake	34013	South Abut	Sandy Loam, Sandy Clay, Sand and Gravel	North Abut	Sandy Loam, Loamy Sand, Peaty Marl	Sand and Gravel, Sandy Loam, Silty Loam	-	-	-	-	CIPC Pipe	CIPC Pipe	South 12" CIPC 1/4" Wall 40 piles 55 ft long	North 12" CIPC 1/4" Wall 39 piles 75 ft long	* * * 16" CIPC 1/4" Wall 18 piles 65 ft long	-	-	-	-
13	TH 171 over Red River	35010	West Abut	Clay, Silty Clay, Fat Clay	East Abut	Silty Clay, Clay	Silty Clay, Clay	Silty Clay, Clay	Silty Clay, Clay	Silty Clay, Clay	Silty Clay, Clay	CIPC Pipe	CIPC Pipe	West 12" CIPC 1/4" Wall 10 piles 175 ft long	East 12" CIPC 1/4" Wall 10 piles 175 ft long	* * * 16" CIPC 1/4" Wall 8 piles 185 ft long	* * * 16" CIPC 1/4" Wall 8 piles 185 ft long	* * * 16" CIPC 1/4" Wall 8 piles 185 ft long	* * * 16" CIPC 1/4" Wall 8 piles 185 ft long	* * * 16" CIPC 1/4" Wall 8/8 piles 185/185 ft long
14	TH 75 over Two Rivers	35012	South Abut	Clay Loam, Clay, Loamy Sand, Fat Clay	North Abut	Org, Silty Clay, Fat Clay, Loamy Sand	No info.	-	-	-	-	CIPC Pipe	CIPC Pipe	South 12" CIPC 1/4" Wall 7 piles 125 ft long	North 12" CIPC 1/4" Wall 7 piles 125 ft long	* * * 16" CIPC 3/8" Wall 7 piles 125 ft long	-	-	-	-
15	TH 15 over Crow River	43016	South Abut	Loamy Sand, Sandy Loam, Loam	North Abut	Loamy Sand, Sandy Loam	Loamy Sand, Sandy Loam	Loamy Sand, Sandy Loam	-	-	-	CIPC Pipe	CIPC Pipe	South 12.75" CIPC 5/16" Wall 28 piles 40 ft long	North 12.75" CIPC 5/16" Wall 28 piles 40 ft long	12.75" CIPC 5/16" Wall 30 piles 25 ft long	12.75" CIPC 5/16" Wall 30 piles 25 ft long	-	-	-

Table 2.2 Mn/DOT Foundation Details of Selected Representative Bridges (Cont. page 3/4)

Case No	Bridge Name	MN Bridge No.	General Soil Condition									Foundation Type		Foundation Size						
			Abutments				Piers					Abut-ments	Piers	Abutments		Piers				
			Desig-nation	Soil	Desig-nation	Soil	1	2	3	4	5					1	2	3	4	5
16	TH 371 over CSAH 46	49037	South Abut	Sand, Sand and Gravel, Phyllite	North Abut	Sand, Sand and Gravel, Phyllite	Sand, Sand and Gravel, Phyllite	Sand, Sand and Gravel, Phyllite	-	-	-	H-Pile	H-Pile	South HP 10x42 8 piles 65 ft long	North HP 10x42 8 piles 65 ft long	* * * HP 12x53 16 piles 40 ft long	* * * HP 12x53 16 piles 40 ft long	-	-	-
17	TH 371 over CSAH 46	49038	South Abut	Org. Loam, Sand, Sandy Loam, Phyllite	North Abut	Org. Silty Loam, Sand, Silty Loam, Phyllite	Loamy Sand, Sand, Silty Loam, Phyllite	Org. Sandy Loam, Sand, Sandy Loam, Phyllite	-	-	-	H-Pile	H-Pile	South HP 10x42 8 piles 70 ft long	North HP 10x42 8 piles 70 ft long	* * * HP 12x53 16 piles 45 ft long	* * * HP 12x53 16 piles 45 ft long	-	-	-
18	TH 371 over CSAH 47	49039	South Abut	Sand, Sandy Loam, Silty Loam, Schist	North Abut	Sand, Sandy Loam, Clayey Shale, Phyllite	Sand, Sandy Loam, Clayey Shale, Phyllite	Sand, Sandy Loam, Phyllite	-	-	-	H-Pile	H-Pile	South HP 10x42 8 piles 45 ft long	North HP 10x42 8 piles 45 ft long	* * * HP 12x53 22 piles 30 ft long	* * * HP 12x53 22 piles 30 ft long	-	-	-
19	TH 371 over CSAH 47	49040	South Abut	Sand, Cobble, Loamy Sand, Loam, Phyllite	North Abut	Sand, Cobble, Silty Loam, Phyllite	Sand, Cobble, Sandy Loam, Phyllite	Sand, Cobble, Sandy Loam, Phyllite	-	-	-	H-Pile	H-Pile	South HP 10x42 8 piles 40 ft long	North HP 10x42 8 piles 40 ft long	* * * HP 12x53 22 piles 25 ft long	* * * HP 12x53 22 piles 25 ft long	-	-	-
20	48th Street over TH 63	55068	West Abut	Clay Loam, Clay, Lime-stone	East Abut	Sandy Clay, Silty Clay Loam, Lime-stone	Clay Loam, Silty Clay Loam, Lime-stone	-	-	-	-	H-Pile	H-Pile	West HP 12x53 44 piles 45 ft long	East HP 12x53 44 piles 45 ft long	HP 12x53 40 piles 35 ft long	-	-	-	-
21	TH 63 over Willow Creek	55073	South Abut	Loam, Sandy Loam, Sand w/ Gravel, Sand-stone	North Abut	No info.	Sand, Sandy Loam, Gravel, Sand, Loamy Sand	No info.	-	-	-	H-Pile	H-Pile	South HP 10x42 11 piles 50 ft long	North HP 10x42 10 piles 50 ft long	* * * HP 12x53 14 piles 55 ft long	* * * HP 12x53 14 piles 55 ft long	-	-	-
22	Woodlake Dr. over Willow Creek	55075	South Abut	No info.	North Abut	Loam, Sandy Loam, Loamy Sand, Sand-stone	Sandy Clay, Loamy Sand, Sand	Sandy Clay, Loamy Sand, Sand	-	-	-	H-Pile	H-Pile	South HP 10x42 7 piles 50 ft long	North HP 10x42 7 piles 50 ft long	* * * HP 12x53 10 piles 55 ft long	* * * HP 12x53 10 piles 55 ft long	-	-	-

Table 2.2 Mn/DOT Foundation Details of Selected Representative Bridges (Cont. page 4/4)

Case No	Bridge Name	MN Bridge No.	General Soil Condition									Foundation Type		Foundation Size						
			Abutments				Piers					Abut-ments	Piers	Abutments		Piers				
			Desig-nation	Soil	Desig-nation	Soil	1	2	3	4	5					1	2	3	4	5
23	35E Ramp over TH 694	62902	North Abut	Loamy Sand, Silty Loam, Sand, Sandy Clay	South Abut	Loamy Sand, Fine Sand, Sand, Sandy Loam	Pier1/2 Loam, Sand, Clay, Sandy Clay	Pier 3/4 Clay, Fine Sand, Sand, Loam	Pier 5/6 Clay, Silty Loamy Sand, Sand	Pier 7 Loamy Sand, Silty Clay, Sand	Pier 8 Sand, Clay, Sand and Gravel	CIPC Pipe	CIPC Pipe	North 12" CIPC 1/4" Wall 49 piles 90 ft long	South 12" CIPC 1/4" Wall 29 piles 65 ft long	Pier 1/2 * * * 16" CIPC 1/4" Wall 24/28 piles 70/60 ft long	Pier 3/4 * * * 16" CIPC 1/4" Wall 34/30 piles 60/90 ft long	Pier 5/6 * * * 16" CIPC 1/4" Wall 32/30 piles 60/70 ft long	Pier 7 * * * 16" CIPC 1/4" Wall 28 piles 50 ft long	Pier 8 * * * 16" CIPC 1/4" Wall 32 piles 70 ft long
24	TH 22 over Horseshoe Lake	73035	South Abut	Sand and Gravel, Fine Sand	North Abut	Gravel, Sand and Gravel, Silty Clay, Granite	Loamy Fine Sand, Sand, Loose Sand, Granite	No data.	Sand, Marl, Fine Sand, Silty Clay, Gravel	-	-	H-Pile	CIPC Pipe	South HP 10x42 6 piles 85 ft long	North HP 10x42 6 piles 85 ft long	* * * 20" CIPC 3/8" Wall 5 piles 100 ft long	* * * 20" CIPC 3/8" Wall 5 piles 100 ft long	* * * 20" CIPC 3/8" Wall 5 piles 100 ft long	-	-
25	TH 14 over CSAH 60	81003	North Abut	Silty Clay, Clay, Fine Sand, Silty Loam	South Abut	Clay, Clay Loam, Silty Loam, Sandy Loam	Clay Loam, Loamy Sand, Silty Loam, Sand	-	-	-	-	CIPC Pipe	CIPC Pipe	North 12" CIPC 1/4" Wall 45 piles 80 ft long	South 12" CIPC 1/4" Wall 41 piles 55 ft long	12" CIPC 1/4" Wall 36 piles 70 ft long	-	-	-	-
26	TH 14 over CSAH 60	81004	North Abut	Silty Clay, Clay, Fine Sand, Silty Loam	South Abut	Clay, Clay Loam, Silt, Sand and Gravel	Clay, Clay Loam, Sandy Loam, Sand	-	-	-	-	CIPC Pipe	CIPC Pipe	North 12" CIPC 1/4" Wall 41 piles 65 ft long	South 12" CIPC 1/4" Wall 41 piles 55 ft long	12" CIPC 1/4" Wall 36 piles 65 ft long	-	-	-	-
27	CSAH 3 over TH 14	81005	South Abut	Loam, Sandy Loam, Sand	North Abut	Loam, Sand, Loamy Sand	Loamy Sand, Loam, Clay Loam, Sand	-	-	-	-	CIPC Pipe	CIPC Pipe	South 12" CIPC 1/4" Wall 26 piles 60 ft long	North 12" CIPC 1/4" Wall 26 piles 50 ft long	12" CIPC 1/4" Wall 48 piles 50 ft long	-	-	-	-
28	TH 74 over Whitewater River	85024	West Abut	Sand and Gravel, Coarse Sand and Gravel	East Abut	Sand and Gravel, Coarse Sand and Gravel	Sand and Gravel, Coarse Sand and Gravel	-	-	-	-	H-Pile	H-Pile	West HP 10x42 10 piles 40 ft long	East HP 10x42 10 piles 40 ft long	* * * HP 12x53 9 piles 50 ft long	-	-	-	-

Table 2.3 Summary of Side and Tip Soil Strata

Case No.	Bridge	Pile Case Number	Pile Type	Length (ft)	Weight of Pile + Capblock (lbs)	Boring Used	Side	Tip	Hammer Type	Final Energy (lbs-ft)	Weight of Ram (lbs)	Final Set (in)	BPI	Mn/DOT Equation (kips)	Equation Variation
1	27V66	27V66-TP5	CEP 16"x.3125"	75	7063.88	B736	SL, CL, S, G	Sandstone	APE D30-42	52920	6615	0.125	8.0	915	None
2	27V66	27V66-TP7	CEP 16"x.25"	105	8184.5	B735	O,LS,S,L,S	Sand	APE D30-42	59535	6615	0.1	10.0	1047	None
3	27V75	27V75-TP5	CEP 16"x.3125"	90	7427.4	B707	O,S,LS,CL,S	Clay	APE D30-42	59535	6615	0.175	5.7	873	None
4	27V84	27V84-TP5	CEP 12"x.25"	62	3856	T337	S	Silt	APE 19-42	31425	4190	0.025	40.0	834	None
5	34027	34027-TP8	CEP 12"x.25"	70	4796	T1	S,G,S,M	Loamy Sand	Delmag D19-42	26700	4190	0.1	10.0	486	3.5E
6	35010	35010-TP1	CEP 12"x.25"	169	8708	C37	M	Clay	Delmag D30-32	58212	6615	0.1333	7.5	896	None
7	35010	35010-TP8	CEP 16"x.25"	171	10685	C32	M	Clay	Delmag D30-32	62800	6615	0.0423	23.6	1209	None
8	49037	49037-TP2	HP10x42	75	4670	B04	S,Phyllite	Phyllite	Delmag D25-32		5513			0	Unknown
9	49037	49037-TP3	HP12x53	50	4670	B03	S,G,M,Phyllite	Phyllite	Delmag D25-32		5513			0	Unknown
10	49040	49040-TP2	HP10x42	55	4330	B12	O,S	Metagraywacke	Delmag D25-32		5513			0	3.5E&.2M
11	49040	49040-TP6	HP12x53	50	4670	B10	O,S	Phyllite	Delmag D25-32	49617	5513	0.25	4.0	680	3.5E&.2M
12	55075	55075-TP8	HP10x42	51	3875	T4	O,S,LS	Sandstone	Delmag 19-32	33520	4190	0.125	8.0	615	3.5E&.2M
13	55075	55075-TP4	HP12x53	53	5200	ST17	O,S,C,S	Sandstone	Delmag 19-32	35615	4190	0.07	14.3	695	3.5E&.2M
14	81003	81003-TP4	CEP 12"x.25"	38	3902	T5	C,S	Sandy Loam	Delmag 19-32	31800	4190	0.1625	6.2	521	3.5E
15	85024	85024-TP1	HP10x42	55	5248	T4	S	Sand & Gravel	Delmag 19-32	32100	4190	0.125	8.0	518	3.5E&.2M
16	85024	85024-TP4	HP12x53	60	5695	T1	M,S	Sand & Gravel	Delmag 19-32	33520	4190	0.1	10.0	565	3.5E&.2M
17	27V69	27V69-TP3	CEP 12"x.25"	81	5079	B702	F,PT,S	Sand & Gravel	APE 19-42	23045	4190	0.48	2.1	180	None
18	27V78	27V78-TP4	CEP 16"x.25"	67	4483.5	T249	S	Loamy Sand	Delmag D25-32	55130	5513	0.163	6.1	951	None
19	03009	03009-TP1	CEP 12"x.25"	130	6255	T1	SG,C,S,C	Clay	Delmag D19-42	32263	4190	0.21	4.8	381	None
20	34028	34028-TP3	CEP 12"x.25"	28	4226	T1	LS,S	Sand & Gravel	Delmag D19-42	29000	4190	0.3	3.3	334	3.5E
21	35012	35012-TP2	CEP 12"x.25"	130	7140	T01	O,C,M	Sand & Gravel	Delmag D30-32	52920	6615	0.1965	5.1	747	None
22	35012	35012-TP3	CEP 20"x.375"	126	13516	T02	C,LS,M,S	Sand & Gravel	Delmag D30-32	58212	6615	0.096	10.4	817	None
23	49038	49038-TP1	HP10x42	67	4834	B08	LS,S,M	Phyllite	Delmag D25-32		5513			0	Unknown
24	49038	49038-TP3	HP12x53	38	4670	B07	O,S,M	Phyllite	Delmag D25-32		5513			0	Unknown
25	55068	55068-TP5	HP12x53	40	4405	ST15	S,MC,C	Limestone	Delmag D30-32	62842.5	6615	0.15	6.7	1207	3.5E&.2M
26	62902	62902-TP2	CEP 12"x.25"	48	3915	T3	L,M,C,S	Sandy Clay	Delmag D25-32	49617	5513	0.1	10.0	1088	3.5E
27	62902	62902-TP13	CEP 16"x.25"	68	6179	T103	L,S,M,C,SC	Loamy Sand	Delmag D30-32	52920	6615	0.1	10.0	1047	3.5E
28	81004	81004-TP4	CEP 12"x.25"	59	5157	T5	C,S,SL	Silty Clay Loam	Delmag D19-32	31425	4190	0.113	8.8	531	3.5E
29	27V73	27V73-TP3	HP14x73	51	7032	B726	S	Sandstone	APE D30-42	56227.5	6615	0.174	5.7	847	.2M
30	27V79	27V79-TP5	CEP 16"x.3125"	66	7430	B721	L,S	Loamy Sand	APE D30-42	62843	6615	0.2	5.0	864	None
31	25027	25027-TP2	HP10x42	54	4030	T1	S,C,S,SG	Sandstone	Delmag 19-42	33520	4190	0.2	5.0	492	3.5E&.2M
32	25027	25027-TP6	CEP 16"x.25"	53	5109	T3	SM,S,GS	Sandstone	Delmag D25-32	44104	5513	0.1125	8.9	840	3.5E
33	34013	34013-TP2	CEP 12"x.25"	47	4636	T3	S,C	Sand & Gravel	Delmag D19-32	29800	4190	0.075	13.3	600	3.5E
34	34013	34013-TP4	CEP 16"x.25"	59	5614	T2	S,C,M	Till	Delmag D19-32	31200	4190	0.025	40.0	706	3.5E
35	43016	43016-TP8	CEP 12.75"x.3125"	59	5403	B1	LS	Sandy Loam	Delmag D25-32	42100	5510	0.225	4.4	577	3.5E
36	49039	49039-TP1	HP10x42	47	4330	B16	S,M	Schist	Delmag D25-32	52345	5510				Unknown
37	49039	49039-TP5	HP12x53	40	4670	B14	S	Phyllite	Delmag D25-32		5510				Unknown
38	55073	55073-TP2	HP10x42	50	4010	T5	SL,SG	Sandstone	Delmag 19-32	29330	4190	0.18	5.6	454	3.5E&.2M
39	55073	55073-TP5	HP12x53	55	4935	ST18	SL,G,S	Sandstone	Delmag 19-32	31425	4190	0.1	10.0	565	3.5E&.2M
40	73035	73035-TP2	HP10x42	97	5640	T04	SG,S,SG	Gravel	Delmag DE50B	37140	5000	0.24	4.2	463	3.5E&.2M
41	73035	73035-TP8	CEP 20"x.375"	109	10506	T01	LS,S,M,SG,MC	Sand & Gravel	Delmag D30-02	55836	6600	0.1	10.0	874	3.5E
42	81005	81005-TP4	CEP 12"x.25"	41	3902	B2-3	G,L,CL	Loam	Delmag D25-32	49617	5513	0.2625	3.8	706	3.5E

Notes: G = gravel, S = sand, M = silt, C = Clay, L = loam, O = organics, F = fill

Table 2.4 Summary of Pile Type, Number and Length of Piles and loads per Project

Bridge	Pile Type	No. of Piles	Average Pile Length (ft)	Total Length Of Piles (ft)	Design Load Per Pile (kips)	Total Load (kips)	Range of Lengths (ft)	Comments
03009	CEP 12"x.25"	176	99.2	17465	175.4	30862	25 - 120	
34013	CEP 12"x.25"	79	63.3	4997.9	154.4	12201	40 - 85	2
34027	CEP 12"x.25"	96	82.8	7953.1	132.5	12716	33.6 - 130	2
34028	CEP 12"x.25"	58	33.9	1967.7	164.3	9532	30 - 50	2
35010	CEP 12"x.25"	20	173.3	3465	142.0	2840	150 - 185	
35012	CEP 12"x.25"	14	131.4	1840	186.0	2604	125 - 135	
62902	CEP 12"x.25"	78	76.7	5985	160.5	12515	*	1,2
81003	CEP 12"x.25"	122	49.0	5973	115.2	14054	35 - 80	
81004	CEP 12"x.25"	118	53.6	6326.8	112.4	13269	35 - 75	
81005	CEP 12"x.25"	100	46.0	4596.3	162.6	16264	34.2 - 70	2
27V69	CEP 12"x.25"	50	69.8	3488	188.0	9400	*	1
27V84	CEP 12"x.25"	144	67.01	9649.44	189.4	27280	60 - 82.5	
43016	CEP 12.75"x.3125"	116	51.1	5931	119.5	13864	35 - 65	
25027	CEP 16"x.25"	22	34.9	768.3	147.0	3235	25 - 70	
34013	CEP 16"x.25"	18	68.3	1230	512.6	9227	60 - 80	2
35010	CEP 16"x.25"	48	177.2	8505	258.0	12384	150 - 195	
62902	CEP 16"x.25"	238	61.8	14700	262.6	62499	*	1,2
27V66	CEP 16"x.25"	62	92.7	5749	246.0	15252	*	1
27V78	CEP 16"x.25"	53	62.8	3330	315.6	16728	60 - 70	
27V66	CEP 16"x.3125"	60	78.2	4690	264.0	15840	*	1
27V75	CEP 16"x.3125"	299	68.3	20410	260.9	78000	*	1
27V79	CEP 16"x.3125"	294	60.1	17658	229.3	67416	*	1
35012	CEP 20"x.375"	7	127.9	895	240.0	1680	125 - 135	
73035	CEP 20"x.375"	15	108.0	1620	197.4	2961	95 - 115	
25027	HP10x42	40	41.9	1675.5	99.8	3990	55 - 94	
49037	HP10x42	16	60.0	960	104.0	1664	*	1
49038	HP10x42	16	57.5	920	104.0	1664	*	1
49039	HP10x42	16	47.5	760	106.6	1706	*	1
49040	HP10x42	16	30.0	480	106.6	1706	*	1
55073	HP10x42	21	51.9	1090	142.3	2989	50 - 60	2
55075	HP10x42	14	56.4	790	144.5	2023	55 - 60	2
73035	HP10x42	12	94.2	1130	130.7	1568	90 - 100	
85024	HP10x42	20	55.3	1105	135.6	2712	55 - 58	
49037	HP12x53	32	36.5	1168	105.4	3372	*	1
49038	HP12x53	32	36.5	1168	105.4	3372	*	1
49039	HP12x53	44	30.9	1360	131.2	5772	*	1
49040	HP12x53	44	30.0	1320	131.2	5772	*	1
55068	HP12x53	128	40.9	5230	189.5	24251	30 - 55	2
55073	HP12x53	28	56.5	1582	185.6	5196	55 - 65	2
55075	HP12x53	20	57.0	1140	194.1	3882	55 - 65	2
85024	HP12x53	9	63.3	570	155.8	1402	60 - 75	
27V73	HP14x73	96	54.8	5262	209.2	20082	50 - 65	
Total		**2891**	**N/A**	**186904**	**N/A**	**555746**	**N/A**	

Note:
1. Lengths estimated using Mn/DOT design pile lengths
2. ASD projects: F.S. = 1.4167/ϕ was implemented (Paikowsky, 2004)

Table 2.5 Summary of Total Pile Length and Design Loads Per Pile Type

Pile Type	No. Of Piles	Total Length of Piles (ft)	% of Total Use	Range of Lengths (ft)	Average Pile Length +/- SD (ft)	Total Load (kips)	Average Load Per Pile (kips)
CEP 12"x.25"	1055	73707	39.4%	25 - 185	70 +/- 39.6	163536	155
CEP 12.75"x.3125"	116	5931	3.2%	35 - 65	51.1 +/- 0	13864	120
CEP 16"x.25"	441	34282	18.3%	25 - 195	77.7 +/- 49.7	119325	271
CEP 16"x.3125"	653	42758	22.9%	Note 1	65.5 +/- 9.1	161256	247
CEP 20"x.375"	22	2515	1.3%	95 - 135	114.3 +/- 14	4641	211
HP10x42	171	8911	4.8%	50 - 100	52.1 +/- 17.4	20022	117
HP12x53	337	13538	7.2%	30 - 75	40.2 +/- 13	53019	157
HP14x73	96	5262	2.8%	50 - 65	54.8 +/- 0	20082	209
Totals	**2891**	**186904**	**100.00%**	**N/A**	**avg = 66**	**555746**	**avg = 186**

Note:
1. Lengths estimated using Mn/DOT design pile lengths

Table 2.6 Summary of Indicator Pile Cases Categorized based on Soil Conditions

Soil Condition / Pile Location	Rock	Till	Sand & Gravel	Sand	Silt	Clay	Organics
Tip	17	1	9	7	1	6	1
Side	0	0	1	25	12	3	1

Note:
1. Total number of cases is 84 (for 42 piles see Table 2.3)

Table 2.7 Summary of Driving Criteria – Pile Performance

Drivng Resistance (BPI)	0 - 4	4 - 8	>8
Number of Indicator Piles	3	14	17
% of Cases	8.8	41.2	50.0

Note:
1. Number of cases is 34 as the blow count in some projects have not been reported

Table 2.8 Equipment Summary

Hammer Type	Maximum Energy (kips-ft)	Ram Weight (lbs)	No. of Projects Used	Total Pile Length Driven (ft)	% of Total Use	Weighted Average
Delmag D19-32	42.4	4000	10	24805	13.4%	9.3%
APE D19-42	47.1	4189	2	13137	7.1%	5.5%
Delmag D19-42	43.2	4010	4	29061	15.6%	11.1%
Delmag D30-02	66.2	6600	1	1620	0.9%	0.9%
Delmag D25-32	66.3	5510	13	28747	15.5%	16.8%
APE D30-42	70.1	6615	5	53769	28.9%	33.3%
Delmag D30-32	75.4	6610	6	34635	18.6%	23.1%
			41	185774	100%	100%

Notes:

1. The project count reflects total number of hammers used and is 42 as multiple hammers were used on various projects.
2. Percent of total use refers to number of projects, and weighted average refers to driven pile length excluding DE50B.

Table 2.6 summarizes the soil conditions along the skin and the pile's tip. For example, out of 42 indicator piles, 17 were driven to rock, 1 to till, and 16 to sand or sand & gravel, meaning that in 80% of the cases (34 out of 42) the piles were driven to a competent bearing layer.

The data are further examined by summarizing the driving resistance at the end of driving as presented in Table 2.7. In 50% of the cases (17 out of 34) the piles were driven to a blow count of or exceeding 8 bpi. Additional 40% were driven to a resistance between 4 to 8 bpi which is the range beyond "easy driving." The data matches quite well with that of Table 2.6 suggesting 90% of the piles were driven to resistance in a competent layer.

Table 2.8 and Figure 2.1 provide a summary of driving equipment used for the driving of the 42 indicator piles. All hammers are diesel hammers ranging in nominal energy from 42 to 75 kip-ft, with the most common hammer per project (13 out of 42) being the Delmag D25-32 and the most length driven using the APE D30-42 (28.8% of all pile length driven or 33.3% excluding DE50B for which exact specs are not available). About 75% of the piles were driven with hammers having nominal energy of about 70kips-ft (ranging from 66.2 to 75.4kip-ft) and ram weight of about 6,000lb (ranging from 5,500 to 6,600lb).

2.7.2 Contractors' Perspective

Appendix B contains the response to a questionnaire that was completed by three contractors familiar with Mn/DOT construction practices. The pile driving hammers available to the contractors are overall diesel hammers ranging in energy according to what was presented in Table 2.8. Other details match well with the data presented in Table 2.5 to 2.7. It seems like jetting is rarely used and pile penetration using vibratory hammers is utilized for initial segment installation only.

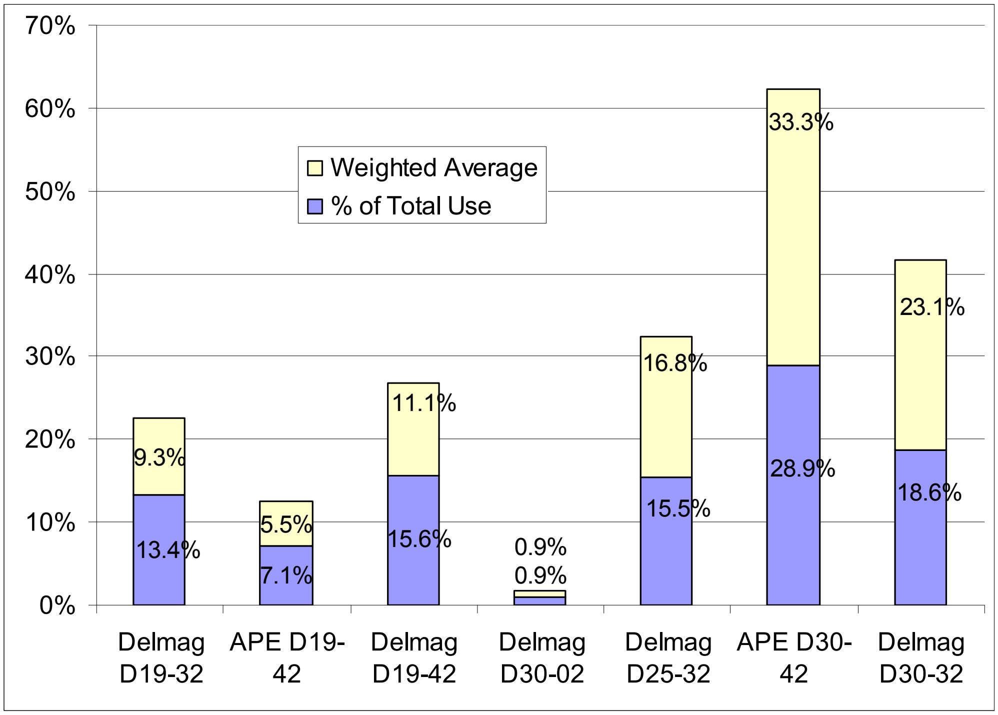

Figure 2.1 Hammer type as percent of total projects use or pile length weighted driven length.

2.8 CONCLUSIONS

The presented summary tables provide quantitative information matching the oral and written reports provided by the Mn/DOT personnel.

1. Majority of bridge foundations are based on Closed Ended Pipe (CEP) and H piles.
2. CEP piles range in diameter from 12 to 20" and comprise of 85% of the driven piles.
3. Most common CEP piles used are 12" x 0.25" and 16" x 0.3125", installed as 40% and 25% of the total foundation length, respectively (based on 28 bridge projects).
4. H piles comprise 15% of the driven pile foundations with sizes ranging between 10x42 to 14x73.
5. Typical (average) driven pile length is 66 feet with a load of 186 kips. More specific categorization is provided in Table 2.5, e.g. Average CEP 12" x 0.25" pile length is 77 feet and it carries 155 kips design (factored) load.
6. Diesel hammers are most commonly used for driving piles ranging in size from D 19-32 (42.4 kip-ft) to D 30-32 (75.4 kip-ft).
7. Over 90% of the piles are driven beyond the easy driving resistance zone of 4 bpi, hence allowing more accurate capacity evaluation when utilizing the dynamic methods. Fifty percent (50%) of the piles were driven to a final penetration of 8 or more bpi.

CHAPTER 3 DATABASE COMPILATION

3.1. OBJECTIVES AND OVERVIEW

The objective of this chapter is to present the development of a new database (Mn/DOT LT 2008) addressing the specific needs of Minnesota DOT pile foundation practices as established in Chapter 2. The database was developed in two stages. In the first stage, two robust H and Pipe pile databases were constructed and analyzed. This effort was presented in a preliminary report entitled “Task 2 – Databases Compilation” submitted on March 16, 2008. The second stage was carried out following comments made by Mn/DOT review team after the preliminary submittal of Task 3 and 4 reports on May 23, 2008. In that stage a comprehensive review and re-evaluation of the original databases were taken focusing on the driving conditions match to Mn/DOT practices. This review resulted with some modifications and re-evaluation based on hammer type and energy, but by and large, had not affected significantly the original databases. Both database development stages are presented here for the following reasons:

1. The explanations provided regarded the case histories and their evaluation are valid for both databases.
2. Both databases (initial and final stages) are robust and, hence, the relatively small modifications made did not result in a substantial difference in analysis outcome or the trend of the obtained results.
3. The first stage database was accompanied by a large scale analysis that remains valid for the condition examined. All the analyses results are presented in Chapter 4 and hence, it is appropriate to present all the databases associated with those analyses.

3.2. METHOD OF APPROACH

The actions required to develop dedicated databases included the following:

1. Review of all Database PD/LT 2000 cases and elimination of data not relevant to Mn/DOT practices; e.g. different pile types and sizes.
2. Searching for additional case histories relevant to the Mn/DOT practices.
3. Extraction of all relevant information and populating database Mn/DOT LT 2008.
4. Develop the statistics of database Mn/DOT LT 2008 and examine it in light of the foundations’ statistics presented in Chapter 2.
5. Re-evaluation of the data and its sortment according to hammer type and energy in addition to pile type.
6. Developing separately a subset of the database containing dynamic measurements and a control database of cases not used as part of the main databases.

3.3. CASE HISTORIES

3.3.1. Past Databases

A database containing dynamic measurements of piles along with static load test results was originally developed by Paikowsky et al. (1994) for examining the reliability of the dynamic measurements and establishing the effectiveness of the Energy Approach method. This database was further enhanced by Stenersen (2001) to become database PD/LT 2000 as presented by Paikowsky and Stenersen (2000) and Paikowsky et al. (2004). Database PD/LT 2000 was the backbone of the AASHTO LRFD calibration for dynamic analyses of driven piles as described by Paikowsky et al. (2004). Database PD/LT 2000 contained information regarding 210 piles out of which 44 were H-Piles, 69 CEP (Closed Ended Pipe) and 24 OEP (Open Ended Pipe). Since 2000, the database was further enhanced to contain 66 H-Piles and 108 pipe piles. Upon establishing the Mn/DOT practices (described in Chapter 2), the enhanced PD/LT 2000 database was sieved and cases relevant to the Mn/DOT pile foundation practices have been identified to form the basis for Mn/DOT/LT 2008 database. This database contained 40 H-Pile case histories, establishing Mn/DOT/LT 2008 H-Pile database. Mn/DOT/LT 2008 Pipe Pile database was also established containing 65 CEP and 12 OEP case histories.

3.3.2. Database Enhancement

A search for additional case histories was undertaken in order to enhance the aforementioned Mn/DOT databases aspiring for optimal calibration conditions. Additional case histories had been obtained in four ways:

1. Request for information was sent to all state DOT engineers and other related officials. The request and a summary of the responses are presented in Appendix C of this report. Six states had responded to our request providing relevant data. A large number of valuable case histories were obtained from Connecticut.
2. Consulting companies and personal communication were used to obtain case histories. Some of this effort was specifically taken to address the need for as many case histories as possible for 16 inch diameter pipe piles.
3. Available reports and publications at the UML Geotechnical Engineering Research Laboratory. These newer reports were accumulated over the past five years and were not used in the enhanced PD/LT 2000 database. The reports examined, case histories were identified, classified and extracted to Mn/DOT/LT 2008.
4. The old FHWA pile database was physically researched and relevant case histories were extracted.

The developed databases at the first stage of analyses are described below. The modified databases are described in Section 3.6 and differ only slightly from the databases described in the following section.

3.4. MN/DOT/LT 2008 H PILES DATABASE

3.4.1. Data Summary

The Mn/DOT/LT 2008 H-Pile database was increased by 126 new case histories from 40 relevant past available cases to 166 cases. It should be noted that the 166 case histories refer to only 137 different piles, such that 48 cases are essentially multiple dynamic and/or static data for only 19 different piles. For example, cases 41 and 42 refer to dynamic data at the end of driving (EOD) and dynamic data at a later time, at the beginning of restrike (BOR) for the same pile. A summary of the information sorted by pile type, geometry and failure load is presented in Table 3.1 for all the H pile cases considering each case history as a separate pile. This way of analysis while provides the information for all possible data cases may cause some distortion in the "use" of piles and other statistics, a factor that should be bear in mind while reviewing the information presented below.

3.4.2. Database Information

The current attributes of the database are presented in Table 3.2. Table 3.2 provides example information for two of the case histories. The data are currently sorted in 63 columns, the most relevant information is presented in the 31 columns of Table 3.2 including:

1. Reference information (columns 1-3), case number, original reference identification and UML volume ID.
2. Location (Column 4) usually state or country.
3. Pile Details (Columns 5, 6, 9, 10) section, area, total length, and weight.
4. Soil Details (Column 11) soil type at the side and tip at the end of driving.
5. Driving System (Columns 7, 8, 12, 13, 17) hammer and driving component details, relevant to dynamic analyses.
6. Driving Data (Columns 15, 16, 18) observed stroke, associated driving energy and driving resistance.
7. Static Pile Capacity (Column 19) static pile capacity obtained for the application of Davisson's failure criterion to the measured or extrapolated static load displacement relations.
8. Dynamic Measurements (Columns 14, 28, 30) measured energy (many other related dynamic measurements details were inserted into the database but are not presented in Table 3.2) and calculated capacity using CAPWAP and the Energy Approach method.
9. Evaluated Dynamic Equations (Columns 20, 22, 24, 26) calculated capacity based on various established and researched dynamic equations, unexecuted yet and to be modified as needed.
10. Bias (Columns 21, 23, 25, 27, 29, 31) ratio of measured capacity as determined by Davisson's failure criterion of the static load test over the calculated capacity based on the relevant method of analysis.

Table 3.1 Summary of Mn/DOT/LT H-Pile Database Sorted by Pile Type, Geometry and Load

Pile Type	Cross-Sectional Area (in^2)	Moment of Inertia (Strong/Weak) (in^4)	No. of Pile Cases[1]	No. of Projects	Total Length of Piles (ft)	% of Total Piles	% of Total Length	Range of Lengths (ft)	Average Pile Length +/- 1 SD (ft)	Average Pile Capacity[2] +/- 1 SD (kips)	No. of Cases with PDA Measurements
HP10X42	12.4	210 / 71.7	28	14	2076	16.87	14.01	15 - 160	74 +/- 37	287 +/- 62	6
HP10X57	16.8	294 / 101	4	3	172	2.41	1.16	36 - 50	43 +/- 8	370 +/- 71	3
HP11X75	14.0	472 / 153	2	1	210	1.20	1.42	105	105	461 +/- 48	0
HP12X53	15.5	393 / 127	41	25	3365	24.70	22.70	22 - 151	77 +/- 37	305 +/- 142	6
HP12X63	18.4	472 / 173	10	1	1532	6.02	10.34	147 - 159	153 +/- 6	275 +/- 52	10
HP12X74	21.8	569 / 186	43	24	3730	25.90	25.16	15 - 291	87 +/- 56	468 +/- 166	20
HP12X89	26.2	693 / 226	3	2	349	1.81	2.35	93 - 140	116 +/- 24	517 +/- 189	2
HP14X73	21.4	729 / 261	16	9	1518	9.64	10.24	39 - 196	95 +/- 30	398 +/- 189	11
HP14X89	26.1	904 / 326	10	6	1103	6.02	7.44	40 - 157	110 +/- 33	619 +/- 273	4
HP14X117	34.4	1220 / 443	9	5	768	5.42	5.18	51 - 113	85 +/- 23	988 +/- 248	4
Totals	**N/A**	**N/A**	**166**	**90**	**14823**	**100.00**	**100.00**	**15 - 196**	**88 +/- 44**	**415 +/- 228**	**66**

Notes: [1] The number relate to the total of 166 cases on 137 different piles

[2] Capacity based on Davisson's failure criterion including 17 cases of load-test extrapolations.

Table 3.2 Typical Attributes of Mn/DOT/LT H-Piles Database

No.[1]	Pile-Case[2] Number	Refer.[3] No.	Location[4]	Pile[5] Type (in x lb)	Pile[6] Weight (lbs)	Capblock[7] Weight (lbs)	Pile[8] Weight + Capblock (lbs)	Pile[9] Area (in2)	Total[10] Length (ft)	Soil Type[11] Side	Soil Type[11] Tip	Hammer[12] Type	Rated[13] Hammer Energy (kip-ft)	Delivered[14] Energy (kip-ft)	Final[15] Stroke (ft)	Final[16] Energy (kip-ft)
62	63-151-3	116	Connecticut	HP12X53	1881.5		1882	15.5	35.5	F,M,Till	Rock	Vulcan 1	15			
65	63-138-2	116	Connecticut	HP10X42	2975.7		2976	12.4	70.85	C,Till	Rock	Vulcan 50C	15.1			

Hammer[17] Weight (lbs)	Blow[18] Count (BPI)	Davisson's[19] Criteria (kips)	Gates[20] Formula R_G (kips)	Measured/[21] Calculated K_G	ENR[22] Equation R_E (kips)	Measured/[23] Calculated K_E	Mod. Gates[24] Equation R_F (kips)	Measured/[25] Calculated K_F	Mn/DOT[26] Equation R_M (kips)	Measured/[27] Calculated K_M	CAPWAP[28] TEPWAP (kips)	Measured/[29] Calculated CAPWAP	Energy[30] Appr. Ru (kips)	Ksp[31] Measured/ Calculated Ru
5000	20.57	280												
5000	47	216												

Notes

[1] Database Case Number
[2] Project Number/Pile Number of Original Reference
[3] UMass Lowell Volume Reference Number
[4] Project Location
[5] H-Pile Section
[6] Pile Weight = lb/ft x length of pile
[7] Weight of capblock (if applicable)
[8] Weight of capblock added to weight of pile
[9] Cross-Sectional Area of Pile during driving
[10] Total Driven Length of Pile
[11] Soil type on pile side and at pile tip
[12] Type of Hammer used in final driving
[13] Rated Hammer Energy per Manufacturer (nominal)
[14] Delivered Energy recorded by PDA
[15] Final stroke of hammer at the end of driving
[16] Final Energy (final stroke x ram weight)
[17] Weight of Ram per Manufacturer
[18] Final blow count of pile in blows per inch
[19] Capacity based on Davisson's Failure Criterion
[20] Gates Dynamic Formula
[21] bias = static Davisson capacity / calculated Gates capacity
[22] Engineering News Record Dynamic Formula
[23] bias = static Davisson capacity / calculated ENR capacity
[24] Modified Gates Dynamic Formula
[25] bias = static Davisson capacity / calculated Modified Gates capacity
[26] Mn/DOT Dynamic Formula
[27] bias = static Davisson capacity / calculated Mn/DOT capacity
[28] CAPWAP/TEPWAP Capacity
[29] bias = static Davisson capacity / calculated CAPWAP capacity
[30] Energy Approach Capacity
[31] bias = static Davisson capacity / calculated Energy Approach capacity

3.4.3. Pile Capacity – Static Load Test

The benchmark pile capacity was established by employing the Davisson's failure criterion (Davisson, 1972) to the static load-settlement relations. The Davisson's failure criterion was selected as the preferable geotechnical pile failure criterion following investigations of five different interpretation methods on 186 case histories as presented by Paikowsky et al. (2004). The interpretation provided the best objective and consistent estimate of the pile capacity with a normal distribution ("correct" capacity over Davisson's interpretation) with a mean of 1.103 and a standard deviation of 0.0829 for 186 cases. This uncertainty may be taken into consideration when applicable. For twenty cases out of the 333 case histories currently comprising the Mn/DOT/LT 2008 database, the static load test was not carried out to intersect the curve of the Davisson's failure criterion. Out of these twenty cases, 16 relate to H-Pile case histories and four relate to pipe piles. For these cases, load test extrapolation was carried out following the procedure proposed by Paikowsky and Tolosko (1999). Table 3.3 summarizes the cases for which static load test extrapolation was carried out, providing in addition to the case ID, the failure obtained by the application of Davisson's criterion to the extrapolated curve along with the actual highest load applied to the pile during the load test. The column described by the extrapolation ratio provides the ratio between the failure load to the actual highest static load applied to the pile during the static load test.

Table 3.3 Case Histories of Mn/DOT/LT 2008 Database for which Load Test Extrapolation Curve was used to Define Failure by Davisson's Criterion

Mn/DOT No.	CT Project Number	Davisson's Criterion (kips)	Maximum Load From SLT (kips)	Extrapolation Ratio
H-353	100-60-1	308	280	1.100
H-206	103-38-1	184	140	1.314
H-142	105-172-1	884	700	1.263
H-60	105-172-3	508	400	1.270
H-324	105-172-4	638	475	1.343
H-287	164-176-3	1034	996	1.038
H-18	42-246-1	912	830	1.099
H-9	44-102-3	460	440	1.045
H-58	63-136-2	510	280	1.821
H-61	63-137-1	350	345	1.014
H-346	63-137-4	408	390	1.046
H-211	63-141-1	314	280	1.121
H-221	91-118-2	452	354	1.277
H-203	92-111-1	298	240	1.242
P-9	92-124-1	282	240	1.175
P-10	92-124-2	268	240	1.117
P-11	92-124-3	400	250	1.600
H-347	92-94-1	230	200	1.150
H-348	92-94-2	248	240	1.033
H-1	96-39-1	128	114	1.123

Notes: [1] Extrapolation was carried out using the procedure developed by Paikowsky and Tolosko (1999)

[2] Extrapolation Ratio = Failure load obtained from the extrapolated load-displacement curve over the highest load applied during static testing

Paikowsky and Tolosko (1999) investigated the accuracy of their extrapolation procedure and found out that it is related to the degree of extrapolation required, i.e. the ratio between the extrapolated failure to the maximum load applied. They found out that extrapolation of up to 33% of the maximum load resulted with an accuracy of 0.99 +/- 0.26 (mean +/- 1 S.D.), extrapolation of up to 200% of the maximum load resulted with an accuracy of 0.89 +/- 0.41. The data in Table 3.3 suggests that only in two cases, the ratio between the extrapolated load to the maximum applied load, exceeded 1.33. These cases (H-58 and P-11) were further examined as to their bias performance.

3.4.4. Data Sorting and Evaluation

Tables 3.4 to 3.6 present summaries related to the cases of the Mn/DOT/LT 2008 H-Piles database regarding the soil type, end of driving resistance and range of hammer rated energy, respectively. Beyond the absolute value of the data, the provided information is compared to that presented in Chapter 2. Table 3.4 presents the data regarding the soil conditions in the database and should be compared to Table 2.6 that summarizes soil conditions for Mn/DOT indicator pile cases. For example; 40.4% of all piles are driven to rock by the Mn/DOT and 34.0% of the H-Piles in Mn/DOT/LT 2008 H-Piles database were driven to rock. Similarly, Table 2.7 suggests that 50% of the Mn/DOT piles are driven to refusal (> 8 bpi) and Table 3.5 suggests that 68.7% of the H-Piles in the database also were driven to final driving resistance equal to or exceeding 8 bpi. Table 2.8 suggests that diesel hammers are used for pile driving by the Mn/DOT with energies ranging from 42.4 to 75.4 kips-ft. Table 3.6 shows that 37.4% of the piles in the database were driven with hammers ranging in energy from 40 to 75 kips-ft. Over half of the piles were driven with diesel hammers; 45.5% in the case of the 25 to 40 kips-ft energy range and 62.5% in the case of the 40 to 50 kips-ft energy range.

Table 3.4 Summary of Mn/DOT/LT H-Pile Database Sorted by Soil Type at the Pile's Tip and Side

Soil Condition / Pile Location	Rock	Till	Sand & Gravel	Sand	Silt	Clay
Tip	54	27	11	47	6	14
Side	0	0	10	90	19	40

Note: 159 total number of cases as 7 pile cases had no soil data available.

Table 3.5 Summary of Mn/DOT/LT H-Pile Database Sorted by End of Driving Resistance

Drivng Resistance (BPI)	0 - 4	4 - 8	>8
Number of Indicator Piles	34	18	114
% of Cases	20.5	10.8	68.7

Table 3.6 Summary of Mn/DOT/LT H-Pile Database Sorted by Range of Hammer Rated Energies

Rated Energy (kips-ft)	No. of Piles	% of Piles	No. of Projects	No. of Hammers	No. of Diesel Hammers	% of Diesel Hammers
7 - 25	57	34.3	32	16	4	25.0%
25 - 40	40	24.1	24	11	5	45.5%
40 - 50	25	15.1	13	8	5	62.5%
50 - 75	37	22.3	17	13	10	76.9%
>75	7	4.2	4	5	4	80.0%
Totals	**166**	**100**	**90**	**53**	**28**	**52.83%**

Figures 3.1 and 3.2 present graphically some of the important features of Mn/DOT/LT 2008 database along with a comparison of data reflecting the Mn/DOT foundation practices as presented in Chapter 2. The information in Figure 3.1 presents mean failure load (+/- 1 standard deviation) for each pile type/size category comprising the database, along with the number of cases related to that information. In addition, the mean LRFD factored (design) load for the Mn/DOT for the applicable pile cases is presented along with the number of piles it is based upon. For example, 41 case histories of the database are related to HP12X53. The mean failure load of these cases was 305 kips +/- 142 kips (1 SD). The mean factored load of this type of pile by the Mn/DOT is 157 kips based on 337 HP12X53 piles. These data alone suggests that the mean safety margin of the Mn/DOT is 1.943 +/- 0.904 in comparison with the database information (not including the load factor) or the covering of approximately 1 S.D range (lower value of resistance is 163 kips compared to a load of 157 kips) translates to a target reliability of $\beta = 1$ and a probability of failure $p_f = 15.9\%$. The information in Figure 3.2 presents the distribution of the case histories in the database based on the pile sizes in comparison with the distribution of use of the same pile by Mn/DOT. To be relevant, the frequency of use of the H-Piles by the Mn/DOT, presented in Figure 3.2, reflects the use of the particular pile type out of the H-Piles only and not out of all driven piles. For example, 41 pile cases of HP12X53 are available in the database (24.7% of all cases), while the Mn/DOT uses this pile in 55.5% of the cases where H-Piles are being used.

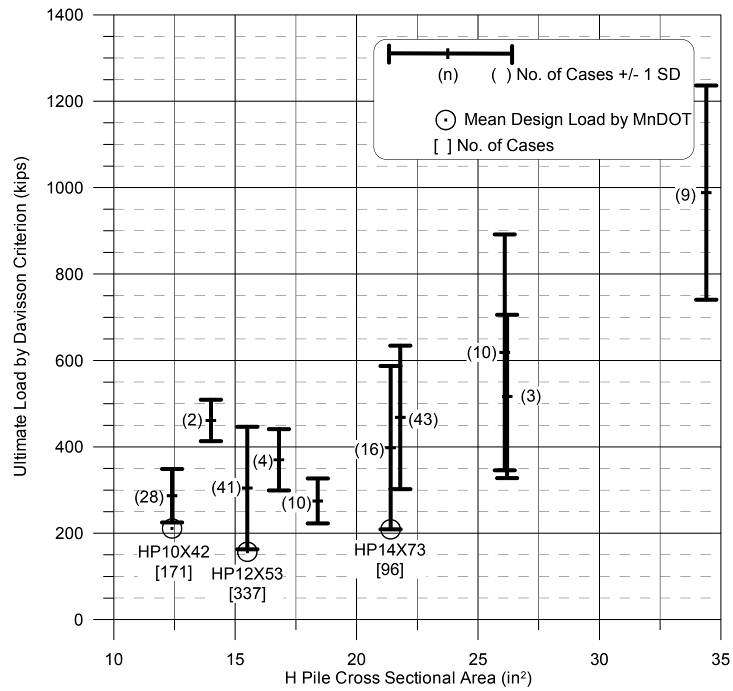

Figure 3.1 Range of pile capacity based on static load test (mean +/- 1 S.D.) and Mn/DOT mean factored design loads sorted by H pile type and cross-sectional area.

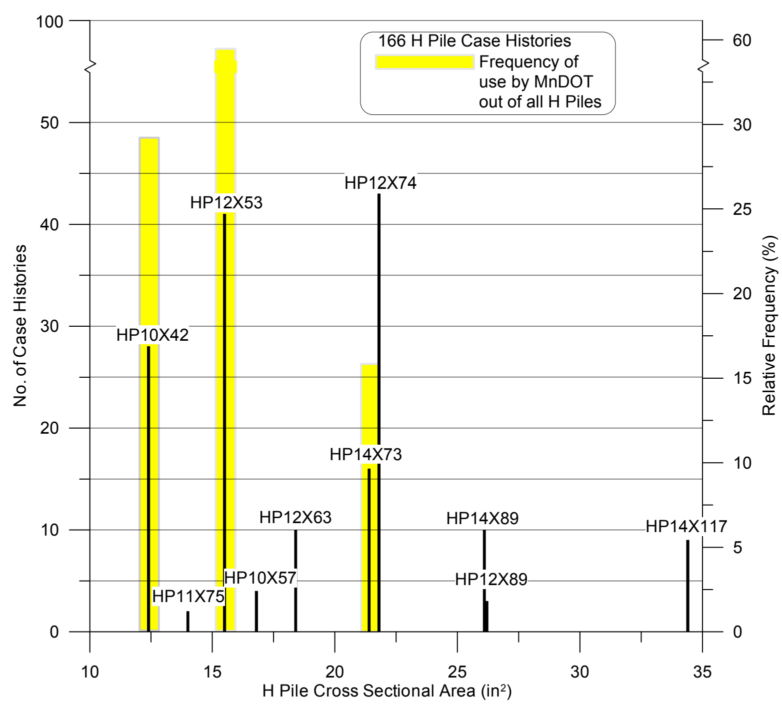

Figure 3.2 Distribution of Database Mn/DOT/LT H-Piles by pile area cross-section along with the frequency and pile type used by Mn/DOT.

3.5. MN/DOT/LT 2008 PIPE PILES DATABASE

3.5.1. Data Summary

The Mn/DOT/LT 2008 Pipe - Pile database was increased by 90 new case histories from 77 relevant past available cases to 167 cases. Although only closed ended pipe piles are used in the Mn/DOT practice, the difficulty in obtaining case histories for 16 inch diameter pipe piles made it logical to include in the database available information regarding four cases of 16 inch open ended pipe piles. It should be noted that the 167 case histories refer to only 138 different piles, such that 54 cases are essentially multiple dynamic and/or static data for only 25 different piles. For example, cases 20 and 21 refer to dynamic data at the end of driving (EOD) and dynamic data at a later time, at the beginning of restrike (BOR) for the same pile. A summary of the information sorted by pile type, geometry and failure load is presented in Table 3.7 for all the pipe pile cases considering each case history as a separate pile. This way of analysis while provides the information for all possible data cases may cause some distortion in the "use" of piles and other statistics, a factor that should be bear in mind while reviewing the information presented below.

3.5.2. Database Information

The current attributes of the database are presented in Table 3.8. Table 3.8 provides example information for two of the case histories. The data are currently sorted in 67 columns, the most relevant information is presented in the 34 columns of Table 3.8 including:

1. Reference information (columns 1-3), case number, original reference identification and UML volume ID.
2. Location (Column 4) usually state or country.
3. Pile Details (Columns 5, 6, 7, 11, 12, 13) type (diameter and closed vs open ended), wall thickness, weight of unit length, total weight, section area and total length.
4. Soil Details (Column 14) soil type at the side and tip at the end of driving.
5. Driving System (Columns 5, 15, 16, 18) hammer and driving component details, relevant to dynamic analyses.
6. Driving Data (Columns 19, 20, 31) observed stroke, associated driving energy and driving resistance.
7. Static Pile Capacity (Column 22) static pile capacity obtained for the application of Davisson's failure criterion to the measured or extrapolated static load displacement relations.
8. Dynamic Measurements (Columns 17, 31, 33) measured energy (many other related dynamic measurements details were inserted into the database but are not presented in Table 3.7) and calculated capacity using CAPWAP and the Energy Approach method.
9. Evaluated Dynamic Equations (Columns 23, 25, 27, 29) calculated capacity based on various established and researched dynamic equations, unexecuted yet and to be modified as needed.
10. Bias (Columns 24, 26, 28, 30, 32, 34) ratio of measured capacity as determined by Davisson's failure criterion of the static load test over the calculated capacity based on the relevant method of analysis.

Table 3.7 Summary of Mn/DOT/LT Pipe Pile Database Sorted by Pile Type, Geometry and Load

Pile Type	Cross-Sectional Area Range (in^2)	No. of Pile Cases[1]	No. of Projects	Total Length Of Piles (ft)	% of Total Piles	% of Total Length	Range of Lengths (ft)	Average Pile Length +/- SD (ft)	Average Pile Capacity[2] +/- SD (kips)	No. of Cases with PDA Measurements
CEP 10" or less	7.9 - 18.4	23	9	2861	13.8%	18.3%	28 - 175	124 +/- 45	422 +/- 160	20
CEP 12"	8.5 - 13.7	12	7	1015	7.2%	6.5%	27 - 134	85 +/- 34	388 +/- 173	3
CEP 12.75"	7.7 - 14.6	65	35	5485	38.9%	35.1%	15 - 175	84 +/- 39	372 +/- 195	30
CEP 14"	10.8 - 21.2	29	11	2777	17.4%	17.8%	31 - 158	96 +/- 38	454 +/- 199	23
CEP 16"	9.3 - 24.3	10	10	863	6.0%	5.5%	24 - 125	86 +/- 30	650 +/- 396	4
CEP 18"	27.5 - 34.1	12	7	1372	7.2%	8.8%	60 - 170	114 +/- 37	545 +/- 198	9
CEP 20" - 26"	36.9 - 67.7	12	4	932	7.2%	6.0%	44 - 166	78 +/- 29	767 +/- 135	12
OEP 16"	24.35	4	1	321	2.4%	2.1%	52 - 109	80 +/- 33	431 +/- 260	3
Totals	**N/A**	**167**	**84**	**15625**	**100.00%**	**100.00%**	**15 - 175**	**94 +/- 42**	**452 +/- 230**	**104**

Notes: [1] The number relate to the total of 167 cases on 138 different piles
[2] Capacity based on Davisson's failure criterion including 3 cases of load-test extrapolations.

Table 3.8 Typical Attributes of Mn/DOT/LT Pipe Piles Database

No.[1]	Pile-Case[2] Number	Refer.[3] No.	Location[4]	Pile[5] Type	Wall[6] Thickness (in)	Pile[7] Unit Weight (lbs/ft)	Pile[8] Weight (lbs)	Capblock[9] Weight (lbs)	Pile[10] Weight + Capblock (lbs)	Pile[11] Area (in2)	Cross[12] Sectional Area (in2)	Total[13] Length (ft)	Soil Type[14]		Hammer[15] Type	Rated[16] Hammer Energy (kip-ft)	Delivered[17] Energy (kip-ft)
													Side	Tip			
25	CNB351-1	117	Tennessee	CEP 16"	0.5	82.8	6207.8		6207.8	201.1	24.3	75.0	C,S	Sand	Vulcan 506	32.5	
73	A-1-137-BOR	10	Canada	CEP 12.75"	0.315	41.8	2510.0		2510.0	127.7	12.3	60	Clay	Till	B-300	40.31	

Hammer[18] Weight (lbs)	Final[19] Stroke (ft)	Final[20] Delivered Energy (kip-ft)	Blow[21] Count (BPI)	Davisson's[22] Criteria (kips)	Gates[23] Formula R_G (kips)	Measured/[24] Calculated K_G	ENR[25] Equation R_E (kips)	Measured/[26] Calculated K_E	Mod. Gates[27] Equation R_F (kips)	Measured/[28] Calculated K_F	Mn/DOT[29] Equation R_M (kips)	Measured/[30] Calculated K_M	CAPWAP[31] TEPWAP (kips)	Measured/[32] Calculated CAPWAP	Energy[33] Appr. Ru (kips)	Ksp[34] Measured/ Calculated Ru
6500	5	32.5	4.50	230												
3750			11.00	384												

Notes:

[1] Database Case Number
[2] Project Number/Pile Number of Original Reference
[3] UMass Lowell Volume Reference Number
[4] Project Location
[5] Pipe Pile Section
[6] Wall Thickness of Pile
[7] Unit Weight of pile per foot
[8] Pile Weight = Unit weight of pile x total driven length
[9] Weight of capblock (if applicable)
[10] Weight of capblock added to weight of pile
[11] Area of Pile at tip
[12] Cross-Sectional Area of Pile during driving
[13] Total Driven Length of Pile
[14] Soil type on pile side and at pile tip
[15] Type of Hammer used in final driving
[16] Rated Hammer Energy per Manufacturer (nominal)
[17] Delivered Energy recorded by PDA
[18] Weight of Ram per Manufacturer
[19] Final stroke of hammer prior at the end of driving
[20] Final Energy (final strokes x ram weight)
[21] Final blow count of pile in blows per inch
[22] Capacity based on Davisson's Failure Criterion
[23] Gates Dynamic Formula
[24] bias = static Davisson capacity / calculated Gates capacity
[25] Engineering News Record Dynamic Formula
[26] bias = static Davisson capacity / calculated ENR capacity
[27] Modified Gates Dynamic Formula
[28] bias = static Davisson capacity / calculated Modified Gates capacity
[29] Mn/DOT Dynamic Formula
[30] bias = static Davisson capacity / calculated Mn/DOT capacity
[31] CAPWAP/TEPWAP Capacity
[32] bias = static Davisson capacity / calculated CAPWAP capacity
[33] Energy Approach Capacity
[34] bias = static Davisson capacity / calculated Energy Approach capacity

3.5.3. Pile Capacity – Static Load Test

Refer to section 3.4.3.

3.5.4. Data Sorting and Evaluation

Tables 3.9 to 3.11 present summaries related to the cases of the Mn/DOT/LT 2008 Pipe Piles database regarding the soil type, end of driving resistance and range of hammer rated energy, respectively. Beyond the absolute value of the data, the provided information is compared to the data presented in Chapter 2. Table 3.9 presents the data regarding the soil conditions in the database and should be compared to Table 2.6. For example 40.4% of all piles driven to rock by the Mn/DOT and only 16.0% of the pipe piles in Mn/DOT/LT 2008 Pipe Piles database were driven to rock. Similarly, Table 2.7 suggests that 50% of the Mn/DOT piles are driven to refusal (> 8 bpi) while Table 3.10 suggests that 37.1% of the pipe piles in the database also were driven to final driving resistance equal to or exceeding 8 bpi. Table 2.8 suggests that diesel hammers are used for pile driving by the Mn/DOT with energies ranging from 42.4 to 75.4 kips-ft. Table 3.11 shows that 40.8% of the piles in the database were driven with hammers ranging in energy from 40 to 75 kips-ft. About half of the piles were driven with diesel hammers; 40.0% in the case of the 25 to 40 kips-ft energy range and 57.1% in the case of the 40 to 50 kips-ft energy range.

Table 3.9 Summary of Mn/DOT/LT Pipe Pile Database Sorted by Soil Type at the Pile's Tip and Side

Soil Condition / Pile Location	Rock	Till	Sand & Gravel	Sand	Silt	Clay
Tip	16	40	7	64	13	27
Side	0	8	4	80	19	56

Notes: [1] Total number of cases is 167

Table 3.10 Summary of Mn/DOT/LT Pipe Pile Database Sorted by End of Driving Resistance

Drivng Resistance (BPI)	0 - 4	4 - 8	>8
Number of Indicator Piles	67	38	62
% of Cases	40.1	22.8	37.1

Table 3.11 Summary of Mn/DOT/LT Pipe Pile Database Sorted by Range of Hammer Rated Energies

Rated Energy (kips-ft)	No. of Piles	% of Piles	No. of Projects	No. of Hammers	No. of Diesel Hammers	% of Diesel Hammers
7 - 25	32	19.2	23	5	2	40.0
25 - 40	41	24.6	14	10	4	40.0
40 - 50	27	16.2	16	7	4	57.1
50 - 75	42	25.1	21	12	9	75.0
>75	25	15.0	10	9	7	77.8
Totals	**167**	**100.0**	**84**	**43**	**26**	**60**

Figures 3.3 and 3.4 present graphically some of the important features of Mn/DOT/LT 2008 database along with a comparison of data reflecting the Mn/DOT foundation practices as presented in the Task 1 report. The information in Figure 3.3 presents mean failure load (+/- 1 standard deviation) for each pile type/size category (by pipe pile diameter) comprising the database, along with the number of cases related to that information. In addition, the mean LRFD factored (design) load for the Mn/DOT for the applicable pile cases is presented along with the number of piles it is based upon. For example, 12 and 65 case histories of the database are related to 12.00 and 12.75 inch diameter piles, respectively. The mean failure load of these cases was 388 +/- 173 kips and 372 +/- 195 kips (1 SD) for the 12 and 12.75 inch diameter piles, respectively. The mean factored load of the 12 and 12.75 inch piles by the Mn/DOT is 155 and 120 kips, based on 1055 and 116 12 and 12.75 inch diameter pipe piles, respectively. These data alone suggests that the mean safety margin of the Mn/DOT 12 and 12.75 inch diameter piles is 2.503 +/- 1.116 and 3.100 +/- 1.625 in comparison with the database information (not including the load factor) or the covering of approximately 1.3 S.D range (lower value of resistance is 1.29 and 1.35 standard deviations from the mean, hence approximately taken as 1.3) translates to a target reliability of $\beta = 1.3$ and a probability of failure $p_f = 9.8\%$. The information in Figure 3.4 presents the distribution of the case histories in the database based on the pile sizes in comparison with the distribution of use of the same pile by Mn/DOT. To be relevant, the frequency of use of the pipe piles by the Mn/DOT, presented in Figure 3.4, reflecting the use of the particular pile type out of the pipe piles only and not out of all driven piles. For example, 77 pile cases of 12 and 12.75 inch diameter piles are available in the database (46.1% of all cases), while the Mn/DOT uses these diameter piles in 50.0% of the projects where pipe piles are being used. The major difficulty of the database as presented in Figure 3.4 is evidently related to the 16 inch diameter closed ended pipe piles. This type of piles are used by the Mn/DOT in 22.9% of all projects and 26.9% of all pipe piles but only 10 closed ended and 4 open ended 16 inch diameter piles are available at the database.

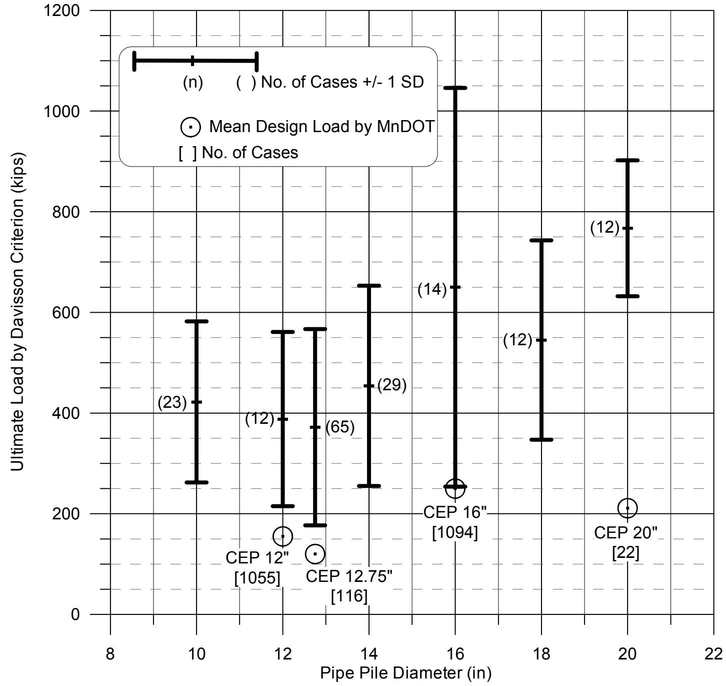

Figure 3.3 Range of pile capacity based on static load test (mean +/- 1 S.D.) and Mn/DOT mean factored design loads sorted by pipe pile type and pipe pile diameter.

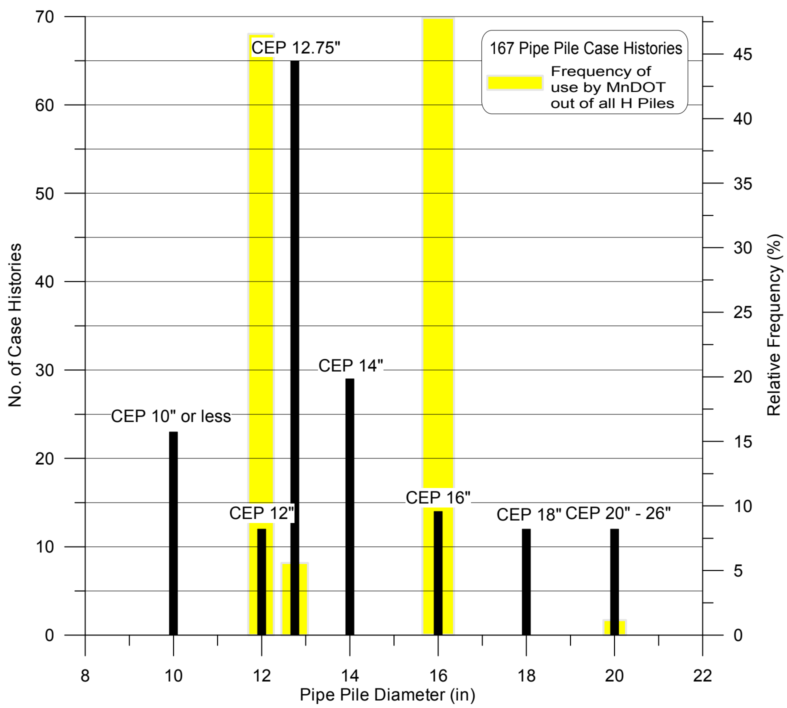

Figure 3.4 Distribution of Database Mn/DOT/LT pipe piles by pile area cross-section along with the frequency and pile type used by Mn/DOT.

3.6. DATABASES MODIFICATION – SECOND RESEARCH STAGE

3.6.1. Overview

Following the TAP meeting that took place in Minnesota on August 8, 2008, an extensive examination of the databases took place primarily to re-check what seems more relevant to the Mn/DOT practice. The databases re-examination consisted of the following:

1. Re-examination of the capacity of all the pipe piles in the database. It was identified that the variability of the data is higher for the pipe piles, contributing to larger variability in the dynamic analyses. Pipe piles are driven empty, but then are being used and statically tested after being filled with concrete. We examined all cases to make sure there was not a discrepancy in the load test interpretation between shell stiffness to that of a concrete filled pipe. It was a tedious task and by and large, the quality of the data were affirmed. We also examined possible corrections for 19 case histories, all found to be ok. We did identify five cases to be removed for various reasons (battered piles, very low blow count, etc.), but added others so overall ended with the same number of cases but three less EOD cases compared to the number of cases that were represented first.
2. Re-examination of all the H-pile cases mostly to double check the determined static pile capacity and the reliability of the dynamic data. We have not changed anything in that pile category. Table 3.12 summarizes our second stage database review including dynamic and static measurements.

Table 3.12 Second Stage Mn/DOT Database Review

Pile Type	Reviewed # All/EOD	Excluded/Added	To be used All/EOD
H	135/125	0/0	135/125
Pipe	128/102	-5/+5/-3	128/99

Notes:
1. Reviewed number relates to 1st stage database.
2. Two H pile cases were excluded from the original H pile database during 1st stage analysis, so 135 piles refer to the original 137 with 2 piles removed.
3. All = all pile cases. EOD = cases for which End of Driving data are available.
4. “To be used” refers to the 2nd stage database and final analysis.

3.6.2. Database Applicability to Mn/DOT Construction Practices

Section 3.4.4 (see Tables 3.5, 3.6), and section 3.5.4 (see Tables 3.10, 3.11) examined the database hammer energy and driving resistances compared to Mn/DOT practices for H and Pipe pile, respectively. Additional examination was performed once more details of assumptions made by Mn/DOT equation application were identified (e.g. assumed hammer energy efficiency of 75% if stroke measurements are not available). The process taken, the findings, and the conclusions are described below.

1. All the original reports were examined to see if records of stroke measurements could be found. Fifteen cases of pipe piles and 58 records of H piles were identified for which the stroke was specified in the reports. Table 3.13 provides a summary of these records.
2. All the cases for which dynamic measurements were available, were examined in order to establish the typical energy transfer and accuracy of the prediction compared to the dynamic equations for the same cases. The original database was updated with the summary presented in Table 3.13.

Table 3.13 Dynamic Data Details for Mn/DOT/LT 2008 Database

Pile Type	Dynamic Measurements			Stroke Measurements		Comments
	No Data	Some	All	No Data	Available	
H	66	6	27	40	59	Some stroke values may be theoretically calculated
Pipe	31	7	56	83	16	

3. Tables 3.14 to 3.16 provide details about the hammers used in driving the piles comprising Mn/DOT/LT 2008 Databases. The data presented in these tables are compared to the data presented in Table 2.8, summarizing the Mn/DOT common equipment based on the bridge construction analyses presented in Chapter 2. The following comments and conclusions can be made when comparing the data in Table 2.8 to that in Tables 3.14 to 3.16:
   a. Based on Table 2.8, about 75% of the piles were driven with hammers having nominal energy of about 70kip-ft (ranging from 66.2 to 75.4kip-ft), and ram weight of about 6,000lb (ranging from 5,500 to 6,600lb).
   b. The details provided in Tables 3.14 to 3.16 of the developed database suggest the following:
      i. 80% of the diesel hammers used for the H piles have a nominal energy of about 50kip-ft (range from 40.6 to 0.885kip-ft) and a ram weight of about 6,000lb (range from 4,910 to 7,930lb), and
      ii. The average of all the diesel hammers used for the Pipe and H piles together (87 cases) is a nominal energy of 61.0kip-ft) and a ram weight of 6,553lb.

   These observations lead to the following conclusions:
      i. The database provides a larger range of hammer sizes and energies compared to Mn/DOT practice, but overall overlaps well with the hammers used in Mn/DOT projects, and
      ii. The research program remained as planned, i.e. work on small and large groups from most selective match cases (e.g. diesel hammer size, energy, pile, driving resistance, etc.) to the most robust cases (all hammers, all piles) and check the influence of the subgroup vs. all group on the statistical results.

Table 3.14 Summary of Hammers Type and Energy Used for Driving the H Piles in the Dataset of Mn/DOT/LT 2008

H Piles – All Hammer Types

Hammer Type	Max. Energy (kips-ft)	Ram Weight (lbs)	No. of Projects Used	Total Pile Length Driven (ft)	% of Total Use	Weighted Ave.
APE D30-32	70.1		1	40	0.5%	0.9%
B-300	34.0	3750	4	331	4.1%	3.7%
B-400	46.0	5000	1	121	1.5%	1.8%
Conmaco 125E5	62.5	12500	6	940	11.7%	19.2%
Delmag D-12	23.7	2750	4	224	2.8%	1.7%
Delmag D19-32	42.4	4000	1	35	0.4%	0.5%
Delmag D-22	40.6	4910	1	100	1.2%	1.3%
Delmag D25-32	61.5	5510	2	213	2.7%	4.3%
Delmag D30-32	73.8	6600	3	250	3.1%	6.0%
Delmag D-36	83.8	7930	1	157	2.0%	4.3%
Delmag D36-32	88.5	7930	1	102	1.3%	2.9%
ICE 1070	72.6	10000	1	54	0.7%	1.3%
ICE 520	30.4	5070	2	139	1.7%	1.4%
ICE 640B	40.6	6000	2	180	2.2%	2.4%
ICE 70S	70.0	7000	1	94	1.2%	2.1%
IHC S-70	51.3	7730	1	131	1.6%	2.2%
Junttan HHK 4a	34.7	8818	2	264	3.3%	3.0%
Junttan HHK 7a	61.6	15431	1	104	1.3%	2.1%
LB 660	51.6	7570	8	930	11.6%	15.7%
MKT 10B3	13.1	3000	1	68	0.8%	0.3%
MKT 11B3	19.2	5000	3	290	3.6%	1.8%
MKT 9B3	8.8	1600	1	59	0.7%	0.2%
MKT DE30	22.4	2800	1	69	0.9%	0.5%
MKT DE-30B	23.8	2800	2	80	1.0%	0.6%
MKT S8	26.0	8000	3	377	4.7%	3.2%
Raymond 65C	19.5	6500	1	90	1.1%	0.6%
Vulcan 06	19.5	6500	3	78	1.0%	0.5%
Vulcan 1	15.0	5000	16	988	12.3%	4.8%
Vulcan 1 Mod.	19.5		3	278	3.5%	1.8%
Vulcan 2	7.3	3000	1	40	0.5%	0.1%
Vulcan 506	32.5	6500	5	355	4.4%	3.8%
Vulcan 50C	15.1	5000	7	561	7.0%	2.8%
Vulcan 80C	24.5	8000	3	292	3.6%	2.3%
	38.6	6200	93	8033	100%	100%
	Average*		Totals			

H Piles – Diesel Hammers

Hammer Type	Max. Energy (kips-ft)	Ram Weight (lbs)	No. of Projects Used	Total Pile Length Driven (ft)	% of Total Use	Weighted Ave.
APE D30-32	70.1	0	1	40	1.3%	1.8%
B-300	34.0	3750	4	331	10.6%	7.1%
B-400	46.0	5000	1	121	3.9%	3.5%
Delmag D-12	23.7	2750	4	224	7.2%	3.4%
Delmag D19-32	42.4	4000	1	35	1.1%	0.9%
Delmag D-22	40.6	4910	1	100	3.2%	2.6%
Delmag D25-32	61.5	5510	2	213	6.8%	8.3%
Delmag D30-32	73.8	6600	3	250	8.0%	11.7%
Delmag D-36	83.8	7930	1	157	5.0%	8.3%
Delmag D36-32	88.5	7930	1	102	3.3%	5.7%
ICE 1070	72.6	10000	1	54	1.7%	2.5%
ICE 520	30.4	5070	2	139	4.5%	2.7%
ICE 640B	40.6	6000	2	180	5.8%	4.6%
ICE 70S	70.0	7000	1	94	3.0%	4.2%
LB 660	51.6	7570	8	930	29.8%	30.5%
MKT DE30	22.4	2800	1	69	2.2%	1.0%
MKT DE-30B	23.8	2800	2	80	2.6%	1.2%
	50.4	5601	36	3118	100%	100%
	Average*		Totals			

*excluding hammer APE D30-32

*excluding hammer APE D30-32

Table 3.15 Summary of Hammers Type and Energy Used for Driving the Pipe Piles in the Dataset of Mn/DOT/LT 2008

Pipe Piles – All Hammer Types

Hammer Type	Max. Energy (kips-ft)	Ram Weight (lbs)	No. of Projects Used	Total Pile Length Driven (ft)	% of Total Use	Weighted Ave.
B-225	29.0	3000	3	418	4.5%	2.6%
B-300	34.0	3750	5	349	3.8%	2.5%
B-400	46.0	5000	4	498	5.4%	4.9%
Delmag D30	59.7	6600	1	60	0.6%	0.8%
Delmag D30-32	73.8	6600	4	326	3.5%	5.1%
Delmag D-12	23.7	2750	12	856	9.3%	4.3%
Delmag D-22	40.6	4910	3	294	3.2%	2.5%
Delmag D46-32	113.1	10140	4	399	4.3%	9.6%
Delmag D62-22	152.5	13660	1	74	0.8%	2.4%
HMC-86	64.0	16000	6	654	7.1%	8.9%
HPSI 1000	50.0	10000	1	119	1.3%	1.3%
HPSI 2000	80.0	20000	3	446	4.8%	7.6%
ICE 160	64.0	16000	1	135	1.5%	1.8%
ICE 1070	72.6	10000	7	750	8.1%	11.6%
ICE-640	40.6	6000	8	970	10.5%	8.4%
Junttan HHK 7a	61.6	15431	2	237	2.6%	3.1%
K-25	51.5	5510	3	166	1.8%	1.8%
K-45	92.8	9920	3	261	2.8%	5.2%
LB 312	15.0	3860	2	171	1.9%	0.5%
MKT DE110C	150.0	15000	1	63	0.7%	2.0%
Vulcan 80C	24.5	8000	4	488	5.3%	2.5%
Vul-010	32.5	10000	5	797	8.6%	5.5%
Vul-200C	50.2	20000	2	266	2.9%	2.8%
Vulcan 1	15.0	5000	3	284	3.1%	0.9%
Vulcan 506	32.5	6500	2	161	1.7%	1.1%
	60.0	9610	90	9240	100%	100%
	Average*		Totals			

*excluding hammer B-225

Pipe Piles – Diesel Hammers

Hammer Type	Max. Energy (kips-ft)	Ram Weight (lbs)	No. of Projects Used	Total Pile Length Driven (ft)	% of Total Use	Weighted Ave.
B-225	29.0	3000	3	418	9.0%	4.7%
B-300	34.0	3750	5	349	7.5%	4.6%
B-400	46.0	5000	4	498	10.8%	8.9%
Delmag D30-32	73.8	6600	4	326	7.0%	9.3%
Delmag D-12	23.7	2750	12	856	18.5%	7.8%
Delmag D-22	40.6	4910	3	294	6.3%	4.6%
Delmag D46-32	113.1	10140	4	399	8.6%	17.4%
Delmag D62-22	152.5	13660	1	74	1.6%	4.4%
ICE 1070	72.6	10000	7	750	16.2%	21.0%
K-25	51.5	5510	3	166	3.6%	3.3%
K-45	92.8	9920	3	261	5.6%	9.3%
LB 312	15.0	3860	2	171	3.7%	1.0%
MKT DE110C	150.0	15000	1	63	1.4%	3.7%
	72.1	7592	52	4624	100%	100%
	Average*		Totals			

*excluding hammer B-225

Table 3.16 Summary of Diesel Hammers Used for Driving H and Pipe Piles in the Dataset of Mn/DOT/LT 2008

Pipe & H Piles - Diesel Hammers						
Hammer Type	Max. Energy (kips-ft)	Ram Weight (lbs)	No. of Projects Used	Total Pile Length Driven (ft)	% of Total Use	Weighted Ave.
APE D30-32	70.1	0	1	40	0.5%	0.7%
B-225	29.0	3000	3	418	5.4%	2.9%
B-300	34.0	3750	9	680	8.8%	5.5%
B-400	46.0	5000	5	619	8.0%	6.8%
Delmag D-12	23.7	2750	16	1080	13.9%	6.1%
Delmag D19-32	42.4	4000	1	35	0.4%	0.4%
Delmag D-22	40.6	4910	4	394	5.1%	3.8%
Delmag D25-32	61.5	5510	2	213	2.8%	3.1%
Delmag D30-32	73.8	6600	7	576	7.4%	10.2%
Delmag D-36	83.8	7930	1	157	2.0%	3.2%
Delmag D36-32	88.5	7930	1	102	1.3%	2.2%
Delmag D46-32	113.1	10140	4	399	5.2%	10.8%
Delmag D62-22	152.5	13660	1	74	1.0%	2.7%
ICE 1070	72.6	10000	8	804	10.4%	14.0%
ICE 520	30.4	5070	2	139	1.8%	1.0%
ICE 640B	40.6	6000	2	180	2.3%	1.8%
ICE 70S	70.0	7000	1	94	1.2%	1.6%
K-25	51.5	5510	3	166	2.1%	2.1%
K-45	92.8	9920	3	261	3.4%	5.8%
LB 312	15.0	3860	2	171	2.2%	0.6%
LB 660	51.6	7570	8	930	12.0%	11.5%
MKT DE110C	150.0	15000	1	63	0.8%	2.3%
MKT DE30	22.4	2800	1	69	0.9%	0.4%
MKT DE-30B	23.8	2800	2	80	1.0%	0.5%
	61.3	6553	88	7742	100%	100%
	Average*		Totals			

*excluding hammer APE D30-32

4. Separate databases were examined, providing rates of energy transfer based on dynamic measurements. These databases contain independent data for which no other data are available, but the hammer and pile types match the Mn/DOT practice. Figure 3.5 presents the most updated information available from all the different sources we have and was provided by GRL, Inc. of Cleveland, Ohio. It matches well previously published data, only it is more extensive than we knew of before. The information in Figure 3.5 refers to 1103 case histories. Based on personal communications with Mr. Garland Likins of Pile Dynamics, Inc., each case refers to an average of a site (not a single pile!), hence the information reflects many more piles than 1103.
5. The data has been analyzed and summarized in Table 3.17 in order to check the adequacy of the databases built for the Mn/DOT and presented in this chapter (having all the information including load test results to failure) to the large database of GRL in Figure 3.5 (for only energy transfer). The data analysis in Table 3.17 clearly shows that the mean energy transfer for diesel hammers on H and Pipe Piles in the databases developed for the Mn/DOT was 37.4% and 39.8%, respectively, compared to 37.7% of GRL database for all steel piles. The standard deviations of the Mn/DOT databases are a bit higher, 11.9% and 13.6% compared to 9.8% of GRL's; something one can expect from 20 and 34 case databases compared to thousands.

   The aforementioned observations verify that the piles in the Mn/DOT database are very much typical of thousands of sites where steel piles are being driven with diesel hammers (the typical Mn/DOT practice).

Table 3.17 Summary of Driving Data Statistics for Mn/DOT/LT 2008 Databases

Pile Type	Driving System Efficiency (PDA)						Stroke Measurments					
	All Hammers			Diesel Hammers			All Hammers			Diesel Hammers		
	n	Mean %	S.D. %	n	Mean %	S.D. %	n	Mean %	S.D. %	n	Mean %	S.D. %
H	27	41.2	15.1	20	37.4	11.9	59	83.8	23.9	11	79.0	13.4
Pipe	56	47.8	18.5	34	39.8	13.6	16	70.2	25.9	6	62.5	24.3

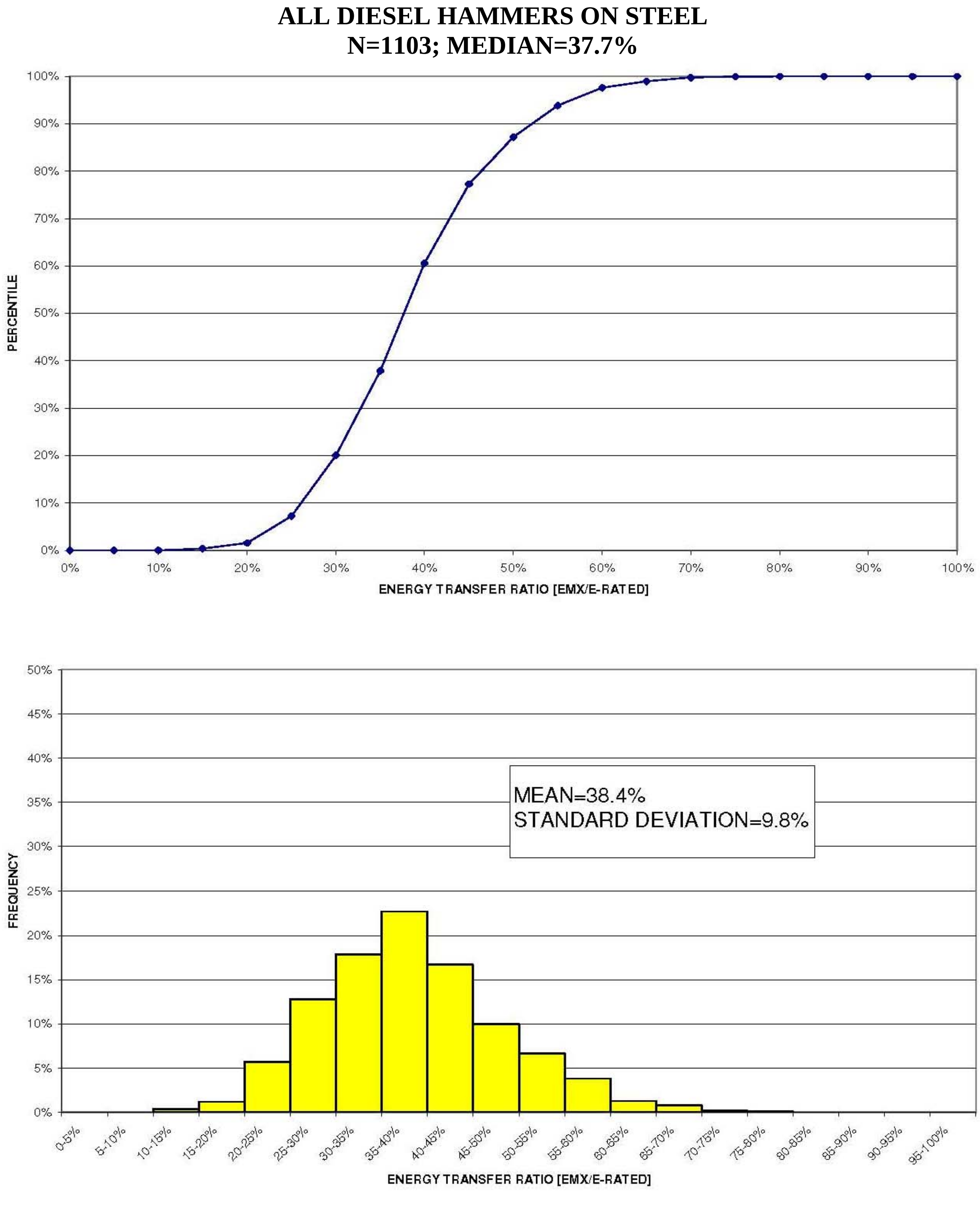

Figure 3.5 Probability Distribution Function (PBD) and Cumulative Distribution Function (CDF) for energy transfer when driving steel piles with diesel hammers (This chart has been assembled from data collected by GRL engineers and may only be copied with the express written permission of GRL Engineers, Inc.).

6. The stroke measurements available in the assembled databases are presented in Table 3.17. The following can be noted regarding these data:
   a. Measured energy allows calculating the total efficiency, i.e. the ratio between energy delivered to the pile itself to the nominal energy specified to the hammer. However, this low number may be somehow misleading due to the operation principle of diesel hammers. Energy manufactured by the hammer depends upon the setting of the fuel pump as well as the driving resistance. Only full setting and high blow count would allow the hammer to produce nominal energy (neglecting hammer internal losses and problematic operation like early ignition). Thus, unless actual dynamic measurements are available, it is useful just for checking the data or WEAP analysis, but not related to stroke measurements.
   b. The efficiency related to stroke measurements provides the ratio between the calculated potential energy (based on stroke times the ram weight) relative to the nominal energy. This is only an indirect indication as to the energy arriving to the pile, which is greatly affected by the losses in the driving system (cushion, helmet, cap block, etc.).
   c. The use of stroke is beneficial to evaluate typical hammer operation, i.e. 'actual' produced energy (subjected to the accuracy of stroke measurements), but it is only indirectly helpful for estimating the energy transferred to the pile.
   d. The above stroke measurements suggest that typically the diesel hammers' stroke is 79% for H piles and 62.5% for Pipe piles. These values compare quite well with the assumed stroke recommended by the Mn/DOT (i.e. 75% of nominal energy) when stroke information is not recorded.

3.6.3. Subset Database of Dynamic Measurements

Two subset databases containing dynamic analysis results of signal matching (CAPWAP) or information to calculate the Energy Approach predictions (see section 1.7.2), were developed for the H and pipe piles out of Mn/DOT/LT 2008. While Table 3.13 presents the number of cases used to evaluate the energy transfer based on measurements, Table 3.18 details the number and type of dynamic analysis predictions available under each category of driving conditions, e.g. 74 CAPWAP analyses and 59 Energy Approach analyses for all pipe piles' conditions to only 12 cases related to EOD with Diesel hammers within the energy range of Mn/DOT practice on pipe piles driven to 4 or more bpi.

The capacity predictions based on dynamic measurements are presented in Chapter 7 for comparison with the static load test in order to examine the prediction ability of dynamic analyses based on measured data to that based on field observations without measurements.

Table 3.18 Summary of Cases in Mn/DOT/LT 2008 Database for which Dynamic Analyses Based on Dynamic Measurements are Available

Condition	H Piles		Pipe Piles	
	CAPWAP	Energy Approach	CAPWAP	Energy Approach
All Cases	38	33	74	59
EOD	31	26	58	43
Diesel Hammers	24	20	36	32
EOD/Diesel BC ≥ 4BPI	17	16	21	19
EOD/Diesel BC ≥ 4BPI/ Mn/DOT Energy Range	4	2	12	12

3.6.4. Control Database

To enable independent evaluation of the research findings, a separate set of data was developed not used in the development of uncertainty for the new equation. This database denoted as Mn/DOT/LT 2008 Control contains only H pile cases as detailed in Table 3.19. The database was developed from information becoming available while the research took place. Due to the scarcity of pipe pile information and in particular data related to sizes most commonly used by the Mn/DOT (i.e. 16inch diameter), no control database is available for pipe piles. It should be noted regarding Mn/DOT/LT 2008 Control, that only two of the 24 cases (or 20 when referring to EOD with BC ≥ 4BPI) are for piles driven with diesel hammers. Chapter 8 presents the control database analysis in the evaluation of the recommendations made based on the major database Mn/DOT/LT 2008.

Table 3.19 Summary of H Pile Cases Compiled in a Control Database (Mn/DOT/LT 2008 Control) for Independent Evaluation of the Research Findings

Condition	No. of Cases
All Cases	24
EOD / BC ≥ 4BPI	20
EOD / Diesel Hammers	2

3.7. CONCLUSIONS

3.7.1. First Stage Database Development

Robust databases of driven H and pipe piles were assembled, answering to the Mn/DOT bridge foundation design practices established in Chapter 2. The databases contain 333 case histories related to 274 different piles. Each case history includes as a minimum requirement, the data regarding the pile type and geometry, subsurface conditions, driving equipment, driving resistance obtained in field observations and static load test results. Twenty load test results require extrapolation to failure, two of which are in the range of possible increased error and require further monitoring. Large number of the cases contain dynamic measurements and relate to different driving times, allowing the examination of the actual driving system efficiency (energy transfer) and the variation of driving resistance with time. The developed database faces only one difficulty because the use of 16 inch diameter piles is very common in Minnesota bridges but not so common elsewhere. As a result, only 14 cases of 16 inch diameter piles had been acquired. The 14 obtained 16 inch diameter cases along with a large number of pipe piles with diameters marginally smaller (e.g. 29 cases of 14 inch pipes) and marginally larger (e.g. 12 cases of 18 inch pipes) should allow reliable evaluation of the dynamic equations and development, representing the 16 inch diameter cases.

3.7.2. Database Examination and Modification – Second Stage

Re-examination of the databases and some elimination and addition, essentially ended up with similar size database for both H and Pipe piles as were initially analyzed. The closer scrutiny as to the comparison between the assembled databases to Mn/DOT practices revealed that the energy transfer measured in the cases available in the database are very much similar to that measured on a very large number of piles, and the typical diesel hammer stroke is very similar to that recommended by the Mn/DOT to be used when actual stroke measurements are not available.

3.7.3. Relevance for Analysis

The presented databases are ready for the analyses and research for which they were developed. As Mn/DOT practice relates to diesel hammers only and typically pile driving to 4bpi or more at the end of driving, sub-categorization based on hammer type and blow count will be followed.

CHAPTER 4 DATABASE ANALYSES - PART I

4.1 OBJECTIVES

Analysis of all relevant case histories of the databases using at least four dynamic equations including (1) Mn/DOT equation, (2) FHWA modified Gates, (3) ENR, and (4) Washington State DOT. The analyses presented in Chapter 4 are related to the databases developed in the first stage of the research (see Chapter 3 sections 3.1 to 3.6).

4.2 PLAN OF ACTION

The required actions included:

1. Evaluate the static capacity of all tested piles using Davisson's failure criterion (described in Chapter 3).
2. Final review of the databases and eliminate inadequate/questionable cases.
3. Evaluate the pile capacity of the database case histories using five different dynamic equations.
4. Evaluate the bias of each method, being the ratio between the measured capacity (static load test, #1 above) to the capacity calculated by the specific method (as outlined in #3 above).
5. Examine the above calculated values and relations in various ways in order to obtain insight as to the obtained results.
6. Develop the resistance factors associated with the different equations and their condition of application.

4.3 INVESTIGATED EQUATIONS

Table 4.1 summarizes the investigated dynamic equations. The format of the ENR equation presented in Table 4.1 is the original equation and not the so called "modified" or "new" ENR, which has a 2 instead of a 12 in the numerator, hence contains a factor of safety of 6. This is the equation presented in the AASHTO specification calibrations but not the one traditionally used and calibrated in Paikowsky et al. (2004). The format of the Mn/DOT equation is the one in which a uniform equation is applied to all pile types. This format was initially presented as the preferable format for the LRFD application and calibration.

4.4 DATA ANALYSIS – H PILES

4.4.1 Summary of Results

Table 4.2 presents a summary of the statistics and other information related to the dynamic equations presented in Table 4.1, along with the new Mn/DOT dynamic equation, to be presented in Chapter 6. The information and graphs related to the new Mn/DOT equation were kept in this section for completion only, allowing its presentation next to the examined equations. The number of cases analyzed in Table 4.2 refers to the following:

Table 4.1 – Investigated Equations

Eq #	Equation	Description	Reference
4.1	$R_u = \frac{12(W_r * h)}{S + 0.1}$	Drop Hammer	Engineering News-Record (1892)
4.2	$R_u = 27.11\sqrt{E_n * e_h}(1 - \log s)$		Gates (1957)
4.3	$R_u = 1.75\sqrt{E_n} * \log(10 * N) - 100$	Modified Gates Equation	FHWA (1982)
4.4	$R_u = 6.6 * F_{eff} * E * Ln(10N)$		Washington State DOT (Allen, 2005)
4.5	$R_u = \frac{10.5E}{S + 0.2} x \frac{W + 0.1M}{W + M}$	Uniform Format for all piles	Minnesota DOT (2006)
4.6	$R_u = 35\sqrt{E_h} \times \log(10N)$	See Chapter 6 for details	First Stage Proposed New Mn/DOT Equation

Notes:

R_u= ultimate carrying capacity of pile, in kips
W= mass of the striking part of the hammer in pounds
M= total mass of pile plus mass of the driving cap in pounds
E= developed energy, equal to W times H, in foot-kips (1.4)
E= energy per blow for each full stroke in foot-pounds (1.5)
e_h= efficiency
E_n= rated energy of hammer per blow, in kips-foot
Ln= the natural logarithm, in base "e"
W_r= weight of falling mass, in kips
s= final set of pile, in inches
N= blows per inch (BPI)
h= height of free fall of ram, in feet
F_{eff}= hammer efficiency factor

Table 4.2 – Dynamic Equation Predictions for all H-Piles

Equation	No. of Cases (n)	Mean Bias Measured/ Calculated (m_λ)	Stand. Dev. (σ_λ)	Coef. of Var. (COV_λ)	Best Fit Line Equation (least square)	Coefficient of Determina-tion (r^2)	Resistance Factor ϕ β=2.33, p_f=1%, Redundant			ϕ/λ Efficiency Factor (%)
							FOSM	MC[3]	Recom	
ENR	135	0.2936	0.2163	0.7365	Ru[1]=5.069*[2]Rs	0.777	0.063	0.067 0.066	0.05	22.1
Gates	135	1.4470	0.5208	0.3599	Ru=0.612*Rs	0.880	0.697	0.781 0.771	0.75	51.8
Modified Gates	135	0.8182	0.3237	0.3956	Ru=1.168*Rs	0.875	0.365	0.408 0.400	0.40	48.9
WSDOT	135	0.8697	0.3254	0.3742	Ru=1.225*Rs	0.851	0.406	0.454 0.448	0.45	51.7
Mn/DOT	135	0.8408	0.5470	0.6796	Ru=1.574*Rs	0.761	0.203	0.217 0.213	0.20	23.8
New Mn/DOT	135	1.0291	0.3704	0.3599	Ru=0.860*Rs	0.880	0.496	0.556 0.548	0.55	53.4

Notes: 1. Ru is the calculated capacity using each of the dynamic formulae.
2. Rs is the Static Capacity of the pile determined by Davisson's Failure Criterion.
3. MC - Monte Carlo Simulation upper values for 10,000 simulations, lower values for 100,000 simulations

1. 137 H pile cases were presented in section 3.4.1.
2. Two (2) cases were excluded as one (1) case had a large load extrapolation ratio (case MH-92, see H-234 in Table 3.3 HP14×84), and one case had incomplete driving data (MH-24, HP12×89).
3. This 135 piles refer to 163 cases when multiple restrikes are included.
4. Out of the 135 cases, 125 cases have EOD data and 10 of the cases have BOR only. Hence, first restrike data was used in Table 4.2 for the presented information. A further separation to 125 EOD cases only is presented in section 4.4.3.

The analyzed data in Table 4.2 are presented in the following way (referring to the columns from left to right):

1. Equation – see Table 4.1 and for the new Mn/DOT details, see Chapter 6.
2. Number of piles analyzed including 125 EOD and 10 first restrike data.
3. m_λ the mean of the bias of all cases. The bias being the ratio of the measured static capacity (Davisson failure criterion) to the predicted capacity of the same case using the relevant equation presented in column 1.
4. Standard deviation of the bias.
5. Coefficient of Variation ($COV_\lambda = \sigma_\lambda/m_x$).
6. The equation of the best fit line (using linear regression analysis by the least square error method) between the measured (R_s) to the calculated (R_u) pile capacity (graphical presentation to follow).
7. Coefficient of determination (r^2) of the equation presented in column 6 where $r^2 = 1$ is a perfect match. Paikowsky et al. (1994) suggested the following guidelines for r^2 when applied to geotechnical data interpretations: $r^2 \geq 0.80$ good correlation, $0.60 \leq r^2 < 0.80$ moderate correlation, and $r^2 < 0.60$ poor correlation.
8. Resistance factor, ϕ, evaluated in three ways:
   a. FOSM – First Order Second Moment, using the closed form solution proposed by Barker et al. (1991):

$$\phi = \frac{\lambda_R\left(\frac{\gamma_D Q_D}{Q_L}+\gamma_L\right)\sqrt{\left[\frac{\left(1+COV_{Q_D}^2+COV_{Q_L}^2\right)}{\left(1+COV_R^2\right)}\right]}}{\left(\frac{\lambda_{Q_D} Q_D}{Q_L}+\lambda_{Q_L}\right)\exp\left\{\beta_T\sqrt{\ln\left[\left(1+COV_R^2\right)\left(1+COV_{Q_D}^2+COV_{Q_L}^2\right)\right]}\right\}} \tag{4.7}$$

   λ_R = resistance bias factor; COV_R = COV of the resistance
   COV_{Q_L} = COV of the live load; COV_{Q_D} = COV of the dead load
   β_T = target reliability index; γ_D, γ_L = dead and live load factors
   Q_D/Q_L = dead to live load ratio; λ_{QD},λ_{QL} = dead & live load bias factors

   b. MC – Monte Carlo Simulation. Using two sets of simulations, 10,000 simulations (upper value) and 100,000 simulations (lower values).
   c. Recommended resistance factors, considering the results obtained by FOSM and MC simulation and rounded for practicality to the closest 0.05 accuracy.

9. Efficiency factor, ϕ/λ, is a measure for evaluating the relative efficiency of the design methods. The ratio is systematically higher for methods which predict more accurately and hence more economically effective to be used, regardless of the absolute value of the resistance factor, for more details see Paikowsky et al. (2004).

All load factors and distributions were those selected by Paikowsky et al. (2004) for calibration of piles under vertical-axial load, namely: for live loads $\gamma_L = 1.75$, $\lambda_{QL} = 1.15$, $COV_{QL} = 0.20$, and for dead loads $\gamma_D = 1.25$, λ_{QD}, = 1.05, $COV_{QD} = 0.10$. The target reliability of $\beta = 2.33$, $p_f = 1\%$ associated with redundant pile support (five or more piles) is used.

4.4.2 Presentation of Results

The uncertainty of the 135 H-pile cases analyzed by the different dynamic equations and summarized in Table 4.2 are presented graphically in this section. The data, related to each of the six (6) investigated methods, are presented repetitively in Figures 4.1 through 4.6 in a format of four (4) relations in the following way:

i) *Figure (a)* – presenting the scatter of the data using the vertical axis for the calculated capacity and the horizontal axis for the measured static capacity. The data are subdivided to the major pile types such that the 135 H-pile cases are categorized into five (5) size groups ranging from HP 10×92 and HP 11×75 to HP 14×117. Two lines are added to each of the scatter graphs; a best fit line equation presented as a dashed line, and measured capacity equal to calculated capacity presented as a continuous black line. The scatter of the data allows the evaluation of the prediction as well as the amount of conservatism or risk associated with the prediction. For example, all data above the solid line means that the calculated capacity is higher than the measured capacity and hence on the unsafe side. See, for example, the large number of overpredicted cases in Figure 4.5(a) relating to the current Mn/DOT equation.
ii) *Figure (b)* – presenting the scatter of the data using the vertical axis for the bias calculated for each case (ratio of measured to calculated capacity) and the horizontal axis as the measured capacity, in a similar way to Figure (a). The presentation comes to identify if the bias of the method is associated with the capacity of the pile. In particular, for the cases in which the bias is smaller than one, the predicted capacity is higher than the measured capacity, therefore being on the unsafe condition. In order to assist with the evaluation of the bias's magnitude, two lines were added; one presenting the mean bias for all cases and the other the two (2) standard deviation boundary beyond which the cases are clear outliers of the method, in this case on the conservative side. For example, examining the Gates method in Figure 4.2(b) suggests increase in the bias with increase in the capacity and six (6) cases being very conservative and most significant un-conservative (dangerous) cases to be in the zone of static capacity smaller than 200kips. In contrast, examining the existing Mn/DOT method in Figure 4.5(b) suggests no correlation between the bias and the magnitude of the static capacity and large number of unsafe cases over a large range of capacity (0 to 800kips).
iii) *Figures (c) and (d) – Factors affecting the Dynamic Methods* – Paikowsky et al. (1994) theorized and demonstrated that the inaccuracy of the dynamic methods

(especially those simulated by the one-dimensional wave equation) is associated with theoretical limitation of the problem formulation by which the inertia of the soil displaced during penetration is not being taken into consideration. As such, larger soil inertia will result in a large energy loss that is not connected to the work done by the pile in resisting the penetration, resulting in a larger inaccuracy in the prediction. The displaced soil inertia is mostly pronounced at the tip of the pile and should be associated with the size of the pile tip and its acceleration. The area of the tip is a varying factor more associated with the relative importance of the soil at the tip to that in the circumference and hence the parameter area ratio was developed:

$$A_R = A_{skin} / A_{tip} = \text{Area of soil in contact with the pile skin/tip area} \qquad (4.8)$$

The effect of the tip soil movement becomes smaller as the pile penetration is getting larger, for example, assuming a closed-ended pipe pile:

$$A_R = \frac{2\pi R \times D}{\pi R^2} = \frac{2D}{R}$$

D = penetration depth
R = pile diameter

such that a 14inch O.D. pile has an area ratio of 69 at a depth of 20ft and an area ratio of 360 at a depth of 105ft. Area ratio smaller than 350 was found to be of importance (Paikowsky and Stenersen, 2000). The acceleration of the tip is associated with the measured blow count, hence the lower the blow count the higher the acceleration. A boundary of 4BPI was identified as significant by Paikowsky and Stenersen (2000), suggesting lower soil inertia effects for pile penetrations above 4BPI. These data are presented in the following way:

Figure (c) – presenting the relations between the bias on the vertical axis to the pile's area ratio on the horizontal scale.

Figure (d) – presenting the relations between the bias on the vertical axis to the driving resistance on the horizontal axis.

For example, examining the current Mn/DOT dynamic equation performance, Figure 4.5(c) suggests that the scatter increases when the area ratio exceeds a certain value (about 3000 to be checked). It is also evident that the performance of the equation becomes more consistent with a significantly lower scatter when the blow count exceeds 4BPI (referring to Figure 4.5(d)).

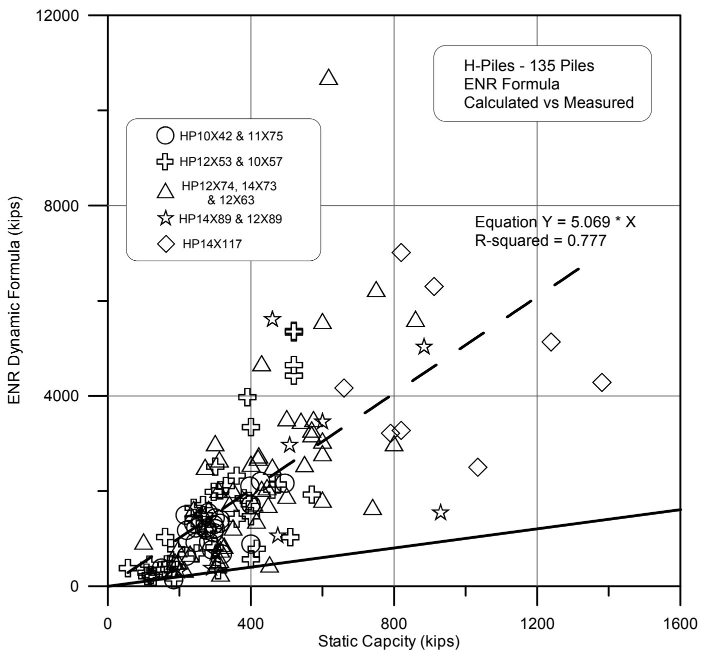

(a) Static Capacity vs. ENR Dynamic Formula

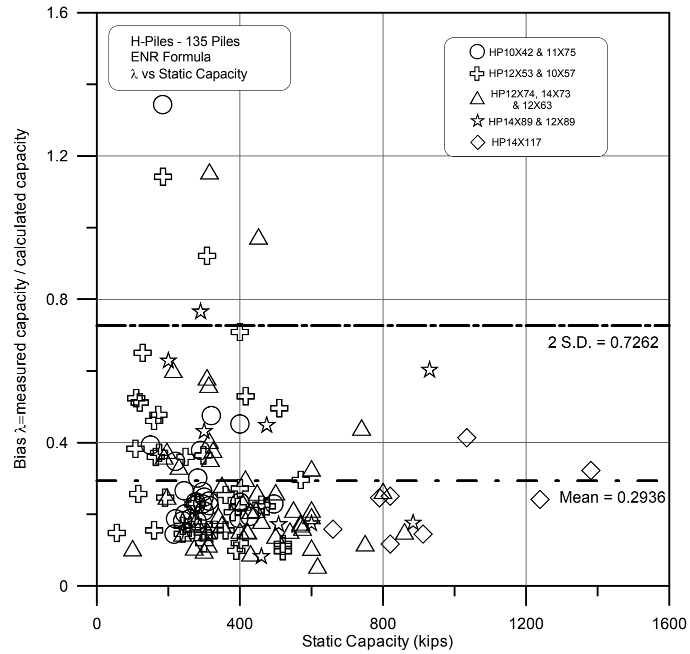

(b) Static Capacity vs. Bias

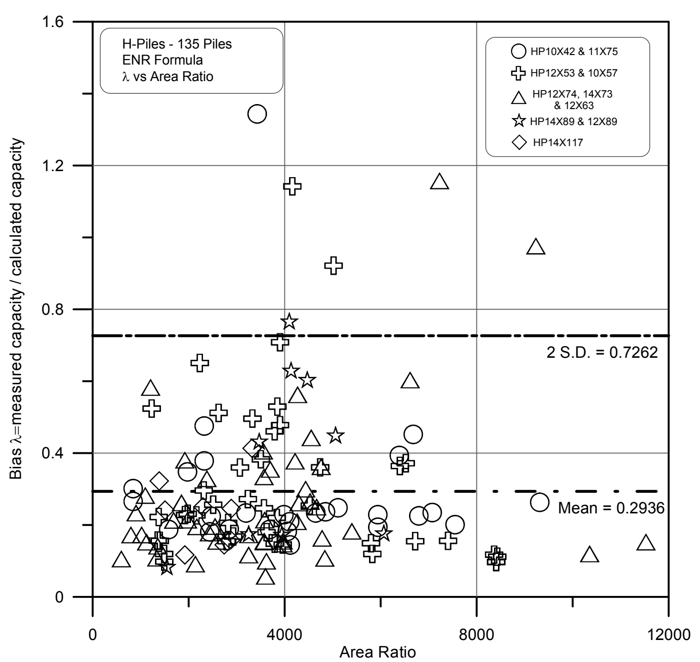

(c) Area Ratio vs. Bias

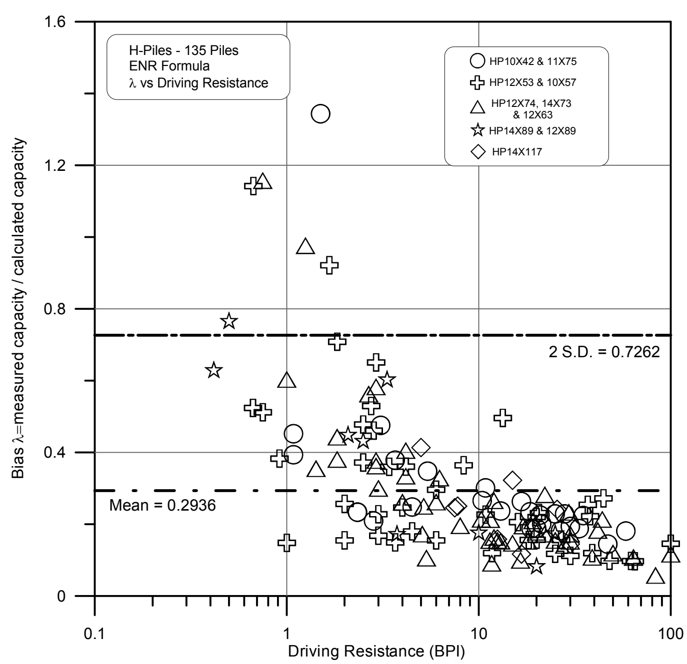

(d) Driving Resistance vs. Bias

Figure 4.1 ENR presentation of H-pile results (a) static capacity vs. ENR dynamic formula (b) Static capacity vs. bias (c) area ratio vs. bias (d) driving resistance vs. bias

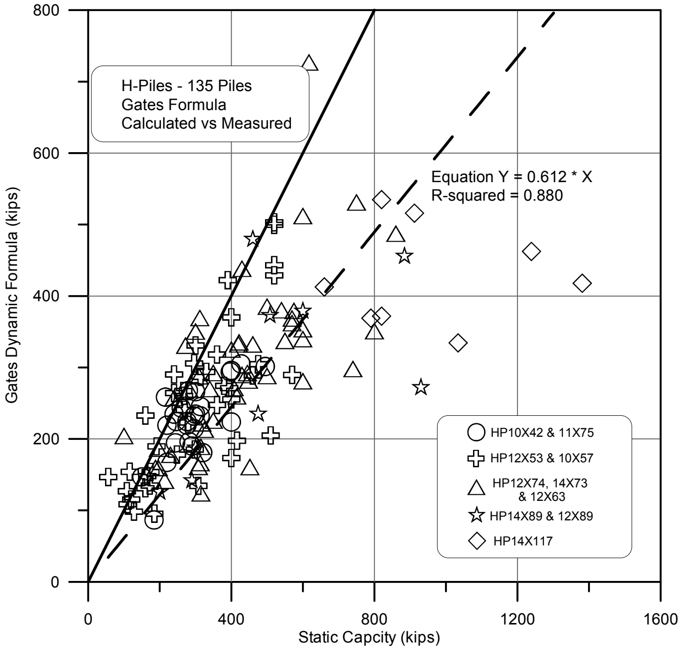

(a) Static Capacity vs. Gates Dynamic Formula

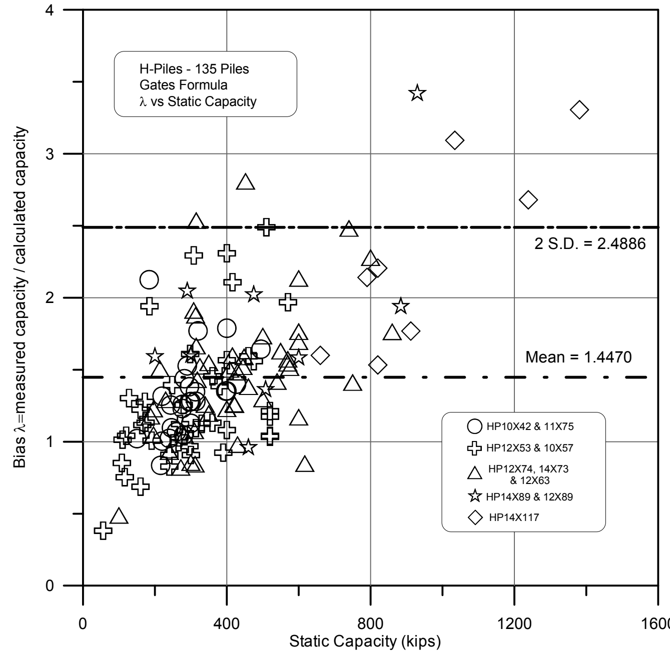

(b) Static Capacity vs. Bias

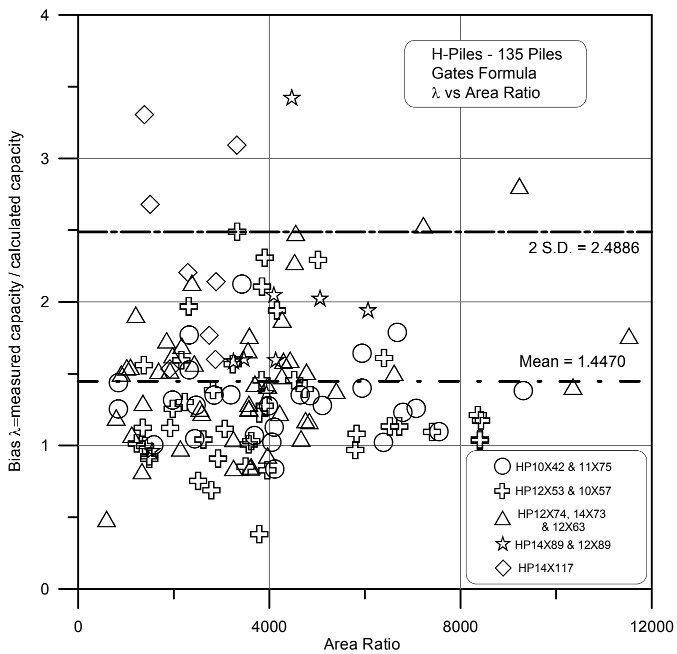

(c) Area Ratio vs. Bias

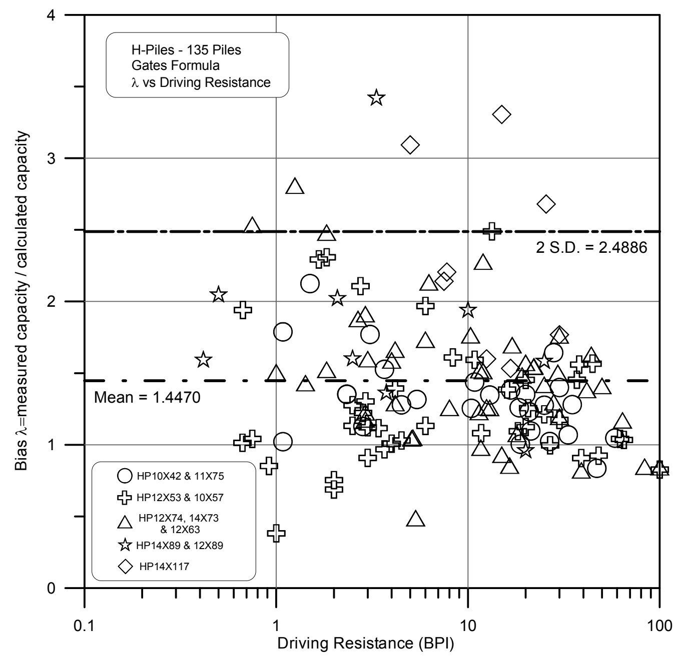

(d) Driving Resistance vs. Bias

Figure 4.2 Gates presentation of H-pile results (a) static capacity vs. gates dynamic formula (b) static capacity vs. bias (c) area ratio vs. bias (d) driving resistance vs. bias

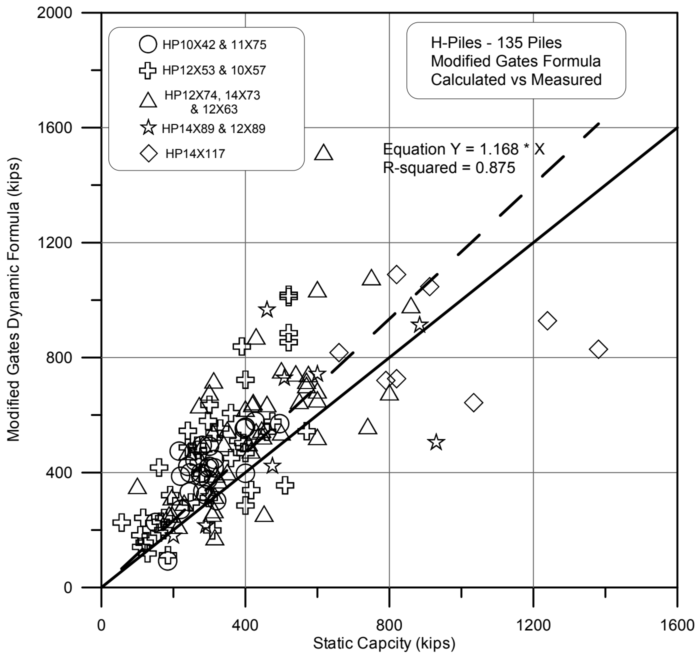

(a) Static Capacity vs. Modified Gates Dynamic Formula

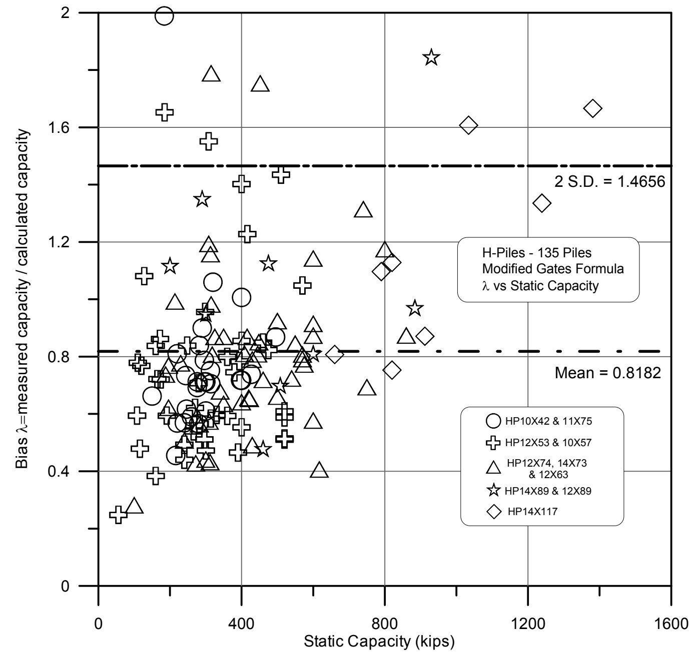

(b) Static Capacity vs. Bias

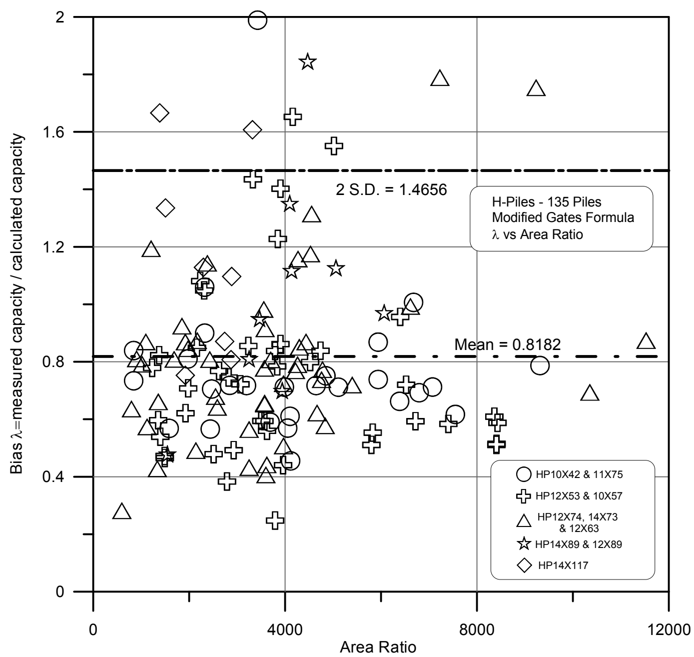

(c) Area Ratio vs. Bias

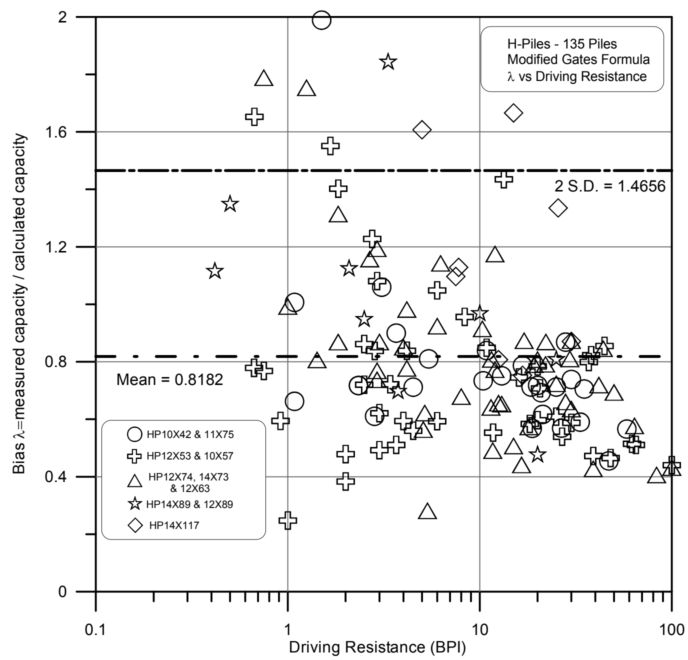

(d) Driving Resistance vs. Bias

Figure 4.3 Modified Gates presentation of H-pile results (a) static capacity vs. Modified Gates dynamic formula (b) static capacity vs. bias (c) area ratio vs. bias (d) driving resistance vs. bias

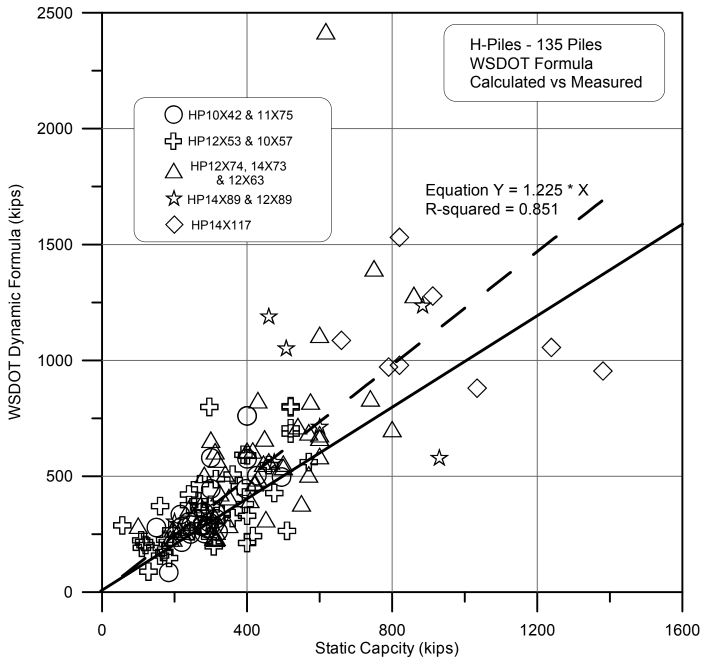

(a) Static Capacity vs. WSDOT Dynamic Formula

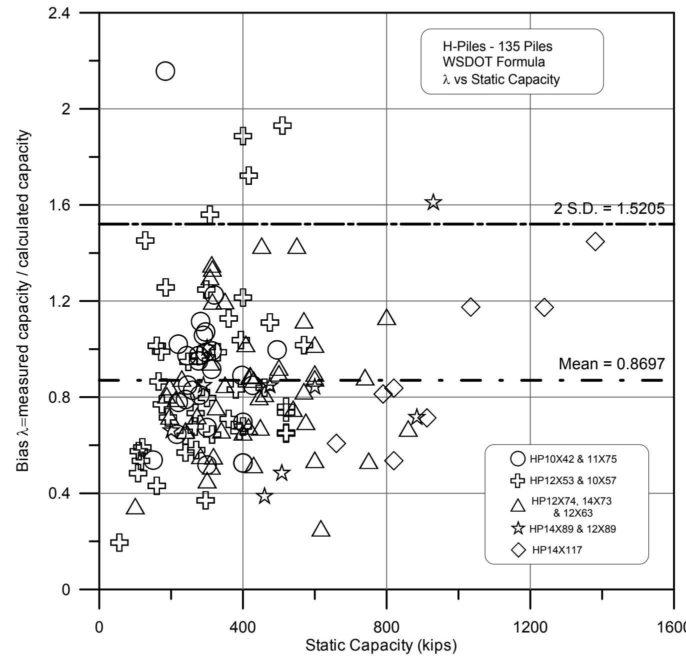

(b) Static Capacity vs. Bias

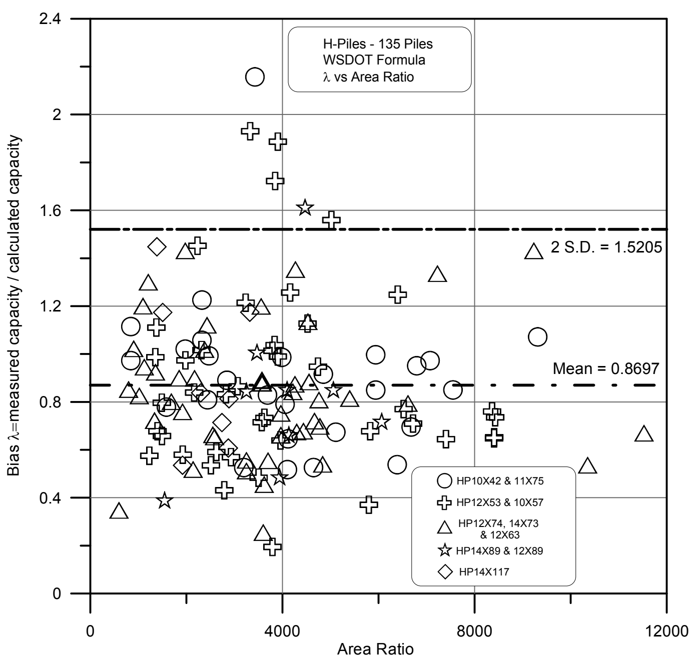

(c) Area Ratio vs. Bias

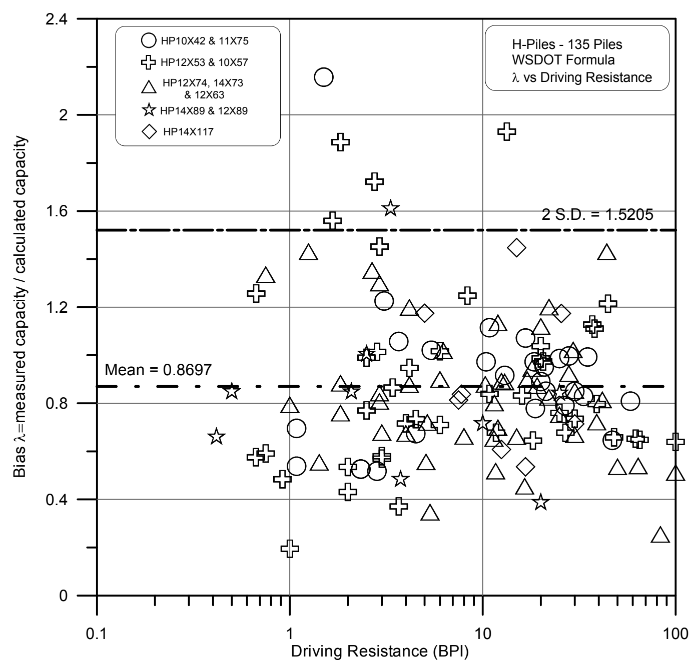

(d) Driving Resistance vs. Bias

Figure 4.4 WSDOT presentation of H-pile results (a) static capacity vs. WSDOT dynamic formula (b) static capacity vs. bias (c) area ratio vs. bias (d) driving resistance vs. bias

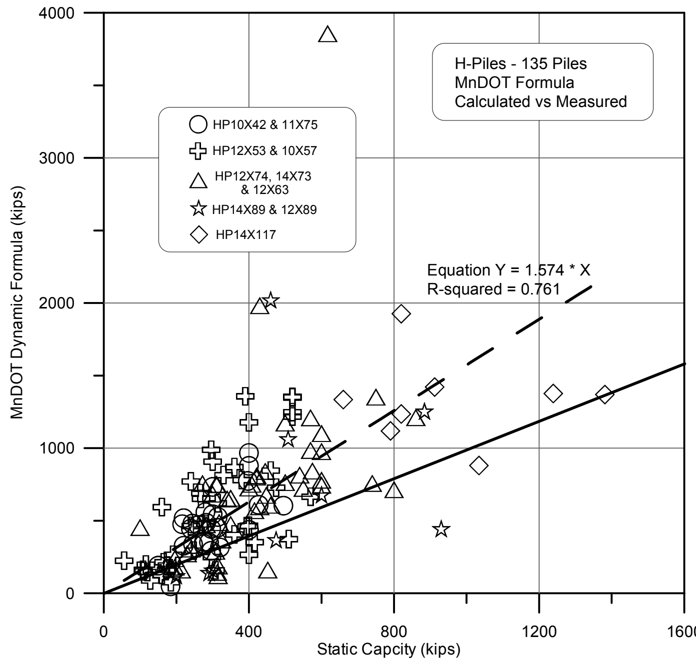

(a) Static Capacity vs. Mn/DOT Dynamic Formula

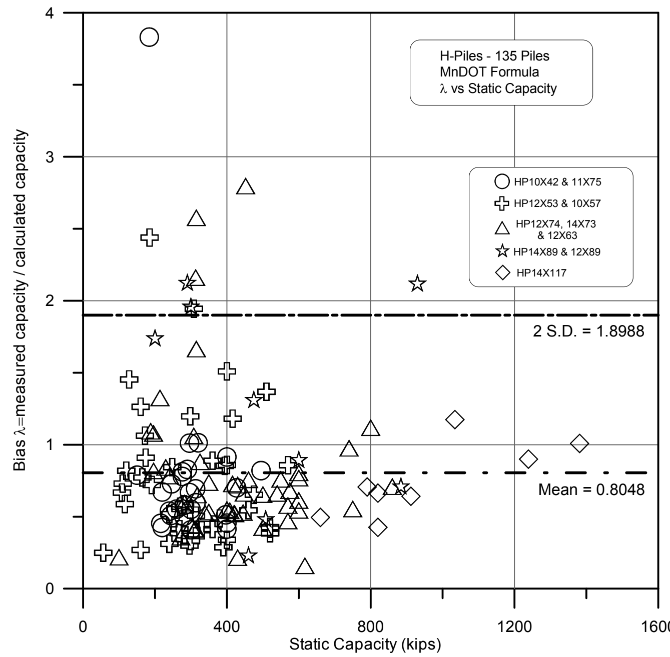

(b) Static Capacity vs. Bias

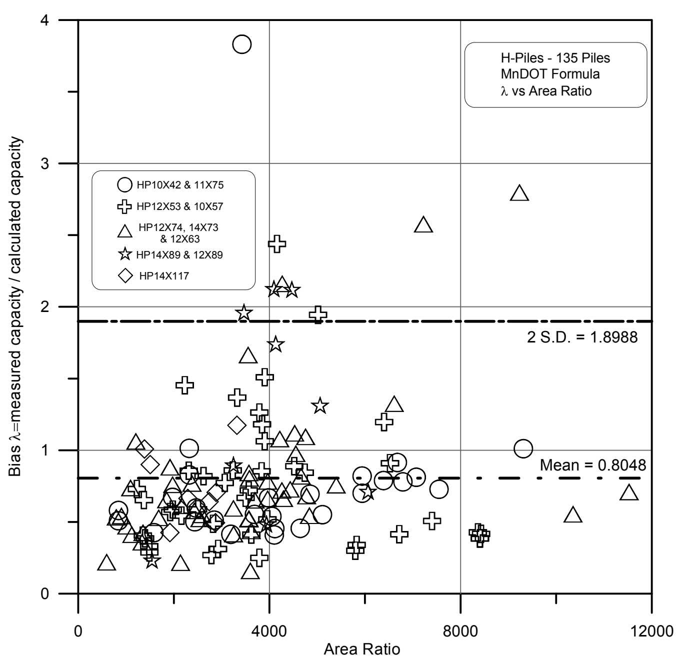

(c) Area Ratio vs. Bias

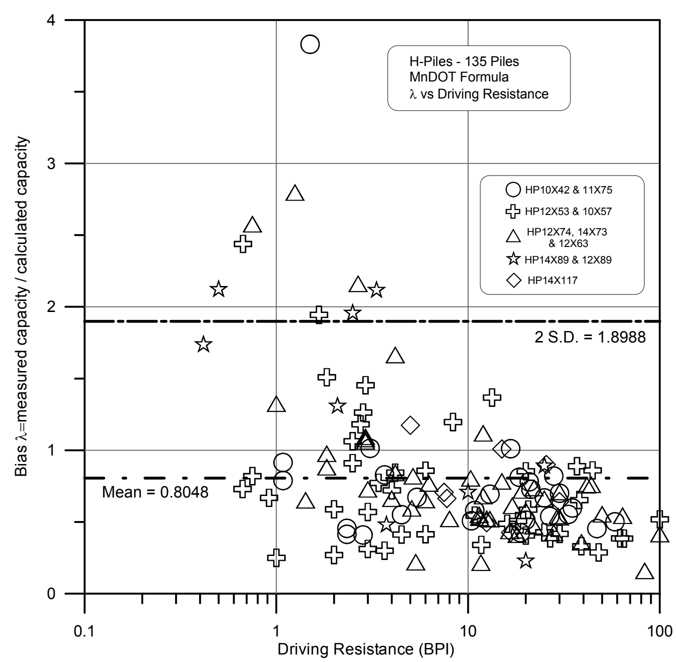

(d) Driving Resistance vs. Bias

Figure 4.5 Mn/DOT presentation of H-pile results (a) static capacity vs. Mn/DOT dynamic formula (b) static capacity vs. bias (c) area ratio vs. bias (d) driving resistance vs. bias

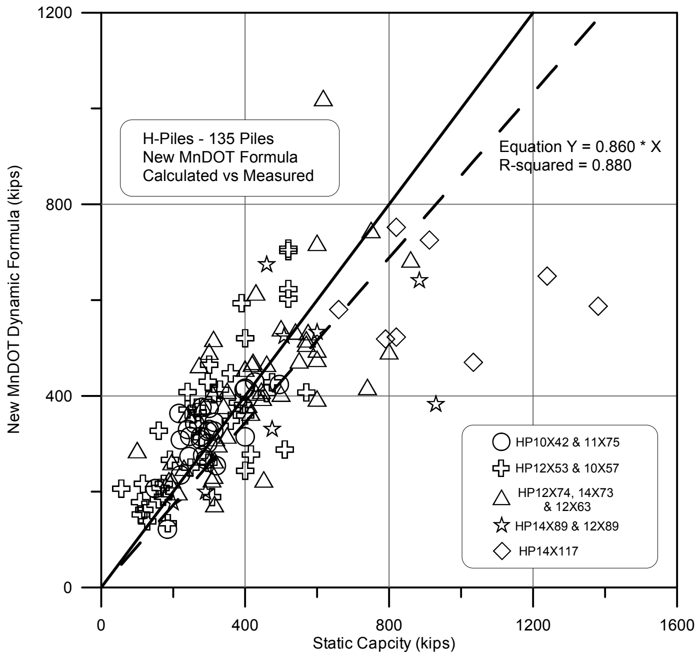

(a) Static Capacity vs. New Mn/DOT Dynamic Formula

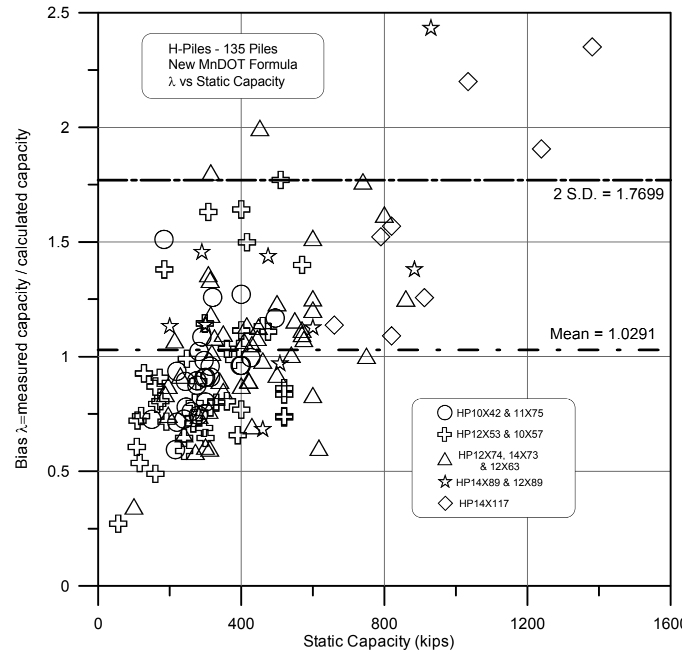

(b) Static Capacity vs. Bias

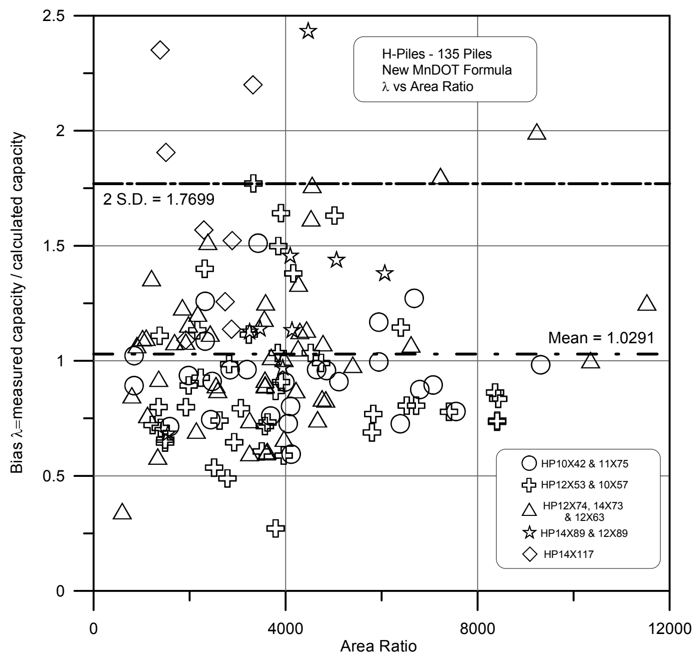

(c) Area Ratio vs. Bias

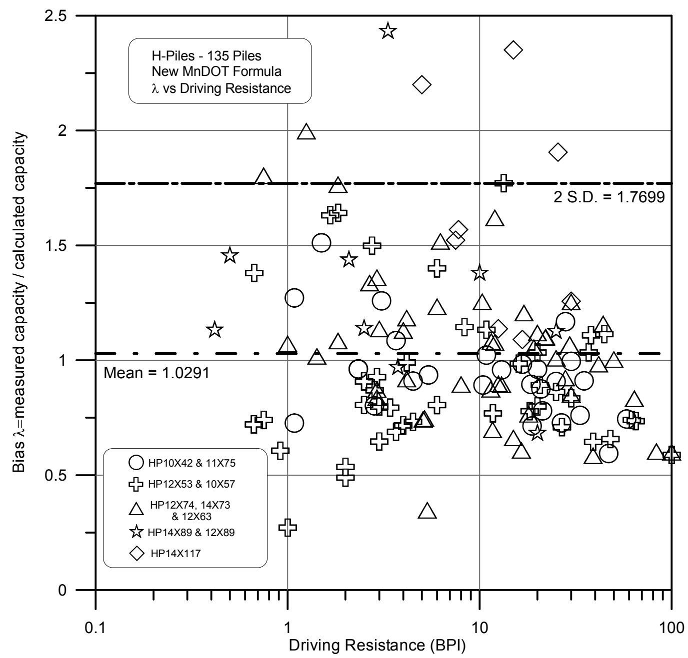

(d) Driving Resistance vs. Bias

Figure 4.6 New Mn/DOT presentation of H-pile results (a) static capacity vs. New Mn/DOT dynamic formula (b) static capacity vs. bias (c) area ratio vs. bias (d) driving resistance vs. bias

4.4.3 Analysis of EOD Data Only

While section 4.4.1 presented the data for all the H pile cases for which either EOD or BOR was provided, a subset of those cases was investigated for EOD only. Dynamic equations are aimed at EOD analyses. However, in some cases (e.g. capacity gain with time) the pile response during a restrike is evaluated as a better representation of the pile capacity. Similarly some states analyze EOD for refusal/end bearing piles and BOR for all other cases. As such, subsets of only EOD cases were evaluated and presented. The format of Table 4.3 is identical to that of Table 4.2, as outlined in section 4.4.1, hence, the explanation provided in section 4.4.1 for Table 4.2 should be used in reference to Table 4.3 as well.

Table 4.3 Dynamic Equation Predictions for H-Piles EOD Condition Only

Equation	No. of Cases (n)	Mean Bias Measured/ Calculated (m_λ)	Stand. Dev. (σ_λ)	Coef. of Var. (COV_λ)	Best Fit Line Equation (least square)	Coefficient of Determination (r^2)	Resistance Factor ϕ β=2.33, p_f=1%, Redundant			ϕ/λ Efficiency Factor (%)
							FOSM	MC[3]	Recom	
ENR	125	0.2976	0.2221	0.7465	Ru[1]=5.027*[2]Rs	0.819	0.062	0.066	0.05	16.8
Gates	125	1.4296	0.5056	0.3536	Ru=0.625*Rs	0.896	0.698	0.782	0.75	52.5
Modified Gates	125	0.8133	0.3229	0.3970	Ru=1.118*Rs	0.893	0.362	0.404	0.40	49.2
WSDOT	125	0.8718	0.3275	0.3756	Ru=1.223*Rs	0.901	0.406	0.454	0.45	51.6
Mn/DOT	125	0.8060	0.5537	0.6870	Ru=1.555*Rs	0.822	0.191	0.204	0.20	24.8
New Mn/DOT	125	1.0168	0.3596	0.3536	Ru=0.879*Rs	0.896	0.496	0.557	0.55	54.1

Notes: 1. Ru is the calculated capacity using each of the dynamic formulae.
2. Rs is the Static Capacity of the pile determined by Davisson's Failure Criterion.
3. MC – Monte Carlo Simulation for 10,000 simulations.

Comparison between the data analysis presented in Table 4.2 to that presented in Table 4.3 suggests very little variation in the H-piles performance when using the two data sets of 135 cases including 10 restriked piles (for which EOD data were not available), and the 125 cases database consisting only of the EOD H-pile cases of Table 4.3.

4.5 DATABASE ANALYSIS – PIPE PILES

4.5.1 Summary of Results

Table 4.4 presents a summary of the statistics and other information related to the dynamic equations presented in Table 4.1, along with the new Mn/DOT dynamic equation (for comparison only), to be presented in Chapter 6. The number of cases analyzed in Table 4.4 refer to the following:

1. 138 Pipe pile cases were presented in section 3.5.1.

2. Ten (10) cases were excluded as one (1) case had a large load extrapolation ratio (case P-11 in Table 3.3), and nine cases had incomplete data that could not have been obtained, resulting with 128 cases.
3. This 128 piles refer to 158 cases when multiple restrikes are included.
4. Out of the 128 cases, 102 cases have EOD data and 26 of the cases have BOR only. Hence, first restrike data was used in Table 4.4 for the presented information. A further separation to 102 EOD only cases is presented in section 4.5.3.

Refer to section 4.4.1 for details regarding the analyzed data in Table 4.4, being identical in format to that presented in Table 4.2.

Table 4.4 Dynamic Equation Predictions for all Pipe Piles

Equation	No. of Cases (n)	Mean Bias Measured/ Calculated (m_λ)	Stand. Dev. (σ_λ)	Coef. of Var. (COV_λ)	Best Fit Line Equation (least square)	Coefficient of Determination (r^2)	Resistance Factor ϕ β=2.33, p_f=1%, Redundant			ϕ/λ Efficiency Factor (%)
							FOSM	MC[3]	Recom.	
ENR	128	0.3047	0.3181	1.0439	Ru[1]=4.493*[2]Rs	0.767	0.0360	0.038	0.05	9.8
Gates	128	1.4947	0.7722	0.5157	Ru=0.387*Rs	0.907	0.5140	0.558	0.55	36.8
Modified Gates	128	0.8381	0.5031	0.6003	Ru=1.132*Rs	0.854	0.2400	0.256	0.25	29.8
WSDOT	128	0.7941	0.4510	0.5680	Ru=1.268*Rs	0.874	0.2430	0.262	0.25	31.5
Mn/DOT	128	0.7311	0.6606	0.9035	Ru=1.656*Rs	0.779	0.1120	0.118	0.10	13.7
New Mn/DOT	128	1.0650	0.5492	0.5157	Ru=.840*Rs	0.861	0.3660	0.397	0.35	32.9

Notes: 1. Ru is the calculated capacity using each of the dynamic formulae.
2. Rs is the Static Capacity of the pile determined by Davisson's Failure Criterion.
3. MC – Monte Carlo Simulation for 10,000 simulations.

4.5.2 Presentation of Results

Refer to section 4.4.2 for detailed explanation regarding the figures format and interpretations.

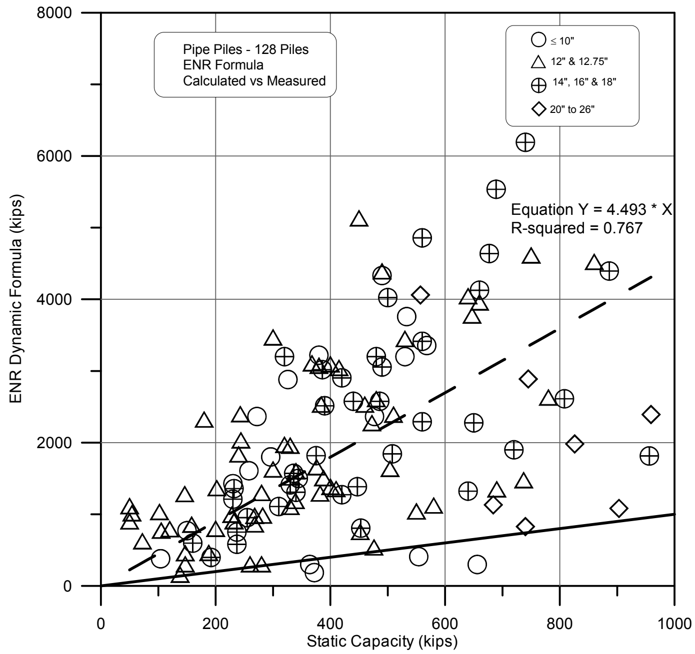

(a) Static Capacity vs. ENR Dynamic Formula

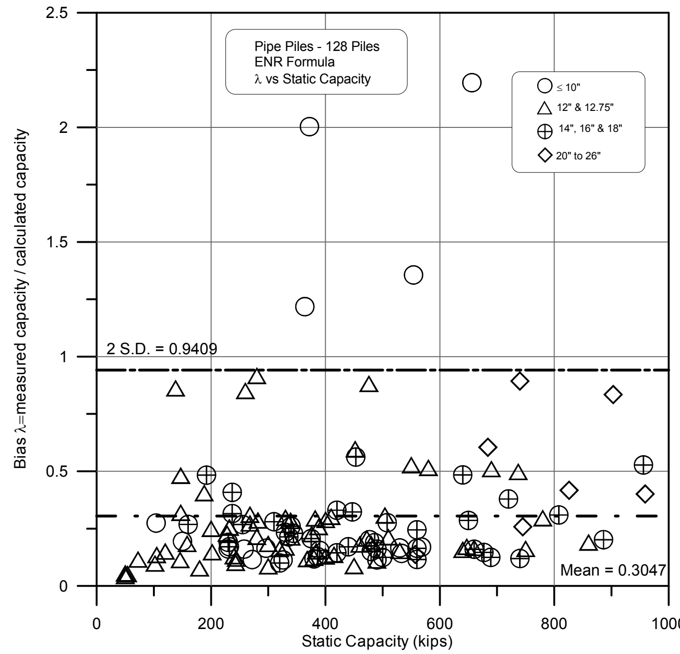

(b) Static Capacity vs. Bias

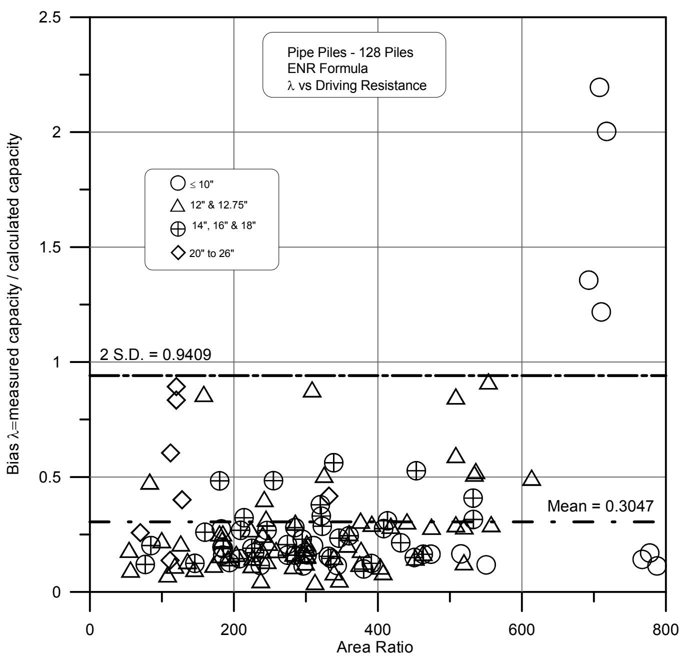

(c) Area Ratio vs. Bias

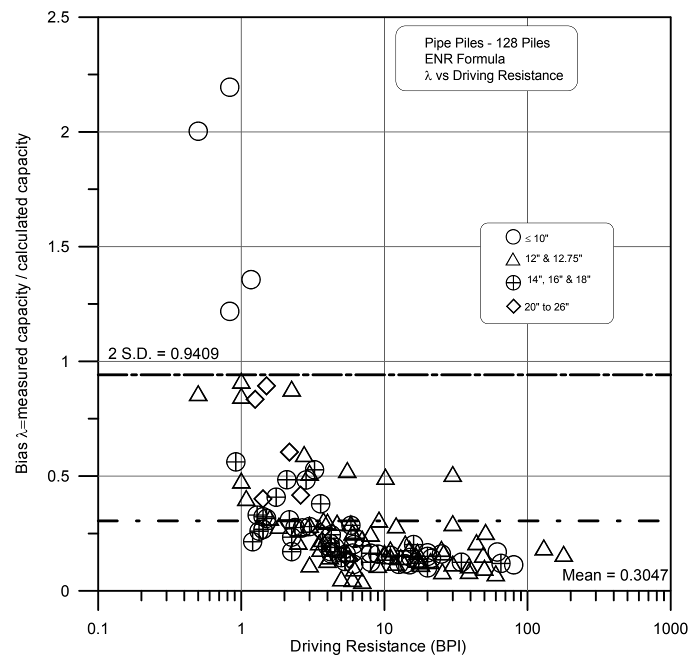

(d) Driving Resistance vs. Bias

Figure 4.7 ENR presentation of pipe pile results (a) static capacity vs. ENR dynamic formula (b) static capacity vs. bias (c) area ratio vs. bias (d) driving resistance vs. bias

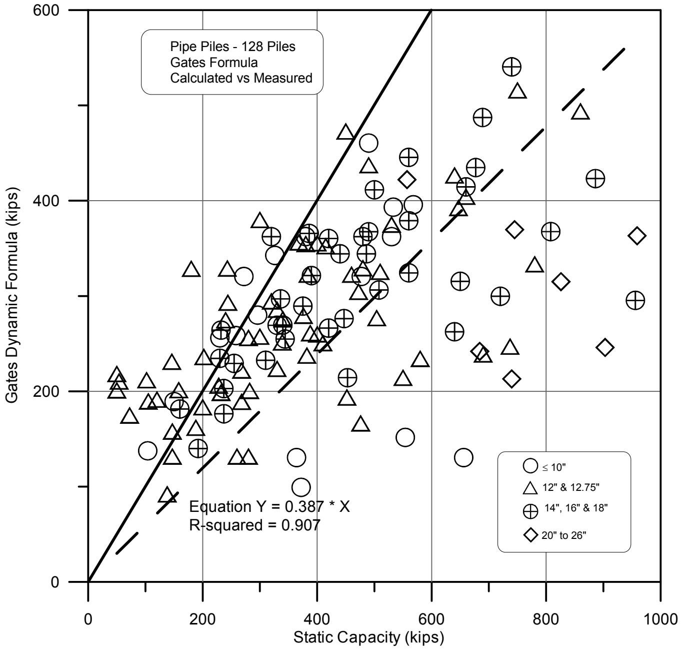

(a) Static Capacity vs. Gates Dynamic Formula

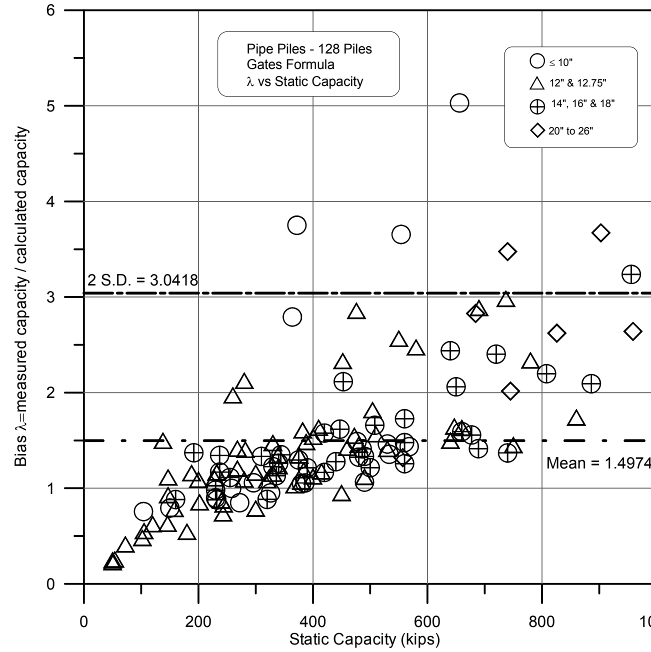

(b) Static Capacity vs. Bias

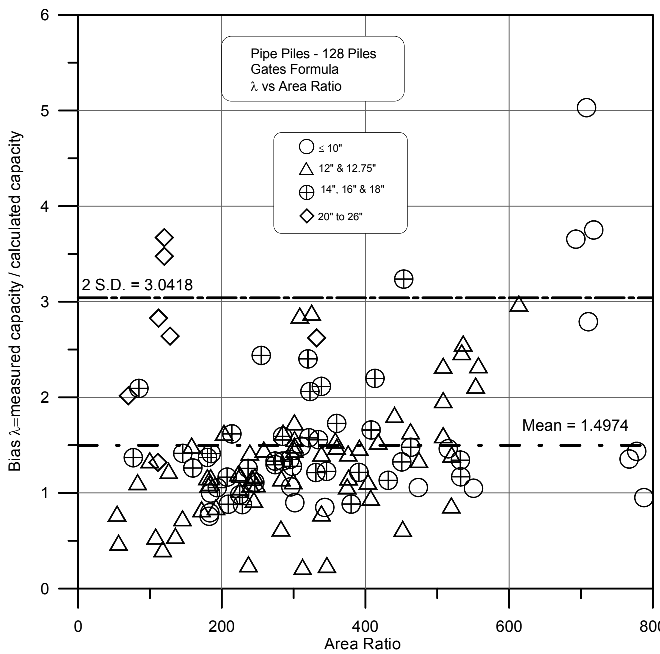

(c) Area Ratio vs. Bias

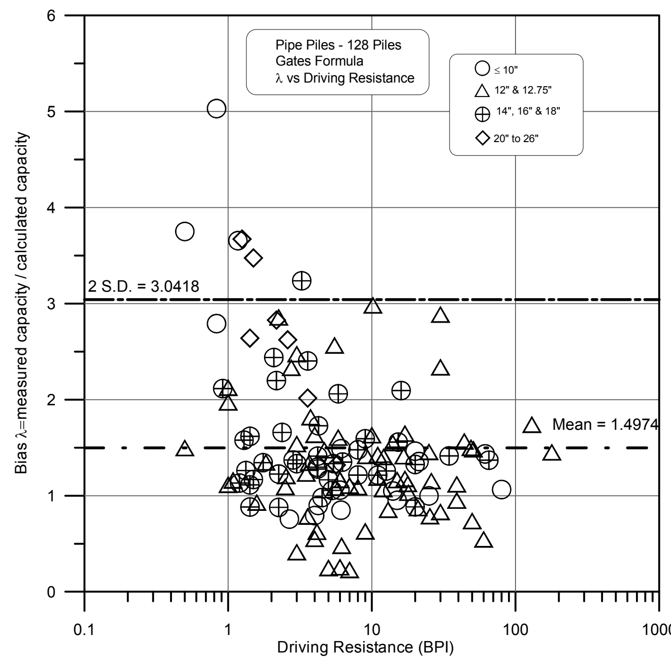

(d) Driving Resistance vs. Bias

Figure 4.8 Gates presentation of pipe pile results (a) static capacity vs. Gates dynamic formula (b) static capacity vs. bias (c) area ratio vs. bias (d) driving resistance vs. bias

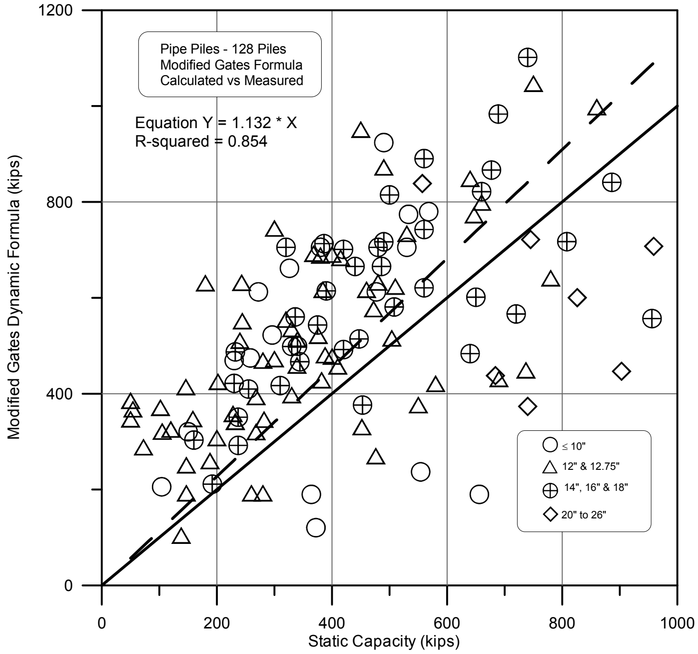

(a) Static Capacity vs. Modified Gates Dynamic Formula

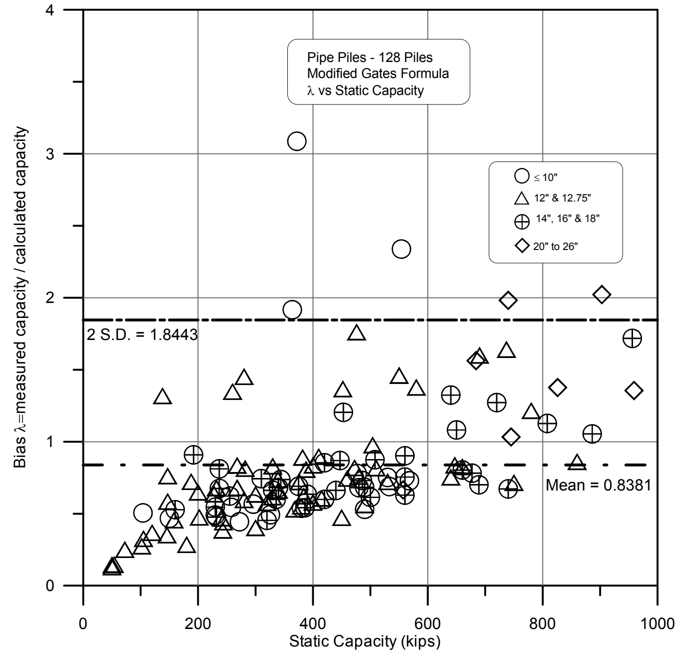

(b) Static Capacity vs. Bias

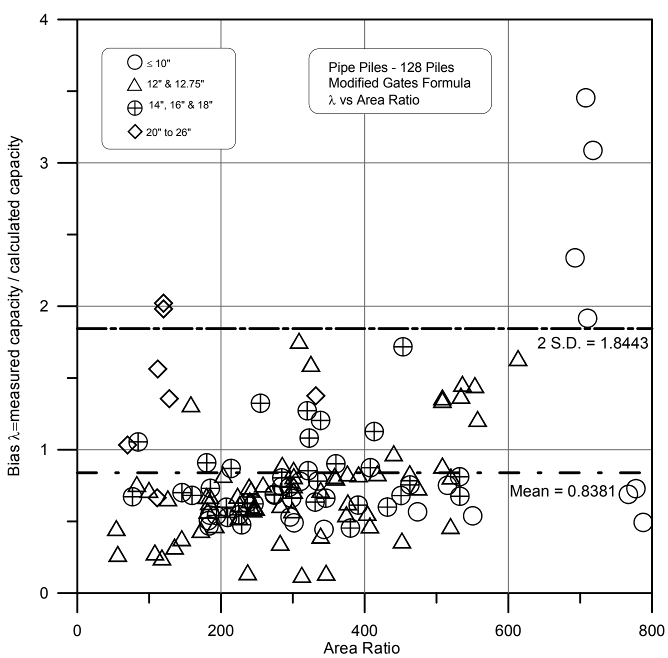

(c) Area Ratio vs. Bias

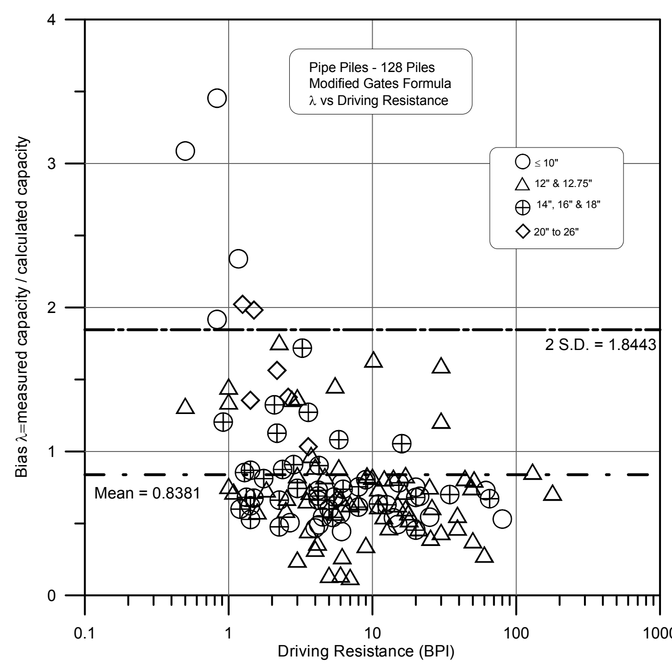

(d) Driving Resistance vs. Bias

Figure 4.9 Modified Gates presentation of pipe pile results (a) static capacity vs. Modified Gates dynamic formula (b) static capacity vs. bias (c) area ratio vs. bias (d) driving resistance vs. bias

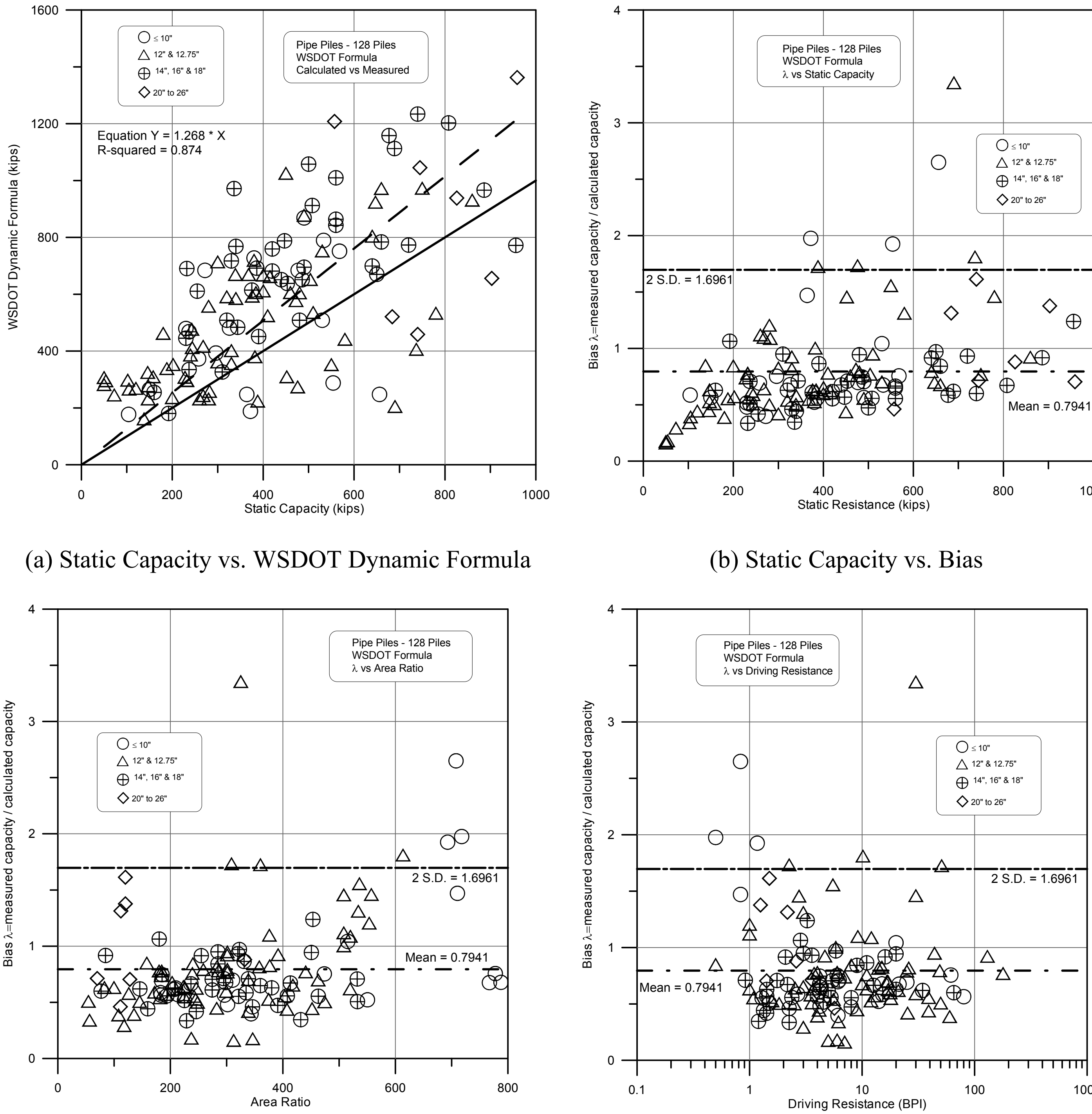

(a) Static Capacity vs. WSDOT Dynamic Formula

(b) Static Capacity vs. Bias

(c) Area Ratio vs. Bias

(d) Driving Resistance vs. Bias

Figure 4.10 WSDOT presentation of pipe pile results (a) static capacity vs. WSDOT dynamic formula (b) static capacity vs. bias (c) area ratio vs. bias (d) driving resistance vs. bias

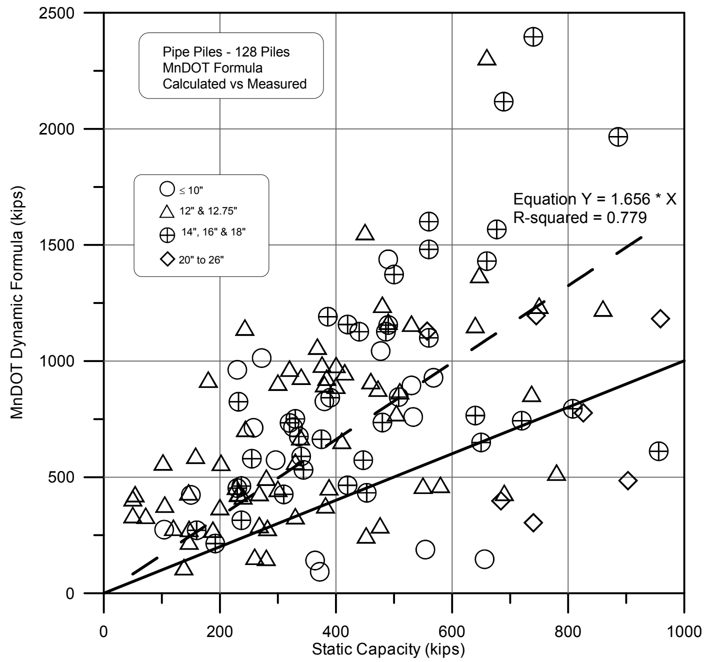

(a) Static Capacity vs. Mn/DOT Dynamic Formula

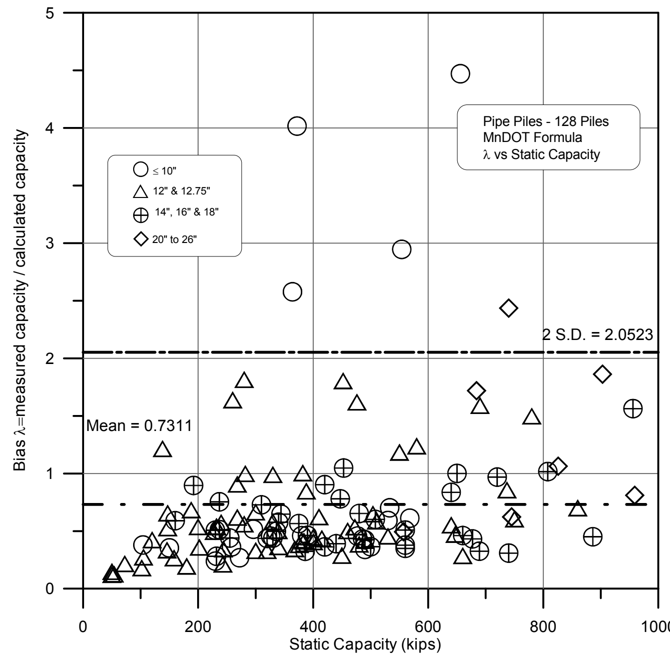

(b) Static Capacity vs. Bias

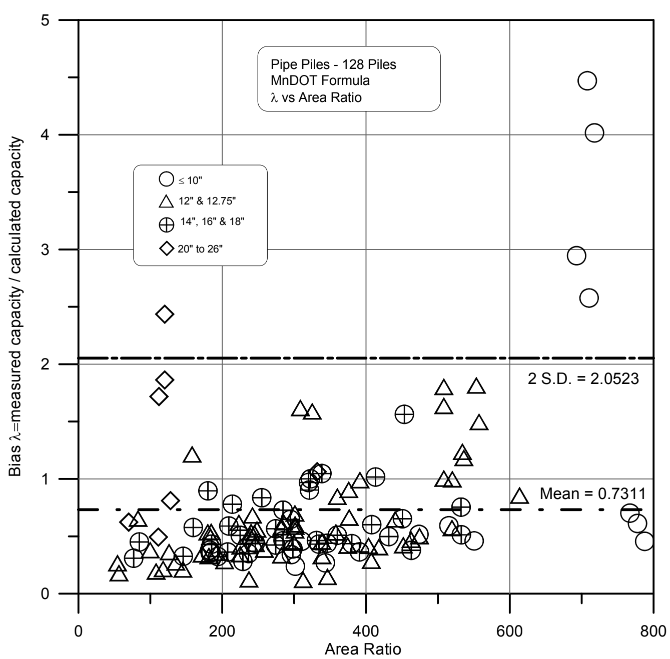

(c) Area Ratio vs. Bias

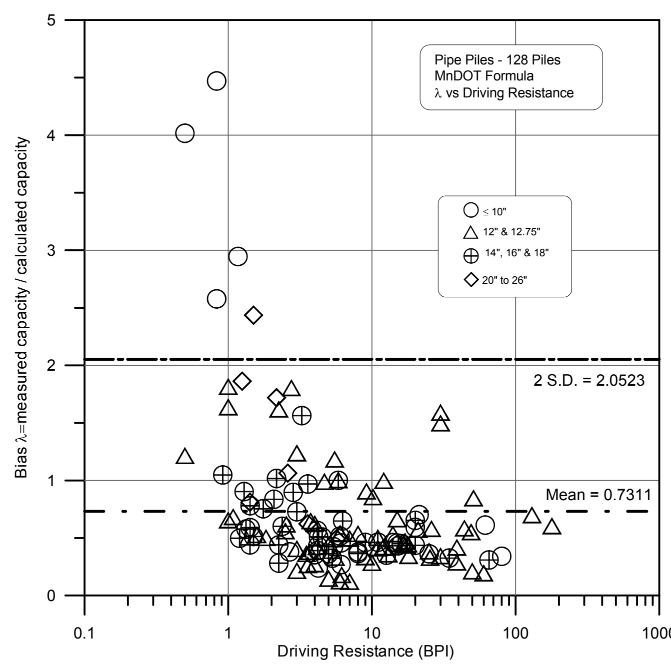

(d) Driving Resistance vs. Bias

Figure 4.11 Mn/DOT presentation of pipe pile results (a) static capacity vs. Mn/DOT dynamic formula (b) static capacity vs. bias (c) area ratio vs. bias (d) driving resistance vs. bias

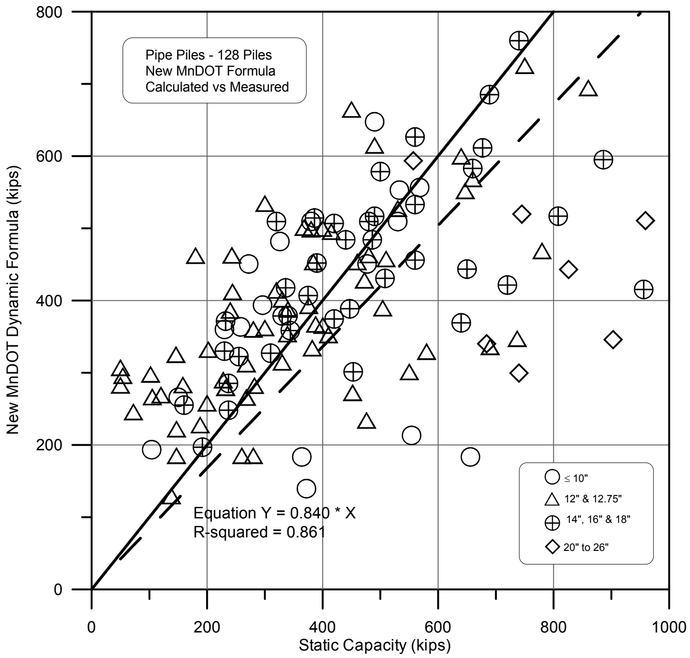

(a) Static Capacity vs. New Mn/DOT Dynamic Formula

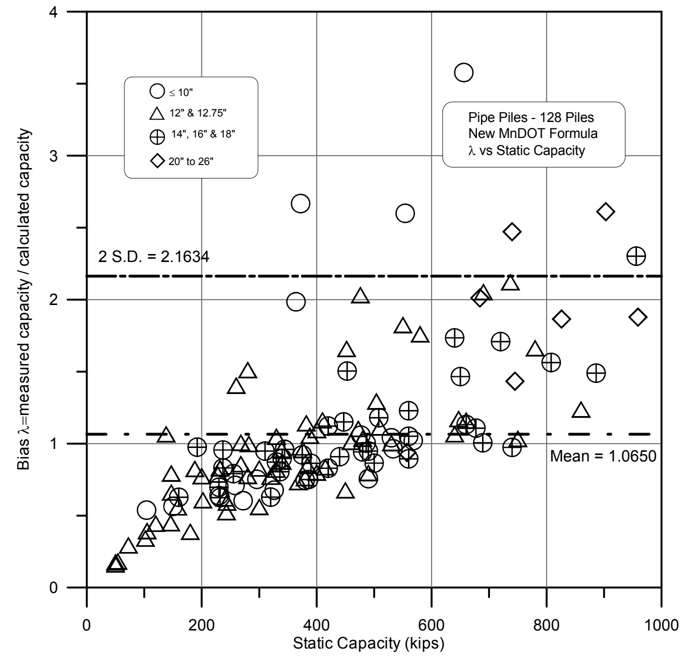

(b) Static Capacity vs. Bias

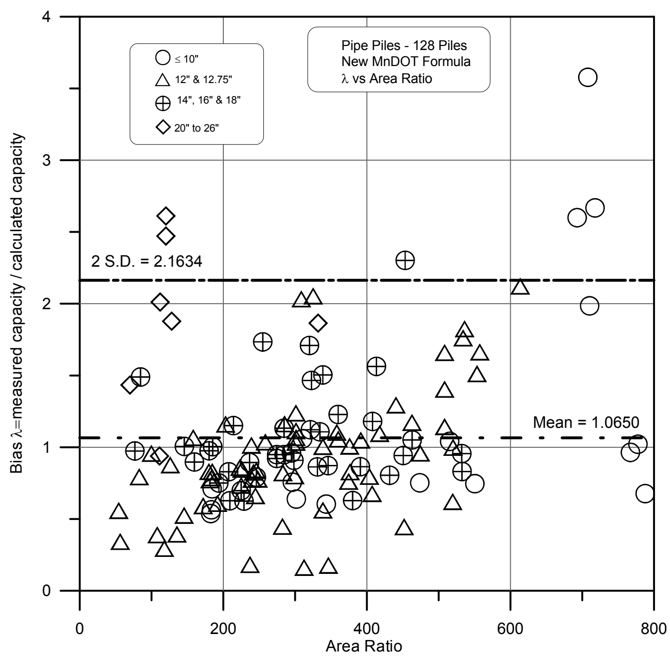

(c) Area Ratio vs. Bias

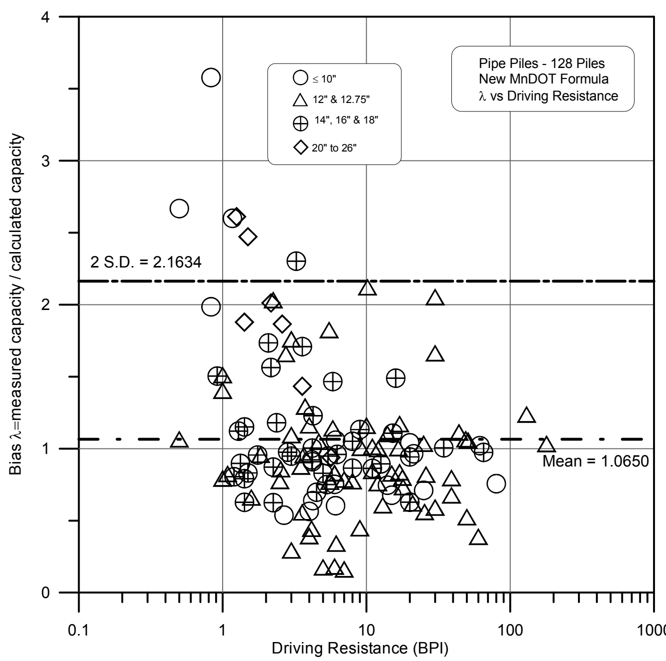

(d) Driving Resistance vs. Bias

Figure 4.12 New Mn/DOT presentation of pipe pile results (a) static capacity vs. New Mn/DOT dynamic formula (b) static capacity vs. bias (c) area ratio vs. bias (d) driving resistance vs. bias

4.5.3 Analysis of EOD Data Only

While section 4.5.1 presented the data for all the pipe pile cases for which either EOD or BOR was provided, a subset of those cases was investigated for EOD only. Dynamic equations are aimed at EOD analyses. However, in some cases (e.g. capacity gain with time) the pile response during a restrike is evaluated as a better representation of the pile capacity. Similarly some states analyze EOD for refusal/end bearing piles and BOR for all other cases. As such, subsets of only EOD cases were evaluated and presented. The format of Table 4.5 is identical to that of Table 4.2, as outlined in section 4.4.1, hence, the explanation provided in section 4.4.1 for Table 4.2 should be used in reference to Table 4.5 as well.

Table 4.5 Dynamic Equation Predictions for Pipe Piles EOD Condition Only

Equation	No. of Cases (n)	Mean Bias Measured/ Calculated (m_λ)	Stand. Dev. (σ_λ)	Coef. of Var. (COV_λ)	Best Fit Line Equation (least square)	Coefficient of Determination (r^2)	Resistance Factor ϕ β=2.33, p_f=1%, Redundant			ϕ/λ Efficiency Factor (%)
							FOSM	MC[3]	Recom	
ENR	102	0.3389	0.3474	1.0249	Ru[1]=4.157*[2]Rs	0.730	0.041	0.043	0.05	11.8
Gates	102	1.5754	0.8314	0.5278	Ru=0.570*Rs	0.850	0.527	0.572	0.55	34.9
Modified Gates	102	0.8913	0.5454	0.6119	Ru=1.079*Rs	0.841	0.248	0.265	0.25	28.0
WSDOT	102	0.8315	0.4934	0.5934	Ru=1.238*Rs	0.858	0.241	0.259	0.25	30.1
Mn/DOT	102	0.8107	0.7180	0.8856	Ru=1.495*Rs	0.755	0.128	0.136	0.15	18.5
New Mn/DOT	102	1.1205	0.5913	0.5278	Ru=0.802*Rs	0.851	0.375	0.407	0.40	35.7

Notes: 1. Ru is the calculated capacity using each of the dynamic formulae.
2. Rs is the Static Capacity of the pile determined by Davisson's Failure Criterion.
3. MC – Monte Carlo Simulation for 10,000 simulations.

Comparison between the data analysis presented in Table 4.3 to that presented in Table 4.5 suggests that elimination of the 26 cases associated with the beginning of restrike had resulted in a slight increase in the bias (approximately by 5% with 11% for the existing Mn/DOT equation) and a very small variation in the scatter as expressed by the COV; hence, resulting with similar calculated resistance factors other than a rounded up (by 0.05) resistance factors for the existing and new Mn/DOT equations.

4.6 PRELIMINARY CONCLUSIONS AND RECOMMENDATIONS

4.6.1 Mn/DOT Dynamic Equation – General Formulation

The following conclusions relate to the investigated format of the equation as presented in Table 4.1, i.e. uniform format for H and Pipe pile and the use of the nominal hammer energy and not 75% of that value if measured stroke is not available.

1. The investigated Mn/DOT equation provides on the average an over-predictive (unsafe) capacity resulting in a mean bias of 0.81 (statically measured capacity over dynamically predicted) for both H and pipe piles (total 227 cases) at the end of driving.
2. The investigated Mn/DOT equation performs poorly as the scatter of its predictions is very large, represented by coefficient of variation ratios for EOD predictions of 0.69 and 0.89 for H and pipe piles, respectively.
3. The recommended resistance factors to be used with the investigated Mn/DOT equation for EOD prediction and redundant pile support (5 or more piles per cap) are $\phi = 0.20$ for H piles, $\phi = 0.15$ for pipe piles.
4. An approximation of the equivalent safety factor can be performed by using the following relations based on Paikowsky et al. (2004):

$$F.S. \approx 1.4167 / \phi$$

   This means that the approximate Factor of Safety requires for the Mn/DOT is 8.0 due to the poor prediction reliability.
5. The use of $\phi = 0.40$ (F.S. ≈ 3.5) currently in place means that the probability of failure is greater than 1% overall. Special attention needs to be given to low capacity piles (statically less than 200kips) that for now should be avoided by keeping a driving criterion at the EOD of 4BPI or higher, and restrike friction piles in particular in clays and silty or mix soil conditions.

4.6.2 Other Examined Dynamic Equations

All other examined equations performed as expected, reasonably well. While their scatter is similar, having a COV of about 0.35 to 0.40 for H-piles and 0.52 to 0.61 for pipe piles, the bias of these methods is either too high (1.43 – 1.58) for the Gates equation, or too low (0.81 – 0.89) for the other equations. A rationale for the development of an independent Mn/DOT new dynamic equation is, therefore, presented and followed up in Chapter 6.

CHAPTER 5 DATABASE ANALYSES - PART II

5.1 OVERVIEW

Chapter 4 presented the basic analyses of all the evaluated dynamic formulas concentrating mostly on all cases (i.e., all pile sizes and all hammer types) and End of Driving (EOD) conditions. The Mn/DOT dynamic equation used in Chapter 4 relates to the uniform format (identical to both H and pipe piles) as presented in equation 4.5 (Table 4.1) without applying a measured stroke or alternatively, 75% of the hammer energy, being the Mn/DOT form of application, as reported by the Technical Advisory Panel (TAP).

Following comments made by the Technical Advisory Panel (TAP) for the project, a re-evaluation of the database was undertaken (described in section 3.6) and a new database analysis was conducted. This analysis and its relevance to Mn/DOT construction practices is described in the present chapter.

5.2 OBJECTIVES

Analysis of all case histories of the updated databases including: (1) five dynamic equations, and (2) detailed performance of the Mn/DOT equation under various conditions (e.g. time of driving, hammer type, energy level and driving resistance).

5.3 PLAN OF ACTION

The required actions include:

1. Evaluate the static capacity of all tested piles using Davisson's failure criterion (described in Chapter 3).
2. Evaluate the pile capacity of the database case histories using five different dynamic equations.
3. Evaluate the bias of each method, being the ratio between the measured capacity (static load test, #1 above) to the capacity calculated by the specific method (as outlined in #2 above).
4. Examine the above calculated values and relations under different driving conditions and criteria in order to obtain insight as to the sensitivity of the results to variation and the performance of the Mn/DOT under most strict sub-categorization of the general cases, e.g. all hammers vs. diesel hammers, and diesel hammers of specific energy range to all diesel hammers, etc.
5. Develop the resistance factors associated with the different equations and their condition of application.

5.4 INVESTIGATED EQUATIONS

Table 5.1 summarizes the investigated dynamic equations. The format of the ENR equation presented in Table 5.1 is the original equation and not the so called "modified" or "new" ENR, which has a 2 instead of a 12 in the numerator, hence contains a factor of safety of 6. This is the equation presented in the AASHTO specification calibrations but not the one traditionally used and calibrated in Paikowsky et al. (2004). The format of the Mn/DOT equation is the one in which a different factor is applied to the driven mass for driven H or pipe piles.

Table 5.1 Investigated Equations

Eq #	Equation	Description	Reference
5.1	$R_u = \frac{12(W_r * h)}{S + 0.1}$	Drop Hammer	Engineering News-Record (1892)
5.2	$R_u = 27.11\sqrt{E_n * e_h}(1 - \log s)$		Gates (1957)
5.3	$R_u = 1.75\sqrt{E_n} * \log(10 * N) - 100$	Modified Gates Equation	FHWA (1982)
5.4	$R_u = 6.6 * F_{eff} * E * Ln(10N)$		Washington State DOT (Allen, 2005)
5.5	$R_u = \frac{10.5E}{S + 0.2} x \frac{W + C * M}{W + M}$	Different format for H and pipe piles	Minnesota DOT (2006)
5.6	$R_u = 35\sqrt{E_h} \times \log(10N)$	See Chapter 6 for details	Proposed General New Mn/DOT Dynamic Equation

Notes:

R_u= ultimate carrying capacity of pile, in kips
W= mass of the striking part of the hammer in pounds
M= total mass of pile plus mass of the driving cap in pounds
E= developed energy, equal to W times H, in foot-kips (1.4)
E= energy per blow for each full stroke in foot-pounds (1.5)
e_h= efficiency
E_n= rated energy of hammer per blow, in kips-foot
C = 0.1 for timber, concrete and shell type piles, 0.2 for steel H piling
Ln= the natural logarithm, in base "e"
W_r= weight of falling mass, in kips
s= final set of pile, in inches
N= blows per inch (BPI)
h= height of free fall of ram, in feet
F_{eff}= hammer efficiency factor

5.5 DATABASE ANALYSIS – H PILES

5.5.1 Summary of Results

Table 5.2 presents a summary of the statistics and other information related to the dynamic equations presented in Table 5.1 under End of Driving conditions. The results of the equations are presented, along with the new General Mn/DOT dynamic equation (for comparison only), developed and detailed in Chapter 6. The number of cases analyzed in Table 5.2 refers to125 H pile cases at EOD as presented in section 3.6.1. These cases do not differ from the cases used in the analysis presented in section 4.4.3.

Table 5.2 Dynamic Equation Predictions for H-Piles EOD Condition Only

Equation	No. of Cases (n)	Mean Bias Measured/ Calculated (m_λ)	Stand. Dev. (σ_λ)	Coef. of Var. (COV_λ)	Best Fit Line Equation (least square)	Coefficient of Determination (r^2)	Resistance Factor ϕ β=2.33, p_f=1%, Redundant			ϕ/λ Efficiency Factor (%)
							FOSM	MC[3]	Recom	
ENR	125	0.2972	0.2223	0.7479	Ru[1]=5.031*Rs[2]	0.819	0.062	0.066	0.07	23.6
Gates	125	1.4289	0.5060	0.3542	Ru=0.626*Rs	0.896	0.697	0.761	0.75	52.5
Modified Gates	125	0.8129	0.3232	0.3976	Ru=1.189*Rs	0.893	0.361	0.393	0.40	49.2
WSDOT	125	0.8738	0.3290	0.3765	Ru=1.221*Rs	0.900	0.406	0.443	0.45	51.5
Mn/DOT	125	0.9842	0.6499	0.6604	Ru=1.268*Rs	0.833	0.247	0.260	0.25	25.4
New Mn/DOT[4]	125	1.0163	0.3599	0.3542	Ru=0.880*Rs	0.896	0.495	0.542	0.55	54.1

Notes: 1. Ru is the calculated capacity using each of the dynamic formulae.
2. Rs is the Static Capacity of the pile determined by Davisson's Failure Criterion.
3. MC - Monte Carlo Simulation for 10,000 simulations
4. New Mn/DOT formula uses a coefficient of 35.

The analyzed data in Table 5.2 are presented in the following way (referring to the columns from left to right):

1. Equation – see Table 5.1 and for the new Mn/DOT details, see Chapter 6.
2. Number of piles analyzed including 125 EOD cases.
3. m_λ the mean of the bias of all cases. The bias being the ratio of the measured static capacity (Davisson failure criterion) to the predicted capacity of the same case using the relevant equation presented in column 1.
4. Standard deviation of the bias.
5. Coefficient of Variation ($COV_\lambda = \sigma_\lambda/m_x$).
6. The equation of the best fit line (using linear regression analysis by the least square error method) between the measured (R_s) to the calculated (R_u) pile capacity (graphical presentation to follow).
7. Coefficient of determination (r^2) of the equation presented in column 6 where $r^2 = 1$ is a perfect match. Paikowsky et al. (1994) suggested the following guidelines for r^2 when applied to geotechnical data interpretations: $r^2 \geq 0.80$ good correlation, $0.60 \leq r^2 < 0.80$ moderate correlation, and $r^2 < 0.60$ poor correlation.
8. Resistance factor, ϕ, evaluated in three ways:
   a. FOSM – First Order Second Moment, using the closed form solution proposed by Barker et al. (1991):

$$\phi = \frac{\lambda_R \left(\frac{\gamma_D Q_D}{Q_L} + \gamma_L \right) \sqrt{\left[\frac{\left(1 + COV_{Q_D}^2 + COV_{Q_L}^2\right)}{\left(1 + COV_R^2\right)} \right]}}{\left(\frac{\lambda_{Q_D} Q_D}{Q_L} + \lambda_{Q_L} \right) \exp\left\{ \beta_T \sqrt{\ln\left[\left(1 + COV_R^2\right)\left(1 + COV_{Q_D}^2 + COV_{Q_L}^2\right)\right]} \right\}} \tag{5.7}$$

λ_R = resistance bias factor
COV_R = COV of the resistance
COV_{Q_L} = COV of the live load
COV_{Q_D} = COV of the dead load
β_T = target reliability index
γ_D, γ_L = dead and live load factors
Q_D/Q_L = dead to live load ratio
λ_{QD}.,λ_{QL} = dead & live load bias factors

b. MC – Monte Carlo Simulation. Using two sets of simulations, 10,000 simulations (upper value) and 100,000 simulations (lower values).
c. Recommended resistance factors, considering the results obtained by FOSM and MC simulation and rounded for practicality to the closest 0.05 accuracy.

9. Efficiency factor, ϕ/λ, is a measure for evaluating the relative efficiency of the design methods. The ratio is systematically higher for methods which predict more accurately and hence more economically effective to be used, regardless of the absolute value of the resistance factor, for more details see Paikowsky et al. (2004).

All load factors and distributions were those selected by Paikowsky et al. (2004) for calibration of piles under vertical-axial load, namely: for live loads $\gamma_L = 1.75$, $\lambda_{QL} = 1.15$, $COV_{QL} = 0.20$, and for dead loads $\gamma_D = 1.25$, λ_{QD}, = 1.05, $COV_{QD} = 0.10$. The target reliability of $\beta = 2.33$, $p_f = 1\%$ associated with redundant pile support (five or more piles) is used.

5.5.2 Presentation of Results

The uncertainty of the 125 H-pile cases analyzed by the different dynamic equations and summarized in Table 5.2 are presented graphically in this section. The scatter of the data, related to each of the six (6) investigated methods, are graphed in Figures 5.1 through 5.6. The presented relations use the vertical axis for the calculated dynamic capacity and the horizontal axis for the measured static capacity. Two lines are added to each of the scatter graphs; a best fit line equation presented as a dashed line, and measured capacity equal to calculated capacity presented as a continuous black line. The scatter of the data allows the evaluation of the prediction as well as the amount of conservatism or risk associated with the prediction. For example, all data above the solid line means that the calculated capacity is higher than the measured capacity and hence on the unsafe side. See, for example, the large number of overpredicted cases in Figure 5.5 relating to the current Mn/DOT equation compared to that in Figure 5.6 related to the newly proposed Mn/DOT equation.

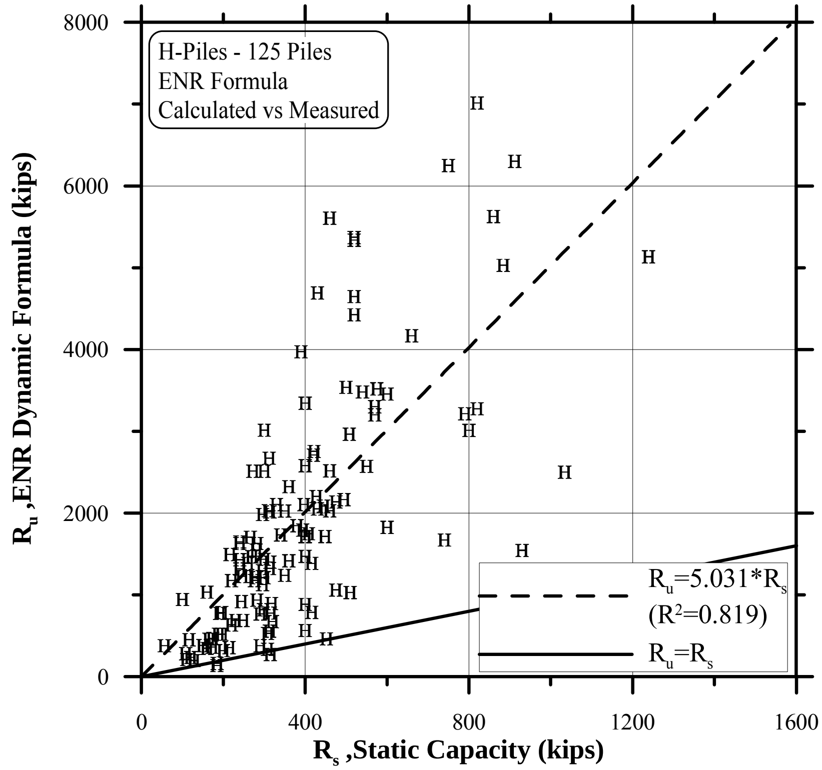

Figure 5.1 Measured static capacity vs. ENR dynamic equation prediction for 125 EOD cases.

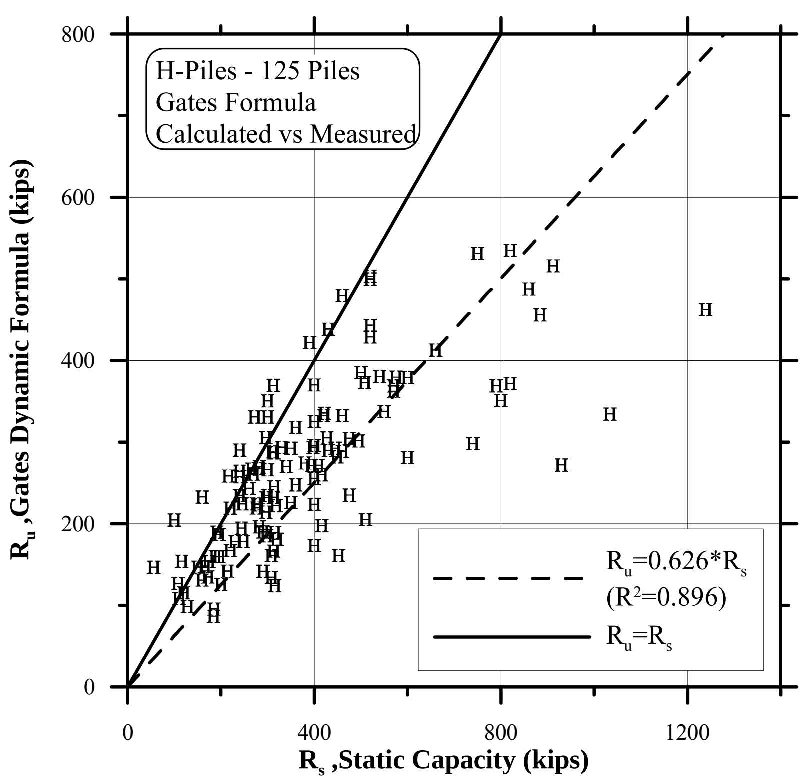

Figure 5.2 Measured static capacity vs. Gates dynamic equation prediction for 125 EOD cases.

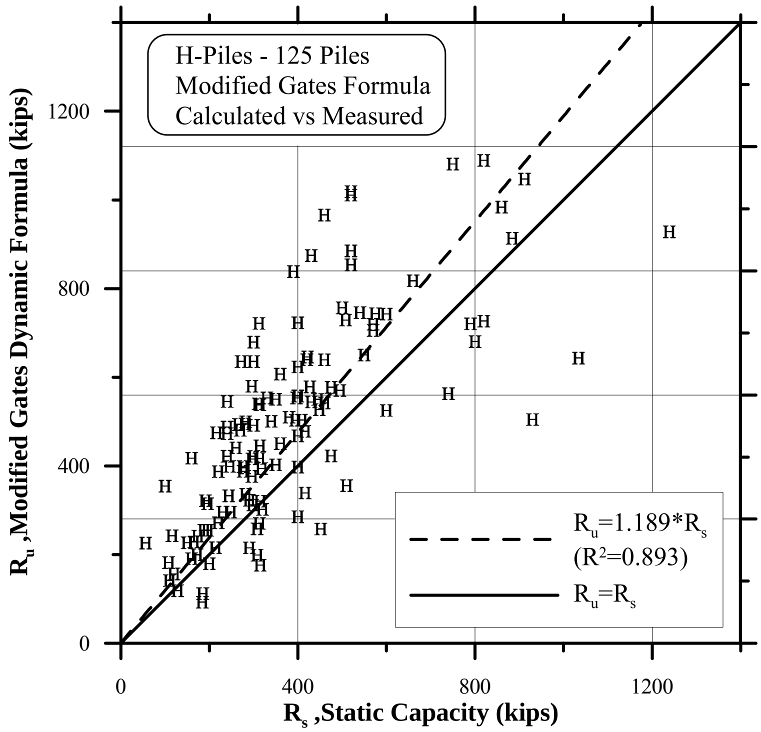

Figure 5.3 Measured static capacity vs. FHWA Modified Gates dynamic equation prediction for 125 EOD cases.

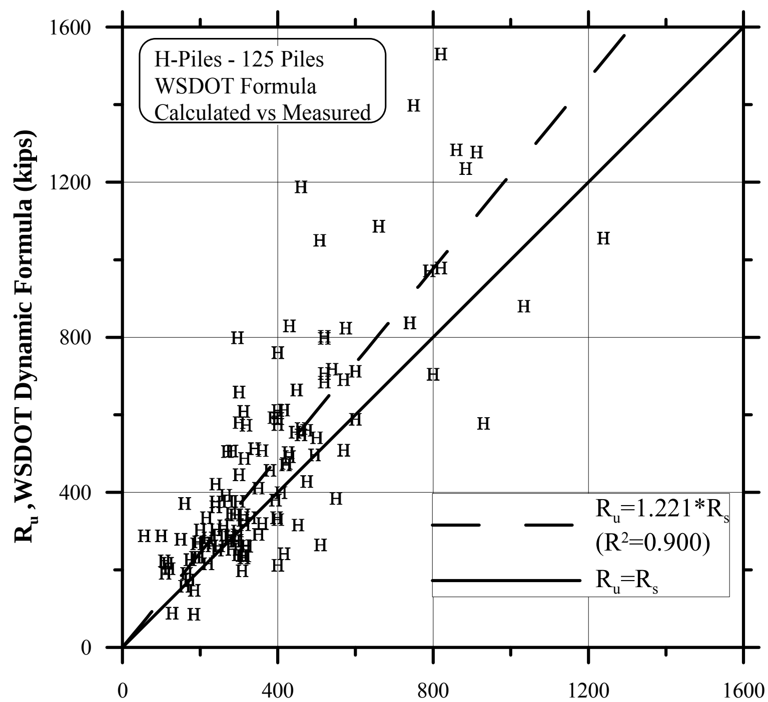

Figure 5.4 Measured static capacity vs. WS DOT dynamic equation prediction for 125 EOD cases.

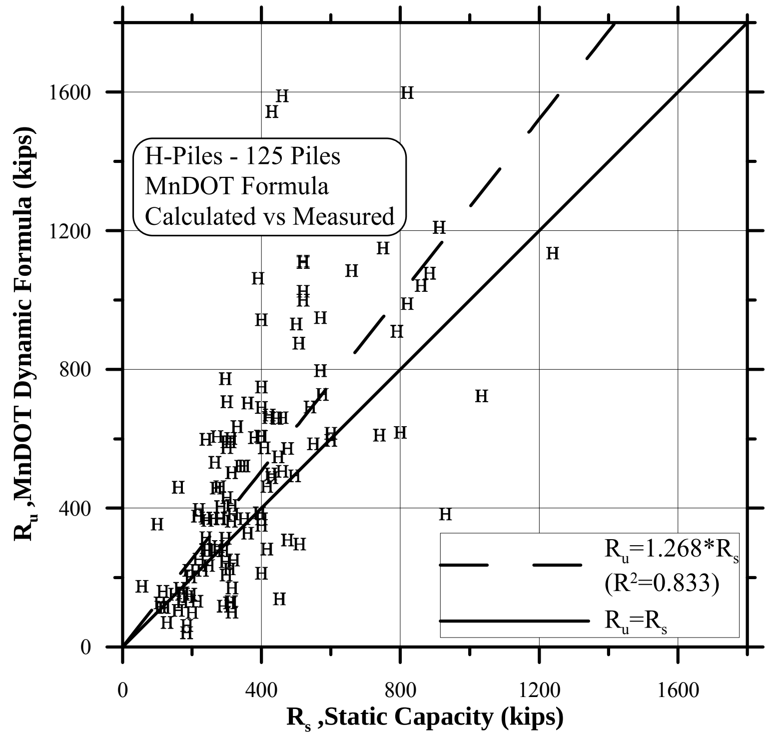

Figure 5.5 Measured static capacity vs. Mn/DOT dynamic equation (C = 0.2, stroke = 75% of nominal) prediction for 125 EOD cases.

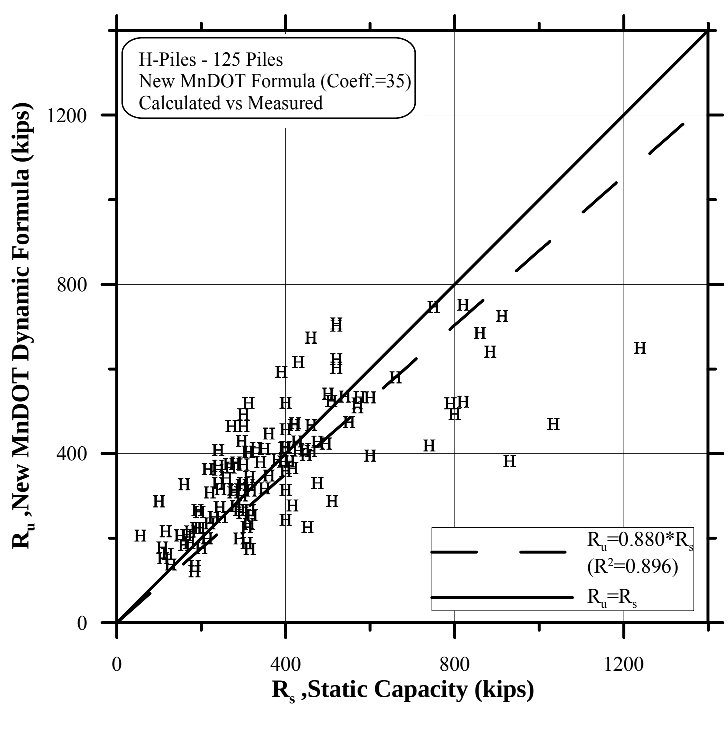

Figure 5.6 Measured static capacity vs. new general Mn/DOT dynamic equation prediction for 125 EOD cases.

5.5.3 Observations

The analysis results presented in Table 5.2 are identical to those presented in Table 4.3 with the exception of those related to Mn/DOT dynamic equation. As the dataset was not changed for the 125 EOD H pile cases, all analyses remain the same. The difference regarding the results of the Mn/DOT equation stems from the application of the equation to H piles. The format of equation 5.5 differs from that of equation 4.5 in the application of 0.2 to the pile and driving system weight (M) and the application of 0.75 to the nominal hammer energy. This variation resulted with a bias increase from 0.8060 to 0.9842 followed, however, by an increase in the standard deviation, bringing to a similar coefficient of variation for both analyses (0.6870 vs. 0.6604). Due to the increase in the bias (from an unsafe level), the calculated resistance factor increased from 0.204 to 0.260 (MC simulation) and, hence, the recommended resistance factor from 0.20 to 0.25. The resistance factor remains relatively low due to the large scatter of the method as evident in Figure 5.5.

As a result of the above, a detailed study of the Mn/DOT dynamic equation under different conditions was carried out, to be presented in section 5.7.

5.6 DATABASE ANALYSIS – PIPE PILES

5.6.1 Summary of Results

Table 5.3 presents a summary of the statistics and other information related to the dynamic equations presented in Table 5.1 under End of Driving conditions. The results of the equations are presented, along with the new General Mn/DOT dynamic equation (for comparison only), developed and detailed in Chapter 6. The number of cases analyzed in Table 5.3 refer to 99 Pipe pile cases at EOD as presented in section 3.6.1, compared to 102 pile cases presented in section 4.5.3. Refer to section 5.5.1 for details regarding the analyzed data in Table 5.3, being identical in format to that presented in Table 5.2.

5.6.2 Presentation of Results

The uncertainty of the 99 pipe pile cases analyzed by the different dynamic equations and summarized in Table 5.3 are presented graphically in this section. The data, related to each of the six (6) investigated methods, are graphed in Figures 5.7 through 5.12 in a format of relations presenting the scatter of the data using the vertical axis for the calculated capacity and the horizontal axis for the measured static capacity. Two lines are added to each of the scatter graphs; a best fit line equation presented as a dashed line, and measured capacity equal to calculated capacity presented as a continuous black line. The scatter of the data allows the evaluation of the prediction as well as the amount of conservatism or risk associated with the prediction. For example, all data above the solid line means that the calculated capacity is higher than the measured capacity and hence on the unsafe side. See, for example, the large number of overpredicted cases in Figure 5.11 relating to the current Mn/DOT equation compared to that in Figure 5.12 related to the newly proposed Mn/DOT equation.

Table 5.3 Dynamic Equation Predictions for Pipe Piles EOD Condition Only

Equation	No. of Cases (n)	Mean Bias Measured/ Calculated (m_λ)	Stand. Dev. (σ_λ)	Coef. of Var. (COV_λ)	Best Fit Line Equation (least square)	Coefficient of Determination (r^2)	Resistance Factor ϕ β=2.33, p_f=1%, Redundant			ϕ/λ Efficiency Factor (%)
							FOSM	MC[3]	Recom.	
ENR	99	0.3306	0.3477	1.0517	Ru[1]=4.183*Rs[2]	0.728	0.038	0.040	0.04	12.1
Gates	99	1.5592	0.8372	0.5370	Ru=0.573*Rs	0.849	0.511	0.542	0.50	32.1
Modified Gates	99	0.8776	0.5490	0.6255	Ru=1.085*Rs	0.839	0.238	0.251	0.25	28.5
WSDOT	99	0.8157	0.4925	0.6038	Ru=1.257*Rs	0.862	0.231	0.244	0.25	30.6
Mn/DOT[4]	99 (96)	1.1031 (0.961)	1.2781 (0.738)	1.1586 (0.767)	Ru=1.142*Rs	0.759	0.106 (0.193)	0.110 (0.204)	0.10 (0.20)	9.1 (20.8)
New Mn/DOT[5]	99	1.1089	0.5955	0.5370	Ru=0.805*Rs	0.849	0.364	0.385	0.35	31.6

Notes:
1. Ru is the calculated capacity using each of the dynamic formulae.
2. Rs is the Static Capacity of the pile determined by Davisson's Failure Criterion.
3. MC – Monte Carlo Simulation for 10,000 simulations.
4. For the Mn/DOT equation results presented in parentheses, see section 5.6.3.
5. New Mn/DOT formula uses a coefficient of 35.

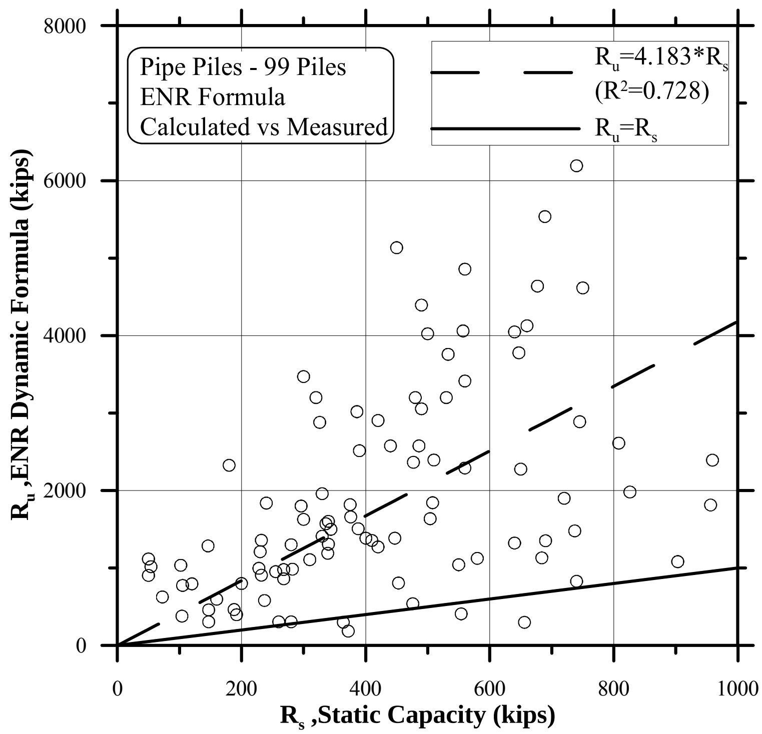

Figure 5.7 Measured static capacity vs. ENR dynamic equation prediction for 99 EOD cases.

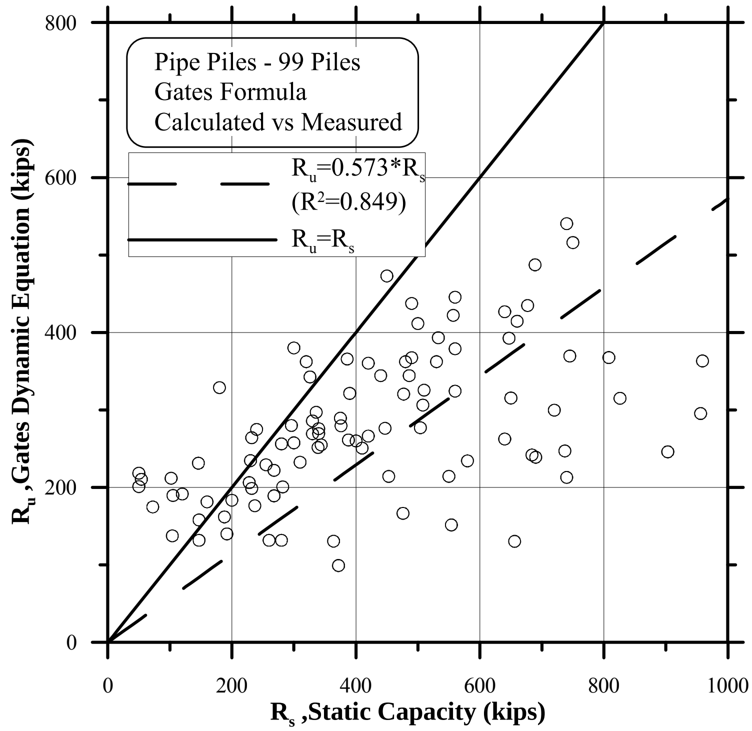

Figure 5.8 Measured static capacity vs. Gates dynamic equation prediction for 99 EOD cases.

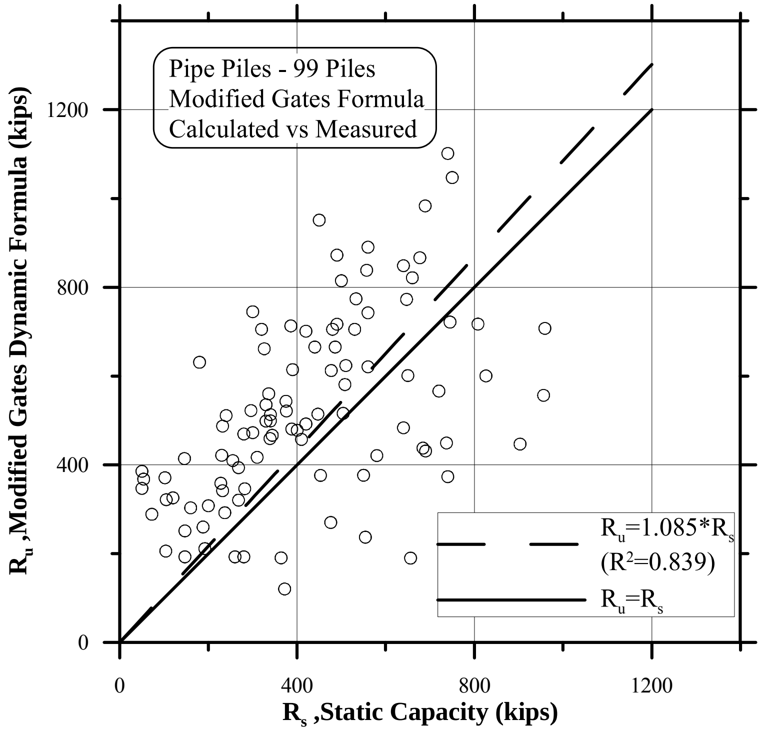

Figure 5.9 Measured static capacity vs. FHWA Modified Gates dynamic equation prediction for 99 EOD cases.

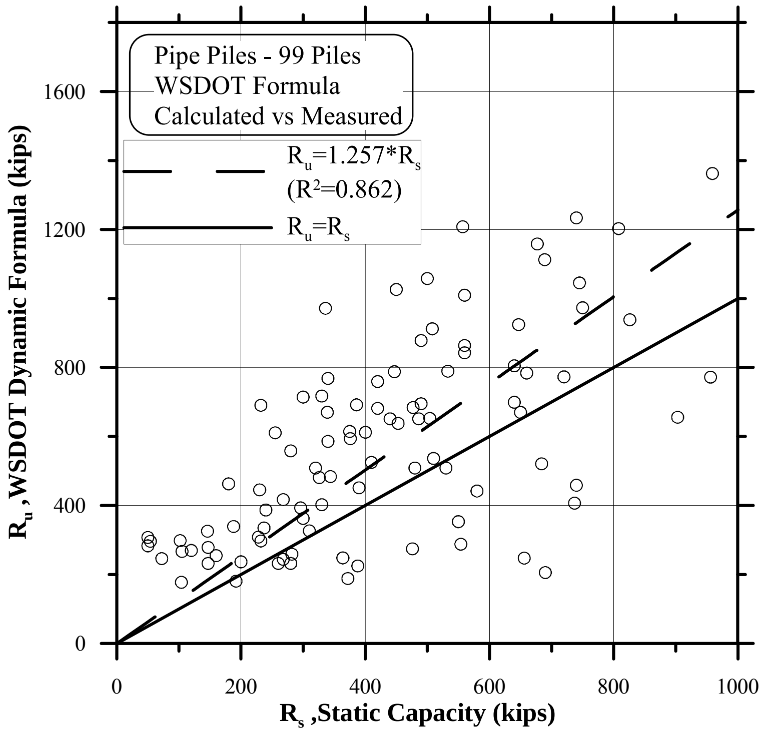

Figure 5.10 Measured static capacity vs. WSDOT dynamic equation prediction for 99 EOD cases.

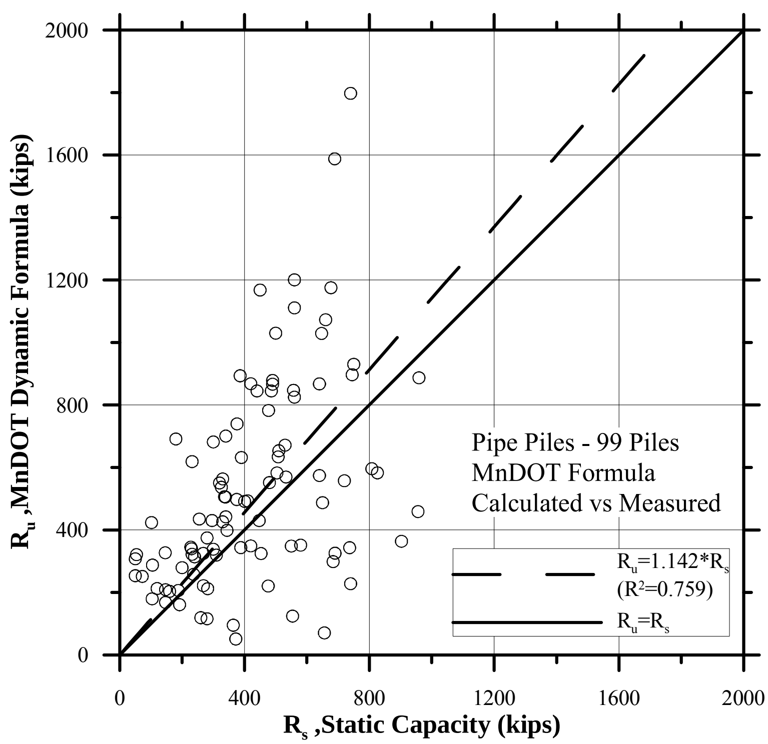

Figure 5.11 Measured static capacity vs. Mn/DOT dynamic equation (C = 0.1, stroke = 75% of nominal) prediction for 99 EOD cases.

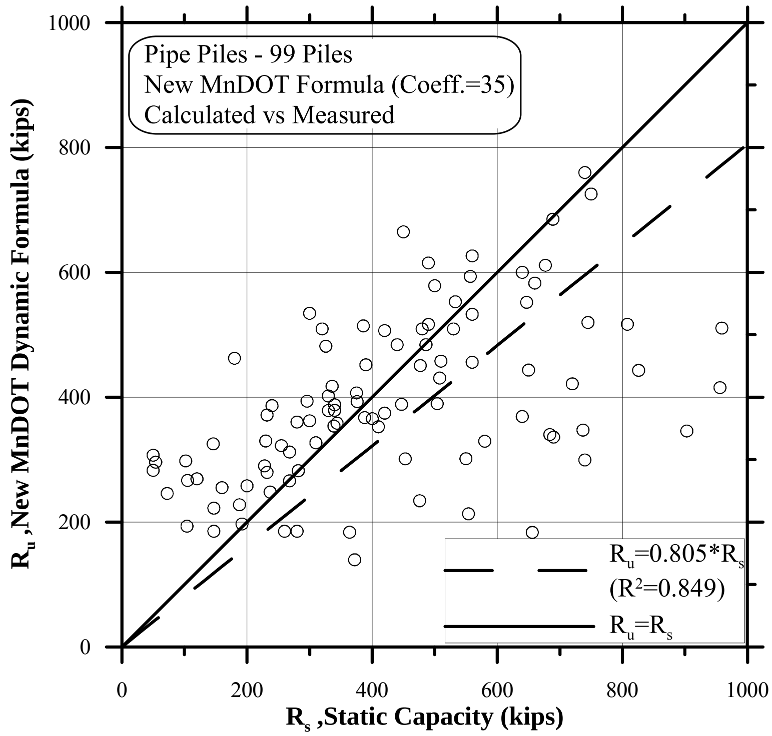

Figure 5.12 Measured static capacity vs. new Mn/DOT dynamic equation prediction for 99 EOD cases.

5.6.3 Observations

The analysis results presented in Table 5.3 compare well to those presented in Table 4.5 with the exception of those related to Mn/DOT dynamic equation. These are an expected outcome as most of the cases in both databases overlap (102 vs. 99 EOD cases). However, the application of the Mn/DOT equation in the format of equation 5.5 and 75% nominal energy has resulted in outlier biases (mostly values in excess of 3.5) that greatly affect the COV and hence, the resistance factor. For example, excluding only three cases with biases 0.30, 7.30 and 9.31 have resulted with a mean bias of 0.961, COV of 0.767 and a resistance factor of 0.20 (ϕ_{MC} = 0.204, ϕ_{FORM} = 0.193). These values are more in line with those presented in Table 4.5 and the other values in Table 5.3.

5.7 DETAILED INVESTIGATION OF THE MN/DOT DYNAMIC EQUATION

5.7.1 Overview

Chapter 3 described in detail the various conditions to be examined in relation to the driving possibilities, i.e. EOD, EOD for diesel hammers only, driving resistance equal or exceeding 4BPI, etc. Many combinations are possible and as the restrictions are compounded (e.g. EOD piles driven with diesel hammers with the energy range typical of Mn/DOT practice to a resistance equal or greater than 4BPI), so is the dataset associated with that 'bin', becoming smaller (i.e. the sets of data answering to the specific conditions). This investigation is important from two reasons:

1. To see the change in the prediction in relation to the increased 'match' between the examined case and the Mn/DOT practice.
2. To examine the confidence of using a more inclusive category to describe a more restrictive condition, e.g. all diesel hammers vs. diesel hammers restricted to the energy level of Mn/DOT practice.

5.7.2 Summary of Results

A summary of the sub-categorization of the driving conditions applied to the Mn/DOT dynamic equation are presented in Figures 5.13 and 5.14 in the form of flow charts. Each flowchart presents the analysis results for both H and pipe piles under all data (EOD and BOR) and EOD data only, respectively. The flowchart provides the statistics and the associated resistance factor from the most general case of all pile cases (denoted as A) to the most restrictive condition (denoted as B8.1 or C8.1). Each cell contains the condition applied, associated number of cases, the mean and coefficient of variation of the bias, and the associated calculated resistance factor. Mn/DOT equation 5.5 was applied to the analyses of the presented cases and 75% of nominal hammer energy was assumed.

As the dynamic equations are mostly applied to the EOD case, a review of the results for the EOD case will be most beneficial. Following the flowchart in Figure 5.14, the following can be observed:

1. All piles without outliers (H and pipe, case A), n = 211, mean = 0.860, resistance factor = 0.317
2. Looking separately (without outliers, cases B1 and C1), for H piles the resistance factor = 0.380 for n = 117, and for the pipe piles, the resistance factor = 0.263 for n = 94 cases.
3. When examining only the cases of diesel hammers (without outliers, cases B2.1 and C2.1) for H piles resistance factor = 0.270 for n = 53, and for the pipe piles resistance factor = 0.214 for n = 58.
4. When further examining the cases of diesel hammers with the range of Mn/DOT experience (without outliers, cases B5.1 and C5.1), for H piles the resistance factor = 0.173 for n = 17, and for the pipe piles the resistance factor = 0.188 for n = 20.
5. When viewing the most restrictive group (i.e. piles at the EOD, driven by diesel hammers within the energy range of Mn/DOT experience and blow count ≥ 4BPI, cases B8.1 and C8.1), for H piles the resistance factor = 0.257 for n = 13 and for the pipe piles the resistance factor = 0.295 for n = 16.

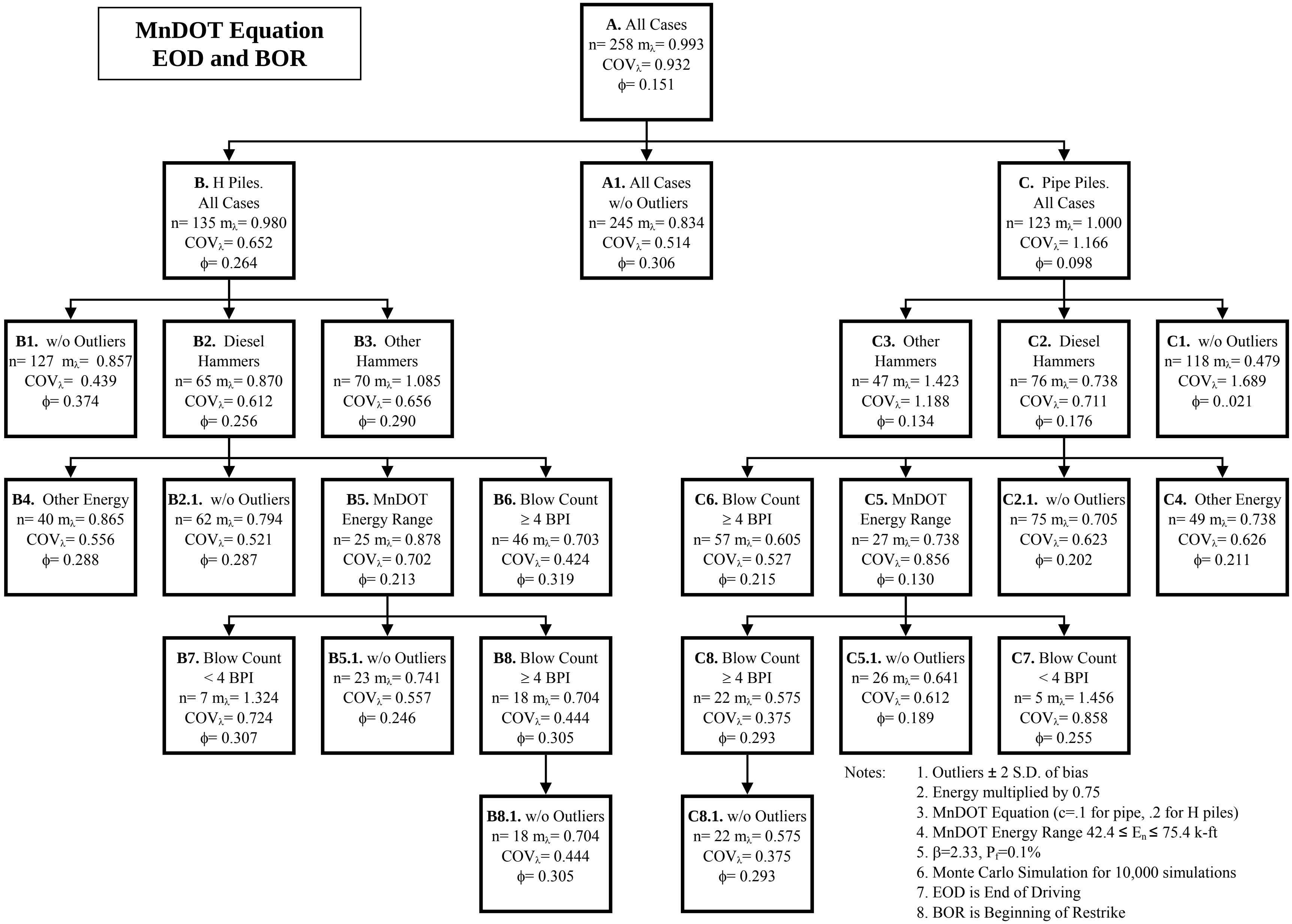

Figure 5.13 Flow chart describing the statistical parameters of a normal distribution for the Mn/DOT dynamic equation grouped by various controlling parameters under EOD and BOR conditions and the resulting resistance factor assuming a lognormal distribution and probability of exceeding criteria ("failure") of 0.1%.

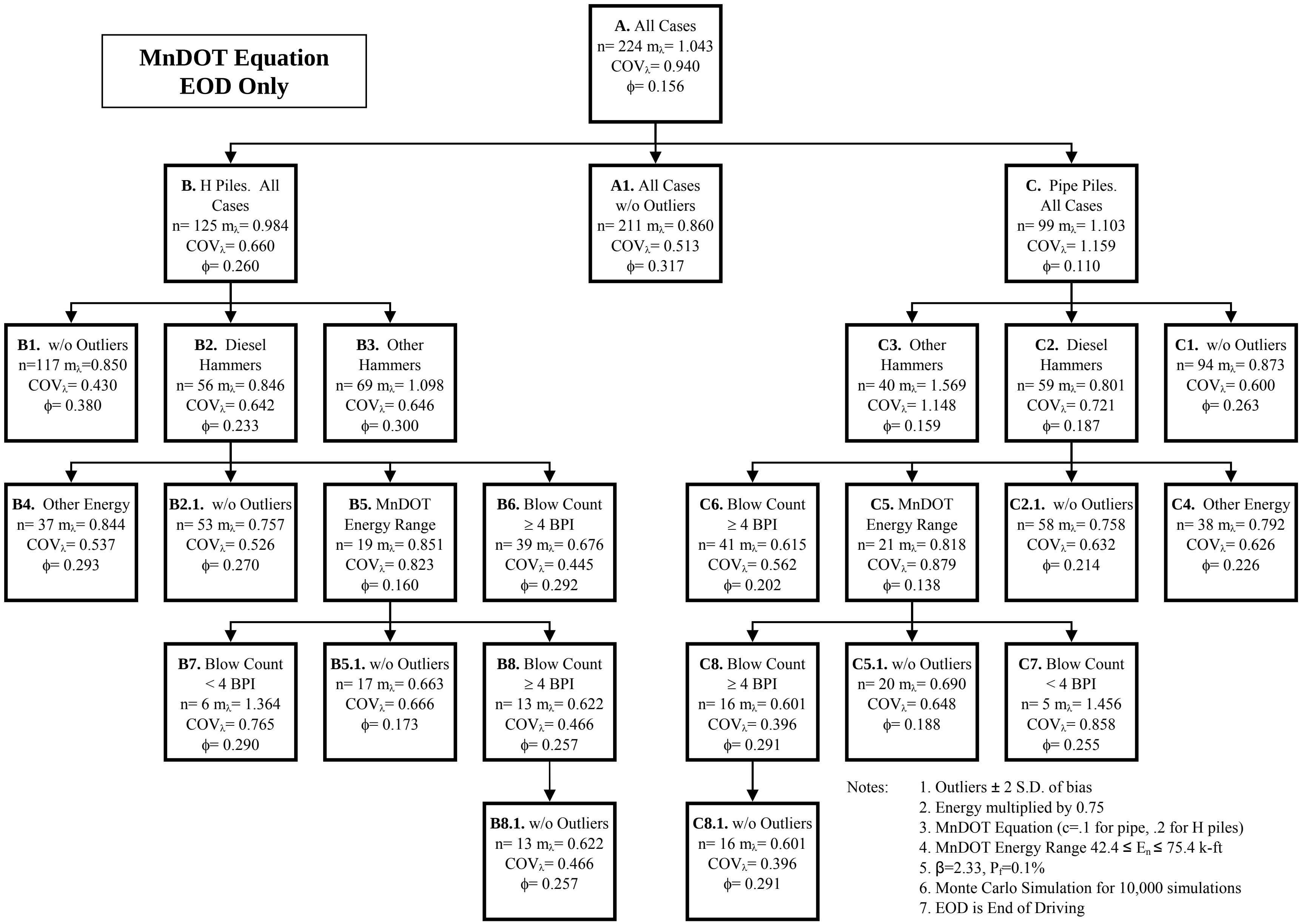

Figure 5.14 Flow chart describing the statistical parameters of a normal distribution for the Mn/DOT dynamic equation grouped by various controlling parameters under end of driving conditions and the resulting resistance factor assuming a lognormal distribution and probability of exceeding criteria ("failure") of 0.1%.

The above observation leads to the conclusion, that there is not much variation in the resistance factors in the entire flowchart. The reason may lie in the fact that once moving from the general case in which the bias is close to 1 but the COV is very large, to the diesel hammer cases in which the bias is lower than 2 (overprediction on the unsafe side) but the COV decreases so overall the resistance factor does not change much. Applying the 0.75 reduction to the energy resulted with higher resistance factors compared to what was obtained in Chapter 4. The most optimal resistance factor to be used would be (ϕ) RF = 0.25 for H piles and possibly RF = 0.30 for pipe piles, or practically using 0.25 for both. While the equation variation and energy limitation resulted with higher RF than previous values, these are still lower than what currently is recommended by the Mn/DOT (RF = 0.4) and suggests that the method altogether is not very efficient.

5.7.3 Detailed Presentation of Selected H Piles Sub-Categories of Mn/DOT Driving Conditions

Selective key sub-categories summarized in Figure 5.14 flowchart are presented in a tabulated and graphical form in this section. Tables 5.4 to 5.7 present the statistical details for the Mn/DOT equation (equation (5.5)) and the new Mn/DOT equation (presented in Chapter 6), while figures 5.15 to 5.18 present graphically the relevant information. The following discussion refers to these data:

1. Table 5.4 presents the EOD cases for all diesel hammers with driving resistances of BC ≥ 4BPI. The graphical detailed presentations of this case are shown in Figures 5.15 to 5.17 in the form of a scatter graph, bias vs. dynamic resistance graph, and bias vs. static capacity graph, respectively. Detailed explanations about such data presentation are provided in section 4.4.2. The analysis results show that the statistical parameters for 53 H piles, EOD driven with diesel hammers (case B.2.1) have very similar statistics to the 39 cases when resistance is limited to BC ≥ 4BPI (case B6 detailed in Table 5.4). These statistics did not change significantly when one outlier is removed as detailed in Table 5.5 (not shown in Figure 5.14).
2. Table 5.6 presents the statistical parameters for the more restrictive sub-category in which all aspects match the typical Mn/DOT pile driving conditions, i.e. EOD, diesel hammer within the energy range of Mn/DOT hammers and BC ≥ 4BPI. Table 5.7 presents the same condition with one Cook outlier removed (to be detailed in Chapter 6). In spite of the limited number of cases (n = 13 and 12, respectively), the statistics does not change in any significant way for the one related to all diesel hammers with BC ≥ 4BPI (n = 39), or all diesel hammers (n = 56 cases), or practically for all EOD cases all together (n = 125 cases). The conclusion derived, therefore, is that the type of hammer or the end of driving resistance has a limited importance in the accuracy of the Mn/DOT dynamic equation when applied to H piles.
3. The above observations are further supported by the graphical presentation of Figures 5.16 to 5.18 showing little correlation to the magnitude of the capacity, or the magnitude of the blow count and presenting similar scatter for the most restrictive (Figure 5.18) compared to the more generic cases (Figures 5.15 and 5.5).

Table 5.4 End of Driving Prediction for H-Piles Driven with Diesel Hammers to a Driving Resistance of 4 BPI or Higher (All Cases)

Equation	No. of Cases (n)	Mean Bias Measured/ Calculated (m_λ)	Stand. Dev. (σ_λ)	Coef. of Var. (COV_λ)	Best Fit Line Equation (least square)	Coefficient of Determination (r^2)	Resistance Factor ϕ β=2.33, p_f=1%, Redundant			ϕ/λ Efficiency Factor (%)
							FOSM	MC[3]	Recom.	
Mn/DOT	39	0.6757	0.3003	0.4445	Ru=1.505*Rs	0.857	0.271	0.292	0.30	44.4
New Mn/DOT[5]	39	1.0760	0.3417	0.3176	Ru=0.812*Rs	0.907	0.566	0.628	0.60	55.8

Notes: 1. Ru is the calculated capacity using each of the dynamic formulae.
2. Rs is the Static Capacity of the pile determined by Davisson's Failure Criterion.
3. MC – Monte Carlo Simulation for 10,000 simulations.
4. BPI is blows per inch.
5. The New Mn/DOT Formula uses a coefficient of 30.

Table 5.5 End of Driving Prediction for H-Piles Driven with Diesel Hammers to a Driving Resistance of 4 BPI or Higher (Cook's Outliers Removed)

Equation	No. of Cases (n)	Mean Bias Measured/ Calculated (m_λ)	Stand. Dev. (σ_λ)	Coef. of Var. (COV_λ)	Best Fit Line Equation (least square)	Coefficient of Determination (r^2)	Resistance Factor ϕ β=2.33, p_f=1%, Redundant			ϕ/λ Efficiency Factor (%)
							FOSM	MC[3]	Recom.	
Mn/DOT	38	0.6647	0.2964	0.4459	Ru=1.605*Rs	0.873	0.266	0.286	0.25	37.6
New Mn/DOT[5]	38	1.0458	0.2888	0.2762	Ru=0.873*Rs	0.935	0.598	0.674	0.65	62.2

Notes: 1. Ru is the calculated capacity using each of the dynamic formulae.
2. Rs is the Static Capacity of the pile determined by Davisson's Failure Criterion.
3. MC – Monte Carlo Simulation for 10,000 simulations.
4. BPI is blows per inch.
5. The New Mn/DOT Formula uses a coefficient of 30.

Table 5.6 End of Driving Prediction for H-Piles Driven with Diesel Hammers in the Mn/DOT Energy Range to a Driving Resistance of 4 BPI or Higher (All Cases)

Equation	No. of Cases (n)	Mean Bias Measured/ Calculated (m_λ)	Stand. Dev. (σ_λ)	Coef. of Var. (COV_λ)	Best Fit Line Equation (least square)	Coefficient of Determination (r^2)	Resistance Factor ϕ β=2.33, p_f=1%, Redundant			ϕ/λ Efficiency Factor (%)
							FOSM	MC[3]	Recom.	
Mn/DOT	13	0.6221	0.2899	0.4661	Ru=1.468*Rs	0.822	0.238	0.257	0.25	40.2
New Mn/DOT[6]	13	1.1419	0.4531	0.3968	Ru=0.759*Rs	0.870	0.508	0.553	0.55	48.2

Notes: 1. Ru is the calculated capacity using each of the dynamic formulae.
2. Rs is the Static Capacity of the pile determined by Davisson's Failure Criterion.
3. MC – Monte Carlo Simulation for 10,000 simulations.
4. BPI is blows per inch.
5. Mn/DOT Energy Range is $42.4 \leq E_n \leq 75.4$ k-ft
6. The New Mn/DOT Formula uses a coefficient of 30.

Table 5.7 End of Driving Prediction for H-Piles Driven with Diesel Hammers in the Mn/DOT Energy Range to a Driving Resistance of 4 BPI or Higher (Cook's Outliers Removed)

Equation	No. of Cases (n)	Mean Bias Measured/ Calculated (m_λ)	Stand. Dev. (σ_λ)	Coef. of Var. (COV_λ)	Best Fit Line Equation (least square)	Coefficient of Determination (r^2)	Resistance Factor ϕ β=2.33, p_f=1%, Redundant			ϕ/λ Efficiency Factor (%)
							FOSM	MC[3]	Recom.	
Mn/DOT	12	0.5830	0.2646	0.4539	Ru=1.701*Rs	0.857	0.229	0.247	0.25	42.9
New Mn/DOT[6]	12	1.0518	0.3297	0.3135	Ru=0.889*Rs	0.924	0.558	0.620	0.60	57.0

Notes: 1. Ru is the calculated capacity using each of the dynamic formulae.
2. Rs is the Static Capacity of the pile determined by Davisson's Failure Criterion.
3. MC – Monte Carlo Simulation for 10,000 simulations.
4. BPI is blows per inch.
5. Mn/DOT Energy Range is $42.4 \leq E_n \leq 75.4$ k-ft
6. The New Mn/DOT Formula uses a coefficient of 30.

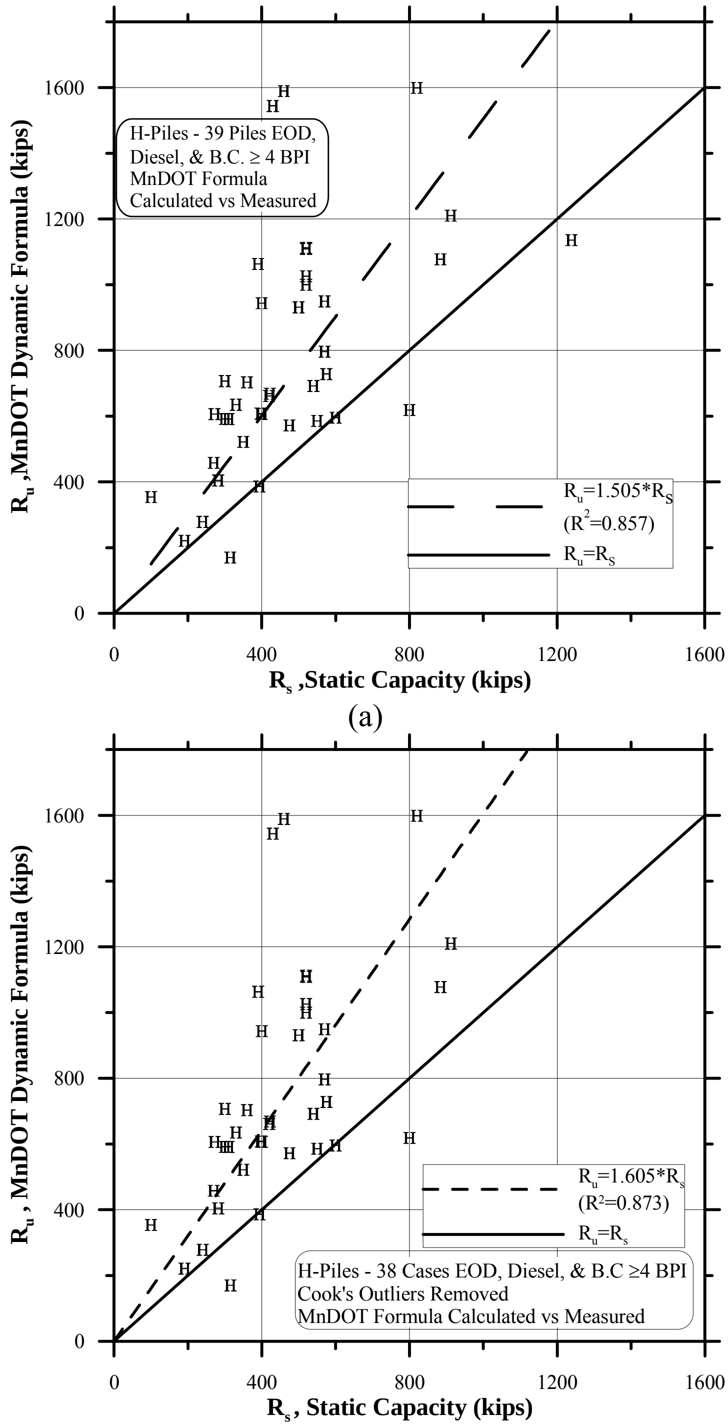

(a)

(b)

Figure 5.15 Measured static capacity vs. Mn/DOT Dynamic equation (C = 0.2, stroke = 75% of nominal) applied to EOD cases of diesel hammers with BC ≥ 4BPI (a) all subset cases, and (b) with outliers removed.

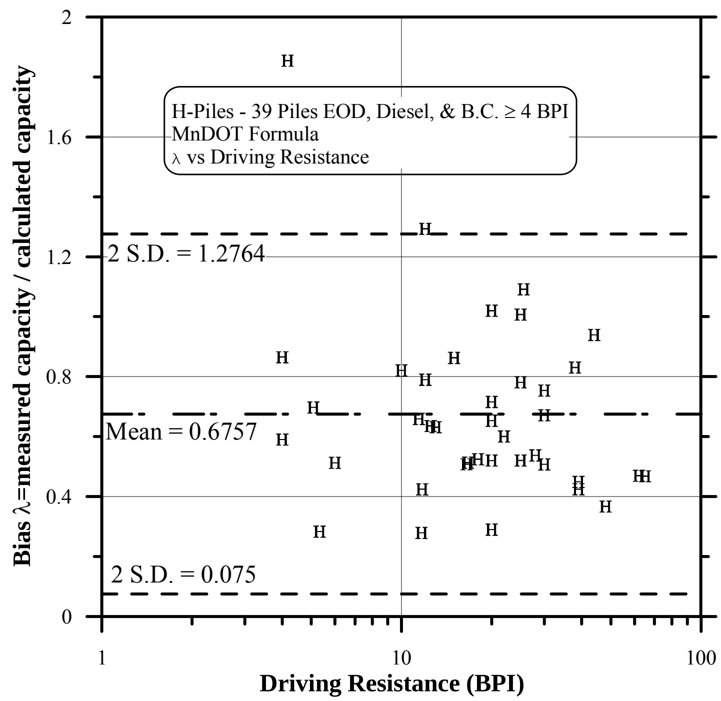

Figure 5.16 Driving resistance vs. bias (measured over predicted capacity) using Mn/DOT dynamic equation (C = 0.2, stroke = 75% of nominal) applied to EOD cases of diesel hammers with BC ≥ 4BPI.

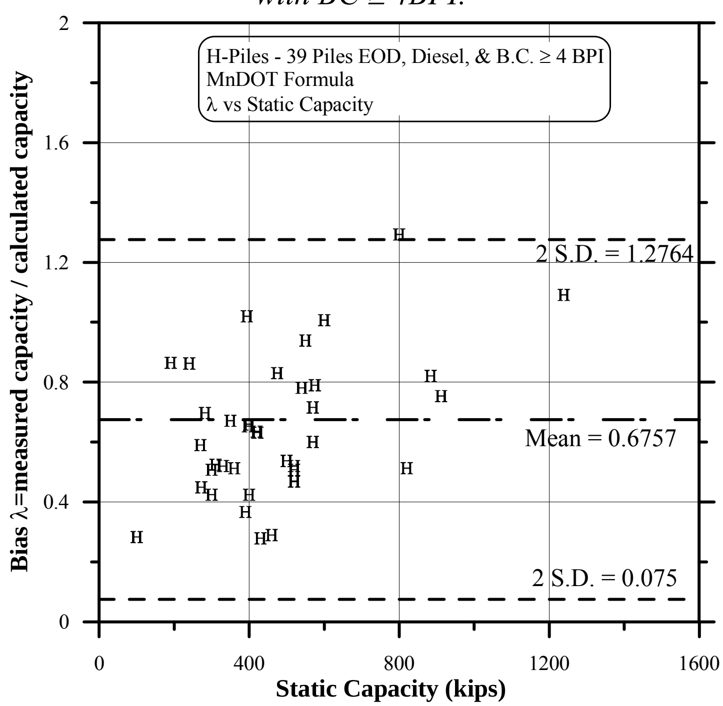

Figure 5.17 Measured static capacity vs. bias (measured over predicted capacity) using Mn/DOT dynamic equation (C = 0.2, stroke = 75% of nominal) applied to EOD cases of diesel hammers with BC ≥ 4BPI.

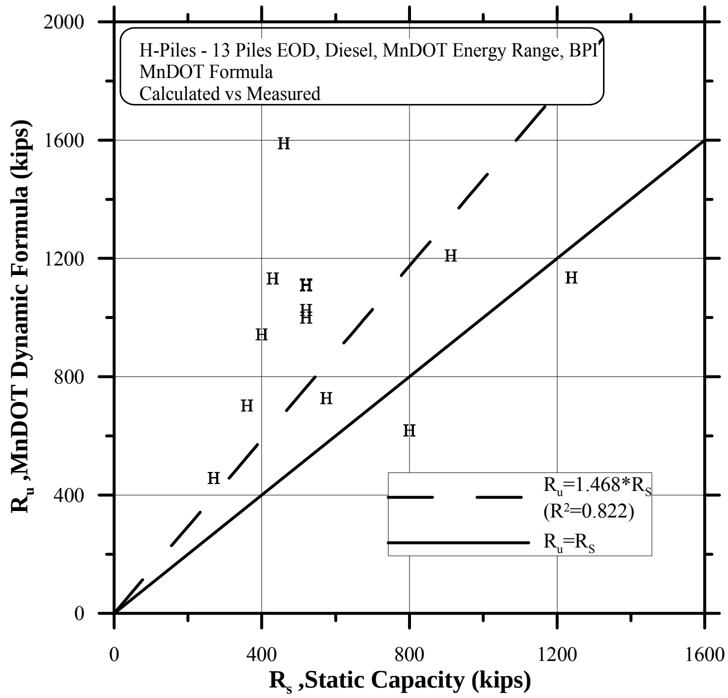

(a)

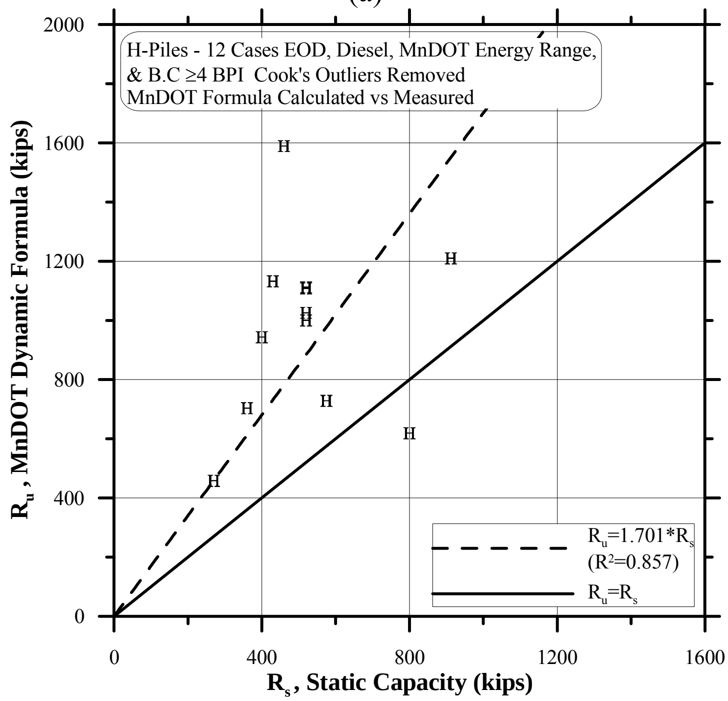

(b)

Figure 5.18 Measured static capacity vs. Mn/DOT Dynamic equation (C = 0.2, stroke = 75% of nominal) applied to EOD cases of diesel hammers within the energy range of Mn/DOT practice with BC ≥ 4BPI (a) all subset cases, and (b) with outliers removed.

5.7.4 Detailed Presentation of Selected Pipe Piles Sub-Categorization of Mn/DOT Driving Conditions

Selective key sub-categories summarized in Figure 5.14 flowchart are presented in a tabulated and graphical form in this section. Tables 5.8 to 5.11 present the statistical details for the Mn/DOT equation (equation (5.5)) and the new Mn/DOT equation (presented in Chapter 6), while figures 5.19 to 5.22 present graphically the relevant information. The following discussion refers to these data:

1. Table 5.8 presents the EOD cases for all diesel hammers with driving resistances of BC ≥ 4BPI. The graphical detailed presentations of this case are shown in Figures 5.19 to 5.21 in the form of a scatter graph, bias vs. dynamic resistance graph, and bias vs. static capacity graph, respectively. Detailed explanations about such data presentation are provided in section 4.4.2. The analysis results show that the statistical parameters for 58 pipe piles, EOD driven with diesel hammers (case C.2.1) have very similar statistics to the 41 cases when resistance is limited to BC ≥ 4BPI (case C6 detailed in Table 5.8). These statistics did not change significantly when one outlier is removed as detailed in Table 5.9 (not shown in Figure 5.14).
2. Table 5.10 presents the statistical parameters for the more restrictive sub-category in which all aspects match the typical Mn/DOT pile driving conditions, i.e. EOD, diesel hammer within the energy range of Mn/DOT hammers and BC ≥ 4BPI. Table 5.11 presents the same condition with one Cook outlier removed (to be detailed in Chapter 6). In spite of the limited number of cases (n = 16 and 14, respectively), the statistics does not change in any significant way for the one related to all diesel hammers with BC ≥ 4BPI (n = 41), though a decrease in the COV suggests a more consistent subset as a result of a large group of piles within the subset relating to a single site. The general trend of the pipe pile data suggests a decrease in the bias and the COV as the sub-categorization of the set leads to smaller subsets. The conclusion derived, therefore, is that the type of hammer or the end of driving resistance affects the accuracy of the Mn/DOT dynamic equation when applied to pipe piles.
3. The above observations are further supported by the graphical presentation of Figures 5.19 to 5.22 showing increased bias with the magnitude of the capacity, and the magnitude of the blow count and presenting less scatter for the most restrictive (Figure 5.22) vs. the more generic cases (Figures 5.19 and 5.11).

Table 5.8 End of Driving Prediction for Pipe Piles Driven with Diesel Hammers to a Driving Resistance of 4 BPI or Higher (All Cases)

Equation	No. of Cases (n)	Mean Bias Measured/ Calculated (m_λ)	Stand. Dev. (σ_λ)	Coef. of Var. (COV_λ)	Best Fit Line Equation (least square)	Coefficient of Determination (r^2)	Resistance Factor ϕ β=2.33, p_f=1%, Redundant			ϕ/λ Efficiency Factor (%)
							FOSM	MC[3]	Recom.	
Mn/DOT	41	0.6149	0.3454	0.5616	Ru=1.653*Rs	0.872	0.191	0.202	0.20	32.5
New Mn/DOT[5]	41	0.9519	0.4078	0.4284	Ru=0.902*Rs	0.918	0.396	0.427	0.40	42.0

Notes: 1. Ru is the calculated capacity using each of the dynamic formulae.
2. Rs is the Static Capacity of the pile determined by Davisson's Failure Criterion.
3. MC – Monte Carlo Simulation for 10,000 simulations.
4. BPI is blows per inch.
5. The New Mn/DOT Formula uses a coefficient of 30.

Table 5.9 End of Driving Prediction for Pipe Piles Driven with Diesel Hammers to a Driving Resistance of 4 BPI or Higher (Cook's Outliers Removed)

Equation	No. of Cases (n)	Mean Bias Measured/ Calculated (m_λ)	Stand. Dev. (σ_λ)	Coef. of Var. (COV_λ)	Best Fit Line Equation (least square)	Coefficient of Determination (r^2)	Resistance Factor ϕ β=2.33, p_f=1%, Redundant			ϕ/λ Efficiency Factor (%)
							FOSM	MC[3]	Recom.	
Mn/DOT	38	0.5657	0.2187	0.3865	Ru=1.773*Rs	0.919	0.257	0.280	0.25	44.2
New Mn/DOT[5]	38	0.9071	0.3149	0.3472	Ru=0.946*Rs	0.946	0.449	0.492	0.45	49.6

Notes: 1. Ru is the calculated capacity using each of the dynamic formulae.
2. Rs is the Static Capacity of the pile determined by Davisson's Failure Criterion.
3. MC – Monte Carlo Simulation for 10,000 simulations.
4. BPI is blows per inch.
5. The New Mn/DOT Formula uses a coefficient of 30.

Table 5.10 End of Driving Prediction for Pipe Piles Driven with Diesel Hammers in the Mn/DOT Energy Range to a Driving Resistance of 4 BPI or Higher (All Cases)

Equation	No. of Cases (n)	Mean Bias Measured/ Calculated (m_λ)	Stand. Dev. (σ_λ)	Coef. of Var. (COV_λ)	Best Fit Line Equation (least square)	Coefficient of Determination (r^2)	Resistance Factor ϕ β=2.33, p_f=1%, Redundant			ϕ/λ Efficiency Factor (%)
							FOSM	MC[3]	Recom.	
Mn/DOT	16	0.6007	0.2379	0.3960	Ru=1.832*Rs	0.929	0.268	0.291	0.30	49.9
New Mn/DOT[6]	16	1.1284	0.2051	0.1818	Ru=0.878*Rs	0.974	0.766	0.905	0.85	75.3

Notes: 1. Ru is the calculated capacity using each of the dynamic formulae.
2. Rs is the Static Capacity of the pile determined by Davisson's Failure Criterion.
3. MC – Monte Carlo Simulation for 10,000 simulations.
4. BPI is blows per inch.
5. Mn/DOT Energy Range is $42.4 \leq E_n \leq 75.4$ k-ft
6. The New Mn/DOT Formula uses a coefficient of 30.

Table 5.11 End of Driving Prediction for Pipe Piles Driven with Diesel Hammers in the Mn/DOT Energy Range to a Driving Resistance of 4 BPI or Higher (Cook's Outliers Removed)

Equation	No. of Cases (n)	Mean Bias Measured/ Calculated (m_λ)	Stand. Dev. (σ_λ)	Coef. of Var. (COV_λ)	Best Fit Line Equation (least square)	Coefficient of Determination (r^2)	Resistance Factor ϕ β=2.33, p_f=1%, Redundant			ϕ/λ Efficiency Factor (%)
							FOSM	MC[3]	Recom.	
Mn/DOT	14	0.5591	0.1425	0.2549	Ru=1.930*Rs	0.960	0.333	0.379	0.35	62.6
New Mn/DOT[6]	14	1.1065	0.1273	0.1151	Ru=0.895*Rs	0.988	0.825	1.012	0.90	81.3

Notes: 1. Ru is the calculated capacity using each of the dynamic formulae.
2. Rs is the Static Capacity of the pile determined by Davisson's Failure Criterion.
3. MC – Monte Carlo Simulation for 10,000 simulations.
4. BPI is blows per inch.
5. Mn/DOT Energy Range is $42.4 \leq E_n \leq 75.4$ k-ft
6. The New Mn/DOT Formula uses a coefficient of 30.

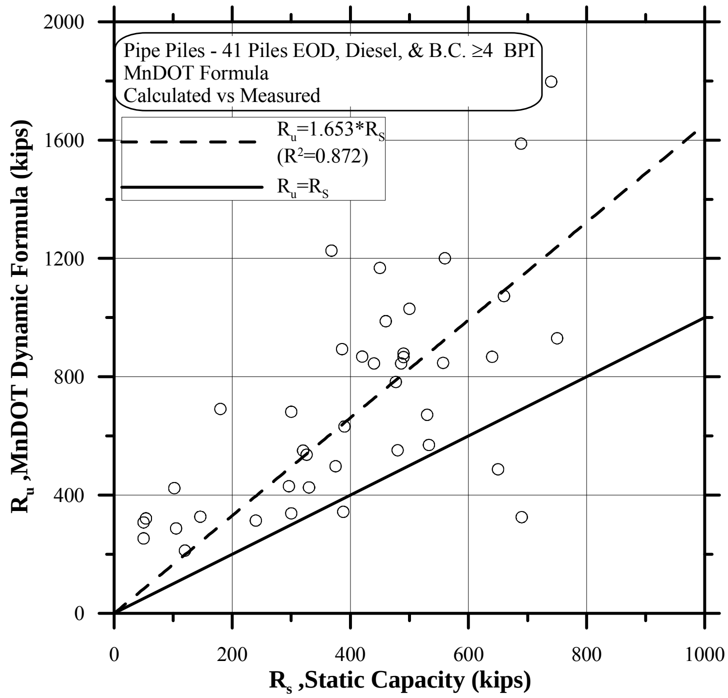

(a)

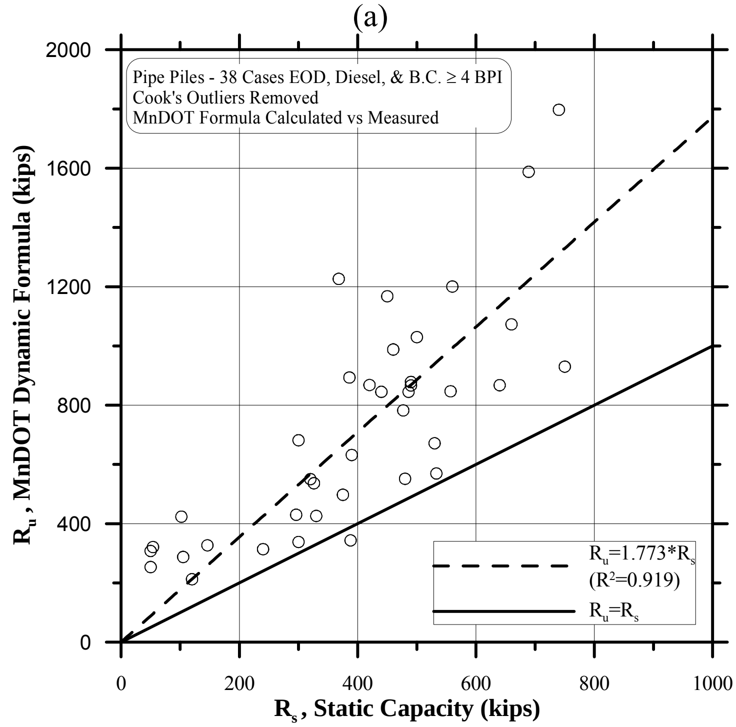

(b)

Figure 5.19 Measured static capacity vs. Mn/DOT Dynamic equation (C = 0.1, stroke = 75% of nominal) applied to EOD cases of diesel hammers with BC ≥ 4BPI (a) all subset cases, and (b) with outliers removed.

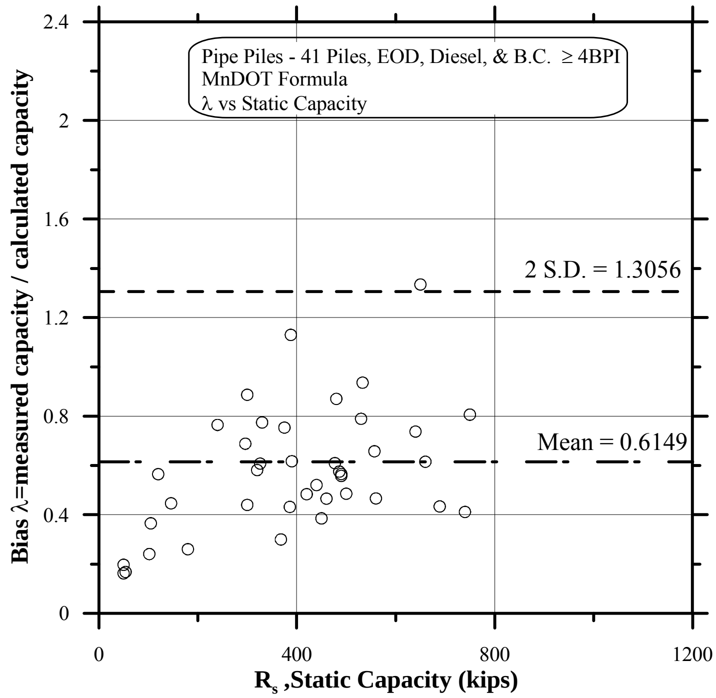

Figure 5.20 Driving resistance vs. bias (measured over predicted capacity) using Mn/DOT dynamic equation (C = 0.1, stroke = 75% of nominal) applied to EOD cases of diesel hammers with BC ≥ 4BPI.

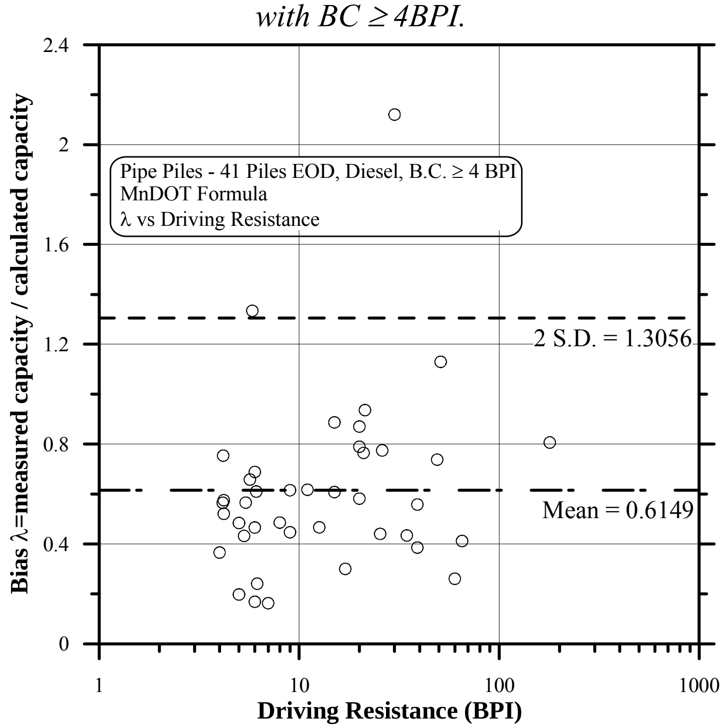

Figure 5.21 Measured static capacity vs. bias (measured over predicted capacity) using Mn/DOT dynamic equation (C = 0.1, stroke = 75% of nominal) applied to EOD cases of diesel hammers with BC ≥ 4BPI.

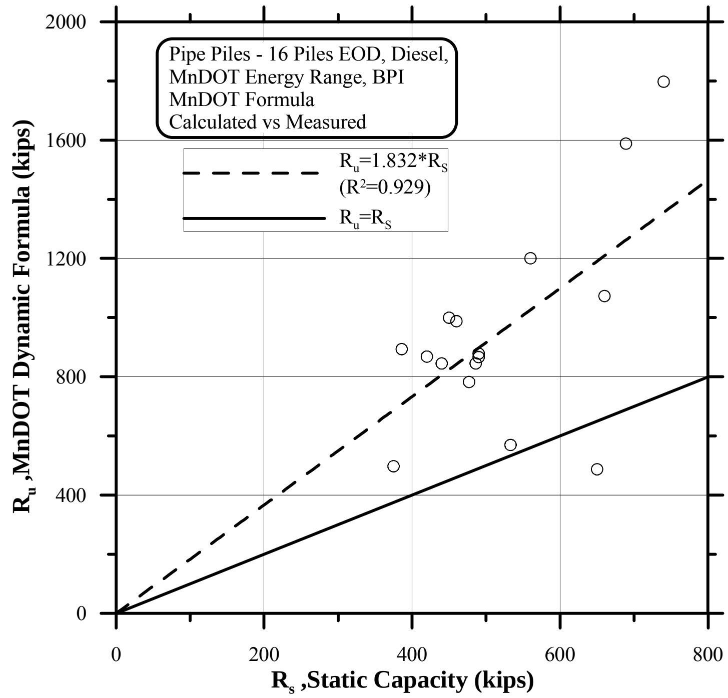

(a)

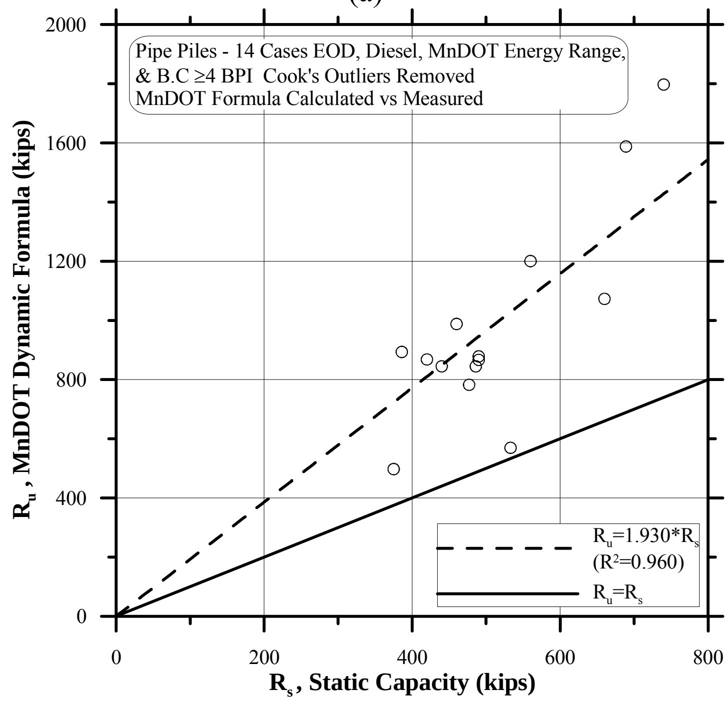

(b)

Figure 5.22 Measured static capacity vs. Mn/DOT Dynamic equation (C = 0.2, stroke = 75% of nominal) applied to EOD cases of diesel hammers within the energy range of Mn/DOT practice with BC ≥ 4BPI (a) all subset cases, and (b) with outliers removed.

5.8 IN-DEPTH EXAMINATION OF THE MN/DOT EQUATION DISTRIBUTION FUNCTIONS FIT FOR LRFD CALIBRATION

Chapters 4 and 5 present the resistance factors calculation for various calibrated conditions. As explained in section 4.4, the calibrations were carried out assuming resistance in agreement with a lognormal distribution for which the statistical parameters are presented. In actuality, the normal distribution function parameters are detailed while in the calibration a translation to a lognormal distribution is made. The mathematical and graphical examination of this hypothesis are presented in this section in the following way:

1. The χ-square goodness of fit (GOF) tests have been carried out to examine the fit of the theoretical normal and lognormal distributions to bias data. Table 5.12 lists in detail the χ^2 values obtained for various key sub-categorization cases, both for H and pipe piles for log and lognormal distributions. If the χ^2 values obtained for an assumed distribution is greater than the acceptance χ^2 value of a certain significance level (usually of 1% or 5%), then the distribution is rejected. The χ^2 values of the 1 and 5% significance values are provided in Table 5.12 as well. Observing the χ^2 values in Table 5.12 suggests that (a) all lognormal distribution χ^2 values are significantly lower than the χ^2 values for the normal distribution, suggesting a better fit to the distribution, (b) all χ^2 values for the lognormal distribution are below the significance level of 1% and except of one, all are below the significance level of 5%. Hence, the lognormal distribution is accepted by the χ-squared GOF test.
2. Presenting the relevant examined data cases against the theoretical normal and lognormal distributions (as standard normal quantile of bias data) is shown in Figure 5.23 for three examined subsets of H pile cases and in Figure 5.24 for three examined subsets of pipe pile cases. The bias data in Figure 5.23 shows an excellent match to the theoretical lognormal distribution for all investigated subsets, affirming the χ^2 GOF test results of Table 5.12 and suggesting no outliers in all three subsets. The bias data in Figure 5.24 shows also a very good match to the theoretical lognormal distribution for all investigated subsets, also affirming the χ^2 GOF test results of Table 5.12, but also indicate on a lesser quality match as the database decreases, especially for the most restrictive case of pipe piles at the EOD driven by diesel hammers within the Mn/DOT energy range for BC $\geq$ 4BPI.

Table 5.12 Summary of χ^2 values for Mn/DOT Equation

Pile Type	Condition	χ^2 Normal	χ^2 Lognormal
H	EOD Only	9419.2	21.4
H	EOD Only excluding Cook's Outliers	-	-
H	EOD, Diesel Hammer, B.C. ≥4 BPI	101.7	7.8
H	EOD, Diesel Hammer, B.C. ≥4 BPI excluding Cook's Outliers	-	-
H	EOD, Diesel Hammer, Mn/DOT Energy[1], B.C. ≥4 BPI	12.1	8.4
H	EOD, Diesel Hammer, Mn/DOT Energy[1], B.C. ≥4 BPI excluding Cook's Outliers	-	-
Pipe	EOD Only	1.9×10^6	20.6
Pipe	EOD Only excluding Cook's Outliers	-	-
Pipe	EOD, Diesel Hammer, B.C. ≥4 BPI	400.1	12.7
Pipe	EOD, Diesel Hammer, B.C. ≥4 BPI excluding Cook's Outliers	-	-
Pipe	EOD, Diesel Hammer, Mn/DOT Energy[1], B.C. ≥4 BPI	44.8	19.2
Pipe	EOD, Diesel Hammer, Mn/DOT Energy[1], B.C. ≥4 BPI excluding Cook's Outliers	-	-

Chi square (1%) = 21.665994
Chi square (5%) = 16.918978

Notes: [1] Mn/DOT energy range contains hammers with rated energies between 42.4 and 75.4 k-ft

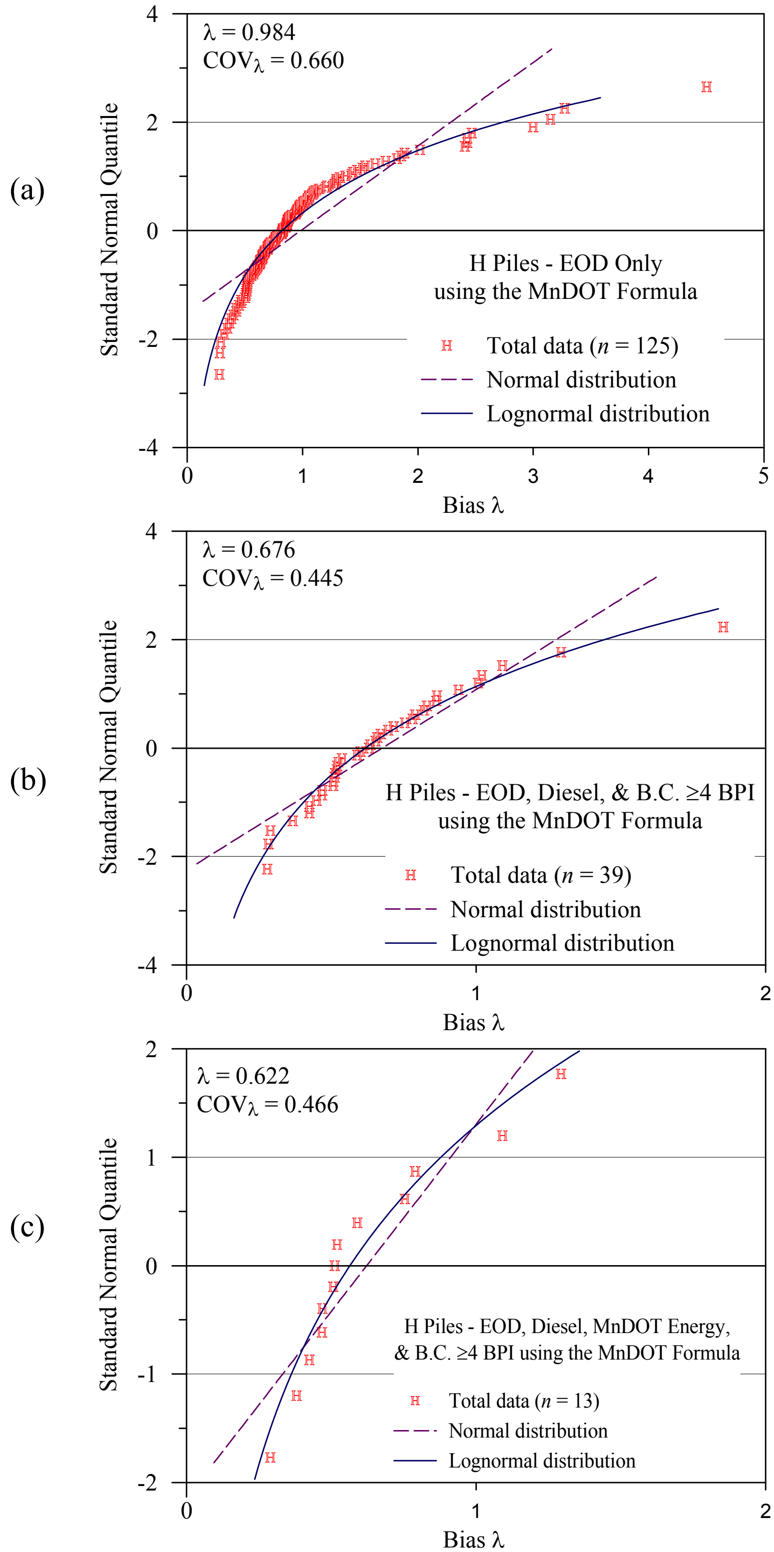

Figure 5.23 Standard normal quantile of bias data (measured capacity over calculated using Mn/DOT equation) and predicted quantiles of normal and lognormal distributions for H piles: (a) all EOD data, (b) EOD all diesel hammers and BC ≥ 4BPI, and (c) EOD, diesel hammers within Mn/DOT energy range and BC ≥ 4BPI.

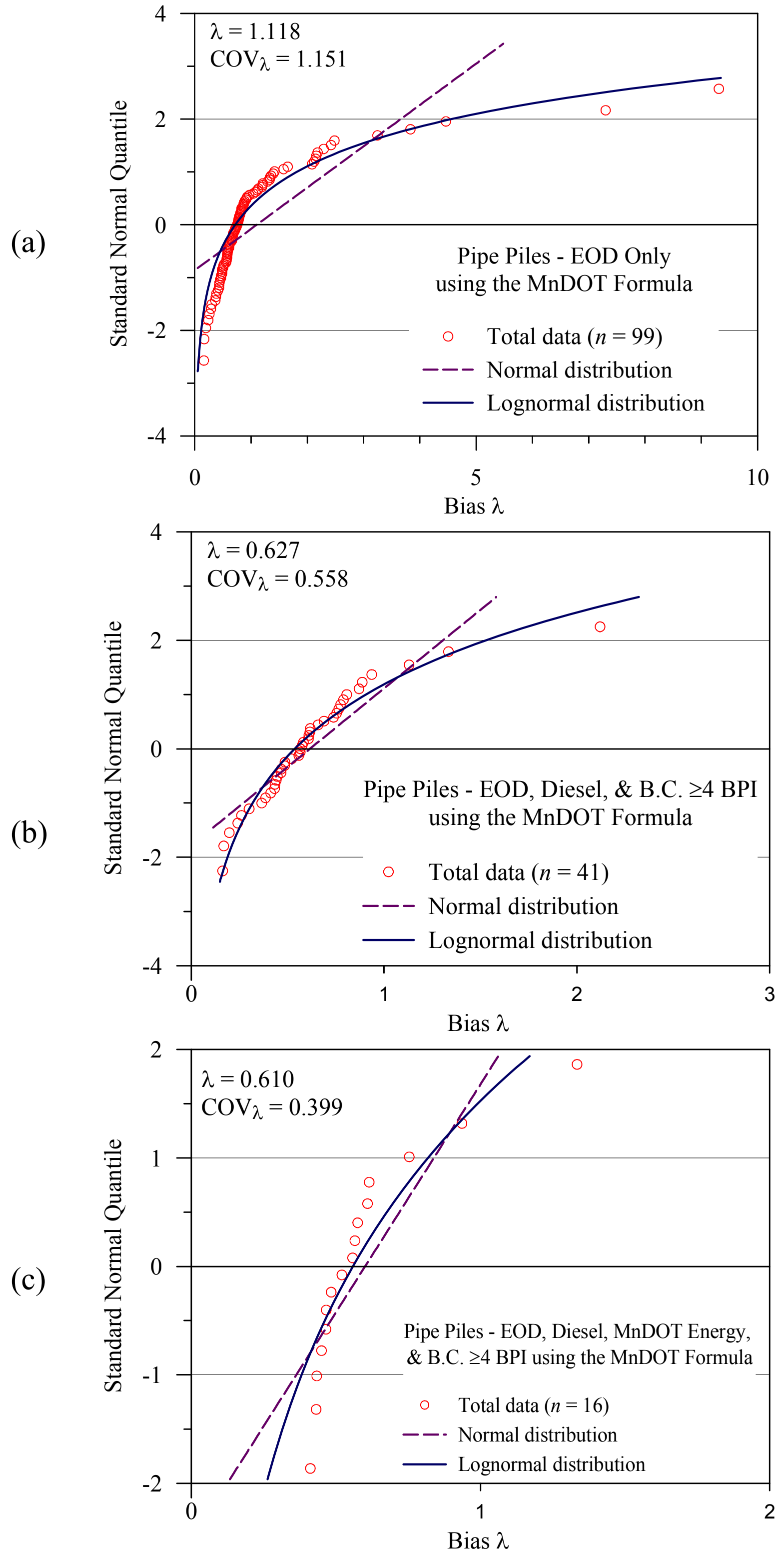

Figure 5.24 Standard normal quantile of bias data (measured capacity over calculated using Mn/DOT equation) and predicted quantiles of normal and lognormal distributions for pipe piles: (a) all EOD data, (b) EOD all diesel hammers and BC ≥ 4BPI, and (c) EOD, diesel hammers within Mn/DOT energy range and BC ≥ 4BPI.

5.9 PRELIMINARY CONCLUSIONS AND RECOMMENDATIONS

5.9.1 Mn/DOT Dynamic Equation – General Formulation

The following conclusions relate to the investigated format of the equation as presented in Table 5.1, i.e. different coefficient for H and Pipe pile and the use of 75% the nominal stroke.

1. The investigated Mn/DOT equation provides on the average an over-predictive (unsafe) capacity when examining the conditions most applicable to Mn/DOT pile driving practices. The general conditions (EOD all hammers) start with a mean bias of approximately 1.0 that decreases with the subset restriction to about 0.60 for both H and pipe piles.
2. The investigated Mn/DOT equation performs poorly as the scatter of its predictions is very large, represented by coefficient of variation ratios for EOD predictions of 0.50 to 0.60 for H piles and 0.40 to 0.80 for pipe piles.
3. The recommended resistance factors to be used with the investigated Mn/DOT equation for EOD prediction and redundant pile support (5 or more piles per cap) are $\phi = 0.25$ for H piles, and pipe piles; to be further detailed and discussed in Chapters 7 and 8.
4. An approximation of the equivalent safety factor can be performed by using the following relations based on Paikowsky et al. (2004):

$$F.S. \approx {}^{1.4167}\!/_{\phi}$$

   This means that the approximate Factor of Safety requires for the Mn/DOT is 5.7 due to the poor prediction reliability.
5. The use of $\phi = 0.40$ (F.S. $\approx$ 3.5) currently in place means that the safety margin is smaller compared to the recommended resistance factors. Special attention needs to be given to low capacity piles (statically less than 200kips) that for now should be avoided by keeping a driving criterion at the EOD of 4BPI or higher, and restrike friction piles in particular in clays and silty or mix soil conditions.

5.9.2 Additional Examined Dynamic Equations

Table 5.13 summarizes the performance of all other investigated methods (in addition to Mn/DOT existing and proposed new equations) and the associated recommended resistance and efficiency factors. The findings in Table 5.13 for the investigated dynamic equations demonstrate the power of pile specific databases. Paikowsky et al. (2004) calibrated the different dynamic equations using inclusive databases, without differentiating between pile types. The recommended resistance factors were $\phi = 0.25$, 0.75 and 0.40 for ENR, Gates and modified Gates, respectively. These values are in line with those presented in Table 5.13 for H piles, excluding ENR that was investigated in its typical formulation in contrast to that presented in AASHTO specifications and Table 5.13 where the equation was modified to exclude the "built-in" factor of safety of 6.0. In contrast to the "typical" values found for the H piles, the resistance factors developed for the pipe piles are significantly lower than those developed for the H piles and do not match the generic parameters proposed by Paikowsky et al. (2004) and appear in the AASHTO specifications. It is important to note that this is the result of the significantly larger scatter that exists in predicting the capacity of pipe piles compared to H piles. While the mean bias of H piles and pipe piles is similar in all cases, the coefficient of variation (COV) of the pipe piles is about 1.5 times larger than that of the H piles.

Table 5.13 Summary of the Performance and Calibration of the Examined Dynamic Equations at EOD Conditions

Equation	H Piles					Pipe Piles				
	No. of Cases (n)	Mean Bias Measured/ Calculated (m_λ)	Coef. of Var. (COV_λ)	Resistance Factor ϕ	ϕ/λ Efficiency Factor (%)	No. of Cases (n)	Mean Bias Measured/ Calculated (m_λ)	Coef. of Var. (COV_λ)	Resistance Factor ϕ	ϕ/λ Efficiency Factor (%)
ENR	125	0.2972	0.7479	0.07	23.6	99	0.3306	1.0517	0.04	12.1
Gates	125	1.4289	0.3542	0.75	52.5	99	1.5592	0.5370	0.50	32.1
Modified Gates	125	0.8129	0.3976	0.40	49.2	99	0.8776	0.6255	0.25	28.5
WSDOT	125	0.8738	0.3765	0.45	51.5	99	0.8157	0.6038	0.25	30.6
Mn/DOT	125	0.9842	0.6604	0.25	25.4	99 (96)	1.1031 (0.961)	1.1586 (0.767)	0.10 (0.20)	9.1 (20.8)
New Mn/DOT[4]	125	1.0163	0.3542	0.55	54.1	99	1.1089	0.5370	0.35	31.6

Notes: 1. Ru is the calculated capacity using each of the dynamic formulae.
2. Rs is the Static Capacity of the pile determined by Davisson's Failure Criterion.
3. MC - Monte Carlo Simulation for 10,000 simulations
4. New Mn/DOT formula using a coefficient of 35.

CHAPTER 6 DEVELOPMENT OF A NEW MN/DOT DYNAMIC EQUATION

6.1 RATIONALE

The development of a new Mn/DOT equation is beyond the scope of the requested and proposed research, but became a necessity as a result of the findings. The data presented in Chapters 4 and 5 strongly suggest that the current Mn/DOT dynamic equation has a poor performance second only to that of the ENR equation. While all other equations (Gates, FHWA modified Gates, and WSDOT) provide a better alternative; each has limitations when considering the very specific Mn/DOT deep foundations practice.

a) Gates equation traditionally presents lower scatter but higher bias. The bias was, therefore, improved by the FHWA modified Gates Equation.
b) FHWA modified Gates equation, while providing a good match for a wide variety of piles, systematically overpredicts (on the unsafe side) H and pipe piles as evident in the bias varying between 0.8 to 0.9 in Tables 4.2 through 4.5 and Tables 5.2 and 5.3.
c) WSDOT equation also shows systematically lower bias (in particular for pipe piles) varying between 0.79 to 0.87 in addition to the need of varying the coefficients based on hammer type. It also should be noted the WSDOT equation was developed using the database presented by Paikowsky et al. (1994) and hence, its relatively lower COV should be cautiously examined.

In light of the above, and considering the fact that Mn/DOT practice is quite focused, it is attractive to try and develop a dynamic equation that specifically answers to the Mn/DOT needs allowing increased accuracy and reduction in scatter, hence, resulting with a measureable economic gain.

6.2 PLAN OF ACTION

1. Developing an independent equation for the Mn/DOT needs, using object oriented programming.
2. Examine the new Mn/DOT dynamic equations by the following steps: (a) evaluate the pile static capacity of all tested piles using Davisson's failure criterion (described in Chapter 3), (b) evaluate the pile capacity of the database case histories using the developed new equation, (c) evaluate the bias of the method as the ratio between measured (stage 'a') to calculated (stage 'b') capacity, and (d) examine the statistical parameters of the bias.
3. Conduct an in-depth evaluation to the new Mn/DOT equation by examining subsets of various conditions.
4. Examine the new Mn/DOT distribution functions fit to LRFD calibration.
5. Develop the resistance factors associated with the different conditions, using both FOSM and MC simulation methods.
6. Examine the recommended resistance facts in comparison to the performance of the existing Mn/DOT and other dynamic equations.

The above steps 1 to 5 are described in this chapter, further examination, comparisons, assessment and recommendations are presented in Chapters 7 and 8.

6.3 PRINCIPLE

A regression analysis can provide parameters that connect the major factors affecting the pile capacity (e.g. energy, driving resistance, etc.) and allow the development of a dynamic equation. A limited attempt was made in that direction, but most obtained equations have no engineering "feel" to them and are constructed of arbitrary terms and parameters.

A different approach was then taken. Recognizing the unique success of the Gates equation in associating the pile capacity to the square of the hammers' nominal energy, and the simplicity in using logarithm of the blow count, a linear regression analysis of the data was performed looking for the best fit parameters to the anticipated formulation. This process is outlined in the following section.

6.4 METHOD OF APPROACH

S-PLUS is a commercial advanced statistics package sold by Insightful Corporation of Seattle, Washington. It features object oriented programming capabilities and advanced analytical algorithms. The source of the S-PLUS program used in this research was a free one year demo from the Insightful Corporation website (http://www.insightful.com/). To develop the New Mn/DOT Dynamic Equation, a linear regression was performed using the S-PLUS program. Static capacity and Gates Parameters (which are square root of hammer energy and log of 10 times the blow count) were provided as input parameters into an S-PLUS worksheet. Linear regression was then performed for each of the eight (8) different examined cases. Report files are obtained as output presenting the coefficient for the New Mn/DOT Dynamic Equation as well as the coefficient of determination, r^2 of the proposed relationship. Another form of output was the Cook's Distance graph enabling to identify the data outliers.

Cook's Distance is a commonly used estimate of the influence of a data point when doing least squares regression. Cook's distance measures the effect of deleting a given observation. Data points with large residuals (outliers) and/or high leverage may distort the outcome and accuracy of a regression. Points with a Cook's distance of 1 or more are considered to merit closer examination in the analysis. Cook's distance is a measurement of the influence of the i^{th} data point on all the other data points. In other words, it tells how much influence the i^{th} case has upon the model. The formula to find Cook's distance, D_i, is, (Cook, 1979):

$$D_i = \frac{\sum \left(\hat{Y}_j - \hat{Y}_{j(i)}\right)^2}{p \bullet MSE} \tag{6.1}$$

where

$\hat{Y}_j$ is the predicted (fitted) value of the i^{th} observation;

$\hat{Y}_{j(i)}$ is the predicted value of the j^{th} observation using a new regression equation found by deleting the i^{th} case;

p is the number of parameters in the model;
and MSE is the Mean Square Error

Using the F distribution to compare with Cook's distance, the influence that the i^{th} data point has on the model can be found. Values in the F distribution table can be used to express the percentage of influence the i^{th} data point has. A percentage of 50% or more would indicate a large influence on the model. The larger the error term implies that the D_i is also larger which means it has a greater influence on the model.

The new Mn/DOT equation was developed in two stages described in the following sections. The most generic form is described in section 6.5 and is investigated in section 6.6. A more specific form is described in section 6.7 and is investigated in section 6.8.

6.5 THE GENERAL NEW MN/DOT DYNAMIC EQUATION DEVELOPMENT

6.5.1 Analysis Results

Appendix D provides the analysis results using the program S-PLUS and a diagram of Cook's outliers for eight investigated cases. Table 6.1 presents a summary of the results, obtained by applying the analysis to all cases and EOD cases of the initial database (stage I) described in sections 3.4 and 3.5 for H and pipe piles, respectively.

Table 6.1 Summary of S-PLUS Linear Regression Analysis Results for the New General Mn/DOT Dynamic Equation

Pile Type	Condition	No. of Cases	Searched Coefficient[1]	Coefficient of Determination r^2
H	All Cases	135	35.814	0.880
H	All excluding Cook's Outliers	132	35.170	0.896
H	EOD Only	125	35.660	0.896
H	EOD excluding Cook Outlier's	123	34.550	0.914
Pipe	All Cases	128	35.866	0.861
Pipe	All excluding Cook's Outliers	125	34.875	0.877
Pipe	EOD Only	102	37.142	0.851
Pipe	EOD excluding Cook Outlier's	99	35.866	0.868

[1]Searched coefficient for the equation Ru = Coeff. $\sqrt{E_h} \bullet \log(10N)$

6.5.2 Conclusions and Recommended General Equation

The obtained results summarized in Table 6.1 suggest the following:

1. For both pile types under all data selection criteria, the recommended coefficient varied between 34.5 to 37.1.

2. All regressions resulted with a coefficient of determination greater than 0.85. As a lower coefficient means a more conservative evaluation and the scatter of the pipe piles predictions is higher than that for the H-piles, it is reasonable to use one coefficient, 35.
3. The final equation recommended as the new Mn/DOT dynamic equation for the most general case (all hammers, all conditions) is therefore:

$$\boxed{R_u = 35\sqrt{E_h} * \log\,(10 * N)} \tag{6.2}$$

R_u = predicted pile capacity in kips
E_h = rated hammer energy kips·ft
N = blows per inch (PBI) at the End of Driving (EOD)

4. Based on the data presented in Tables 4.2 to 4.5 and 5.2 to 5.11, the recommended preliminary resistance factors for equation 6.2 are $\phi = 0.55$ for H-piles and $\phi = 0.40$ for pipe piles. Further details and discussion of these recommendations are presented in section 6.10.

6.6 INVESTIGATION OF THE NEW GENERAL MN/DOT DYNAMIC EQUATION

6.6.1 Overview

Once a dynamic equation for use is developed (and accepted) a thorough investigation needs to be carried out with the following goals:

1. Identify the equations' performance under different conditions and the controlling parameters.
2. Identify the appropriate statistical parameters to be used for the calibration of the equation.
3. Identify the conditions under which the performance of the equation may results in unsafe predictions.
4. Investigate all of the above combined in order to develop a coherent application of the recommended equation and associated parameters in the field.

6.6.2 Initial and Advanced Investigation

Initial examination of the uncertainty of the proposed new equation and the associated resistance factors was presented as part of the dynamic equations investigation outlined in Chapters 4 and 5, specifically summarized in Tables 4.2 to 4.5 and Figure 4.6 for H-piles and Figure 4.12 for pipe piles as well as tables 5.2 and 5.3, Figures 5.6 and 5.12. The presentations of the new equation's performance in Chapters 4 and 5 were presented so comparisons can be held between the proposed new equation and all other investigated methods. Figures 6.1 and 6.2 are identical to Figures 5.6 and 5.12, presenting the scatter of the new equation in the form of static (measured) capacity vs. predicted capacity for H and pipe piles, respectively. The obtained results suggest a consistent higher performance of the equation for H piles (efficiency factor of about 53% to 54%) and a resistance factor of 0.55. The results also suggest the highest performance of the equation for pipe piles (36%) with a recommended resistance factor of 0.40. Further in-depth investigations are presented in the following sections for H and pipe piles, respectively. Section 6.7 follows the more restrictive Mn/DOT pile driving conditions in examining the applicability of the equation or a variation of it.

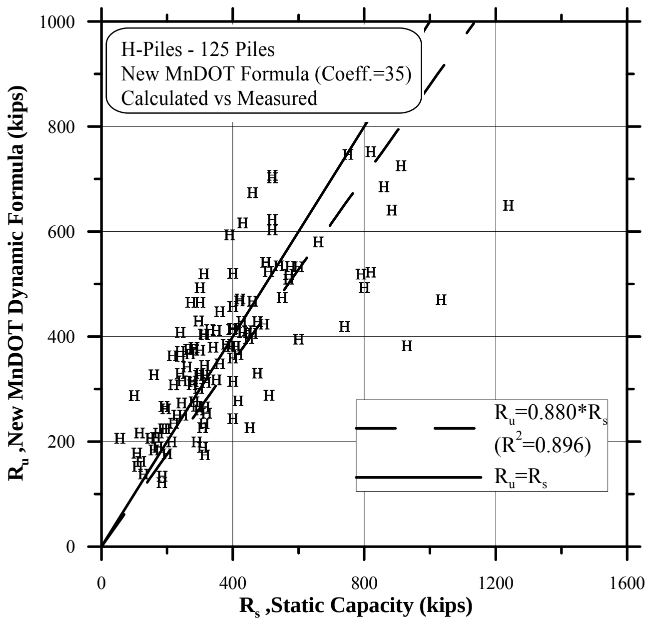

Figure 6.1 Measured static capacity vs. new General Mn/DOT dynamic equation prediction for 125 EOD cases.

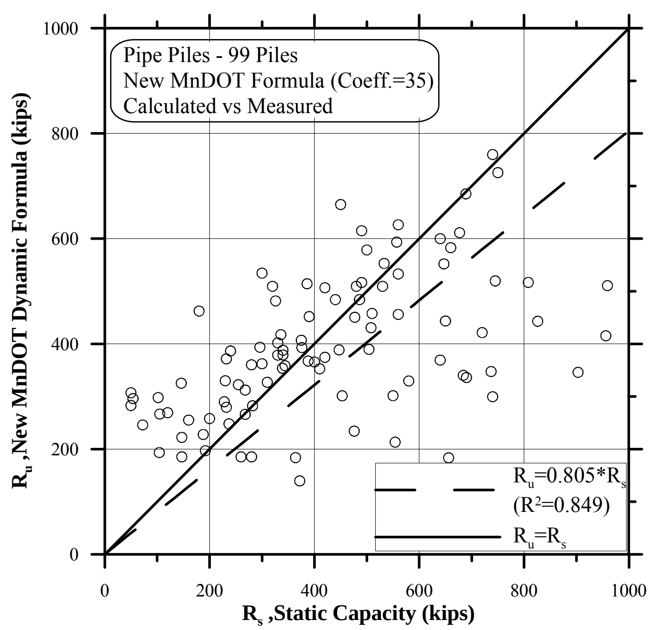

Figure 6.2 Measured static capacity vs. new Mn/DOT dynamic equation prediction for 99 EOD cases.

6.6.3 H-Piles

Table 6.2 summarizes the obtained analyses for an in-depth investigation of the performance obtained by applying the new Mn/DOT equation to different data conditions focusing mostly on EOD, driving resistance and pile capacity, and not on hammer type and energy level. General guidelines for Table 6.2 are provided below. The columns (from left to right) describe the following:

1. The examined case, numbered from 1 to 15
2. Case description for which the subset refers to
3. Number of case histories in the subset
4. mean, standard deviation and coefficient of variation of the bias (m_λ, σ_λ, COV_λ)
5. mean and standard deviation of the static capacity of the examined subset (m_{Rs}, σ_{Rs})
6. Mean and standard deviation of the dynamic capacity of the examined subset (m_{Ru}, σ_{Ru})

Table 6.2 New General Mn/DOT Dynamic Equation Statistics – H-Piles In-Depth Investigation

Case No.	Description	No. of Cases	Mean Bias m_λ	σ_λ	COV_λ	Mean Static Capacity m_{Rs}	σ_{RS}	Mean Dynamic m_{Ru}	σ_{Ru}
1	All Cases	135	1.0291	0.3704	0.3599	399.4	221.4	388.6	155.6
2	w/o Cook's Outliers	132	1.0157	0.3458	0.3404	384.0	191.9	380.3	144.2
3	w/o Outlier's > 2 S.D.	128	0.9724	0.2810	0.2890	375.5	180.2	388.1	154.9
4	w/o Outlier's > 2 S.D. & $\lambda < 0.5$	125	0.9869	0.2677	0.2713	381.9	177.2	390.9	155.5
5	$\lambda < 0.5$	3	0.3695	0.1103	0.2986	105.3	52.2	273.6	61.7
6	$\lambda < 0.61$	11	0.5301	0.1160	0.2189	227.0	156.0	407.9	235.3
7	Restrike Only (No EOD) included in the above	10	1.1838	0.4821	0.4072	576.1	314.7	504.7	226.3
8	Last Restrike Only	28	1.2136	0.5666	0.4669	537.0	287.6	458.7	182.5
9	w/o Restrike EOD Only	125	1.0168	0.3596	0.3536	385.3	207.6	379.3	145.8
10	w/o Restrike & w/o >2 S.D.	119	0.9663	0.2820	0.2919	367.1	180.2	380.0	15.0
11	Ru ≤ 150 kips	3	1.2725	0.3067	0.2410	165.7	32.6	131.3	8.5
12	Ru ≤ 200 kips	13	1.1352	0.3845	0.3388	191.8	72.6	169.2	25.5
13	Ru ≤ 250 kips	27	1.0661	0.4160	0.3902	211.5	92.9	198.8	35.5
14	Ru ≤ 275 kips	35	1.0557	0.3762	0.3564	224.7	88.1	213.7	41.8
15	Rs ≤ 200 kips	20	0.7969	0.2995	0.3758	153.0	40.3	204.1	52.8

The rows of the different subsets are described by the following:

1. Case 1 refers to all H-pile data as presented in Table 4.2.
2. Case 2 is Case 1 without the Cook's outliers for the general case (see Table 6.1 and Appendix D).
3. Case 3 omits the outliers of extreme conservative predictions greater than two standard deviations beyond the mean.
4. Case 4 refers to Case 3 without cases of extreme unsafe predictions with a bias smaller than 0.5.
5. Case 5 checks the statistics of the extreme unsafe predictions (omitted when moving from case 3 to case 4), suggesting a mean bias of 0.37 for 3 cases for which the mean measured capacity was 105kips and the mean predicted capacity 274kips.
6. Case 6 expands the range of unsafe predictions to include biases smaller than 0.61 resulting with 11 cases for which the mean bias was 0.531 and average calculated and measured capacities of 408 and 227kips, respectively.
7. Case 7 investigates the restrike cases including the earlier data, hence the first restrike for piles for which no EOD data are available.
8. Case 8 examines all BOR cases looking at the last BOR if multiple restrikes are available.
9. Case 9 looks at EOD cases only, identical to the cases presented in Table 4.3.
10. Case 10 looks at the data used in Cast 9, eliminating the extreme conservative outliers beyond two standard deviations.
11. Cases 11 to 15 are investigations of different segment of lower capacity piles recognizing that the most unsafe predictions are associated with lower static capacities (refer to Figure 4.6(b)). As static capacity is unknown at the time of the test, different predictions were searched and cases 11 to 14 refer to dynamic predictions and case 15 to static capacity.

Graphical presentation of Case 1 dataset is provided in Figure 4.6 in which the predictions of the new equation are presented against measured data, and the bias of the equation presented against static capacity, area ratio and driving resistance.

6.6.4 Pipe Piles

Table 6.3 summarizes the obtained analyses for an in-depth investigation of the performance obtained by applying the new Mn/DOT equation to different data conditions focusing mostly on EOD, driving resistance and pile capacity, and not on hammer type and energy level. Refer to section 6.6.3 for explanations regarding the Table's attributes. Graphical presentation of Case 1 dataset is provided in Figure 4.12 in which the predictions of the new equation are presented against measured data, and the bias of the equation presented against static capacity, area ratio and driving resistance.

Table 6.3 New General Mn/DOT Dynamic Equation Statistics – Pipe Piles In-Depth Investigation

Case No.	Description	No. of Cases	Mean Bias m_λ	σ_λ	COV_λ	Mean Static Capacity m_{Rs}	σ_{RS}	Mean Dynamic Capacity m_{Ru}	σ_{Ru}
1	All Cases	128	1.0650	0.5492	0.5157	417.2	210.6	401.6	132.6
2	w/o Cook's Outliers	125	1.0362	0.5207	0.5025	404.6	196.6	401.0	133.7
3	w/o Outlier's > 2 S.D.	122	0.9844	0.4104	0.4169	403.4	201.3	408.2	130.5
4	w/o Outlier's > 2 S.D. & $\lambda < 0.5$	113	1.0376	0.3770	0.3634	427.7	188.4	416.4	131.2
5	$\lambda < 0.5$	9	0.3152	0.1160	0.3681	97.7	45.8	305.9	63.3
6	Restrike Only (No EOD) included in the above	26	0.8474	0.2403	0.2836	392.7	192.4	446.8	115.1
7	Last Restrike Only	50	0.9415	0.2984	0.3169	437.7	192.1	459.1	126.5
8	w/o Restrike EOD Only	102	1.1205	0.5913	0.5278	423.4	215.4	390.0	134.8
9	w/o Restrike & w/o >2 S.D.	96	1.0214	0.4391	0.4299	406.3	204.5	397.8	133.0
10	Ru ≤ 250 kips	15	1.4592	0.9329	0.6393	279.2	172.9	198.2	34.7
11	Ru ≤ 300 kips	32	1.1053	0.8181	0.7402	248.7	168.7	240.7	47.8
12	Ru ≤ 350 kips	48	1.1659	0.7804	0.6693	306.8	211.1	268.9	56.6
13	Rs ≤ 200 kips	19	0.5380	0.2639	0.4905	129.7	48.1	261.6	68.8

6.7 THE DETAILED NEW MN/DOT DYNAMIC EQUATION DEVELOPMENT

6.7.1 Overview

The examination of the more restrictive pile driving conditions of Mn/DOT practice led to the re-examination of the dataset and its sub-categorization as described in section 3.6.8. Chapter 5 presented the analyses of these datasets. The approach and method of analysis presented in sections 6.2 to 6.5 were used for searching an optional new Mn/DOT equation that would (if possible) better fit the specific conditions than the general case of equation 6.2 presented earlier.

6.7.2 Analysis Results

Appendix D provides the analysis results using the program S-PLUS and a diagram of Cook's outliers for twelve investigated cases. Table 6.4 presents a summary of the results, obtained by applying the analysis to the modified database (second stage) described in section 3.6.

Table 6.4 Summary of S-PLUS Linear Regression Analysis Results for the New Detailed Mn/DOT Dynamic Equation

Pile Type	Condition	No. of Cases	Searched Coefficient[1]	Coefficient of Determination r^2
H	EOD Only	125	35.637	0.896
H	EOD Only excluding Cook's Outliers	122	34.151	0.925
H	EOD, Diesel Hammer, B.C. ≥4 BPI	39	33.527	0.907
H	EOD, Diesel Hammer, B.C. ≥4 BPI excluding Cook's Outliers	38	32.126	0.935
H	EOD, Diesel Hammer, Mn/DOT Energy[2], B.C. ≥4 BPI	13	34.401	0.870
H	EOD, Diesel Hammer, Mn/DOT Energy[2], B.C. ≥4 BPI excluding Cook's Outliers	12	31.181	0.924
Pipe	EOD Only	99	36.746	0.850
Pipe	EOD Only excluding Cook's Outliers	97	35.839	0.859
Pipe	EOD, Diesel Hammer, B.C. ≥4 BPI	41	30.532	0.918
Pipe	EOD, Diesel Hammer, B.C. ≥4 BPI excluding Cook's Outliers	38	29.983	0.946
Pipe	EOD, Diesel Hammer, Mn/DOT Energy[2], B.C. ≥4 BPI	16	33.294	0.974
Pipe	EOD, Diesel Hammer, Mn/DOT Energy[2], B.C. ≥4 BPI excluding Cook's Outliers	14	33.146	0.989

Notes:

[1]Searched coefficient for the equation Ru = Coeff. $\sqrt{E_h} \bullet \log(10N)$

[2]Mn/DOT energy range contains hammers with rated energies between 42.4 and 75.4 k-ft

6.7.3 Conclusions and Recommended General Equation

The obtained results summarized in Table 6.4 suggest the following:

1. For both pile types under all EOD data selection criteria (with or without the outliers), the recommended coefficient varied between 34.2 to 36.7 reaffirming the coefficient of 35 recommended for the general equation as appeared in equation 6.2.
2. All regressions resulted with a coefficient of determination greater than 0.85 suggesting good performance of the proposed format and obtained coefficients.
3. When restricting the EOD data to diesel hammers only and a blow count of equal or greater to 4BPI (with or without the outliers) the recommended coefficients are 32.1 to 33.5 for the H piles and 30.0 to 30.5 for the pipe piles. Both subsets contain significant number of cases (38 H piles and 38 pipe piles when eliminating outliers).
4. When further restricting the conditions described in (3) above by looking at the energy range of the diesel hammers typically used in Mn/DOT practice, the subsets decrease to 13/12 H pile cases and 16/14 pipe pile cases, with and without outliers, respectively. These are marginal size sets that result with coefficients varying between 31.2 to 34.4 for H piles and 33.1 to 33.3 for pipe piles.
5. Close examination of the most restrictive subsets described in (4) above (i.e. 13 H piles and 16 pipe piles before removing the outliers) show that in both subsets a relatively (to the subset size) large group of cases are of different piles of the same size tested at the same site (e.g. 7 out of the 16 pipe piles are 14" diameter piles from Deer Island project in Massachusetts and 6 of the H piles are 12x53 from site no. 37 in Canada). As such, the data are too biased as not only the set is marginal in size,

but about 50% of the cases are related to the same project. The statistics and coefficient obtained from that subset should, therefore, cautiously be applied.

6. As a lower coefficient means a more conservative evaluation, the above discussion and the observations presented in (3) should serve as the guideline for the new Mn/DOT dynamic equation that suits better to Mn/DOT pile driving practice of diesel hammers and BC ≥ 4BPI.
7. The equation recommended as the new Mn/DOT dynamic equation for the specific practice (diesel hammers) is therefore:

$$R_u = 30\sqrt{E_h} * \log (10 * N) \tag{6.3}$$

R_u = predicted pile capacity in kips
E_h = rated hammer energy kips·ft
N = blows per inch (PBI) at the End of Driving (EOD)

8. Based on the data presented in Tables 5.2 to 5.11, the associated recommended preliminary resistance factors for equation 6.3 are ϕ = 0.60 for H-piles and ϕ = 0.45 for pipe piles. Further details and discussion of these recommendations are presented in section 6.10.

6.8 INVESTIGATION OF THE DETAILED NEW MN/DOT DYNAMIC EQUATION

6.8.1 Overview

The sub-categorizations of the data related to the conditions that were used to examine the Mn/DOT dynamic equation (section 5.7) and to develop equation 6.3 are described in Table 6.4. The same subsets were used to examine the statistical parameters of equation 6.3 under EOD conditions starting from all hammers EOD cases (for which equation 6.2 is applied) to the most restrictive conditions directly related to the Mn/DOT practices and ranges. The results of these analyses are presented below.

6.8.2 H Piles

Table 6.5 presents the statistical details of the new Mn/DOT dynamic equation (equation 63) while Figures 6.3 to 6.7 present graphically the relevant information. For the most generic case of EOD with all piles, the statistics of both equations (6.2 and 6.3) are presented in Table 6.5 and Figures 6.3a and 6.3b. This is done so to examine the applicability of using the detailed equation (6.3) under all driving conditions.

The presented information suggests that the performance of equation 6.3 is consistent and reliable for all H piles driven with diesel hammers regardless of the energy range. The use of equation 6.3 for all type of hammers at EOD and all driving resistances naturally would provide a safer evaluation compared to that of equation 6.2 that was developed for that situation specifically. This can be clearly seen in Figure 6.3 where the cases plotted above the solid line represent the ‘unsafe’ cases for which the prediction was higher than the measured capacity, and the use of a coefficient of 30 vs. 35 essentially reduced the calculated capacity by 6/7. The greater mean bias obtained when using equation 6.3 allows, therefore, to select a consistent resistance factor of ϕ = 0.60 to be used for all the cases when applying equation 6.3. This conclusion is further examined and reaffirmed against an independent control database in section 7.2.

6.8.3 Pipe Piles

Table 6.6 presents the statistical details for the new Mn/DOT dynamic equation (equation 6.3) while Figures 6.8 to 6.12 present graphically the relevant information. For the most generic case of EOD with all piles, the statistics of both equations (6.2 and 6.3) are presented in Table 6.6 and Figures 6.8a and 6.8b. This is done to examine the applicability of using the detailed equation (6.3) under all driving conditions.

The presented information suggests that equation 6.2 provides accurate predictions for all cases (mean about 1.0), however, due to the larger scatter associated with the capacity prediction of pipe piles, the coefficient of variation is typically higher than that for the H piles, and hence, the associated resistance factors are lower. Exception to that are the cases of the most restrictive subsets, matching closely the Mn/DOT practice by the hammers energy range in addition to diesel hammers and BC ≥ 4BPI. These subsets result with an under-prediction and, hence, a bias greater than 1.0 along with low coefficients of variation, resulting with very high resistance factors. The reasons for that behavior were discussed in section 6.7.2, as the small subset is biased due to large number of piles from the same site, the use of these parameters is not safe. However, a consistent resistance factor of 0.45 could be used when applying equation 6.3 for all H pile cases. Figure 6.8 shows that while the scatter remains about the same when using equation 6.3 instead of equation 6.2, the number of under-predicted cases decreases as the prediction decreases by 6/7 when applying equation 6.3 instead of 6.2. Figures 6.9 to 6.11 show that the most unsafe cases are associated with low static capacities of about 50kips that is not well correlated to the driving resistance in the field being approximately 5 to 7BPI.

Table 6.5 Statistical Parameters and Resistance Factors of the New Detailed Mn/DOT Dynamic Equation for H Piles

Case No.	No. of Cases (n)	Coeff.	Condition	Mean Bias Measured/ Calculated (m_λ)	Stand. Dev. (σ_λ)	Coef. of Var. (COV_λ)	Best Fit Line Equation (least square)	Coeff. of Determination (r^2)	Resistance Factor ϕ β=2.33, p_f=1%, Redundant			ϕ/λ Efficiency Factor (%)
									FOSM	MC[3]	Recom	
1	125	35	EOD Only	1.0163	0.3599	0.3542	R_u=0.888R_s	0.896	0.495	0.542	0.55	54.1
		30		1.1856	0.4199	0.3542	R_u=0.754R_s	0.896	0.578	0.632	0.60	50.6
2	39	30	EOD, Diesel, BC ≥ 4BPI	1.0760	0.3417	0.3176	R_u=0.812R_s	0.907	0.566	0.628	0.60	55.8
3	38	30	EOD, Diesel, BC ≥ 4BPI w/o outliers	1.0458	0.2888	0.2762	R_u=0.873R_s	0.935	0.598	0.674	0.65	62.2
4	13	30	EOD, Diesel, Mn/DOT Energy, BC ≥ 4BPI	1.1419	0.4531	0.3968	R_u=0.759R_s	0.870	0.508	0.553	0.55	48.2
5	12	30	EOD, Diesel, Mn/DOT Energy, BC ≥ 4BPI w/o outliers	1.0518	0.3297	0.3135	R_u=0.889R_s	0.924	0.558	0.620	0.60	57.0

Notes: 1. calculated capacity using Mn/DOT new dynamic equation Ru = Coeff. $\sqrt{E_h} \bullet \log(10N)$.

2. Rs is the static capacity of the pile examined by Davisson's failure criterion

3. MC - Monte Carlo Simulation for 10,000 simulations

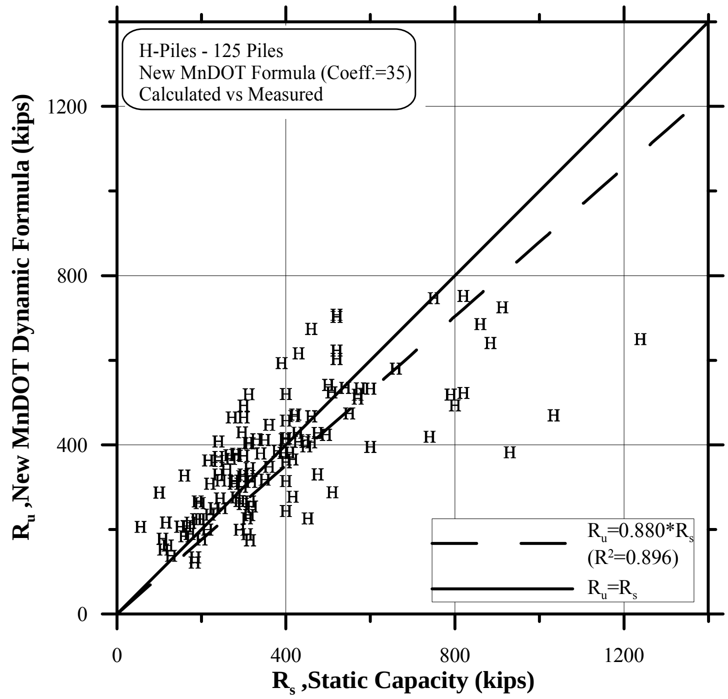

(a)

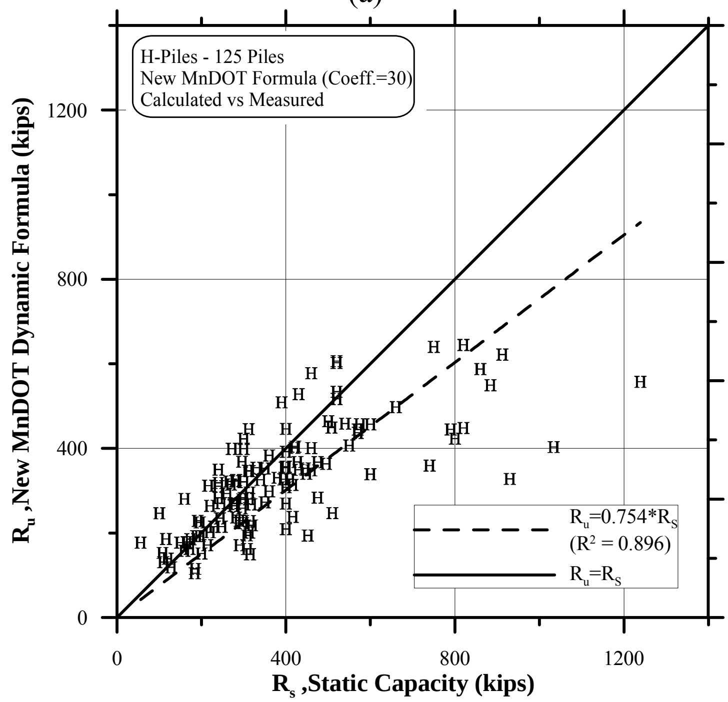

(b)

Figure 6.3 Measured static capacity vs. the new Mn/DOT equation prediction for 125 EOD H pile cases (a) coeff. = 0.35 (equation 6.2), and (b) coeff. = 0.30 (equation 6.3).

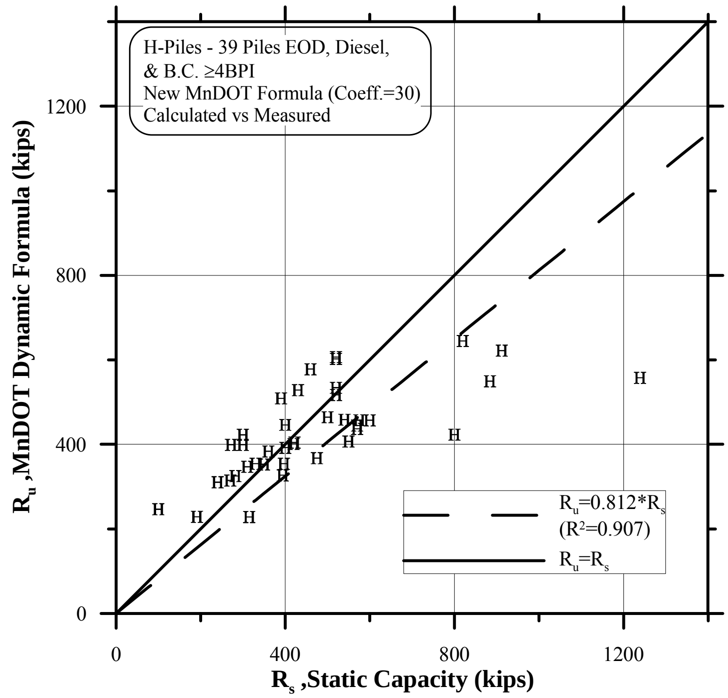

(a)

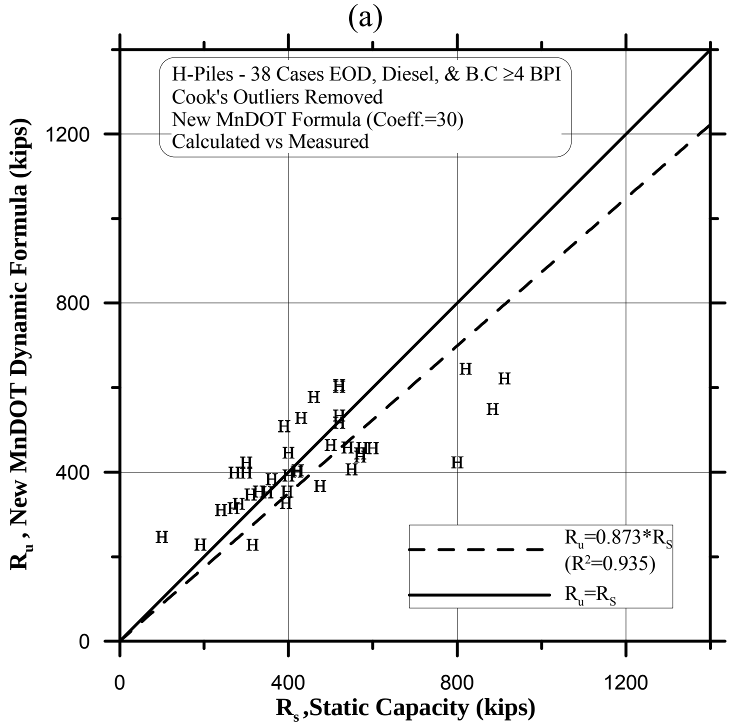

(b)

Figure 6.4 Measured static capacity vs. the new Mn/DOT dynamic equation (coeff. = 0.30) applied to EOD cases of diesel hammers with BC ≥ 4BPI (a) all subset cases and (b) with outliers removed.

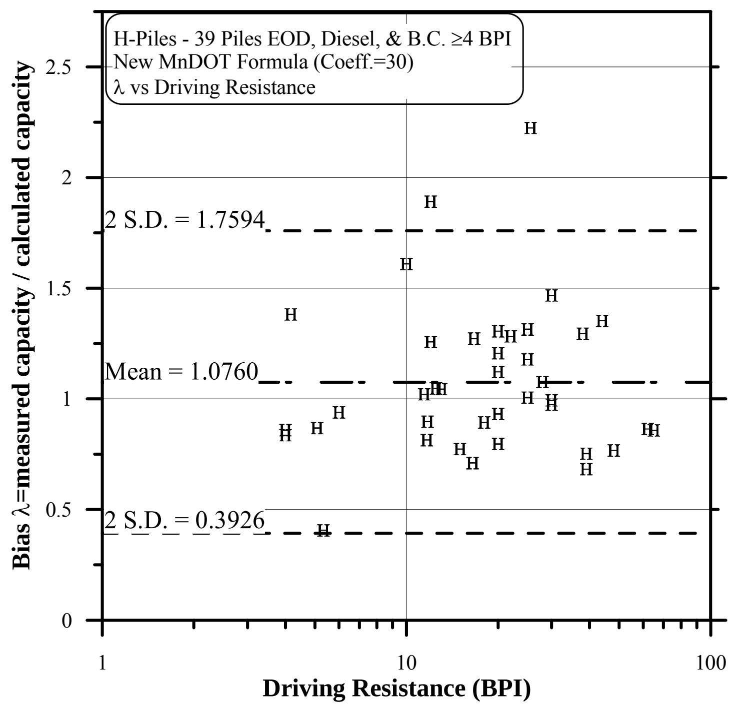

Figure 6.5 Driving resistance vs. bias (measured over predicted capacity) using New Mn/DOT dynamic equation (coeff. = 30) applied to EOD cases of diesel hammers with BC ≥ 4BPI.

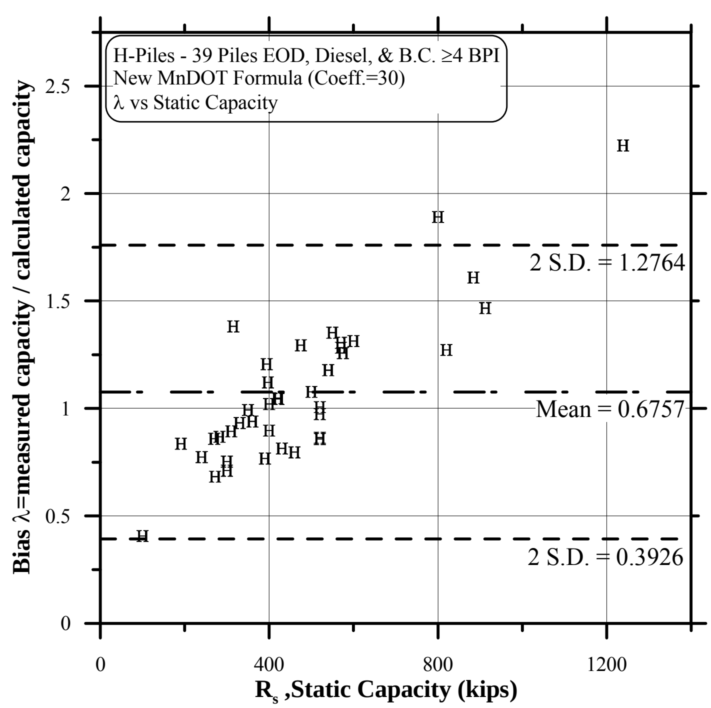

Figure 6.6 Measured static capacity vs. bias (measured over predicted capacity) using New Mn/DOT dynamic equation (coeff. = 30) applied to EOD cases of diesel hammers with BC ≥ 4BPI.

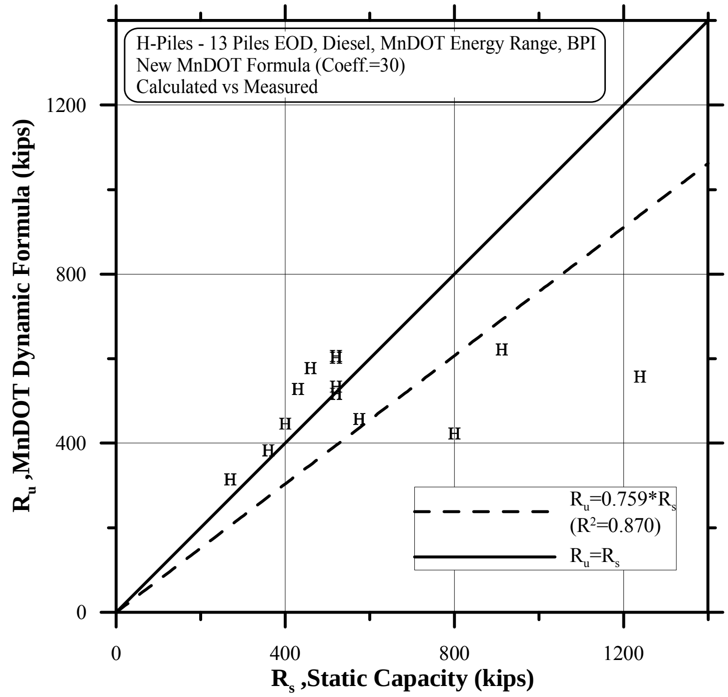

(a)

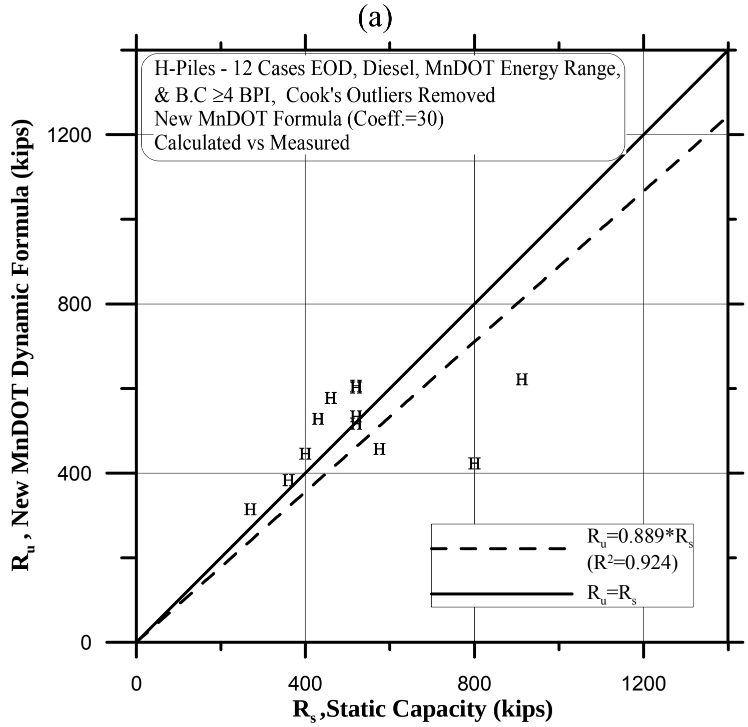

(b)

Figure 6.7 Measured static capacity vs. New Mn/DOT Dynamic equation (coeff. = 30) applied to EOD cases of diesel hammers within the energy range of Mn/DOT practice with BC ≥ 4BPI (a) all subset cases, and (b) with outliers removed.

Table 6.6 Statistical Parameters and Resistance Factors of the New Detailed Mn/DOT Dynamic Equation for Pipe Piles

Case No.	No. of Cases (n)	Coeff.	Condition	Mean Bias Measured/ Calculated (m_λ)	Stand. Dev. (σ_λ)	Coef. of Var. (COV_λ)	Best Fit Line Equation (least square)	Coeff. of Determination (r^2)	Resistance Factor ϕ β=2.33, p_f=1%, Redundant			ϕ/λ Efficiency Factor (%)
									FOSM	MC³	Recom	
1	99	35	EOD Only	1.1089	0.5955	0.5955	R_u=0.805R_s	0.849	0.364	0.385	0.35	31.6
		30		1.2937	0.6947	0.5370	R_u=0.694R_s	0.850	0.424	0.450	0.45	34.8
2	41	30	EOD, Diesel, BC ≥ 4BPI	0.9519	0.4078	0.4284	R_u=0.902R_s	0.918	0.396	0.427	0.40	42.0
3	38	30	EOD, Diesel, BC ≥ 4BPI w/o outliers	0.9071	0.3149	0.3472	R_u=0.946R_s	0.946	0.449	0.492	0.45	49.6
4	16	30	EOD, Diesel, Mn/DOT Energy, BC ≥ 4BPI	1.1284	0.2051	0.1818	R_u=0.878R_s	0.974	0.766	0.905	0.85	45.3
5	14	30	EOD, Diesel, Mn/DOT Energy, BC ≥ 4BPI w/o outliers	1.1065	0.1273	0.1151	R_u=0.895R_s	0.988	0.825	1.012	0.90	81.3

Notes: 1. calculated capacity using Mn/DOT new dynamic equation Ru = Coeff. $\sqrt{E_h} \bullet \log(10N)$.

2. Rs is the static capacity of the pile examined by Davisson's failure criterion

3. MC - Monte Carlo Simulation for 10,000 simulations

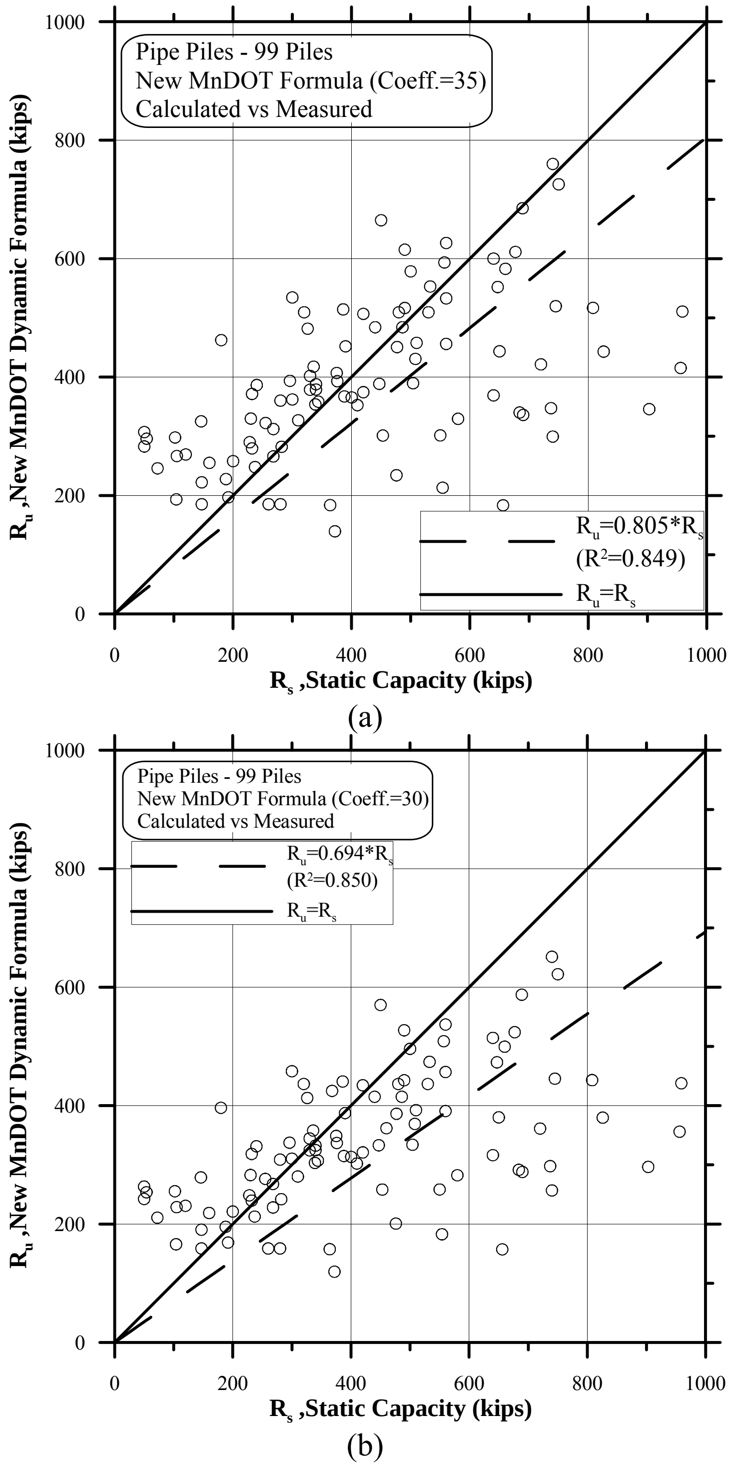

Figure 6.8 Measured static capacity vs. the new Mn/DOT equation prediction for 99 EOD pipe pile cases (a) coeff. = 0.35 (equation 6.2), and (b) coeff. = 0.30 (equation 6.3).

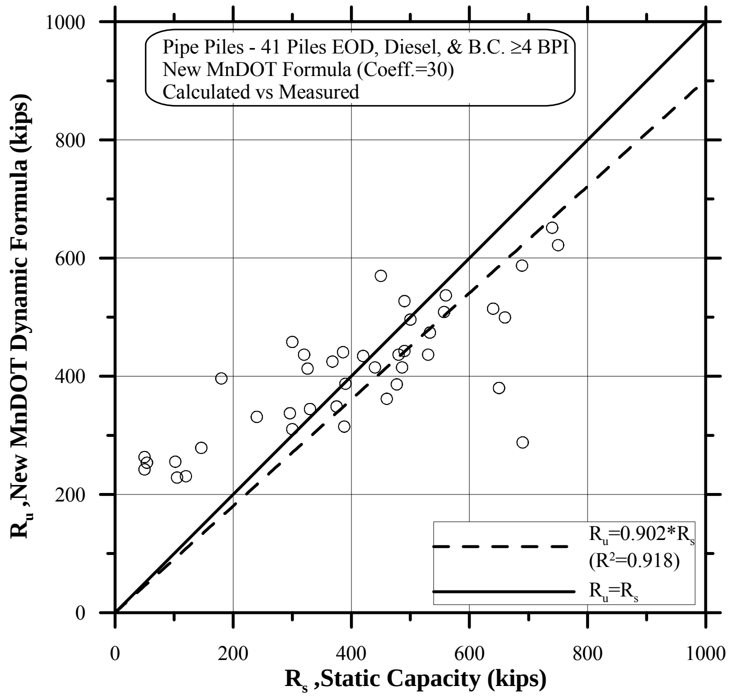

(a)

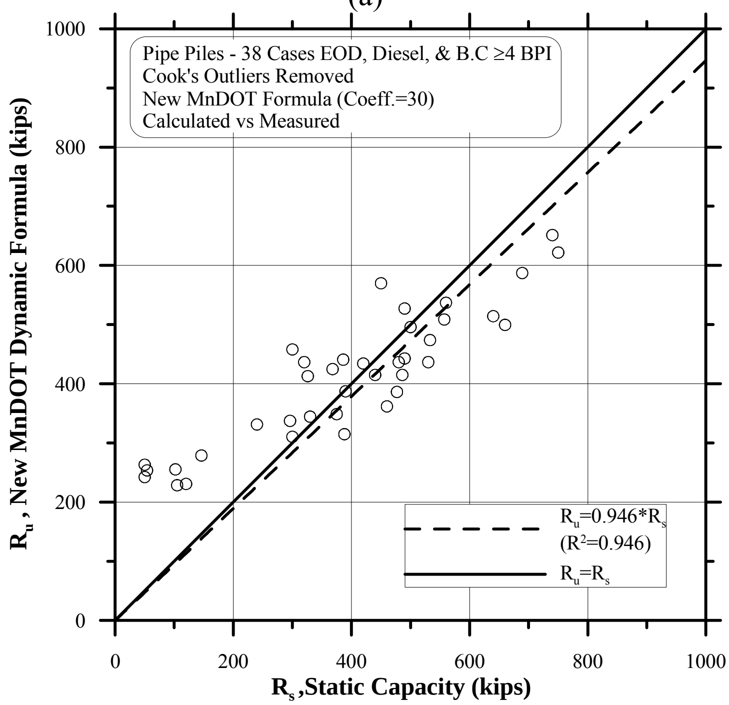

(b)

Figure 6.9 Measured static capacity vs. the new Mn/DOT dynamic equation (coeff. = 0.30) applied to EOD cases of diesel hammers with BC ≥ 4BPI (a) all subset cases and (b) with outliers removed.

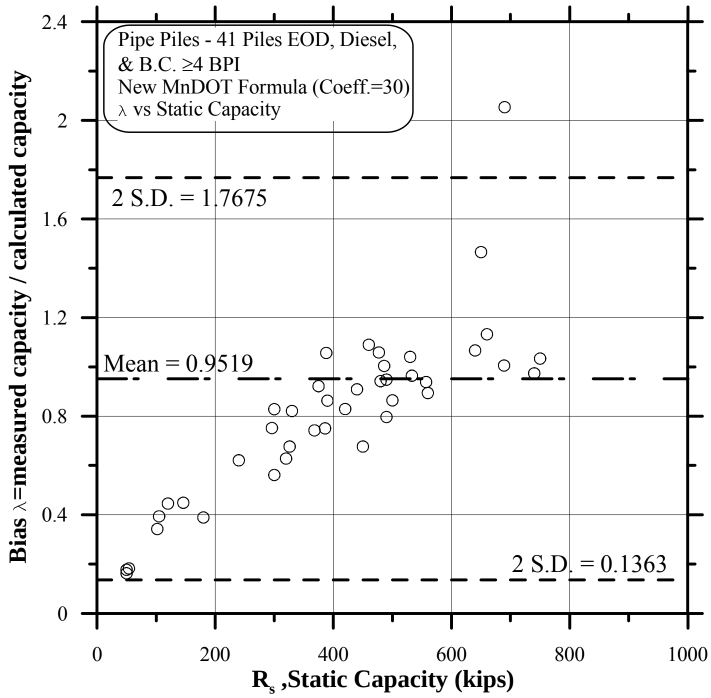

Figure 6.10 Driving resistance vs. bias (measured over predicted capacity) using New Mn/DOT dynamic equation (coeff. = 30) applied to EOD cases of diesel hammers with BC ≥ 4BPI.

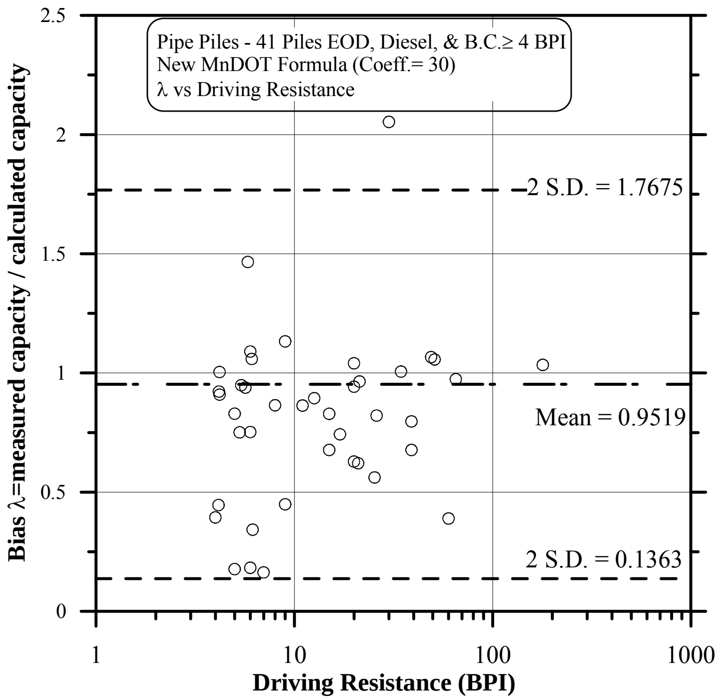

Figure 6.11 Measured static capacity vs. bias (measured over predicted capacity) using New Mn/DOT dynamic equation (coeff. = 30) applied to EOD cases of diesel hammers with BC ≥ 4BPI.

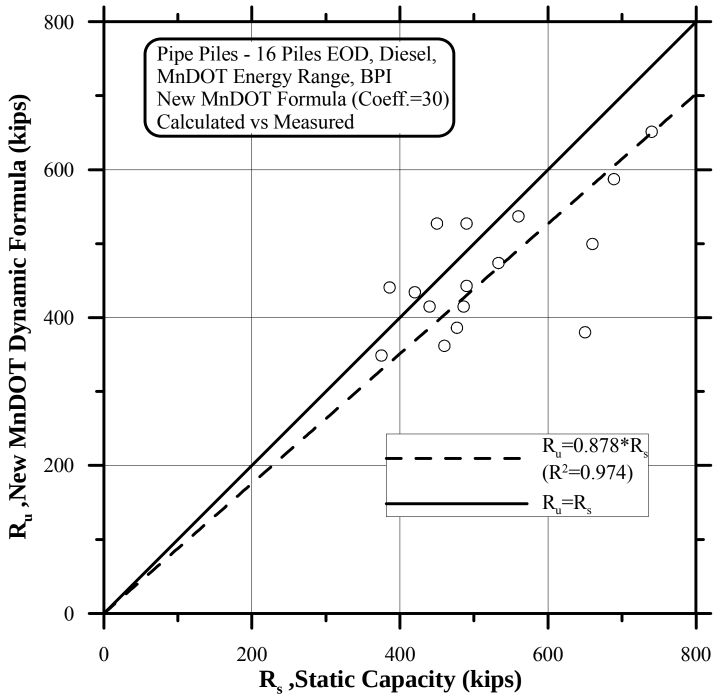

(a)

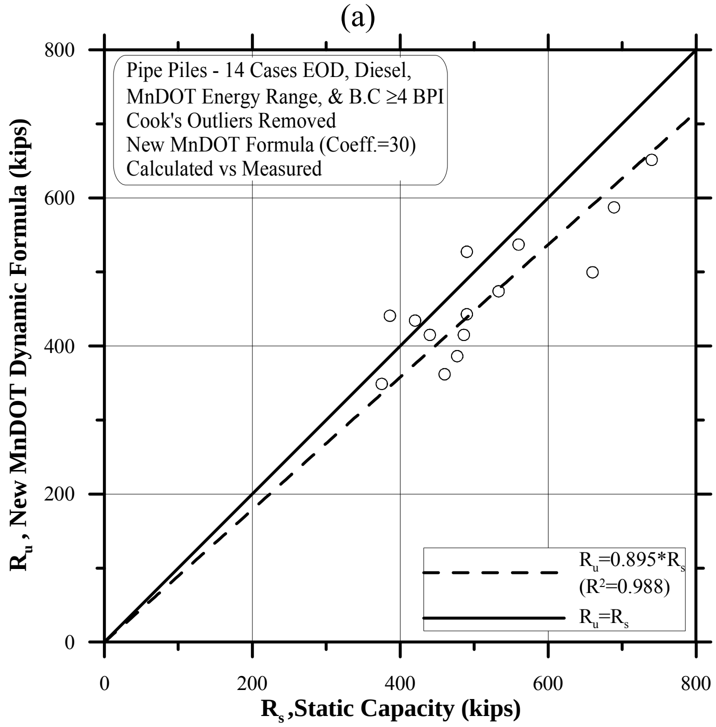

(b)

Figure 6.12 Measured static capacity vs. New Mn/DOT Dynamic equation (coeff. = 30) applied to EOD cases of diesel hammers within the energy range of Mn/DOT practice with BC ≥ 4BPI (a) all subset cases, and (b) with outliers removed.

6.9 IN-DEPTH EXAMINATION OF THE NEW MN/DOT EQUATION DISTRIBUTION FUNCTIONS FIT FOR LRFD CALIBRATION

Tables 6.5 and 6.6 presented the resistance factors calculation for various calibrated conditions. As explained in section 4.4, the calibrations were carried out assuming resistance in agreement with a lognormal distribution for which the statistical parameters are presented. In actuality, the normal distribution function parameters are detailed while in the calibration, a translation to a lognormal distribution is made. The mathematical and graphical examination of this hypothesis are presented in this section in the following way:

1. The χ-square goodness of fit (GOF) tests have been carried out to examine the fit of the theoretical normal and lognormal distributions to bias data. Table 6.7 lists in detail the χ^2 values obtained for various key sub-categorization cases, both for H and pipe piles for log and lognormal distributions. If the χ^2 values obtained for an assumed distribution is greater than the acceptance χ^2 value of a certain significance level (usually of 1% or 5%), then the distribution is rejected. The χ^2 values of the 1 and 5% significance values are provided in Table 6.7 as well. Observing the χ^2 values in Table 6.7 suggests that (a) all lognormal distribution χ^2 values are significantly lower than the χ^2 values for the normal distribution, suggesting a better fit to the distribution, (b) all χ^2 values for the lognormal distribution are below the significance level of 1% except of one. Hence, the lognormal distribution is accepted by the χ-squared GOF test.
2. Presenting the relevant examined data cases against the theoretical normal and lognormal distributions (as standard normal quantile of bias data) is shown in Figure 6.13 for three examined subsets of H pile cases and in Figure 6.14 for three examined subsets of pipe pile cases. The bias data in Figure 6.13 shows a good match to the theoretical lognormal distribution for all investigated subsets, affirming the χ^2 GOF test results of Table 6.7 and suggesting no outliers in all three subsets. The lower fit to the tail in Figure 6.13c shows data on the 'safer' side (higher bias) than the theoretical distribution and, hence, the use of the theoretical distribution is safe. The bias data in Figure 6.14 shows also a reasonably good match to the theoretical lognormal distribution for all investigated subsets. While affirming the χ^2 GOF test results of Table 6.7, it also indicates on a lesser quality match as the database decreases, especially for the case of pipe piles at the EOD driven by diesel hammers with BC $\geq$ 4BPI (Figure 6.14b) for which the use of a lognormal distribution is on the "unsafe" side. In both problematic matches, datasets without outliers had been examined as presented in Table 6.6.

Table 6.7 Summary of χ^2 values for the New Mn/DOT Equation (coeff. = 30)

		χ^2	
Pile Type	**Condition**	**Normal**	**Lognormal**
H	EOD Only	47.8	8.7
H	EOD Only excluding Cook's Outliers	-	-
H	EOD, Diesel Hammer, B.C. ≥4 BPI	24.2	8.1
H	EOD, Diesel Hammer, B.C. ≥4 BPI excluding Cook's Outliers	-	-
H	EOD, Diesel Hammer, Mn/DOT Energy[2], B.C. ≥4 BPI	30.2	21.0
H	EOD, Diesel Hammer, Mn/DOT Energy[2], B.C. ≥4 BPI excluding Cook's Outliers	-	-
Pipe	EOD Only	110.1	19.0
Pipe	EOD Only excluding Cook's Outliers	-	-
Pipe	EOD, Diesel Hammer, B.C. ≥4 BPI	34.7	29.1
Pipe	EOD, Diesel Hammer, B.C. ≥4 BPI excluding Cook's Outliers	-	-
Pipe	EOD, Diesel Hammer, Mn/DOT Energy[2], B.C. ≥4 BPI	18.5	12.5
Pipe	EOD, Diesel Hammer, Mn/DOT Energy[2], B.C. ≥4 BPI excluding Cook's Outliers	-	-

Chi square (1%) = 21.6659943
Chi square (5%) = 16.9189776

Notes: [1] Searched coefficient for the equation Ru = Coeff. $\sqrt{E_h} \bullet \log(10N)$

[2] Mn/DOT energy range contains hammers with rated energies between 42.4 and 75.4 k-ft

(a)

(b)

(c)

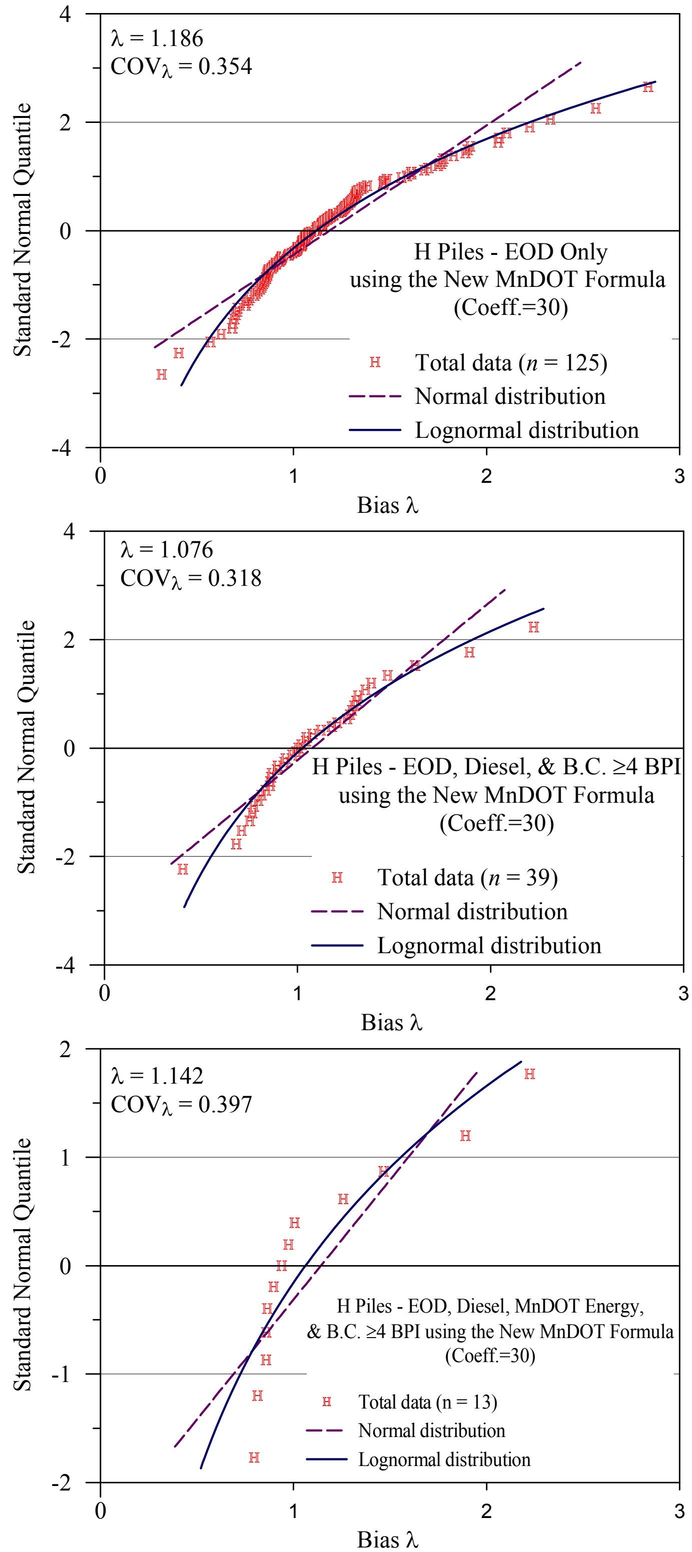

Figure 6.13 Standard normal quantile of bias data (measured capacity over calculated using the New Mn/DOT equation) and predicted quantiles of normal and lognormal distributions for H piles: (a) all EOD data, (b) EOD all diesel hammers and BC ≥ 4BPI, and (c) EOD, diesel hammers within Mn/DOT energy range and BC ≥ 4BPI.

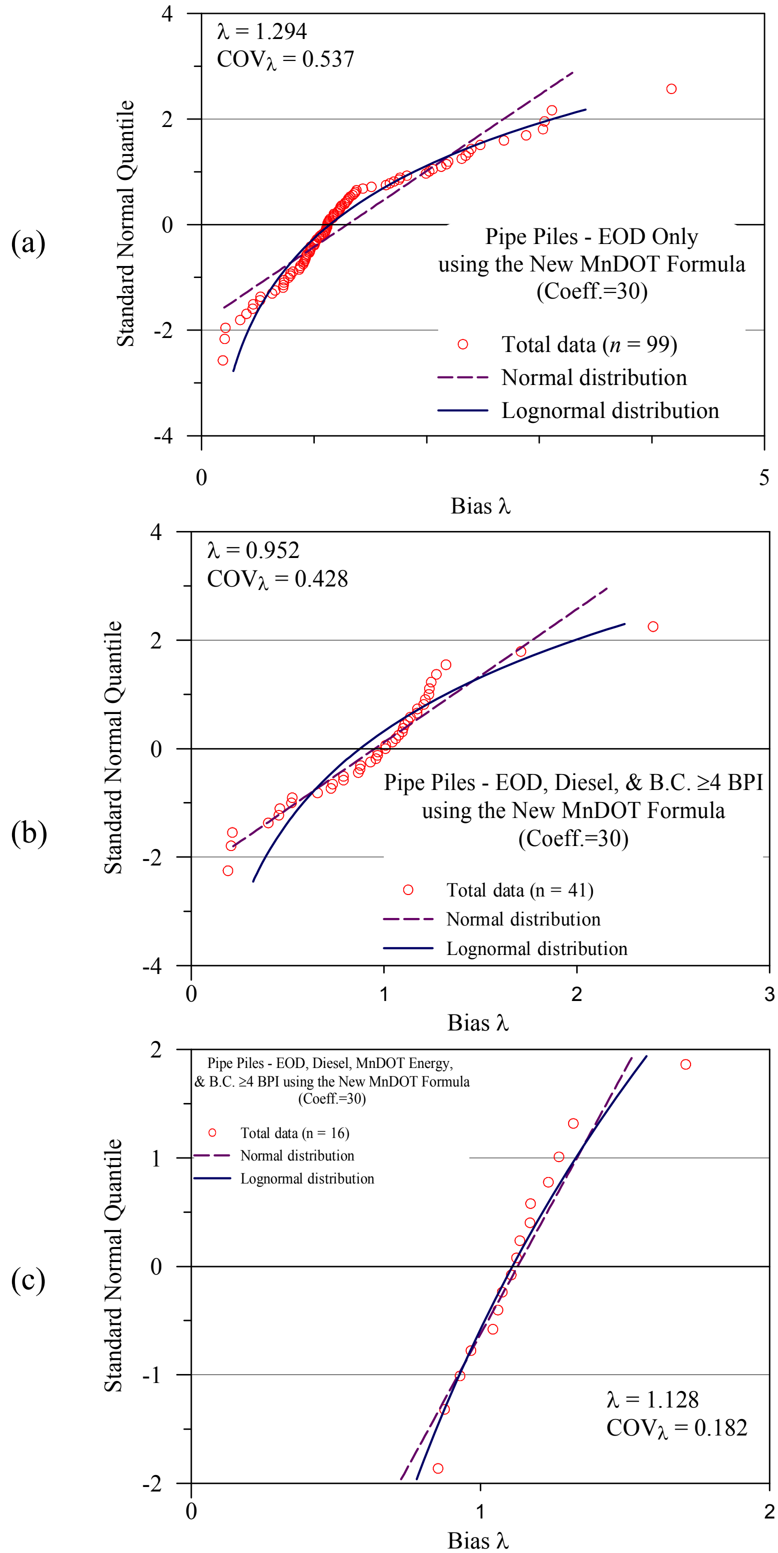

Figure 6.14 Standard normal quantile of bias data (measured capacity over calculated using the New Mn/DOT equation) and predicted quantiles of normal and lognormal distributions for pipe piles: (a) all EOD data, (b) EOD all diesel hammers and BC ≥ 4BPI, and (c) EOD, diesel hammers within Mn/DOT energy range and BC ≥ 4BPI.

6.10 PRELIMINARY CONCLUSIONS AND RECOMMENDATION

1. The development of a new general Mn/DOT dynamic equation addressing EOD conditions of all hammers with all energies and driving resistances resulted with equation (6.2) being:

$$R_u = 35\sqrt{E_h} * \log\ (10 * N) \quad (6.2)$$

R_u = predicted pile capacity in kips
E_h = rated hammer energy kips·ft
N = blows per inch (PBI) at the End of Driving (EOD)

The associated recommended resistance factors using equation 6.2 are ϕ = 0.55 for H-piles and ϕ = 0.40 for pipe piles.

2. The associated Factor of Safety with the use of this equation is F.S. ≈ 2.6 for H piles and F.S. ≈ 3.5 for pipe piles, reflecting the varied confidence in its use.
3. Considering subsets addressing better the Mn/DOT pile driving practices resulted with a new detailed dynamic equation recommended to be used by the Mn/DOT for all conditions:

$$R_u = 30\sqrt{E_h} * \log\ (10 * N) \quad (6.3)$$

R_u = predicted pile capacity in kips
E_h = rated hammer energy kips·ft
N = blows per inch (PBI) at the End of Driving (EOD)

4. The equation was developed specifically for the Mn/DOT pile driving practices (diesel hammers and BC ≥ 4BPI) and is suitable for both H and pipe piles. It was then examined for the general EOD cases.
5. The recommended resistance factors to be used with equation 6.3 are ϕ = 0.60 for H piles, ϕ = 0.45 for pipe piles.
6. The same equation and resistance factors are recommended for all hammers under EOD conditions.
7. Additional investigation of the proposed equation is performed on the separate control group database (see section 3.6.4) is presented in Chapter 7.

CHAPTER 7 PERFORMANCE EVALUATION OF METHODS UTILIZING DYNAMIC MEASUREMENTS AND THE MN/DOT DYNAMIC EQUATIONS UTILIZING A CONTROL DATABASE

7.1 ANALYSIS BASED ON DYNAMIC MEASUREMENTS

7.1.1 Overview

The pursuit of pile capacity prediction during driving remains (like all other engineering discussions) subjected to economic evaluation. While the preceding chapters concentrated on the performance evaluation and the development of dynamic equations, the present section evaluates the performance of dynamic analyses based on dynamic equations. Such performance should be compared to that of the dynamic measurements and the use of dynamic measurements can then be economically evaluated based on the findings. Section 3.6.3 presents the data subset containing dynamic measurements and the following sections present the performance of methods utilizing these data. Two analysis methods utilizing the dynamic measurements are evaluated, the signal matching method (CAPWAP) described in section 1.7.3, and the field method Energy Approach (EA) described in section 1.7.2. Both methods have different datasets (as often only CAPWAP prediction is provided in a report without the measurements' details) and hence, when compared to the performance of the Mn/DOT dynamic equations (existing and new), both datasets had been analyzed.

7.1.2 H Piles

Table 7.1 summarizes the performance of both CAPWAP and the Energy Approach for the following conditions: (a) all the available data cases, (b) EOD only, (c) EOD by diesel hammers, (d) EOD by diesel hammers with BC $\geq$ 4BPI and (e) subset 'd' with the energy range of Mn/DOT practice only. Table 7.2 summarizes for the same data the performance of Mn/DOT equation and the New Mn/DOT equation. In order to allow for accurate comparisons, both equations were evaluated for both datasets.

Figures 7.1 and 7.2 present the measured static capacity (determined using Davisson's Criterion) vs. CAPWAP and Energy Approach predictions for all (EOD and BOR) H pile cases, respectively. Figures 7.3 and 7.4 present the measured static capacity vs. CAPWAP and Energy Approach predictions for EOD, diesel hammer driven H pile cases, respectively.

The data in Tables 7.1 and 7.2, and Figures 7.1 to 7.4 suggests the following:

1. CAPWAP systematically under-predicted the pile capacities, hence, resulted in a mean bias significantly greater than 1.0 for most subsets.
2. The scatter of the CAPWAP method (measured via the COV) is better than the typical dynamic equations excluding the new Mn/DOT equation, which is consistently lower than that of CAPWAP, but also was developed using the analyzed dataset as part of its database.

3. CAPWAP best performed for driving conditions of diesel hammers with BC ≥ 4BPI, however, also for that category the COV was 0.443.
4. The Energy Approach systematically provided a bias closer to 1.0 and a scatter smaller than that of CAPWAP (EA COV ≈ 0.35 vs. CAPWAP COV ≈ 0.45).
5. The Energy Approach marginally over-predicts (mean = 0.89) the conditions for diesel hammers with BC ≥ 4BPI.
6. Due to the above, while CAPWAP results with a higher calculated resistance factor (as a result of a high bias), the Energy Approach shows to have systematically higher efficiency factor and hence, economic advantage for the piles for which dynamic measurements data were available.
7. The Mn/DOT dynamic equation (equation 5.5) had resulted with systematically accurate average predictions, hence, biases around 1.0, however, the scatter of the equation is extremely large expressed as COV around 0.7. The resulting calculated resistance factor was $\phi = 0.25$ which is identical to the one recommended in section 5.9.
8. The new Mn/DOT dynamic equation (equation 6.3) had resulted with exceptional good performance. The systematic higher biases are a result of the fact that equation 6.3 was developed for Mn/DOT practices and, hence, is most suitable for diesel hammers with BC ≥ 4BPI, performing well for that category. Using equation 6.2 that was developed for all cases would result with the mean biases reduced by 6/7 and, hence, more accurate predictions. The COV of the new equation is systematically low, just marginally higher than that of the Energy Approach and lower than that of CAPWAP. These findings need, however to be reviewed in light of the fact that the new equation was developed using in part the data of Table 7.2 for which it was evaluated. The calculated resistance factors in Table 7.2 of $\phi = 0.60$, matches that recommended in section 6.10 and mitigates the under-prediction (higher bias) of the equation when applied to all hammer types.

7.1.3 Pipe Piles

Table 7.3 summarizes the performance of both CAPWAP and the Energy Approach for the following conditions: (a) all the available data cases, (b) EOD only, (c) EOD by diesel hammers, (d) EOD by diesel hammers with BC ≥ 4BPI and (e) subset 'd' with the energy range of Mn/DOT practice only. Table 7.4 summarizes for the same data the performance of Mn/DOT equation and the New Mn/DOT equation. In order to allow for accurate comparisons, both equations were evaluated for both datasets.

Figures 7.5 and 7.6 present the measured static capacity (determined using Davisson's Criterion) vs. CAPWAP and Energy Approach predictions for all (EOD and BOR) pipe pile cases, respectively. Figures 7.7 and 7.8 present the measured static capacity vs. CAPWAP and Energy Approach predictions for all EOD pipe pile cases, respectively. Figures 7.9 and 7.10 present the measured static capacity vs. CAPWAP and Energy Approach predictions for all EOD diesel hammer driven pipe piles, respectively.

Table 7.1 Statistical Parameters of Dynamic Analyses of H Piles Using Dynamic Measurements and the Associated Resistance Factors

Condition	CAPWAP								ENERGY APPROACH							
	No. of Cases (n)	Mean Bias Measured/ Calculated (m_λ)	Stand. Dev. (σ_λ)	Coef. of Var. (COV_λ)	Resistance Factor ϕ β=2.33, p_f=1% Redundant			Efficiency Factor (ϕ/λ) %	No. of Cases (n)	Mean Bias Measured/ Calculated (m_λ)	Stand. Dev. (σ_λ)	Coef. of Var. (COV_λ)	Resistance Factor ϕ β=2.33, p_f=1% Redundant			Efficiency Factor (ϕ/λ) %
					FOSM	MCS	Recom						FOSM	MCS	Recom	
All	38	1.456	0.656	0.451	0.577	0.622	0.60	41.2	33	0.989	0.326	0.329	0.508	0.561	0.55	55.6
EOD	31	1.457	0.635	0.436	0.596	0.642	0.60	41.2	26	0.991	0.346	0.349	0.488	0.535	0.50	50.5
Diesel	24	1.333	0.609	0.457	0.521	0.562	0.55	41.2	20	0.967	0.370	0.383	0.444	0.484	0.45	46.5
B.C. ≥4 BPI	17	1.072	0.475	0.443	0.431	0.464	0.45	42.0	16	0.893	0.337	0.377	0.415	0.453	0.45	50.4
Mn/DOT Energy	4	1.400	0.801	0.572	0.425	0.449	0.45	32.1	2	1.505	0.407	0.270	0.871	0.985	N/A	N/A

Table 7.2 Statistical Parameters of the Mn/DOT Dynamic Equations (Existing and New) Developed for the Dataset Containing Dynamic Measurements on H Piles and the Associated Resistance Factors

CAPWAP Dataset																
Condition	Mn/DOT Equation (75%)								New Mn/DOT Equation (coeff. = 30)							
	No. of Cases (n)	Mean Bias Measured/ Calculated (m_λ)	Stand. Dev. (σ_λ)	Coef. of Var. (COV_λ)	Resistance Factor ϕ β=2.33, p_f=1% Redundant			Efficiency Factor (ϕ/λ) %	No. of Cases (n)	Mean Bias Measured/ Calculated (m_λ)	Stand. Dev. (σ_λ)	Coef. of Var. (COV_λ)	Resistance Factor ϕ β=2.33, p_f=1% Redundant			Efficiency Factor (ϕ/λ) %
					FOSM	MCS	Recom						FOSM	MCS	Recom	
All	38	1.056	0.711	0.674	0.258	0.272	0.25	23.7	38	1.349	0.533	0.395	0.603	0.656	0.60	44.5
EOD	31	1.072	0.743	0.693	0.251	0.265	0.25	23.3	31	1.337	0.513	0.383	0.613	0.668	0.60	44.9
Diesel	24	1.027	0.698	0.680	0.247	0.261	0.25	24.3	24	1.348	0.549	0.407	0.587	0.637	0.60	44.5
B.C. ≥4 BPI	17	0.721	0.392	0.544	0.233	0.247	0.25	34.7	17	1.153	0.413	0.359	0.556	0.607	0.60	52.0
Energy Approach Dataset																
Condition	Mn/DOT Equation (75%)								New Mn/DOT Equation (coeff. = 30)							
	No. of Cases (n)	Mean Bias Measured/ Calculated (m_λ)	Stand. Dev. (σ_λ)	Coef. of Var. (COV_λ)	Resistance Factor ϕ β=2.33, p_f=1% Redundant			Efficiency Factor (ϕ/λ) %	No. of Cases (n)	Mean Bias Measured/ Calculated (m_λ)	Stand. Dev. (σ_λ)	Coef. of Var. (COV_λ)	Resistance Factor ϕ β=2.33, p_f=1% Redundant			Efficiency Factor (ϕ/λ) %
					FOSM	MCS	Recom						FOSM	MCS	Recom	
All	33	1.162	0.456	0.393	0.521	0.567	0.55	47.3	33	1.355	0.533	0.393	0.608	0.662	0.60	44.3
EOD	26	1.028	0.711	0.692	0.241	0.255	0.25	24.3	26	1.343	0.508	0.378	0.622	0.678	0.60	44.7
Diesel	20	0.928	0.626	0.675	0.226	0.238	0.25	26.9	20	1.331	0.551	0.414	0.571	0.618	0.60	45.1
B.C. ≥4 BPI	16	0.749	0.388	0.519	0.256	0.272	0.25	33.4	16	1.201	0.408	0.340	0.603	0.663	0.60	50.0

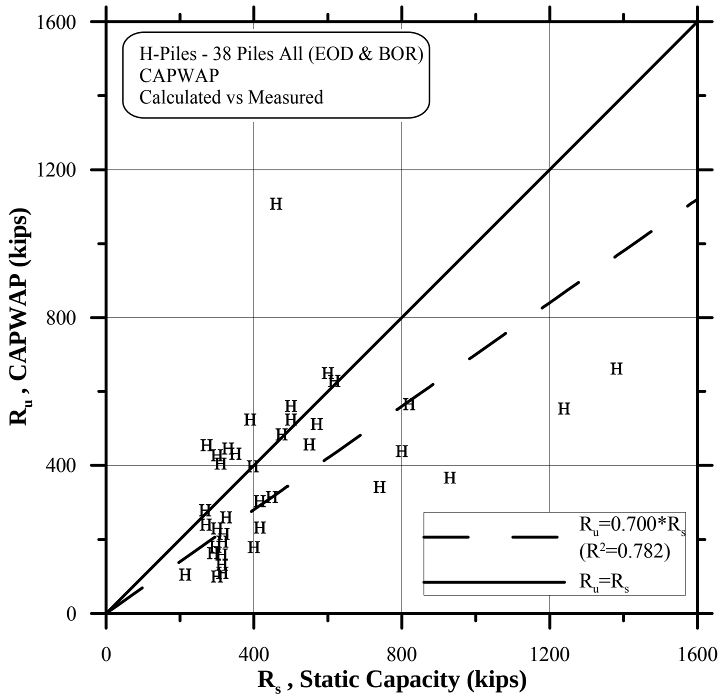

Figure 7.1 Measured static capacity vs. signal matching (CAPWAP) prediction for 38 H pile cases (EOD and BOR).

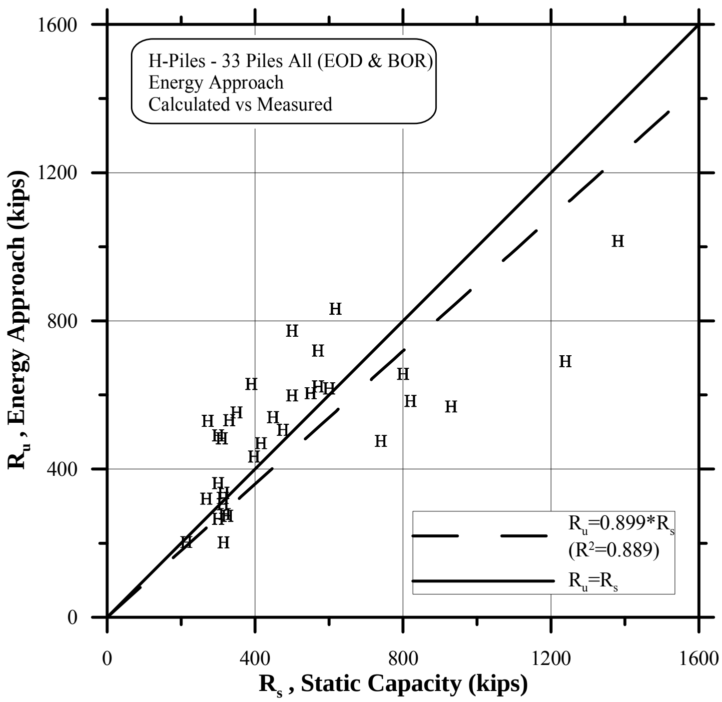

Figure 7.2 Measured static capacity vs. Energy Approach (EA) prediction for 33 H pile cases (EOD and BOR).

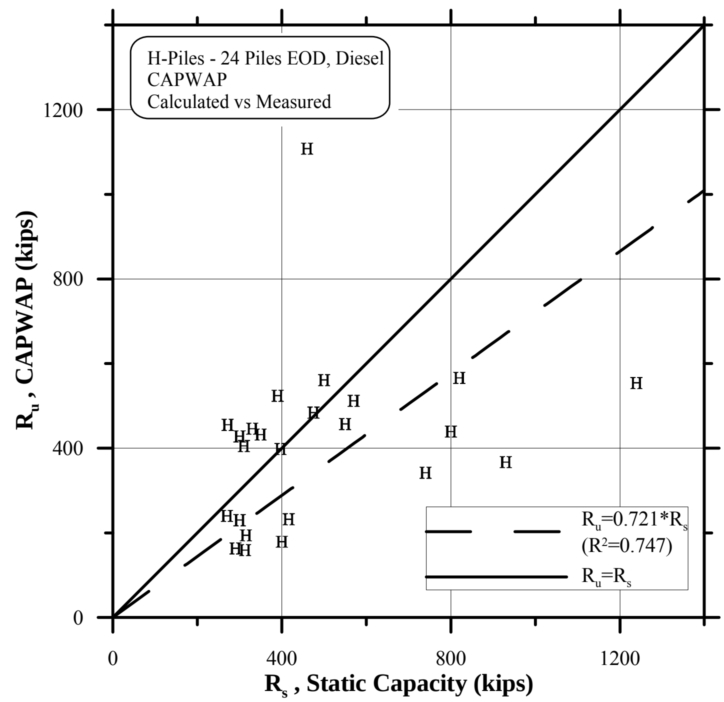

Figure 7.3 Measured static capacity vs. signal matching (CAPWAP) prediction for 24 EOD, diesel driven H pile cases.

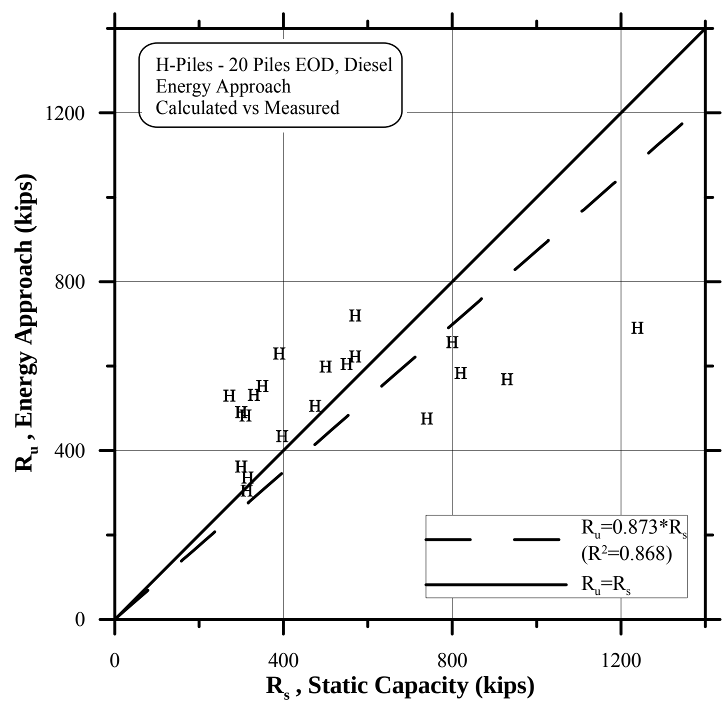

Figure 7.4 Measured static capacity vs. Energy Approach (EA) prediction for 20 EOD, diesel driven H pile cases.

The data in Tables 7.3 and 7.4, and Figures 7.5 to 7.10 suggests the following:

1. CAPWAP systematically under-predicts the pile capacities in all the subsets, typically by a bias factor of about 1.4.
2. The scatter of the CAPWAP method is better than the typical dynamic equations excluding the Mn/DOT equation, and similar to the one obtained for the H piles.
3. The Energy Approach method systematically provided a bias lower than that of CAPWAP (close to 1.0), but a scatter higher than that of CAPWAP for the generic cases (all EOD) as well as lower than that of CAPWAP for all EOD with diesel hammers and those for BC ≥ 4BPI, meaning that the Energy Approach is more suitable for EOD conditions in the field.
4. Due to the above, while CAPWAP results with higher calculated resistance factors (due to the high bias), the Energy Approach shows to have a higher efficiency factor for EOD diesel hammers and with cases having BC ≥ 4BPI.
5. The Mn/DOT dynamic equation (equation 5.5) had resulted with systematically problematic scatter except of the cases for which the combination of diesel hammer and BC ≥ 4BPI were achieved, for which the dataset was biased by 13 cases related to two sites only (6 of the Civic Center project and 7 of the Deer Island project identical piles in each location all obtained from GZA of MA). A low COV for this subset was observed in all analyzed methods. The very large coefficient of variation resulted with resistance factors of about $\phi = 0.10$ for the general cases and 0.20 and 0.35 for the EOD diesel and EOD diesel with BC ≥ 4BPI. The later are compatible with the recommended resistance facto of $\phi = 0.25$ presented in section 5.9.
6. The new Mn/DOT dynamic equation (equation 6.3) had resulted with good performance compared to the other methods' performance for pipe piles. The systematic higher biases are a result of the equation's adjustment to the Mn/DOT diesel hammer and higher blow count as discussed in the previous section for the H piles. The high scatter (COV), though very good compared to all other methods (second only to CAPWAP), results with resistance factors consistent with the $\phi = 0.45$ recommendations of section 6.10. The higher resistance factors calculated for the smaller subgroups are a result of the fact that the equation was developed for those conditions and the large number of piles came from small number of sites as discussed above.

Table 7.3 Statistical Parameters of Dynamic Analysis of Pipe Piles Using Dynamic Measurements and the Associated Resistance Factors

Condition	CAPWAP								ENERGY APPROACH							
	No. of Cases (n)	Mean Bias Measured/ Calculated (m_λ)	Stand. Dev. (σ_λ)	Coef. of Var. (COV_λ)	Resistance Factor ϕ β=2.33, p_f=1% Redundant FOSM	MCS	Recom	Efficiency Factor (ϕ/λ) %	No. of Cases (n)	Mean Bias Measured/ Calculated (m_λ)	Stand. Dev. (σ_λ)	Coef. of Var. (COV_λ)	Resistance Factor ϕ β=2.33, p_f=1% Redundant FOSM	MCS	Recom	Efficiency Factor (ϕ/λ) %
All	74	1.358	0.563	0.415	0.582	0.630	0.60	44.2	59	1.138	0.675	0.593	0.330	0.349	0.35	30.8
EOD	58	1.441	0.597	0.414	0.618	0.668	0.65	45.1	43	1.261	0.744	0.590	0.369	0.389	0.35	27.8
Diesel	36	1.381	0.501	0.363	0.661	0.721	0.70	50.7	32	1.019	0.247	0.243	0.621	0.709	0.70	68.7
B.C. ≥4 BPI	21	1.327	0.455	0.343	0.663	0.728	0.70	52.8	19	0.976	0.166	0.170	0.675	0.802	0.70	71.7
Mn/DOT Energy	12	1.502	0.527	0.351	0.737	0.807	0.75	49.9	12	0.953	0.175	0.183	0.645	0.761	0.70	73.5

Table 7.4 Statistical Parameters of the Mn/DOT Dynamic Equations (Existing and New) Developed for the Dataset Containing Dynamic Measurements on Pipe Piles and the Associated Resistance Factors

CAPWAP Dataset																
Condition	Mn/DOT Equation (75%)								New Mn/DOT Equation (coeff. = 30)							
	No. of Cases (n)	Mean Bias Measured/ Calculated (m_λ)	Stand. Dev. (σ_λ)	Coef. of Var. (COV_λ)	Resistance Factor ϕ β=2.33, p_f=1% Redundant FOSM	MCS	Recom	Efficiency Factor (ϕ/λ) %	No. of Cases (n)	Mean Bias Measured/ Calculated (m_λ)	Stand. Dev. (σ_λ)	Coef. of Var. (COV_λ)	Resistance Factor ϕ β=2.33, p_f=1% Redundant FOSM	MCS	Recom	Efficiency Factor (ϕ/λ) %
All	74	1.073	1.384	1.289	0.083	0.086	0.10	9.3	74	1.368	0.675	0.493	0.492	0.528	0.50	36.5
EOD	58	1.227	1.533	1.249	0.101	0.105	0.10	8.1	58	1.467	0.714	0.487	0.537	0.577	0.55	77.0
Diesel	36	0.874	0.618	0.708	0.198	0.209	0.20	22.9	36	1.280	0.550	0.430	0.530	0.527	0.50	39.1
B.C. ≥4 BPI	21	0.618	0.224	0.362	0.296	0.323	0.30	48.5	21	1.077	0.210	0.195	0.715	0.838	0.80	74.3
Energy Approach Dataset																
Condition	Mn/DOT Equation (75%)								New Mn/DOT Equation (coeff. = 30)							
	No. of Cases (n)	Mean Bias Measured/ Calculated (m_λ)	Stand. Dev. (σ_λ)	Coef. of Var. (COV_λ)	Resistance Factor ϕ β=2.33, p_f=1% Redundant FOSM	MCS	Recom	Efficiency Factor (ϕ/λ) %	No. of Cases (n)	Mean Bias Measured/ Calculated (m_λ)	Stand. Dev. (σ_λ)	Coef. of Var. (COV_λ)	Resistance Factor ϕ β=2.33, p_f=1% Redundant FOSM	MCS	Recom	Efficiency Factor (ϕ/λ) %
All	59	1.196	1.586	1.327	0.087	0.090	0.10	8.4	59	1.369	0.734	0.536	0.450	0.477	0.45	32.9
EOD	43	1.437	1.803	1.255	0.117	0.121	0.10	7.0	43	1.502	0.801	0.533	0.497	0.527	0.50	33.3
Diesel	32	0.899	0.635	0.707	0.205	0.216	0.20	22.2	32	1.288	0.569	0.442	0.520	0.560	0.55	42.7
B.C. ≥4 BPI	19	0.648	0.215	0.332	0.331	0.365	0.35	54.0	19	1.079	0.216	0.200	0.710	0.831	0.75	69.5

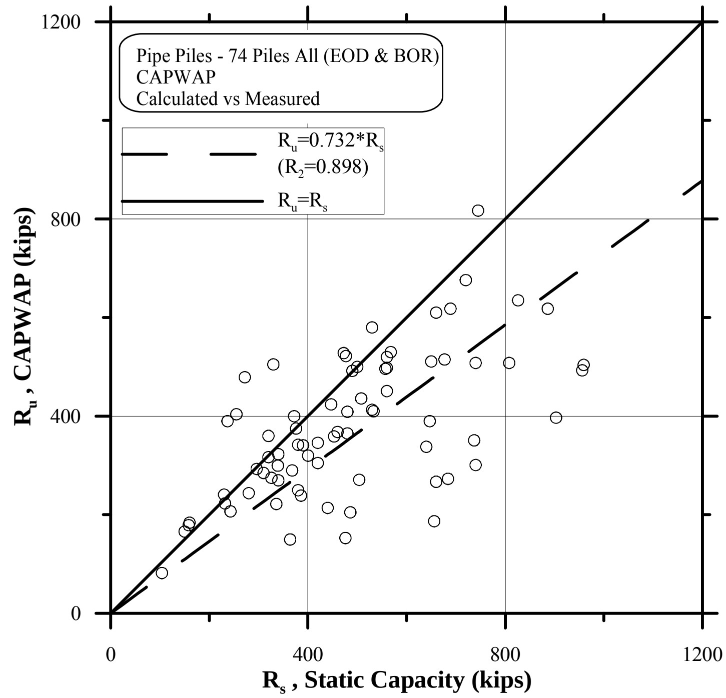

Figure 7.5 Measured static capacity vs. signal matching (CAPWAP) prediction for 74 pipe piles (EOD and BOR).

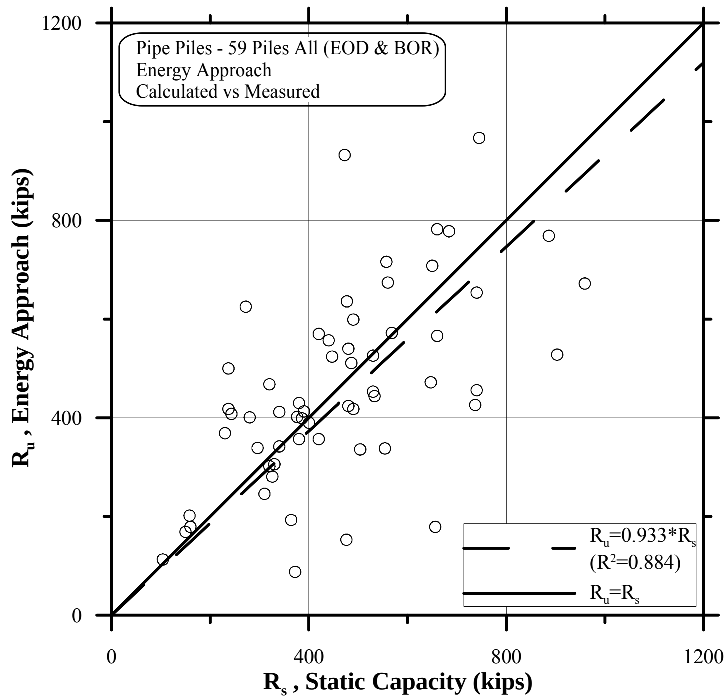

Figure 7.6 Measured static capacity vs. Energy Approach (EA) prediction for 59 pipe piles (EOD and BOR).

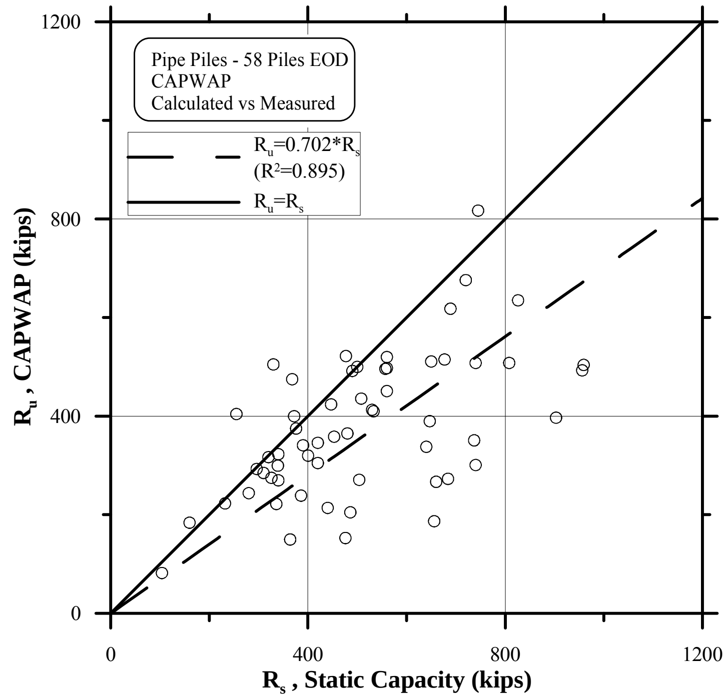

Figure 7.7 Measured static capacity vs. signal matching (CAPWAP) prediction for 58 EOD pipe piles.

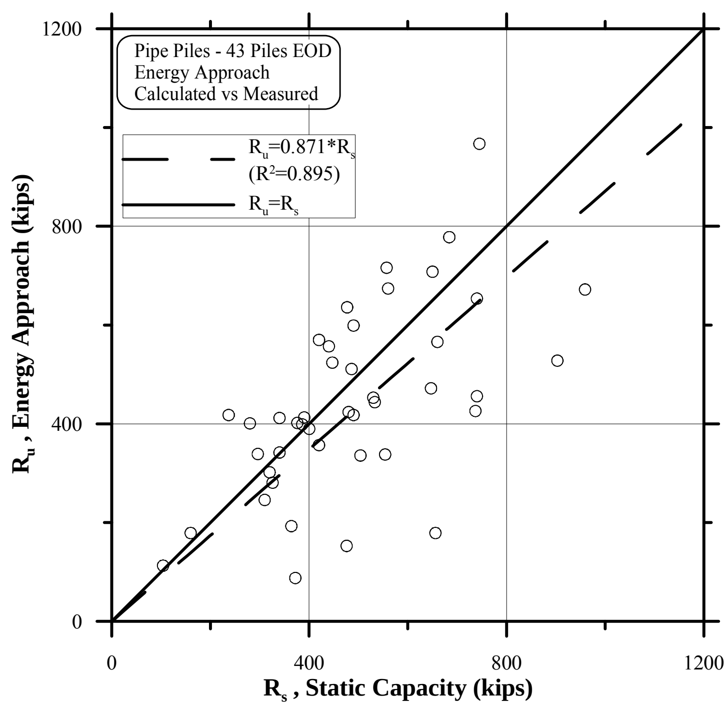

Figure 7.8 Measured static capacity vs. Energy Approach (EA) prediction for 43 EOD pipe piles.

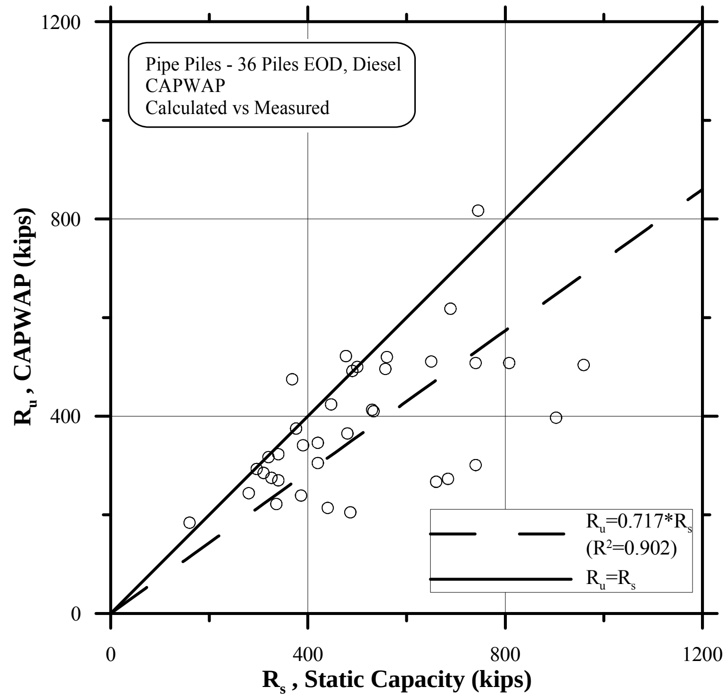

Figure 7.9 Measured static capacity vs. signal matching (CAPWAP) prediction for 36 EOD, diesel hammer driven pipe piles.

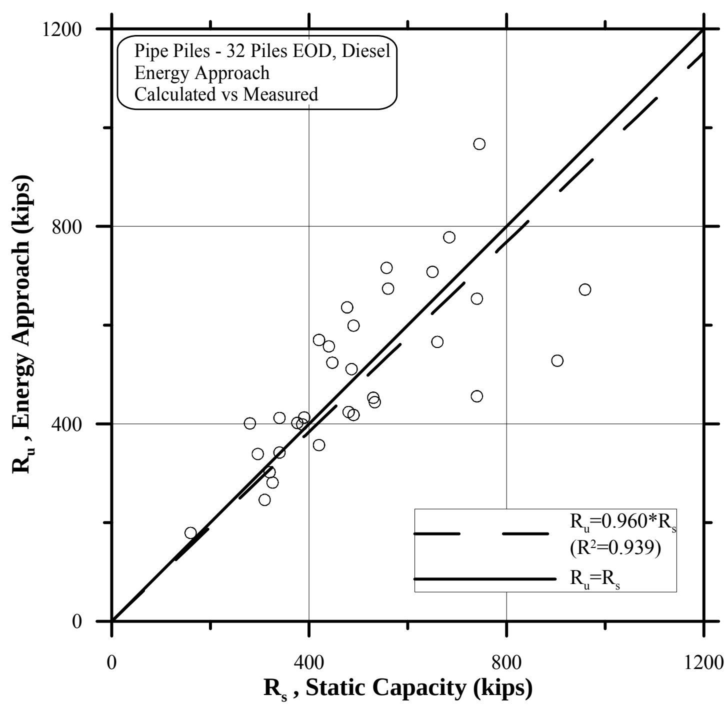

Figure 7.10 Measured static capacity vs. Energy Approach (EA) prediction for 32 EOD, diesel hammer driven pipe piles.

7.1.4 Conclusions

1. The use of dynamic measurements and analyses based on those measurements reduces significantly the scatter in the pile capacity predictions.
2. The Energy Approach field method provides an excellent prediction at the EOD. The recommended resistance factor of $\phi = 0.55$ for the Energy Approach at EOD based on all type of piles (Paikowsky et al., 2004) seems to match the findings for the H piles but needs to be re-examined for the cases of pipe piles.
3. The CAPWAP method recommendations of $\phi = 0.65$ for EOD (except for large displacement piles at easy driving) presented by Paikowsky et al. (2004) seems to match well the findings for both H and pipe piles.
4. The use of the new Mn/DOT equation for the dynamic measurements dataset provided with excellent results, those need, however, to be re-examined with a control dataset for which the data was not used in developing the equation itself.

7.2 CONTROL DATABASE

7.2.1 Overview

The recommendation of resistance factors and the evaluation of a newly developed empirical dynamic equation, can best be examined via independent control databases not being part of the data originally used. Section 3.6.4 presents the database developed for that end and its analysis results are described below.

7.2.2 Results

Tables 7.5 through 7.7 summarize the performance of both the Mn/DOT equation (equation 5.5 and application of 75% of the nominal stroke) and the new Mn/DOT equation (equation 6.3) for the control database under (a) all EOD, (b) all EOD and BC ≥ 4BPI, and (c) EOD with diesel hammers, respectively. Though the data refers mostly to hammers other than diesel hammers, the examination presented is still valid as the analyses in Chapters 4 and 5 revealed that both equations were less sensitive to the use of different hammers (than diesel) for H piles compared to pipe piles.

Figures 7.11 to 7.13 present the static capacity (Davisson's Criterion) vs. the calculated capacity using the Mn/DOT equation for the above described conditions and Figures 7.14 to 7.16 present the same data compared to the calculated capacity using the new Mn/DOT equation.

Table 7.5 End of Driving Prediction for All H-Piles (Control Database)

Equation	No. of Cases (n)	Mean Bias Measured/ Calculated (m_λ)	Stand. Dev. (σ_λ)	Coef. of Var. (COV_λ)	Best Fit Line Equation (least square)	Coefficient of Determination (r^2)	Resistance Factor ϕ β=2.33, p_f=1%, Redundant			ϕ/λ Efficiency Factor (%)
							FOSM	MC[3]	Recom.	
Mn/DOT	24	1.1679	0.9617	0.8234	Ru=1.047*Rs	0.846	0.209	0.219	0.20	17.1
New Mn/DOT[5]	24	0.8494	0.2559	0.3013	Ru=1.092*Rs	0.911	0.462	0.515	0.50	58.9

Notes: 1. Ru is the calculated capacity using each of the dynamic formulae.
2. Rs is the Static Capacity of the pile determined by Davisson's Failure Criterion.
3. MC – Monte Carlo Simulation for 10,000 simulations.
4. BPI is blows per inch.
5. The New Mn/DOT Formula uses a coefficient of 35.

Table 7.6 End of Driving Prediction for All H-Piles Driven to a Driving Resistance of 4 BPI or Higher (Control Database)

Equation	No. of Cases (n)	Mean Bias Measured/ Calculated (m_λ)	Stand. Dev. (σ_λ)	Coef. of Var. (COV_λ)	Best Fit Line Equation (least square)	Coefficient of Determination (r^2)	Resistance Factor ϕ β=2.33, p_f=1%, Redundant			ϕ/λ Efficiency Factor (%)
							FOSM	MC[3]	Recom.	
Mn/DOT	20	0.9455	0.2902	0.3070	Ru=1.094*Rs	0.865	0.508	0.566	0.50	47.3
New Mn/DOT[5]	20	0.9822	0.2794	0.2845	Ru=0.943*Rs	0.914	0.552	0.620	0.60	61.1

Notes: 1. Ru is the calculated capacity using each of the dynamic formulae.
2. Rs is the Static Capacity of the pile determined by Davisson's Failure Criterion.
3. MC – Monte Carlo Simulation for 10,000 simulations.
4. BPI is blows per inch.
5. The New Mn/DOT Formula uses a coefficient of 30.

Table 7.7 End of Driving Prediction for H-Piles Driven with Diesel Hammers (Control Database)

Equation	No. of Cases (n)	Mean Bias Measured/ Calculated (m_λ)	Stand. Dev. (σ_λ)	Coef. of Var. (COV_λ)	Best Fit Line Equation (least square)	Coefficient of Determination (r^2)	Resistance Factor ϕ β=2.33, p_f=1%, Redundant			ϕ/λ Efficiency Factor (%)
							FOSM	MC[3]	Recom.	
Mn/DOT	2	0.5422	0.3799	0.7006	Ru=1.413*Rs	0.832	0.125	0.132	0.10	18.4
New Mn/DOT[5]	2	0.8664	0.6169	0.7120	Ru=0.883*Rs	0.824	0.195	0.206	0.20	23.1

Notes: 1. Ru is the calculated capacity using each of the dynamic formulae.
2. Rs is the Static Capacity of the pile determined by Davisson's Failure Criterion.
3. MC – Monte Carlo Simulation for 10,000 simulations.
4. BPI is blows per inch.
5. The New Mn/DOT Formula uses a coefficient of 30.

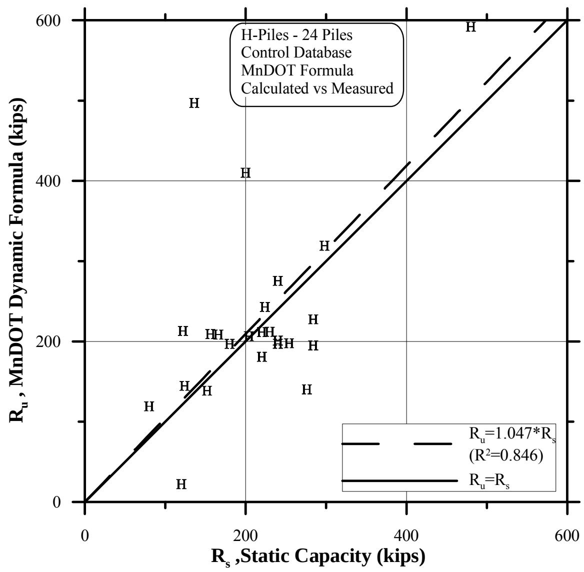

Figure 7.11 Measured static capacity vs. Mn/DOT dynamic equation (C = 0.2, stroke = 75% of nominal) prediction for 24 EOD H pile control database cases.

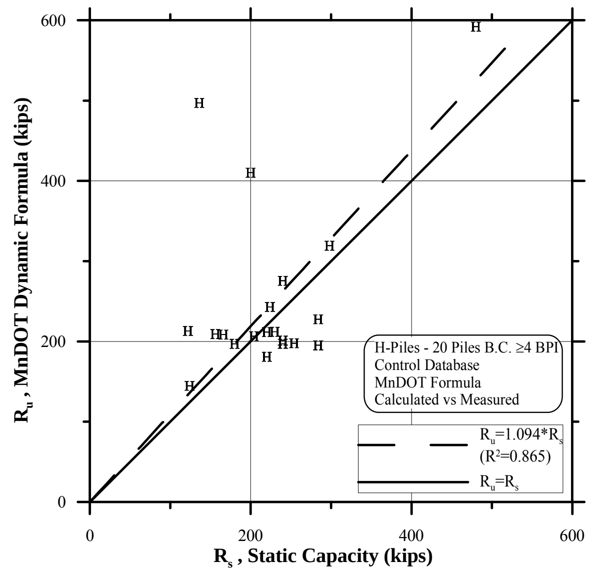

Figure 7.12 Measured static capacity vs. Mn/DOT dynamic equation (C = 0.2, stroke = 75% of nominal) prediction for 20 EOD with B.C. ≥ 4BPI H pile control database cases.

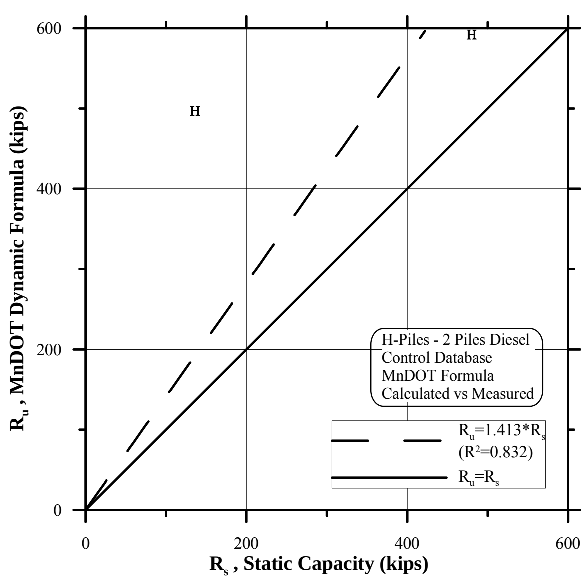

Figure 7.13 Measured static capacity vs. Mn/DOT dynamic equation (C = 0.2, stroke = 75% of nominal) prediction for 2 EOD diesel driven H pile control database cases

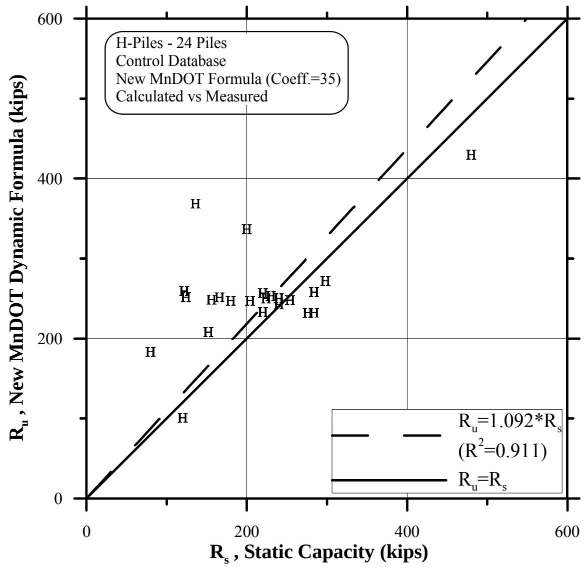

Figure 7.14 Measured static capacity vs. the New Mn/DOT dynamic equation (coeff. = 30) prediction for 24 EOD H pile control database cases.

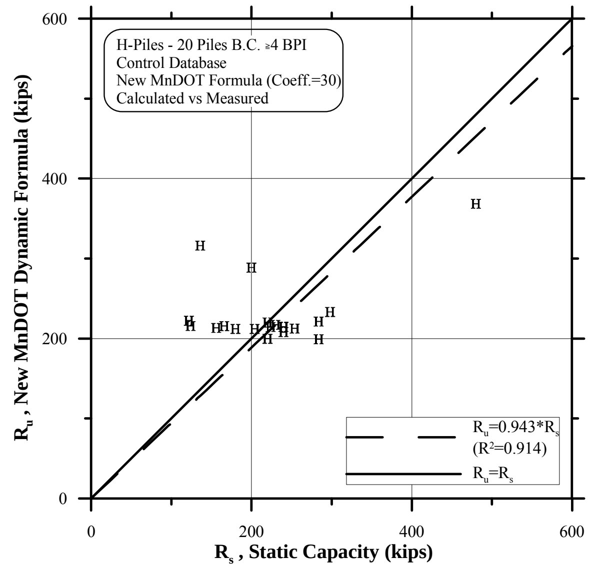

Figure 7.15 Measured static capacity vs. New Mn/DOT dynamic equation (coeff. = 30) prediction for 20 EOD with BC ≥ 4BPI H pile control database cases.

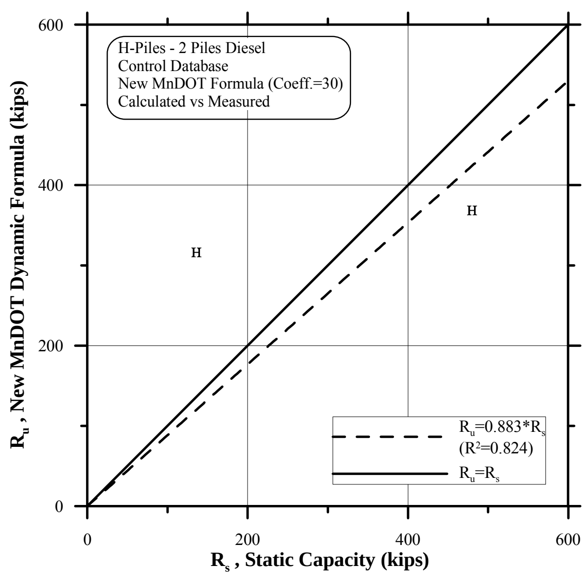

Figure 7.16 Measured static capacity vs. New Mn/DOT dynamic equation (coeff. = 30) prediction for 2 EOD diesel driven H pile control database cases.

7.2.3 Observations and Conclusions

1. The new Mn/DOT equation performed better than the existing Mn/DOT equation in both accuracy and bias.
2. The existing Mn/DOT preformed reasonably well for driving conditions of BC ≥ 4BPI, but extremely poor for all conditions. This means that for the four cases included in Table 7.5 but excluded from Table 7.6, that had BC < 4BPI, the existing Mn/DOT equation performed extremely poorly. Those cases can be identified when observing Figure 7.11 against Figure 7.12.
3. The major importance of the examined analyses relate to the new Mn/DOT equation. As the equation was developed based on databases specifically compiled for Mn/DOT, the use of unrelated data allows for a true independent evaluation of that development. The numerical statistics and the graphical presentation clearly show that (a) the new equation predicted very well the measured capacity under all conditions, and (b) the assigned resistance factors recommended for H piles in section 6.10 ($\phi = 0.45$) are adequate.
4. The resistance factor for the Mn/DOT recommended in section 5.9 ($\phi = 0.25$) was also found to be adequate for the control database.

CHAPTER 8 SUMMARY AND RECOMMENDATIONS

8.1 SUMMARY OF DYNAMIC EQUATIONS AND RESISTANCE FACTORS

8.1.1 Dynamic Equations

The Mn/DOT dynamic equation calibrated in the research is presented in Equation 8.1. The calibration of the equation in this format is presented in Chapter 5 and thereafter. All calibrations assumed a stroke of 75% of the nominal stroke per Mn/DOT practices informed by the Technical Advisory Panel (TAP). The assumed value was found to match typical stroke measurements in the database. The format of equation 8.1 differs from that appearing in the original research request, being uniform for H and other piles (i.e. C = 0.1 for all piles) and not assuming a reduction in the stroke. The format of the original equation (see equation 4.5) was investigated in Chapter 4.

$$R_u = \frac{10.5E}{S + 0.2} x \frac{W + C * M}{W + M} \tag{8.1}$$

where R_u= ultimate carrying capacity of pile, in kips
W= mass of the striking part of the hammer in pounds
M= total mass of pile plus mass of the driving cap in pounds
S= final set of pile, in inches
E= energy per blow for each full stroke in foot-pounds (1.5)
C = 0.1 for timber, concrete and shell type piles, 0.2 for steel H piling

The development of a new general Mn/DOT dynamic equation was also carried out in two stages as presented in Chapter 6. Section 6.5 present the first stage, addressing EOD conditions of all hammers with all energies and driving resistances; resulted with equation (6.2). Its adaptation to the Mn/DOT specific practices of diesel hammers and driving resistance of BC ≥ 4BPI is presented in section 6.7 and resulted in equation 8.2.

$$R_u = 30\sqrt{E_h} * \log\ (10 * N) \tag{8.2}$$

where R_u = predicted pile capacity in kips
E_h = rated hammer energy kips·ft
N = blows per inch (PBI) at the End of Driving (EOD)

Equation 8.2 was then examined to the general driving conditions and appropriate resistance factors were developed as summarized below.

8.1.2 Recommended Resistance Factors

Table 8.1 and Figure 8.1 summarize the findings regarding resistance factors developments for H Piles with the use of relevant databases. Related to the Mn/DOT existing equation (equation 8.1); the use of all End of Driving (EOD) data (125 cases) results with a recommended resistance factor of 0.25. When limiting the data to diesel hammers only and Blow Count (BC) greater or equation to 4 BPI (39 cases), the recommended resistance factor becomes ϕ = 0.30. When omitting one outlier, the factor becomes back ϕ = 0.25. When restricting the data to a subset containing diesel hammers within the range used by Mn/DOT and EOD BC ≥ 4 BPI (13 cases), the recommended resistance factor does not change (ϕ = 0.25), and the same stands when one outlier is omitted. Figures 5.13 and 5.14 presented in a flowchart all the databases analyzed and the resulting resistance factors. Graphical presentation of all the major findings summarized in Table 8.1 are provided in Figure 8.1, expressed as almost a horizontal line regardless of the dataset. In summary, the data in all stages strongly supports the recommendation of a resistance factor of ϕ = 0.25 for the Mn/DOT equation when applied to H Piles, assuming redundant pile use (i.e. five piles or more under one pile cap).

Further examination of these results via a controlled database, is described in section 7.2. The control database included mostly hammers different than Diesel. The calculated resistance factors vary between ϕ = 0.2 for all cases to ϕ = 0.5 for all EOD cases with BC ≥ 4BPI. Case no. 6 of Table 8.1 relates to these findings, suggesting that for the examined cases, the Mn/DOT equation in general applications would require a resistance factor of ϕ = 0.20. As only two out of the 24 cases of the controlled database relate to Diesel hammers and further limiting the data to BC ≥ 4BPI does not lead to reasonable results due to the fact that many of the piles come from a few sites only. The control database findings are presented in Figure 8.1 as well.

The recommendations of the resistance factors for the new dynamic equation proposed to be used by the Mn/DOT (equation 8.2) was investigated in a similar way to the process described for equation 8.1. Table 8.1 and Figure 8.1 present the findings leading to the conclusion that the appropriate resistance factors to be used for H Piles under Mn/DOT practices (and all conditions as well) would be ϕ = 0.60 assuming redundant pile use.

Table 8.1. Summary of Developed Resistance Factors for H-Piles

<table>
<tr><th rowspan="2">Case No.</th><th rowspan="2">No. of Cases</th><th rowspan="2">Condition</th><th colspan="2">Recommended ϕ</th><th rowspan="2">New Mn/DOT Coefficient</th><th rowspan="2">Reference</th><th rowspan="2">Notes</th></tr>
<tr><th>Mn/DOT</th><th>New Mn/DOT</th></tr>
<tr><td rowspan="2">1</td><td rowspan="2">125</td><td rowspan="2">All EOD</td><td rowspan="2">0.25</td><td>0.55</td><td>35</td><td rowspan="2">Table 6.5 & Table 5.2</td><td>General Equation all EOD</td></tr>
<tr><td>0.60</td><td>30</td><td rowspan="5">Specific Equation for EOD, Diesel, and BC ≥ 4 BPI (Equation 8.2)</td></tr>
<tr><td>2</td><td>39</td><td>Diesel & B.C ≥ 4 BPI</td><td>0.30</td><td>0.60</td><td>30</td><td>Table 5.4</td></tr>
<tr><td>3</td><td>38</td><td>Diesel & B.C ≥ 4 BPI w/o Cook's Outlier</td><td>0.25</td><td>0.65</td><td>30</td><td>Table 5.5</td></tr>
<tr><td>4</td><td>13</td><td>Diesel & Mn/DOT Energy Range</td><td>0.25</td><td>0.55</td><td>30</td><td>Table 5.6</td></tr>
<tr><td>5</td><td>12</td><td>Diesel & Mn/DOT Energy Range w/o Cook's Outlier</td><td>0.25</td><td>0.60</td><td>30</td><td>Table 5.7</td></tr>
<tr><td>6</td><td>24</td><td>Control Database All EOD</td><td>0.20</td><td>0.50</td><td>35</td><td>Table 7.5</td><td>General Equation EOD</td></tr>
<tr><td>7</td><td>20</td><td>Control Database B.C ≥ 4 BPI</td><td>0.50</td><td>0.60</td><td>30</td><td>Table 7.6</td><td>Specific Equation</td></tr>
</table>

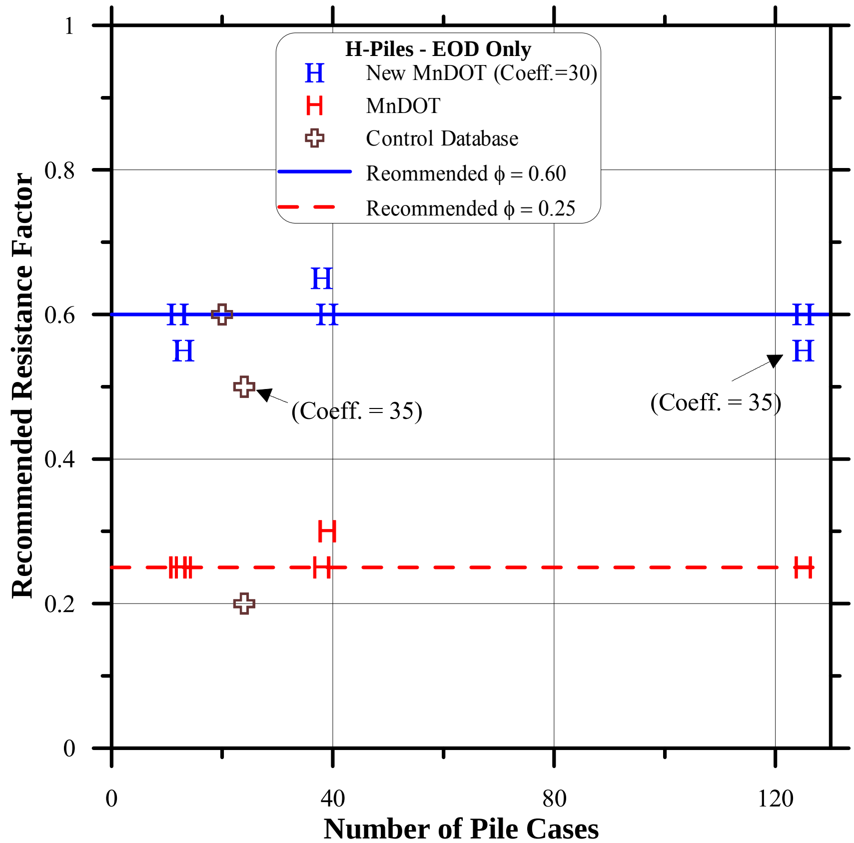

Figure 8.1. Developed and recommended resistance factors as a function of H piles' database and its subsets for existing and proposed Mn/DOT dynamic equations.

Table 8.2 and Figure 8.2 summarize the findings regarding resistance factors developments for Pipe Piles with the use of relevant databases. Related to Mn/DOT existing equation, (equation 8.1); the use of all EOD data (99 cases) results with a recommended resistance factor of 0.10 only. When limiting the data to diesel hammers only and BC ≥ 4BPI (41 cases), the recommended resistance factor increased to ϕ = 0.20. When omitting three outliers, the resistance factor further increases to ϕ = 0.25. When restricting the data to diesel hammers within the energy range of Mn/DOT practice and EOD BC ≥ 4BPI (16 cases), the recommended resistance factor increases to ϕ = 0.30 and further increases to ϕ = 0.35 upon the removal of two outliers (14 cases remaining). The small datasets associated with the best match to the Mn/DOT practices has several sets of identical piles from a small number of sites and hence result with a reduced variability (i.e. COV) and increased resistance factor. Figure 8.2 expresses this trend showing a consistent increase in the resistance factor with the decreased number of cases in the database (or more accurately, with an increased alliance of the database with Mn/DOT practices). Figures 5.13 and 5.14 presented in a flowchart all the databases analyzed and the resulting resistance factors.

In summary, a recommended resistance factor of 0.25 seems to be appropriate for the use with the existing Mn/DOT for Pipe Piles under Mn/DOT practices.

Table 8.2. Summary of Developed Resistance Factors for Pipe-Piles

Case No.	No. of Cases	Condition	Recommended ϕ		New Mn/DOT Coefficient	Reference	Notes
			Mn/DOT	New Mn/DOT			
1	99	All EOD	0.10	0.35	35	Table 6.6 & Table 5.3	General Equation all EOD
				0.60	30		
2	41	Diesel & B.C ≥ 4 BPI	0.20	0.40	30	Table 5.8	Specific Equation for EOD, Diesel, and BC ≥ 4 BPI
3	38	Diesel & B.C ≥ 4 BPI w/o Cook's Outlier	0.25	0.45	30	Table 5.9	
4	16	Diesel & Mn/DOT Energy Range	0.30	0.85	30	Table 5.10	
5	14	Diesel & Mn/DOT Energy Range w/o Cook's Outlier	0.35	0.90	30	Table 5.11	

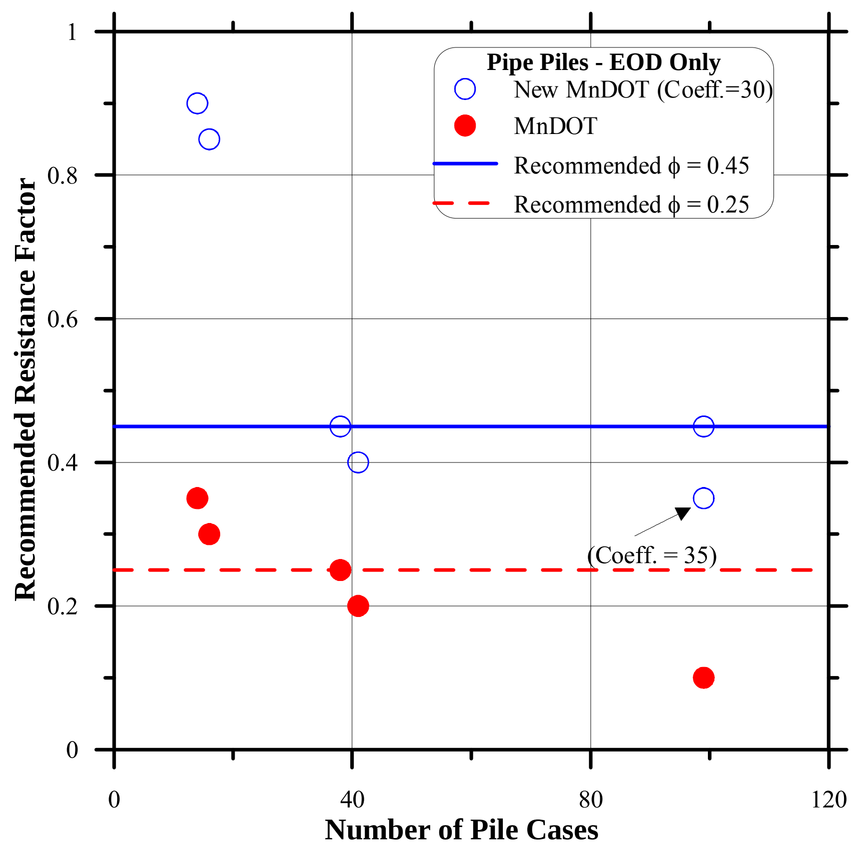

Figure 8. 2. Developed and recommended resistance factors as a function of pipe piles' database and its subsets for existing and proposed Mn/DOT dynamic equations.

The recommendations of the resistance factors for the new dynamic equation proposed to be used by the Mn/DOT (equation 8.2) was investigated in a similar way to the process described for equation 8.1. Table 8.2 and Figure 8.2 present the findings leading to the conclusion that the appropriate resistance factors to be used for Pipe Piles under Mn/DOT practices (and all conditions as well) would be $\phi = 0.45$ assuming redundant pile use.

Discussion: The difference in the behavior of the two pile types is evident. While H Piles are predominantly small displacement piles, pipe piles are large displacement piles and would be, therefore, more sensitive to soil inertia effects expressed via blow count and hammer type and energy. As a result, it is unwise to rely on the smaller subsets that provide resistance factors of ϕ = 0.30. A unique resistance factor is therefore recommended to be used with the Mn/DOT dynamic equation for all H and Pipe Piles, driven by Diesel hammer to EOD BC ≥ 4BPI being ϕ = 0.25.

Table 8.3 summarizes the recommended resistance factors.

Table 8.3. Summary of Recommended Resistance Factors for the Existing and Proposed Mn/DOT Dynamic Equations

Pile Type	Recommended ϕ		Assumptions
	Mn/DOT (Equation 8.1)	New Mn/DOT (Equation 8.2)	
H Piles	**0.25**	**0.60**	Resistance Factors were calculated for a target reliability β=2.33, probability of failure p_f=1%, assuming redundant pile use
Pipe Piles	**0.25**	**0.45**	

8.2 EXAMPLE

8.2.1 Given Details

The following examples are constructed based on typical piles and driving equipment as presented in Chapters 2 and 3.

<u>H Pile:</u>

Pile:	HP 12×53
Length:	40ft
Design Factored Load:	160kips
Hammers:	Delmag 19-42 and APE D30-32
Driving Resistance at EOD:	From 2 to 12 BPI

<u>Pipe Pile:</u>

Pile:	CEP 12”×0.25”
Length:	70ft
Design Factored Load:	160kips
Hammers:	Delmag D19-42 and APE D30-32
Driving Resistance at EOD:	From 2 to 12 BPI

Table 8.4 provides the relevant information for the hammer, pile and driving system required for using equations 8.1 and 8.2.

Table 8.4 Summary of Hammer, Driving System and Pile Parameters

Hammer	Energy E kip•ft	Weight (kips)						
		Hammer			Pile		Mn/DOT Equation	
		Ram W	Impact Block	Helmet	HP 12x53@ 40’	CEP 12x0.25@70’	M H-Pile	M Pipe Pile
Delmag D19-42	42.4	4.02	0.75	6.60	2.12	2.20	9.47	9.55
APE D30-32	70.1	6.61	1.36	8.00	2.12	2.20	11.48	11.56

Notes: 1. Ram weight based on manufacturer’s datasheet (Delmag, and APE)
2. Impact block and helmet weights are based on WEAP (2006)
3. HP 12x53 weight = 40ft x 53lb/ft = 2.12 kips
4. Pipe Pile 12x0.25 weight = 70ft x 31.4lb/ft = 2.20 kips

8.2.2 Example Calculations

Proposed New Mn/DOT (Equation: 8.2): $R_u = 30\sqrt{E_h} * \log\ (10 * N)$

1. Using Delamg D19-42 for all piles, EOD = 6BPI $\rightarrow$ $R_u = 347^k$
2. Using APE D30-32 for all piles, EOD = 6BPI $\rightarrow$ $R_u = 447^k$

Current Mn/DOT (Equation 8.1): $R_u = \dfrac{10.5E}{S+0.2} x \dfrac{W + C * M}{W + M}$

Pile Weight:

H-pile = $40\text{ft} \times 53\, {}^{lb}\!/\!{}_{ft}$ = 2120lb = 2.12kips

Pipe Pile = $70\text{ft} \times 31.4\, {}^{lb}\!/\!{}_{ft}$ = 2197lb = 2.20kips

Using Delamg D19-42:

Ram Weight: W = 4.02kips
Capblock + Helmet Weight: = 7.35kips
$M_{H\text{-pile}}$: 7.35 + 2.12 = 9.47kips
$M_{pipe\ pile}$: 7.35 + 2.20 = 9.55kips

$$R_{u_H} = \frac{10.5 \bullet 42.4 \bullet 0.75}{S+0.2} \times 0.438 \quad R_{u_{Pipe}} = \frac{10.5 \bullet 42.4 \bullet 0.75}{S+0.2} \times 0.367$$

H-pile EOD = 6BPI $\rightarrow$ $R_u = 399^k$
Pipe Pile EOD = 6BPI $\rightarrow$ $R_u = 334^k$

8.2.3 Summary of Calculations

Tables 8.5 and 8.6 summarize the calculations of the examples for Delmag D19-42 and APE D30-32, respectively. Table 8.5 and 8.6 include for both, the H pile and the Pipe Pile, the calculated and factored resistances using the currently employed resistance factor for the Mn/DOT as well as the newly recommended resistance factor for the same equation, alongside the newly recommended dynamic equation and the associated resistance factor.

Figures 8.3 to 8.6 present the findings of Tables 8.5 and 8.6 in a graphical form. Figures 8.3 and 8.4 present the driving resistance vs. pile capacity (and factored resistance) for H and Pipe piles driven with Delmag D19-42, respectively. Figures 8.5 and 8.6 present the driving resistance vs. pile capacity (and factored resistance) for H and Pipe piles driven with APE D30-31, respectively.

Table 8.5. Summary Capacities and Resistances for the Examples Using Delmag D19-42

Pile Type	EOD (BPI)	Current Mn/DOT Equation $R_u = \frac{10.5E}{S+0.2} x \frac{W+0.1M}{W+M}$					Proposed Mn/DOT Equation $R_u = 30\sqrt{E_h} * \log(10*N)$		
		Capacity (kips)	ϕ^1	Factored Resistance (kips)	ϕ^2	Factored Resistance (kips)	Capacity (kips)	ϕ^3	Factored Resistance (kips)
HP 12”×53	2	209	0.25	52	0.40	84	254	0.60	152
HP 12”×53	4	325	0.25	81	0.40	130	313	0.60	188
HP 12”×53	6	399	0.25	100	0.40	160	347	0.60	208
HP 12”×53	8	450	0.25	113	0.40	180	372	0.60	223
HP 12”×53	10	488	0.25	122	0.40	195	391	0.60	234
HP 12”×53	12	517	0.25	129	0.40	207	406	0.60	244
CEP 12”×0.25”	2	175	0.25	44	0.40	70	254	0.45	114
CEP 12”×0.25”	4	272	0.25	68	0.40	109	313	0.45	141
CEP 12”×0.25”	6	334	0.25	83	0.40	134	347	0.45	156
CEP 12”×0.25”	8	377	0.25	94	0.40	151	372	0.45	167
CEP 12”×0.25”	10	408	0.25	102	0.40	163	391	0.45	176
CEP 12”×0.25”	12	432	0.25	108	0.40	173	406	0.45	183

[1]Recommended resistance factors for current Mn/DOT equation
[2]Resistance factor currently used by the Mn/DOT
[3]Recommended resistance factors for the new Mn/DOT equation
Note – Mn/DOT equation application assumes 75% stroke

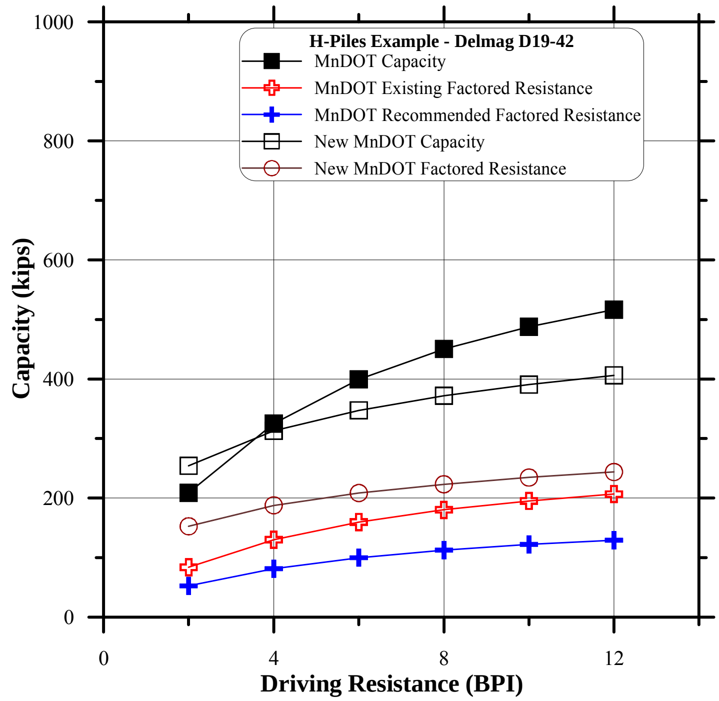

Figure 8.3 Driving resistance vs. capacity (calculated and factored) using the existing and proposed Mn/DOT dynamic equations for H pile driven with Delamg D19- 42.

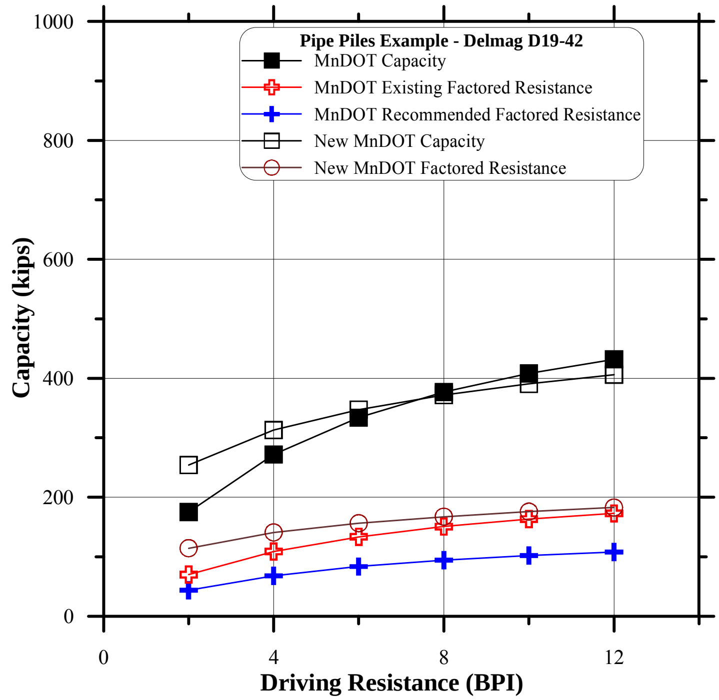

Figure 8.4 Driving resistance vs. capacity (calculated and factored) using the existing and proposed Mn/DOT dynamic equations for pipe pile driven with Delamg D19- 42.

Table 8.6. Summary Capacities and Resistances for the Example Using APE D30-31

Pile Type	EOD (BPI)	Current Mn/DOT Equation $R_u = \frac{10.5E}{S+0.2} x \frac{W+0.1M}{W+M}$					Proposed Mn/DOT Equation $R_u = 30\sqrt{E_h} * \log(10 * N)$		
		Capacity (kips)	ϕ^1	Factored Resistance (kips)	ϕ^2	Factored Resistance (kips)	Capacity (kips)	ϕ^3	Factored Resistance (kips)
HP 12”×53	2	388	0.25	97	0.40	155	327	0.60	196
HP 12”×53	4	604	0.25	151	0.40	242	402	0.60	241
HP 12”×53	6	741	0.25	185	0.40	296	447	0.60	268
HP 12”×53	8	836	0.25	209	0.40	334	478	0.60	287
HP 12”×53	10	906	0.25	226	0.40	362	502	0.60	301
HP 12”×53	12	959	0.25	240	0.40	384	522	0.60	313
CEP 12”×0.25”	2	387	0.25	97	0.40	155	327	0.45	147
CEP 12”×0.25”	4	602	0.25	151	0.40	241	402	0.45	181
CEP 12”×0.25”	6	739	0.25	185	0.40	296	447	0.45	201
CEP 12”×0.25”	8	834	0.25	209	0.40	334	478	0.45	215
CEP 12”×0.25”	10	904	0.25	226	0.40	361	502	0.45	226
CEP 12”×0.25”	12	957	0.25	239	0.40	383	522	0.45	235

[1]Recommended resistance factors for current Mn/DOT equation
[2]Resistance factor currently used by the Mn/DOT
[3]Recommended resistance factors for the new Mn/DOT equation
Note – Mn/DOT equation application assumes 75% stroke

8.2.4 Example Observations

1. The two chosen hammers represent the lower and higher ends of energies within the typical range of Mn/DOT practices applied to two typical piles.
2. The use of the Delmag D19-42 for the H and pipe piles shows that for a low driving resistance, (BC in the range of 4 to 6BPI) the proposed new equation predicts higher capacity than the current Mn/DOT equation. Beyond the range of 4 to 6BPI, the current Mn/DOT equation exceeds the capacity prediction of the new equation.
3. Using a heavier hammer set-up with higher energy (APE D30-32) increases significantly the predicted capacity of the existing Mn/DOT equation compared to the proposed equation. This can be expected as the resistance of the Mn/DOT equation is a function of the hammer energy directly and using a hammer twice the energy will double the capacity. In the new equation the pile capacity is a function of the square of the hammer energy, hence, doubling the hammer energy would increase the capacity by 1.4 ($\sqrt{2}$) only.

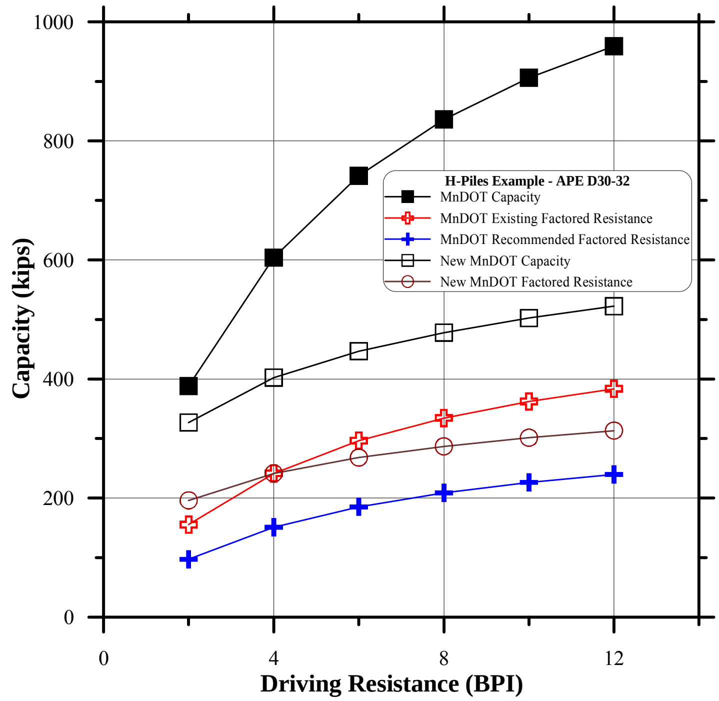

Figure 8.5 Driving resistance vs. capacity (calculated and factored) using the existing and proposed Mn/DOT dynamic equations for H pile driven with APE D30-31.

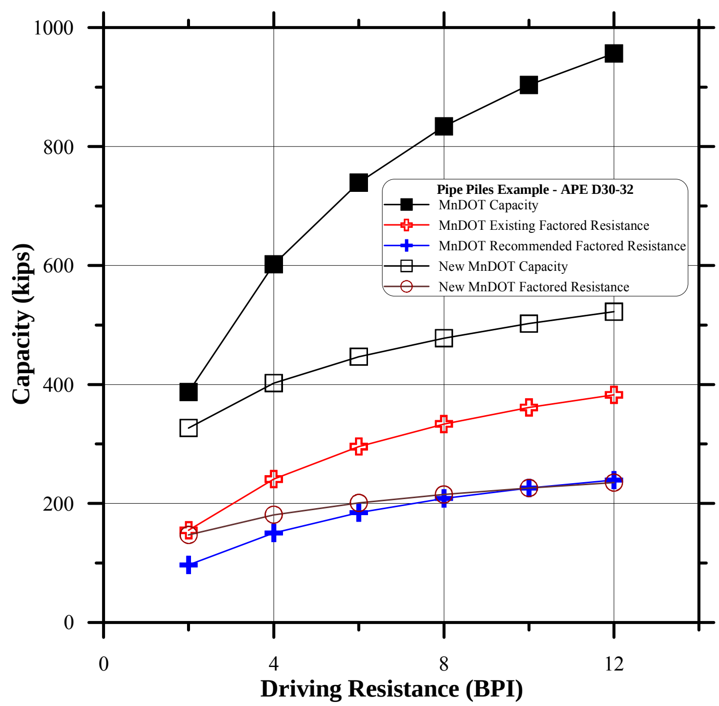

Figure 8.6 Driving Resistance vs. Capacity (Calculated and Factored) using the existing and proposed Mn/DOT dynamic equations for Pipe pile Driven with APE D30-31.

4. Figures 8.3 and 8.4 demonstrate that for the lower energy hammer, in spite of the lower capacities predicted by the Mn/DOT new equation, the factored resistance is higher than that obtained using the current Mn/DOT resistance factor ($\phi = 0.4$), let alone the proposed Mn/DOT equation LRFD calibrated factor ($\phi = 0.25$).
5. Figures 8.5 and 8.6 demonstrate that for the higher energy hammer the use of the existing resistance factor results with capacities exceeding those obtained from using the new equation with the recommended resistance factor and certainly the factored resistance obtained using the Mn/DOT equation with the newly developed resistance factor.
6. The use of the LRFD developed factors with the existing Mn/DOT dynamic equation translates to a decreased capacity by a factor of 0.625 (0.25/0.40), which is a significant economic loss for a gain in safety.
7. The use of the newly proposed equation along with the recommended developed resistance factors may translate to gain or lose in factored resistance, depending on the specific pile/hammer/driving resistance combination. It should, however, provide a consistent level of reliability in the pile construction.

8.3 CONCLUSIONS

8.3.1 Current Mn/DOT Dynamic Equation

1. The current Mn/DOT equation provides on the average an over-predictive (unsafe) capacity resulting in a mean bias of about 0.8 (statically measured capacity over dynamically predicted) for both H and pipe piles (refer to Figure 5.14).
2. The current Mn/DOT equation performs poorly as the scatter of its predictions is very large, represented by coefficient of variation ratios for EOD predictions of 0.50 to 0.80 for H and pipe piles (refer to Figure 5.14).
3. The systematic over-prediction and large scatter resulted with a recommended resistance factor to be used with the current Mn/DOT equation for EOD prediction and redundant pile support (5 or more piles per cap) of $\phi = 0.25$ for both H piles and pipe piles.
4. An approximation of the equivalent safety factor can be performed by using the following relations based on Paikowsky et al. (2004):

$$F.S. \approx 1.4167/\phi \qquad (8.3)$$

   This means that the approximate Factor of Safety requires for the Mn/DOT is 5.7 due to the poor prediction reliability.
5. The use of $\phi = 0.40$ (F.S. $\approx$ 3.5) currently in place means that the probability of failure is greater than 1% overall. Special attention needs to be given to low capacity piles (statically less than 200kips) that for now should be avoided by keeping a driving criterion at the EOD of 4BPI or higher, and restrike friction piles in particular in clays and silt or mix soil conditions. Attention also should be given to piles driven with large hammers for which the Mn/DOT equation tends (due to its structure) to substantially over-predict the capacity.

8.3.2 Other Examined Dynamic Equations

All other examined equations performed as expected, reasonably well. While their scatter is similar, having a COV of about 0.35 to 0.40 for H-piles and 0.52 to 0.61 for pipe piles, the bias of these methods is either too high (1.43 – 1.58) for the Gates equation, or too low (0.81 – 0.89) for the other equations. A rationale for the development of an independent Mn/DOT new dynamic equation is, therefore, presented and followed up in Chapter 6.

8.3.3 New Mn/DOT Dynamic Equation

1. The recommended resistance factor for the use with the newly developed Mn/DOT equation is $\phi = 0.6$ for H piles and $\phi = 0.45$ for pipe piles. The varied resistance factors come from the clear differences in the ability to predict the capacity of the two pile types and, hence, the greater uncertainty in the prediction of pipe pile capacity.
2. The associated Factor of Safety with the use of the newly developed equation is F.S. $\approx$ 2.4 for H piles and F.S. $\approx$ 3.1 for pipe piles, reflecting the higher confidence in the use of the proposed equation.
3. Further investigation of the proposed equation should be carried out as part of its implementation as outlined in the following recommendations.

8.4 RECOMMENDATIONS

1. The resistance factors developed and recommended to be used in this study reflect a decrease to 63% of the factored resistance, when compared to the current practice. There is no question that it is a significant economical constraint, but at the same time it reflects the uncertain nature of the existing equation and to toll demanded to obtain a consistent risk in its use.
2. It is highly recommended to implement the proposed new equation in a transitional process.
3. The implementation of the new equation is proposed to be applied immediately to ongoing projects in the following way:
   a. Calculate pile capacity using the current Mn/DOT dynamic equation.
   b. Apply to the obtained capacity both resistance factors; 0.25 and 0.40, i.e. the new recommended resistance factor and the currently used factor, respectively.
   c. Calculate pile capacity using the new proposed Mn/DOT equation.
   d. Apply to the obtained capacity a resistance factor of 0.60 for the use with H piles and 0.45 for the use with pipe piles.
   e. Maintain the records and apply a safe factored resistance value based on all the results.
4. The data accumulation from large number of projects can enable the analysis and re-evaluation of the recommendation.
5. Devise a systematic program while collecting data as described in item #3. The program should include a series of routine dynamic measurements (with a PDA and/or other instruments to be discussed) along with some static load tests in key projects when possible.

6. The above steps may result with modifications to the new proposed equation and/or to its proposed resistance factors.
7. The long term goal should be a reduction in the prediction scatter so to obtain a systematic increase in the prediction reliability and a decrease in the foundation cost.

REFERENCES

AASHTO (1973-1976). *Standard Specifications for Highway Bridges,* American Association of State Highway and Transportation Officials, Washington, D.C.

AASHTO (1994). *AASHTO LRFD Bridge Design Specifications*, SI unit, 1st Edition, American Association of State Highway and Transportation Officials, Washington, D.C.

AASHTO (1997). *Standard Specifications for Highway Bridges: 16th Edition* (1996 with 1997 interims). American Association of State Highway and Transportation Officials, Washington, D.C.

AASHTO (2006). *LRFD Bridge Design Specifications, Section 10: Foundations,* American Association of State Highway & Transportation Officials, Washington, D.C.

AASHTO (2008). *LRFD Bridge Design Specifications Section 10: Foundations*, American Association of State Highway & Transportation Officials, Washington, D.C.

AIJ (2002). *Recommendations for Limit State Design of Buildings*, Architectural Institute of Japan, Tokyo, Japan (in Japanese).

Ayyub, B., and Assakkaf, I. (1999). *LRFD Rules for Naval Surface Ship Structures: Reliability-Based Load and Resistance Factor Design Rules.* Naval Surface Warfare Center, Carderock Division, U.S. Navy, West Bethesda, MD.

Ayyub, B., Assakkaf, I., and Atua, K. (2000). "Reliability-Based Load and Resistance Factor Design (LRFD) of Hull Girders for Surface Ships". *Naval Engineers Journal,* Vol. 112, No. 4, July, pp. 279-296.

Allen, T. M. (2005). *Development of the WSDOT Pile Driving Formula and Its Calibration for Load and Resistance Factor Design (LRFD).* Final Research Report submitted to Washington State Department of Transportation, Olympia, WA. March.

Barker, R., Duncan, J., Rojiani, K., Ooi, P., Tan, C., and Kim, S. (1991). *NCHRP Report 343: Manuals for the Design of Bridge Foundations.* TRB, National Research Council, Washington, D.C.

Becker, D.E. (2003). "Limit states foundation design code development in Canada", *Proc. International Workshop on Limit State Design in Geotechnical Engineering Practice (LSD2003)*, editors K.K.Phoon, Y.Honjo, and R.B.Gilbert, pp.37-38, full paper in CD-ROM, World Scientific Publishing, Singapore.

Bowles, J.E. (1977). *Foundation Analysis and Design,* 2nd Edition, McGraw-Hill, NY.

Bowles, J.E. (1988). *Foundation Analysis and Design,* 4th Edition, McGraw-Hill, NY.

Canadian Building Code (1975).

CEN (2004). *prEN 1997-1 Geotechnical Design - General Rules*, European Committee for Standardization (CEN), Brussels, Belgium.

Chellis, R. (1961). *Pile Foundations.* 2nd Edition, New York: McGraw-Hill, New York, NY.

Cheney, R.S., and Chassie, R.G. (1982). *Soils and Foundations Workshop Manual,* FHWA Report no. FHWA-NHI-88-009, Washington, D.C., pp. 338.

Cook, R.D. (1979). "Influential Observations in Linear Regression". *Journal of the American Statistical Association*, Vol.74, pp.169-174.

Cornell, C. (1969). A Probability Based Structural Code, *Journal of American Conc. Institute*, Vol. 66, No. 12, pp. 974-985.

Cummings, A.E. (1940). "Dynamic Pile-Driving Formulas", *Boston Society of Civil Engineers Journal,* 1925-1940, January, pp. 392-413.

Davisson, M. (1972). "High Capacity Piles." *Proceedings, Soil Mechanics Lecture Series on Innovations in Foundation Construction,* ASCE, Illinois Section, Chicago, IL, pp. 81-112.

DIN EN 1997-1. (2008). *Geotechnical Design, Part I: General Rules,* Deutsches Institut für Normung (DIN) (German Institute for Standardization), Beuta-Verlag, Berlin.

Ellingwood, B., Galambos, T., MacGregor, J., and Cornell, C. (1980). *Development of a Probability-Based Load Criterion for American National A58.* National Bureau of Standards Publication 577, Washington, D.C.

Ellingwood, B., MacGregor, J.G., Galanbos, T.V., and Cornell, C.A. (1982). "Probability based load criteria: load factors and load combinations", ASCE *J. Struct. Div.,* Vol. 108, No. ST5, pp. 978-997.

Engineering News-Record (1888).

Engineering News-Record (1892).

Engineering News-Record (1965).

FHWA, (1982). Modification of the Gates Equation by Richard Cheney of the FHWA, based on statistical correlations with static load tests as presented in FHWA, 1988.

FHWA, (1988). *Geotechnical Guidline No. 13,* FHWA, Washington, D.C., pp. 37.

Flaate, K. (1964). *An Investigation of the Validity of Three Pile-Driving Formulae in Cohesionless Material,* Norwegian Geotechnical Institute, Publication 56, Oslo, Norway.

Fragaszy, R., Higgins, J., and Lawton, E. (1985). *Development of Guidelines for Construction Control of Pile Driving and Estimation of Pile Capacity: Phase I,* Washington DOT Report WA/RD-68.1, Olympia, WA, pp. 83.

Galambos, T., and Ravindra, M. (1978). "Properties of Steel for use in LRFD", *Journal of Structural Engineering,* Vol. 104, No. 9, pp. 1459-1468.

Gates, M. (1957). "Empirical Formula for Predicting Pile Bearing Capacity". *Civil Engineering*, ASCE, Vol. 27, No. 3. March.

Goble, G.G., Likins, G. and Rausche, F. (1970). *Dynamic Studies on the Bearing Capacity of Piles – Phase III,* Report No. 48, Division of Solid Mechanics, Structures, and Mechanical Design, Case Western Reserve University, Cleveland, OH.

Hasofer, A., and Lind, N. (1974). "Exact and Invariant Second-Moment Code Format", *Journal of Engineering Mechanics Division*, ASCE, Vol. 100, No. EM1, pp. 111-121.

Hiley, A. (1930). "Pile Driving Calculations with Notes on Driving Forces and Ground Resistance", *The Structural Engineer,* Vol. 8, July and August, 1930.

Honjo, Y., and Amatya, S. (2005). "Partial factors calibration based on reliability analyses for square footings on granular soils", *Géotechnique*, Vol. 55, No. 6, pp. 479-491.

Honjo, Y., and Kusakabe, O. (2002). "Proposal of a Comprehensive Foundation Design Code: Geocode 21 ver.2", *Proc. Foundation Design Codes and Soil Investigation in View of International Harmonization and Performance Based Design,* editors. Honjo, Y., Kusakabe, O., Matsui, K., Kouda, M., and Pokharel, G. Kamakura, Malaysia, pp. 95-106, A.A. Balkema Publishers, The Netherlands.

Honjo, Y., Kusakabe, O., Matsui, K., Kikuchi, Y., Kobayashi, K., Kouda, M., Kuwabara, F., Okumura, F., and Shirato, M. (2000). "National Report on Limit State Design in Geotechnical Engineering: Japan", *Proc. International Workshop on Limit State design in Geotechnical Engineering (LSD2000)*, Melbourne, pp. 217-240.

Housel, W.S. (1965). "Michigan Study of Pile-Driving Hammers", *Proceeding of the ASCE Journal of Soil Mechanics and Foundations,* Vol. 91, No. SM5, September, pp. 37-64.

Housel, W.S. (1966). "Pile Load Capacity: Estimates and Test Results", *Journal of Soil Mechanics and Foundations*, ASCE, Vol. 92, No. SM4, July, pp. 1-30.

Kobayashi, K., Kuwabara, F., and Ogura, H. (2003). "Limit state design development for building foundations", *Proc. of 5th Japan Conference on Structural Safety and Reliability,* JCOSSAR, November, Tokyo, Japan, pp. 901-908 (in Japanese).

Kulhawy, F.H., and Phoon, K.K. (2002). "Observations on Geotechnical Reliability-Based Design Development in North America", *Proc. Foundation Design Codes and Soil Investigation in View of International Harmonization and Performance Based Design,* editors Honjo, Y., Kusakabe, O., Matsui, K., Kouda, M., and Pokharel, G. Kamakura, Malaysia, pp. 31-50, A.A. Balkema Publishers, The Netherlands.

Kulicki, J. M., Prucz, A., Clancy, C. M., Mertz, D. R., and Nowak, A. S. (2007). *Updating the calibration report for AASHTO LRFD code, Final Report*, Project No. NCHRP 20-7/186, Transportation Research Board of the National Academies, Washington, D.C.

Long, J., Bozkurt, D., Kerrigan, J., and Wysockey, M. (1999). "Value of Methods for Predicting Axial Pile Capacity, *TRB Transportation Research Record No. 1663,* 76th Annual Meeting, January, Washington, D.C., pp. 57-63.

Mansur, C.I. and Hunter, A.H. (1970). "Pile Tests – Arkansas River Project", *JSMFD*, ASCE, Vol. 96, No. SM5, September, pp. 1545-1582.

Meyerhof, G. (1994). Evolution of Safety Factors and Geotechnical Limit State Design. *Second Spencer J. Buchanan Lecture*, Texas A & M University, Nov. 4, College Station, TX, pp. 32.

Middendorp, P., and van Weel, P.J. (1986). "Application of Characteristic Stress-Wave Method in Offshore Practice", *Proceedings of the 3rd International Conference on Numerical Methods in Offshore Piling*. Nantes, France, May 21-22, Editions Technip.

Middle Tennessee State University Statistics Website, May 19th, 2008 http://mtsu32.mtsu.edu:11308/regression/level3/cook/concept.htm.

Minnesota Department of Transportation. (2006). *Bridge Construction Manual,* November 6, 2006, St. Paul, MN.

Minnesota Department of Transportation (2005). *Bridge Construction Manual,* November 1, 2005, St. Paul, MN. http://www.dot.state.mn.us/bridge/manuals/construction/index.html.

NCHRP 12-66 "*AASHTO LRFD Specifications for Serviceability in the Design of Bridge Foundations*" National Academy of Science, Washington, D.C., ongoing project.

Nowak, A. (1999). *NCHRP Report 368: Calibration of LRFD Bridge Design Code.* National Cooperative Highway Research Program, TRB, Washington, D.C.

Okahara, M., Fukui, J., Shirato, M., Matsui, K., and Honjo, Y. (2003). "National Report on Geotechnical Codes in Japan", *Proc. 12th Asian Regional Conference on Soil Mechanics and Geotechnical Engineering* (in press), 4-8 August, Singapore.

Olsen, R.E., and Flaate, K.S. (1967). "Pile-Driving Formulas for Friction Piles in Sand", *ASCE Journal of Soil Mechanics and Foundations,* Vol. 92, No. 6, pp. 279-297.

Orr, T.L.L. (2002). "Eurocode 7 - a code for harmonized geotechnical design." *Proc. Foundation Design Codes and Soil Investigation in View of International Harmonization and Performance Based Design,* editors Honjo, Y., Kusakabe, O., Matsui, K., Kouda, M., and Pokharel, G., Kamakura, Malaysia, pp. 3-12, A.A. Balkema Publishers, The Netherlands.

Ovesen, N.K. (1989). "General report/discussion session 30: Codes and Standards", *Proc. 12th International Conference Soil Mechanics and Foundation Engineering.* No.4, pp. 2751-2764*,* Rio de Janeiro, Brazil.

Paikowsky, S.G. (1982). "Use of Dynamic Measurements to Predict Pile Capacity under Local Conditions". (M.Sc. Dissertation), submitted to the Dept. of Civil Engineering, Geotechnical Division, Technion - Israel Institute of Technology, Haifa, Israel.

Paikowsky, S.G. (1995). "Using Dynamic Measurements for the Capacity Evaluation of Driven Piles", *Civil Engineering Practice: Journal of the Boston Society of Civil Engineers Section/ASCE*, Vol. 10, No. 2, (Fall/Winter 1995 issue), pp.61-76.

Paikowsky, S.G. (2005). "Serviceability in the Design of Bridge Foundations", *Proceedings of International Workshop on the Evaluation of Eurocode 7.* Trinity College, Dublin, Ireland, March 31 - April 1, pp. 251-261.

Paikowsky, S.G. with contributions by Birgission, G., McVay, M., Nguyen, T., Kuo, C., Baecher, G., Ayyub, B., Stenersen, K., O'Mally, K., Chernauskas, L., and O'Neill, M. (2004). *Load and Resistance Factor Design (LRFD) for Deep Foundations*, NCHRP Report 507, Transportation Research Board, National Research Council, Washington, D.C. , pp. 134 (not including Appendices), http://onlinepubs.trb.org/onlinepubs/nchrp/nchrp_rpt_507.pdf.

Paikowsky, S.G., and Canniff, M.C. (2004). "AASHTO LRFD Specifications for Serviceability in the Design of Bridge Foundations, Appendix A: Questionnaire", Interim Report Appendix A submitted for the research project NCHRP 12-66 to the National Academies, Geosciences Testing & Research, Inc., N. Chelmsford, MA.

Paikowsky, S.G., and Chernauskas, L.R. (1992). "Energy Approach for Capacity Evaluation of Driven Piles", *Proceedings of the 4th International Conference on the Application of Stress-Wave Theory to Piles*, September 21–24, pp. 595-604, discussion pp. 714, A.A. Balkema Publishers, The Netherlands.

Paikowsky, S.G., and LaBelle, V.A. (1994). "Examination of the Energy Approach for Capacity Evaluation of Driven Piles" *US FHWA International Conference on Design and Construction of Deep Foundations*, Orlando, FL, December 6-8, Vol. II, pp. 1133-1149.

Paikowsky, S.G., Lesny, K., Kisse, A., Amatya, S., Muganga, R., and Canniff, M.C. (2009). *LRFD Design Specifications for Shallow Foundations*, Final Report, submitted to the National Academies for the research project NCHRP 24-31, Geosciences Testing & Research, Inc., N. Chelmsford, MA, September 30, 2009, pp. 446.

Paikowsky, S.G., and Lu, Y. (2006). "Establishing Serviceability Limit State in the Design of Bridge Foundations", *Foundation Analysis and Design – Innovative Methods*, Proc. GeoShanghai International Conference, Shanghai, China, June 6-8, GSP No. 153, ASCE, pp. 49-58.

Paikowsky, S.G., Regan, J.E., and McDonnell, J.J. (1994). *A Simplified Field Method for Capacity Evaluation of Driven Piles*, FHWA research report. No. RD - 94-042, 1994, McLean, VA, pp. 291 (HNR publication).

Paikowsky, S.G., and Stenersen, K.L. (2000). "The Performance of the Dynamic Methods, their Controlling Parameters and Deep Foundation Specifications", Keynote lecture in the *Proceeding of the Sixth International Conference on the Application of Stress-Wave Theory to Piles*, editors Niyama S. and Beim J. September 11- 13, São Paulo, Brazil, pp. 281-304, A.A. Balkema Publishers, The Netherlands.

Paikowsky, S., and Tolosko, T. (1999). "Extrapolation of Pile Capacity From Non-Failed Load Tests". FHWA Report No. FHWA-RD-99-170, December, 1999, McLean, VA.

Paikowsky, S.G., and Whitman, R.V. (1990). "The Effect of Plugging on Pile Performance and Design", *Canadian Geotechnical Journal*, August, Vol. 27, No. 4, pp. 429–440.

Phoon, K., Kulhawy, F., and Grigoriu, M. (1995). *Reliability-Based Design of Foundations for Transmission Line Structures.* Report TR-105000. Electrical Power Research Institute (EPRI), Palo Alto, TX.

Phoon, K.K., Kulhawy, F.H., and Grigoriu, M.D. (2000). "Reliability based design for transmission line structure foundations", *Computers and Geotechnics* Vol. 26, pp. 169-185.

Rosenblueth, E., and Esteva, L. (1972). *Reliability Basis for Some Mexican Codes*. ACI Publication SP-31. American Concrete Institute, Detroit, MI.

Rubinstein, R.Y. (1981). *Simulation and the Monte Carlo Method*, John Wiley and Sons, New York, NY, pp. 278.

Schmertmann, J.H. (1970). Static cone to compute static settlement over sand, *Journal of Soil Mechanics and Foundation Div.*, ASCE, Vol. 96, No. SM3, pp. 1011-1043.

Schmertmann, J.H., and Hartman, J.P., and Brown, P.R. (1978). "Improved Strain Influence Factor Diagrams," *Journal of the Geotechnical Engineering Division*, ASCE, Vol. 104, No. GT8, pp. 113-1135.

Simpson, B., and Driscoll, R. (1998). *Eurocode 7 a commentary*, Construction Research Communications, Peterborough, United Kingdom.

Stenersen, K. (2001). *"Load and Resistance Factor Design (LRFD) for Dynamic Analyses of Driven Piles"* (M.Sc. Ths.) submitted to the University of Massachusetts at Lowell, Lowell, MA.

Taylor, D.W. (1948). *Fundamentals of Soil Mechanics,* 12th edition, John Wiley and Sons, Inc., New York, NY.

Thoft-Christensen, P., and Baker, M. (1982). *Structural Reliability Theory and Its Application.* Springer-Verlag, New York.

Wellington. (1892). Discussion of "the Iron Wharf at Fort Monroe, VA." By J.B. Cuncklee. Transactions, ASCE, Vol.27, paper no. 543, August, pp. 129-137.

Wikipedia Website. "Cook's Distance", May 19, 2008, http://en.wikipedia.org/wiki/Cook%27s_distance.

Withiam, J.L. (2003). "Implementation of the AASHTO LRFD Bridge Design Specifications for Substructure Design", *Proc. International Workshop on Limit State Design in Geotechnical Engineering Practice (LSD2003)*, editors Phoon, K.K., Honjo, Y., and Gilbert, R.B. Singapore, pp.37-38, full paper in CD-ROM, World Scientific.

Withiam, J., Voytko, E., Barker, R., Duncan, M., Kelly, B., Musser, S., and Elias, V. (1998). *Load and Resistance Factor Design (LRFD) of Highway Bridge Substructures.* Federal Highway Administration Report FHWA HI-98-032. FHWA, McLean, VA.

Zhang, L. (2003). "Limit State Design Experiences in Hong Kong and Mainland China", *Proc. 12th Asian Regional Conference on Soil Mechanics and Geotechnical Engineering* (in press), 4-8 August, Singapore.

APPENDIX A

Mn/DOT FOUNDATION CONSTRUCTION DETAILS OF 28 REPRESENTATIVE BRIDGES

Table A-1. Mn/DOT Foundation Construction Details of Bridge No. 27V66

Case No.	Bridge No.		Details	Abutments N	Abutments S	Piers 1	Piers 2	Piers 3	Piers 4	Piers 5	Comments
1	27V66	1.	Structure Type	**A6**	**A6**	**D2**	**D2**	-	-	-	
		2.	Design load total (kips)	**6888** (LRFD)	**8364** (LRFD)	**8280** (LRFD)	**7560** (LRFD)	-	-	-	
		3.	Design load per pile vert./horiz. (kips)	**246** (LRFD)	**246** (LRFD)	**276** (LRFD)	**252** (LRFD)	-	-	-	
		4.	Driving equipment	**APE D30-42**	**APE D30-42**	**APE D30-42**	**APE D30-42**	-	-	-	
		5.	Penetration criterion	**C**	**C**	**C**	**C**	-	-	-	
		6.	Final driving Resistance (typ.)	**0.150 in/blow** (avg 28 piles EOID) **0.100 in/blow** (TP 7 EIOD) **0.013 in/blow** (TP 8 "restrike" drove 4 ft to refusal)	-	-	**0.235 in/blow** (avg 30 piles EOID) **0.923 in/blow** (TP 5 EOID) **0.125 in/blow** (TP 5 restrike) **0.225 in/blow** (TP 6 EIOD)	-	-	-	
			Blows/ft (avg.)	**80 bpf** (avg 28 piles) **120 bpf** (TP 7 EOID) **1000 bpf** (TP 8 restrike)	-	-	**50 bpf** (avg 30 piles) **13 bpf** (TP 5 EOID) **100 bpf** (TP 5 restrike) **50 bpf** (TP 6 EOID)	-	-	-	
			Blows/inch (detail)	**6.7 bpi for 12 inches** (avg. 28 piles) **10.0 bpi for 12 inches** (TP 7) **75.0 bpi for 12 inches** (TP 8 "restrike" drove 4 ft to refusal)	-	-	**4.3 bpi for 12 inches** (avg. 30 piles EIOD) **1.1 bpi for 12 inches** (TP 5 EIOD) **8.0 bpi for 12 inches** (TP 5 restrike) **4.4 bpi for 12 inches** (TP 6 EIOD)	-	-	-	
		7.	Estimated field capacity (kips)	**28 Pile Avg. 812** (Mn/DOT formula) ------------- **TP 7A (EOID) 1050** (Mn/DOT formula) **439.2**	-	-	**30 Pile Avg. 726** (Mn/DOT formula) ------------- **TP 5 (EOID) 232** (Mn/DOT formula) **336.5**	-	-	-	

				(CAPWAP) **409.4** (Case Method) --------------- **TP 7 (Restrike)** **228.6** (CAPWAP) **409.4** (Case Method) --------------- **TP 8 (EOID)** **209.6** (CAPWAP) **409.4** (Case Method) --------------- **TP 8 ("restrike" to refusal)** **1375** (Mn/DOT formula) **451.9** (CAPWAP)			(CAPWAP) **420.6** (Case Method) --------------- **TP 5 (Restrike)** **915** (Mn/DOT formula) **451.8** (CAPWAP) **420.6** (Case Method) -------------- **TP 6 (EOID)** **730** (Mn/DOT formula) **439.3** (CAPWAP) **420.6** (Case Method)				

Table A-2. Mn/DOT Foundation Construction Details of Bridge No. 27V69

Case No.	Bridge No.	Details		Abutments W	Abutments E	Piers 1	Piers 2	Piers 3	Piers 4	Piers 5	Comments
2	27V69	1.	Structure Type	**A6**	**A6**	**D1M**	-	-	-	-	
		2.	Design load total (kips)	**3196** (LRFD)	**2820** (LRFD)	**3384** (LRFD)	-	-	-	-	
		3.	Design load per pile vert./horiz. (kips)	**188** (LRFD)	**188** (LRFD)	**188** (LRFD)	-	-	-	-	
		4.	Driving equipment	**APE D19-42**	**APE D19-42**	**APE D19-42**	-	-	-	-	
		5.	Penetration criterion	**C**	**C**	**C**	-	-	-	-	
		6.	Final driving Resistance (typ.)	-	-	**0.34 in/blow** (avg 16 piles) **0.480 in/blow** (TP3 EOID) **0.462 in/blow** (TP4 EOID)		-	-	-	
			Blows/ft (avg.)	-	-	**35 bpf** (avg 16 piles) **25 bpf** (TP3 EOID) **26 bpf** (TP4 EOID)		-	-	-	
			Blows/inch (detail)	-	-	**3/8 inch per 5 blows (2.67 bpi)** (TP 3 BOR) **3/8 inch per 5 blows (2.67 bpi)** (TP 4 BOR)		-	-	-	
		7.	Estimated field capacity (kips)	-	-	**16 Pile Avg. 294** (Mn/DOT formula) ------------ **TP 3 (EOID) 180** (Mn/DOT formula) **138** (CAPWAP) **328** (Case Method) ------------ **TP 3 (Restrike) 566** (Mn/DOT formula) **343** (CAPWAP)		-	-	-	

						328 (Case Method) ------------ **TP 4 (EOID)** **190** (Mn/DOT formula) **148** (CAPWAP) **328** (Case Method) ------------ **TP 4 (Restrike)** **620** (Mn/DOT formula) **421** (CAPWAP) **328** (Case Method)					

Table A-3. Mn/DOT Foundation Construction Details of Bridge No. 27V73

Case No.	Bridge No.		Details	Abutments W	Abutments E	Piers 1	Piers 2	Piers 3	Piers 4	Piers 5	Comments
3	27V73	1.	Structure Type	**A6**	**A6**	**D2**	**D2**	-	-	-	
		2.	Design load total (kips)	**6302** (LRFD)	**2260** (LRFD)	**5740** (LRFD)	**5780** (LRFD)	-	-	-	
		3.	Design load per pile vert./horiz. (kips)	**274** (LRFD)	**274** (LRFD)	**287** (LRFD)	**289** (LRFD)	-	-	-	
		4.	Driving equipment	**APE D40-32 D30-42 D30-32**	**APE D40-32 D30-42 D30-32**	**APE D40-32 D30-42 D30-32**	**APE D40-32 D30-42 D30-32**	-	-	-	
		5.	Penetration criterion	**C**	**C**	**C**	**C**	-	-	-	
		6.	Final driving Resistance (typ.)	**0.240 in/blow** (avg 21 piles) **0.235 in/blow** (TP1 EOID) **0.231 in/blow** (TP2 EOID)	**0.230 in/blow** (avg 31 piles) **0.150 in/blow** (TP7 EOID) **0.200 in/blow** (TP8 EOID)	**0.230 in/blow** (avg 18 piles) **0.174 in/blow** (TP3 EOID) **0.203 in/blow** (TP4 EOID)	**0.230 in/blow** (avg 18 piles) **0.200 in/blow** (TP5 EOID) **0.194 in/blow** (TP6 EOID)	-	-	-	
			Blows/ft (avg.)	**50 bpf** (avg 21 piles) **51 bpf** (TP1 EOID) **52 bpf** (TP2 EOID)	**52 bpf** (avg 31 piles) **80 bpf** (TP7 EOID) **60 bpf** (TP8 EOID)	**52 bpf** (avg 18 piles) **69 bpf** (TP3 EOID) **59 bpf** (TP4 EOID)	**52 bpf** (avg 18 piles) **60 bpf** (TP5 EOID) **62 bpf** (TP6 EOID)	-	-	-	
			Blows/inch (detail)	**4.2 bpi for 12 inches** (avg. 21 piles) **4.2 bpi for 12 inches** (TP 1) **4.3 bpi for 12 inches** (TP 2)	**4.3 bpi for 12 inches** (avg. 31 piles) **6.7 bpi for 12 inches** (TP 7) **5.0 bpi for 12 inches** (TP 8)	**4.3 bpi for 12 inches** (avg. 18 piles) **5.7 bpi for 12 inches** (TP 3) **4.9 bpi for 12 inches** (TP 4)	**4.3 bpi for 12 inches** (avg. 18 piles) **5.0 bpi for 12 inches** (TP 5) **5.2 bpi for 12 inches** (TP 6)	-	-	-	
		7.	Estimated field capacity (kips)	**21 Pile Avg. 816** (Mn/DOT formula) ------------ **TP 1 (EOID) 816** (Mn/DOT formula) **638** (CAPWAP) **456** (Case Method) ------------ **TP 2 (EOID) 824** (Mn/DOT formula)	**31 Pile Avg. 840** (Mn/DOT formula) ------------ **TP 7 (EOID) 1050** (Mn/DOT formula) **820** (CAPWAP) **456** (Case Method) ------------ **TP 8 (EOID) 970** (Mn/DOT formula)	**18 Pile Avg. 806** (Mn/DOT formula) ------------ **TP 3 (EOID) 928** (Mn/DOT formula) **635** (CAPWAP) **478** (Case Method) ------------ **TP 4 (EOID) 860** (Mn/DOT formula)	**18 Pile Avg. 800** (Mn/DOT formula) ------------ **TP 5 (EOID) 868** (Mn/DOT formula) **482** (CAPWAP) **498** (Case Method) ------------ **TP 6 (EOID) 882** (Mn/DOT formula)	-	-	-	

Table A-4. Mn/DOT Foundation Construction Details of Bridge No.27V75

Case No.	Bridge No.		Details	Abutments W	Abutments E	Piers 1	Piers 2	Piers 3	Piers 4	Piers 5	Comments
4	27V75	1.	Structure Type	**A6**	**A6**	**D1S**	**D1S**	**D1S**	**D1S**	**D1S**	
		2.	Design load total (kips)	**13,888** (LRFD)	**9240** (LRFD)	**9792** (LRFD)	**10,640** (LRFD)	**12,600** (LRFD)	**11,200** (LRFD)	**10,640** (LRFD)	
		3.	Design load per pile vert./horiz. (kips)	**248** (LRFD)	**220** (LRFD)	**272** (LRFD)	**266** (LRFD)	**280** (LRFD)	**280** (LRFD)	**266** (LRFD)	
		4.	Driving equipment	**APE D30-42**	**APE D30-42**	**APE D30-42**	**APE D30-42**	**APE D30-42**	**APE D30-42**	**APE D30-42**	
		5.	Penetration criterion	**C**	**C**	**C**	**C**	**C**	**C**	**C**	
		6.	Final driving Resistance (typ.)	-	-	-	**0.175 in/blow** (TP5 EOID) **0.200 in/blow** (TP6 EOID)	-	-	-	
			Blows/ft (avg.)	-	-	-	**69 bpf** (TP5 EOID) **60 bpf** (TP6 EOID)	-	-	-	
			Blows/inch (detail)	-	-	-	**5.7 bpi for 12 inches** (TP 5) **5.0 bpi for 12 inches** (TP 6)	-	-	-	
		7.	Estimated field capacity (kips)	-	-	-	**TP 5 (EOID)** **873** (Mn/DOT formula) **550** (CAPWAP) ------------ **TP 6 (EOID)** **819** (Mn/DOT formula) **545** (CAPWAP)	-	-	-	

Table A-5. Mn/DOT Foundation Construction Details of Bridge No. 27V78

Case No.	Bridge No.		Details	Abutments W	Abutments E	Piers 1	Piers 2	Piers 3	Piers 4	Piers 5	Comments
5	27V78	1.	Structure Type	**A6**	**A6**	-	-	-	-	-	
		2.	Design load total (kips)	**8364** (LRFD)	**8364** (LRFD)	-	-	-	-	-	
		3.	Design load per pile vert./horiz. (kips)	**246** (LRFD)	**246** (LRFD)	-	-	-	-	-	
		4.	Driving equipment	**DELMAG D19-32 D25-32**	**DELMAG D19-32 D25-32**	-	-	-	-	-	
		5.	Penetration criterion	**C**	**C**	-	-	-	-	-	
		6.	Final driving Resistance (typ.)	**0.080 in/blow** (avg 25 piles) **0.040 in/blow** (TP1 EOID) **0.025 in/blow** (TP2 EOID)	**0.260 in/blow** (avg 24 piles) **0.138 in/blow** (TP3 EOID) **0.163 in/blow** (TP4 EOID)	-	-	-	-	-	
			Blows/ft (avg.)	**46 bpf** (avg 25 piles) **300 bpf** (TP1 EOID) **480 bpf** (TP2 EOID)	**46 bpf** (avg 24 piles) **87 bpf** (TP3 EOID) **74 bpf** (TP4 EOID)	-	-	-	-	-	
			Blows/inch (detail)	**3.8 bpi for 12 inches** (avg. 25 piles) **41 blows for 1.625 inches (25.2 bpi)** (TP 1) **10 blows for 0.25 inch (0.025 bpi)** (TP 2)	**3.8 bpi for 12 inches** (avg. 24 piles) **7 2 bpi for 12 inches** (TP 3) **6.1 bpi for 12 inches** (TP 4)	-	-	-	-	-	
		7.	Estimated field capacity (kips)	**25 Pile Avg. 586** (Mn/DOT formula) ------------ **TP 1 (EOID) 740** (Mn/DOT formula) **TP 1 (Restrike) 399** (CAPWAP) ------------ **TP 2 (EOID) 740** (Mn/DOT	**24 Pile Avg. 700** (Mn/DOT formula) ------------ **TP 3 (EOID) 1023** (Mn/DOT formula) **481** (CAPWAP) ------------ **TP 4 (EOID) 952** (Mn/DOT formula) **523**	-	-	-	-	-	

				formula) **411** (CAPWAP)	(CAPWAP)						

Table A-6. Mn/DOT Foundation Construction Details of Bridge No. 27V79

Case No.	Bridge No.		Details	Abutments W	Abutments E	Piers 1	Piers 2	Piers 3	Piers 4	Piers 5	Comments
6	27V79	1.	Structure Type	**A6**	**A6**	**D1S**	**D1S**	**D1S**	**D1S**	**D1S**	
		2.	Design load total (kips)	**9460** (LRFD)	**6288** (LRFD)	**9216** (LRFD)	**9360** (LRFD)	**11,700** (LRFD)	**11,096** (LRFD)	**10,296** (LRFD)	
		3.	Design load per pile vert./horiz. (kips)	**220** (LRFD)	**262** (LRFD)	**256** (LRFD)	**260** (LRFD)	**260** (LRFD)	**292** (LRFD)	**286** (LRFD)	
		4.	Driving equipment	**APE D30-42**	**APE D30-42**	**APE D30-42**	**APE D30-42**	**APE D30-42**	**APE D30-42**	**APE D30-42**	
		5.	Penetration criterion	**C**	**C**	**C**	**C**	**C**	**C**	**C**	
		6.	Final driving Resistance (typ.)	-	-	-	**0.110 in/blow** (avg 34 piles) **0.200 in/blow** (TP5 EOID) **0.200 in/blow** (TP6 EOID)	-	-	-	
			Blows/ft (avg.)	-	-	-	**109 bpf** (avg 34 piles) **60 bpf** (TP5 EOID) **60 bpf** (TP6 EOID)	-	-	-	
			Blows/inch (detail)	-	-	-	**4.9.1 bpi for 12 inches** (avg. 34 piles) **5.0 bpi for 12 inches** (TP 5) **5.0 bpi for 12 inches** (TP 6)	-	-	-	
		7.	Estimated field capacity (kips)	-	-	-	**34 Pile Avg. 1071** (Mn/DOT formula) ----------- **TP 5 (EOID) 864** (Mn/DOT formula) ----------- **TP 6 (EOID) 818** (Mn/DOT formula)	-	-	-	

Table A-7. Mn/DOT Foundation Construction Details of Bridge No. 27V84

Case No.	Bridge No.	Details		Abutments W	Abutments E	Piers 1	Piers 2	Piers 3	Piers 4	Piers 5	Comments
7	27V84	1.	Structure Type	**A6**	**A6**	**D2**	-	-	-	-	
		2.	Design load total (kips)	**11,776** (LRFD)	**8448** (LRFD)	**7056** (LRFD)	-	-	-	-	
		3.	Design load per pile vert./horiz. (kips)	**184** (LRFD)	**192** (LRFD)	**196** (LRFD)	-	-	-	-	
		4.	Driving equipment	**APE DELMAG D19-42**	**APE DELMAG D19-42**	**APE DELMAG D19-42**	-	-	-	-	
		5.	Penetration criterion	**C**	**C**	**C**	-	-	-	-	
		6.	Final driving Resistance (typ.)	**0.240 in/blow** (avg 33 piles Abutment) **0.330 in/blow** (avg 29 piles Wing Wall) **0.238 in/blow** (TP1 EOID) **0.700 in/blow** (TP2 EOID)	**0.130 in/blow** (avg 42 piles) **0.025 in/blow** (TP5 EOID) **0.056 in/blow** (TP6 EOID)	**0.150 in/blow** (avg 34 piles) **0.100 in/blow** (TP3 EOID) **0.545 in/blow** (TP4 EOID) **0.088 in/blow** (TP4 Restrike)	-	-	-	-	
			Blows/ft (avg.)	**50.0 bpf** (avg 33 piles Abutment) **36.4 bpf** (avg 29 piles Wing Wall) **50.4 bpf** (TP1 EOID) **17.1 bpf** (TP2 EOID)	**92 bpf** (avg 42 piles) **480 bpf** (TP5 EOID) **214 bpf** (TP6 EOID)	**80 bpf** (avg 34 piles) **120 bpf** (TP3 EOID) **22 bpf** (TP4 EOID) **137 bpf** (TP4 EOID)	-	-	-	-	
			Blows/inch (detail)	**10 blows for 3.375 inches (3.0 bpi)** ------------ **5 blows for 1.500 inches (3.3 bpi)** ------------ **10 blows for 2.375 inches (4.2 bpi)** ------------ **5 blows for 3.500 inches (1.4 bpi)** ------------ **4.2 bpi for 12 inches** (avg. 33 piles) **3.0 bpi for 12**	**7.7 bpi for 12 inches** (avg. 42 piles) **40.0 bpi for 12 inches** (TP 5) **17.9 bpi for 12 inches** (TP 6)	**6.7 bpi for 12 inches** (avg. 34 piles) **10.0 bpi for 12 inches** (TP 3) **1.8 bpi for 12 inches** (TP 4) **10 blows for 0.875 inches** (11.4 bpi for 12 inches) (TP 4 - Restrike)	-	-	-	-	

				inches (avg. 29 piles) **4.2 bpi for 12 inches** (TP 1) **1.4 bpi for 12 inches** (TP 2)							
		7.	Estimated field capacity (kips)	**33 Pile Avg.** **475** (Mn/DOT formula - Abutment) ------------ **29 Pile Avg.** **388** (Mn/DOT formula – Wing Wall) ------------ **TP 1 (EOID)** **457** (Mn/DOT formula) **171** (CAPWAP) **306** (Case Method) ------------ **TP 1 (Restrike)** **325** (CAPWAP) **306** (Case Method) ------------ **TP 2 (EOID)** **195** (Mn/DOT formula) **177** (CAPWAP) **256** (Case Method) ------------ **TP 2 (Restrike)** **273** (CAPWAP) **256** (Case Method)	**42 Pile Avg.** **626** (Mn/DOT formula) ------------ **TP 5 (EOID)** **818** (Mn/DOT formula) **349** (CAPWAP) **320** (Case Method) ------------ **TP 6 (EOID)** **730** (Mn/DOT formula) **356** (CAPWAP) **320** (Case Method)	**34 Pile Avg.** **628** (Mn/DOT formula) ------------ **TP 3 (EOID)** **750** (Mn/DOT formula) **337** (CAPWAP) **325** (Case Method) ------------ **TP 4 (EOID)** **235** (Mn/DOT formula) **201** (CAPWAP) **325** (Case Method) ------------ **TP 4 (Restrike)** **740** (Mn/DOT formula) **332** (CAPWAP)	-	-	-	-	

Table A-8. Mn/DOT Foundation Construction Details of Bridge No.03009

Case No.	Bridge No.	Details		Abutments W	Abutments E	Piers 1	Piers 2	Piers 3	Piers 4	Piers 5	Comments
8	03009	1.	Structure Type	**?**	**?**	**D2**	**D2**	**D2**	**D2**	-	
		2.	Design load total (kips)	**2550** (LRFD)	**4750** (LRFD)	**5338** (LRFD)	**6120** (LRFD)	**6392** (LRFD)	**5712** (LRFD)	-	
		3.	Design load per pile vert./horiz. (kips)	**170** (LRFD)	**190** (LRFD)	**157** (LRFD)	**180** (LRFD)	**188** (LRFD)	**168** (LRFD)	-	
		4.	Driving equipment	**APE** **D25-32** **D19-42**	**APE** **D25-32** **D19-42**	**APE** **D25-32** **D19-42**	**APE** **D25-32** **D19-42**	**APE** **D25-32** **D19-42**	**APE** **D25-32** **D19-42**	-	
		5.	Penetration criterion	**C**	**C**	**C**	**C**	**C**	**C**	-	
		6.	Final driving Resistance (typ.)	**0.860 in/blow** (avg 5 piles – stage 1) **0.600 in/blow** (avg 8 piles – stage 2) **0.92 in/blow** (TP1 EOID) **0.38 in/blow** (TP1 Restrike) **0.92 in/blow** (TP2 EOID) **0.20 in/blow** (TP2 Restrike)	**0.190 in/blow** (avg 10 piles – stage 1) **0.220 in/blow** (avg 13 piles – stage 2) **0.30 in/blow** (TP11 EOID) **0.12 in/blow** (TP12 EOID) **0.05 in/blow** (TP12 Restrike)	**0.570 in/blow** (avg 20 piles – stage 2) **0.92 in/blow** (TP3 EOID) **0.05 in/blow** (TP3 Restrike) **0.57 in/blow** (TP4 EOID) **0.13 in/blow** (TP4 Restrike)	**0.620 in/blow** (avg 12 piles – stage 1) **0.480 in/blow** (avg 20 piles – stage 2) **0.86 in/blow** (TP5 EOID) **0.05 in/blow** (TP5 Restrike) **0.63 in/blow** (TP6 EOID) **0.11 in/blow** (TP6 Restrike)	**0.690 in/blow** (avg 19 piles – stage 1) **0.530 in/blow** (avg 12 piles – stage 2) **0.71 in/blow** (TP7 EOID) **0.10 in/blow** (TP7 Restrike) **0.48 in/blow** (TP8 EOID) **0.14 in/blow** (TP8 Restrike)	**0.250 in/blow** (avg 12 piles – stage 1) **0.560 in/blow** (avg 20 piles – stage 2) **0.57 in/blow** (TP9 EOID) **0.10 in/blow** (TP9 Restrike) **0.21 in/blow** (TP10 EOID) **0.05 in/blow** (TP10 Restrike)	-	
			Blows/ft (avg.)	**14 bpf** (avg 5 piles – stage 1) **20 bpf** (avg 8 piles – stage 2) **13 bpf** (TP1 EOID) **32 bpf** (TP1 Restrike) **13 bpf** (TP2 EOID) **60 bpf** (TP2 Restrike)	**63 bpf** (avg 10 piles – stage 1) **55 bpf** (avg 13 piles – stage 2) **40 bpf** (TP11 EOID) **100 bpf** (TP12 EOID) **240 bpf** (TP12 Restrike)	**21 bpf** (avg 20 piles – stage 2) **13 bpf** (TP3 EOID) **240 bpf** (TP3 Restrike) **21 bpf** (TP4 EOID) **92 bpf** (TP4 Restrike)	**19 bpf** (avg 12 piles – stage 1) **25 bpf** (avg 20 piles – stage 2) **14 bpf** (TP5 EOID) **240 bpf** (TP5 Restrike) **19 bpf** (TP6 EOID) **110 bpf** (TP6 Restrike)	**17 bpf** (avg 19 piles – stage 1) **23 bpf** (avg 12 piles – stage 2) **17 bpf** (TP7 EOID) **120 bpf** (TP7 Restrike) **25 bpf** (TP8 EOID) **86 bpf** (TP8 Restrike)	**48 bpf** (avg 12 piles – stage 1) **21 bpf** (avg 20 piles – stage 2) **21 bpf** (TP9 EOID) **120 bpf** (TP9 Restrike) **57 bpf** (TP10 EOID) **240 bpf** (TP10 Restrike)	-	
			Blows/inch (detail)	**1.2 bpi for 12 inches** (avg 5 piles – stage 1) **1.7 bpi for 12 inches** (avg 8 piles – stage 2) **1.1 bpi for 12 inches** (TP1 EOID) **5.0 bpi for 12**	**5.3 bpi for 12 inches** (avg 10 piles – stage 1) **4.5 bpi for 12 inches** (avg 13 piles – stage 2) **3.3 bpi for 12 inches** (TP11 EOID)	**1.8 bpi for 12 inches** (avg 20 piles – stage 2) **1.1 bpi for 12 inches** (TP3 EOID) **20.0 bpi for 12**	**1.6 bpi for 12 inches** (avg 12 piles – stage 1) **2.1 bpi for 12 inches** (avg 20 piles – stage 2) **1.2 bpi for 12 inches** (TP5 EOID) **20.0 bpi for 12**	**1.4 bpi for 12 inches** (avg 19 piles – stage 1) **1.9 bpi for 12 inches** (avg 12 piles – stage 2) **1.4 bpi for 12 inches** (TP7 EOID) **10.0 bpi for 12**	**4.0 bpi for 12 inches** (avg 12 piles – stage 1) **1.8 bpi for 12 inches** (avg 20 piles – stage 2) **1.8 bpi for 12 inches** (TP9 EOID) **10.0 bpi for 12**	-	

				inches (TP1 Restrike) **1.1 bpi for 12 inches** (TP2 EOID) **2.6 bpi for 12 inches** (TP2 Restrike)	**8.3 bpi for 12 inches** (TP12 EOID) **20.0 bpi for 12 inches** (TP12 Restrike)	**inches** (TP3 Restrike) **1.8 bpi for 12 inches** (TP4 EOID) **7.7 bpi for 12 inches** (TP4 Restrike)	**inches** (TP5 Restrike) **1.6 bpi for 12 inches** (TP6 EOID) **9.1 bpi for 12 inches** (TP6 Restrike)	**inches** (TP7 Restrike) **2.1 bpi for 12 inches** (TP8 EOID) **7.1 bpi for 12 inches** (TP8 Restrike)	**inches** (TP9 Restrike) **4.8 bpi for 12 inches** (TP10 EOID) **20.0 bpi for 12 inches** (TP10 Restrike)		
		7.	Estimated field capacity (kips)	**Mn/DOT formula** ---------------- **346** (avg 5 piles – stage 1) **226** (avg 8 piles – stage 2) **194** (TP1 EOID) **438** (TP1 Restrike) **200** (TP2 EOID) **670** (TP2 Restrike)	**Mn/DOT formula** ---------------- **582** (avg 10 piles – stage 1) **696** (avg 13 piles – stage 2) **544** (TP11 EOID) **654** (TP12 EOID) **846** (TP12 Restrike)	**Mn/DOT formula** ---------------- **324** (avg 20 piles – stage 2) **198** (TP3 EOID) **1124** (TP3 Restrike) **280** (TP4 EOID) **816** (TP4 Restrike)	**Mn/DOT formula** ---------------- **302** (avg 12 piles – stage 1) **364** (avg 20 piles – stage 2) **224** (TP5 EOID) **998** (TP5 Restrike) **278** (TP6 EOID) **834** (TP6 Restrike)	**Mn/DOT formula** ---------------- **270** (avg 19 piles – stage 1) **356** (avg 12 piles – stage 2) **258** (TP7 EOID) **946** (TP7 Restrike) **358** (TP8 EOID) **882** (TP8 Restrike)	**Mn/DOT formula** ---------------- **378** (avg 12 piles – stage 1) **318** (avg 20 piles – stage 2) **236** (TP9 EOID) **662** (TP9 Restrike) **376** (TP10 EOID) **650** (TP10 Restrike)	-	

Table A-9. Mn/DOT Foundation Construction Details of Bridge No. 25027

Case No.	Bridge No.	Details		Abutments S	Abutments N	Piers 1	Piers 2	Piers 3	Piers 4	Piers 5	Comments
9	25027	1.	Structure Type	**A6**	**A6**	**D2**	**D2**	-	-	-	
		2.	Design load total (kips)	**1930** (LFD)	**2060** (LFD)	**1635** (LFD)	**1600** (LFD)	-	-	-	
		3.	Design load per pile vert./horiz. (kips)	**102** (LFD)	**98** (LFD)	**150** (LFD)	**146** (LFD)	-	-	-	
		4.	Driving equipment	**DELMAG D19-42**	**DELMAG D19-42**	**DELMAG D25-42**	**DELMAG D25-42**	-	-	-	
		5.	Penetration criterion	**C**	**C**	**C**	**C**	-	-	-	
		6.	Final driving Resistance (typ.)	**0.27 in/blow** (avg 17 piles) **0.167 in/blow** (TP1 EOID) **0.200 in/blow** (TP2 EOID)	**0.20 in/blow** (avg 19 piles) **0.1125 in/blow** (TP7 EOID) **0.126 in/blow** (TP8 EOID)	**0.14 in/blow** (avg 9 piles) **0.0875 in/blow** (TP3 EOID) **0.0875 in/blow** (TP4 EOID)	**0.24 in/blow** (avg 9 piles) **0.175 in/blow** (TP5 EOID) **0.1125 in/blow** (TP6 EOID)	-	-	-	
			Blows/ft (avg.)	**44 bpf** (avg 17 piles) **72 bpf** (TP1 EOID) **60 bpf** (TP2 EOID)	**60 bpf** (avg 19 piles) **107 bpf** (TP7 EOID) **95 bpf** (TP8 EOID)	**86 bpf** (avg 9 piles) **137 bpf** (TP3 EOID) **137 bpf** (TP4 EOID)	**50 bpf** (avg 9 piles) **69 bpf** (TP5 EOID) **107 bpf** (TP6 EOID)	-	-	-	
			Blows/inch (detail)	**3.7 bpi for 12 inches** (avg. 17 piles) **6.0 bpi for 12 inches** (TP 1) **5.0 bpi for 12 inches** (TP 2)	**5.0 bpi for 12 inches** (avg. 19 piles) **8.9 bpi for 12 inches** (TP 7) **7.9 bpi for 12 inches** (TP 8)	**7.1 bpi for 12 inches** (avg. 9 piles) **11.4 bpi for 12 inches** (TP 3) **11.4 bpi for 12 inches** (TP 4)	**4.2 bpi for 12 inches** (avg. 9 piles) **5.7 bpi for 12 inches** (TP 5) **8.9 bpi for 12 inches** (TP 6)	-	-	-	
		7.	Estimated field capacity (kips)	**17 Pile Avg. 134** (Mn/DOT formula) ------------ **TP 1 (EOID) 173** (Mn/DOT formula) ------------ **TP 2 (EOID) 178** (Mn/DOT formula)	**19 Pile Avg. 160** (Mn/DOT formula) ------------ **TP 7 (EOID) 270** (Mn/DOT formula) ------------ **TP 8 (EOID) 172** (Mn/DOT formula)	**9 Pile Avg. 240** (Mn/DOT formula) ------------ **TP 3 (EOID) 248** (Mn/DOT formula) ------------ **TP 4 (EOID) 272** (Mn/DOT formula)	**9 Pile Avg. 240** (Mn/DOT formula) ------------ **TP 5 (EOID) 264** (Mn/DOT formula) ------------ **TP 6 (EOID) 280** (Mn/DOT formula)	-	-	-	

Table A-10. Mn/DOT Foundation Construction Details of Bridge No. 34027

Case No.	Bridge No.		Details	Abutments W	Abutments E	Piers 1	Piers 2	Piers 3	Piers 4	Piers 5	Comments
10	34027	1.	Structure Type	**A6**	**A6**	**D2**	**D2**	-	-	-	
		2.	Design load total (kips)	**1800** (ASD)	**1800** (ASD)	**2688** (ASD)	**2688** (ASD)	-	-	-	
		3.	Design load per pile vert./horiz. (kips)	**90** (ASD)	**90** (ASD)	**84** (ASD)	**84** (ASD)	-	-	-	
		4.	Driving equipment	**DELMAG D19-32**	**DELMAG D19-32**	**DELMAG D19-32**	**DELMAG D19-32**	-	-	-	
		5.	Penetration criterion	**C**	**C**	**C**	**C**	-	-	-	
		6.	Final driving Resistance (typ.)	**0.12 in/blow** (avg 18 piles) **0.100 in/blow** (TP1 EOID) **0.138 in/blow** (TP2 EOID)	**0.16 in/blow** (avg 17 piles) **0.125 in/blow** (TP7 EOID) **0.100 in/blow** (TP8 EOID)	**0.11 in/blow** (avg 30 piles) **0.050 in/blow** (TP3 EOID) **0.050 in/blow** (TP4 EOID)	**0.13 in/blow** (avg 24 piles) **0.088 in/blow** (TP5 EOID) **0.088 in/blow** (TP6 EOID)	-	-	-	
			Blows/ft (avg.)	**100 bpf** (avg 18 piles) **120 bpf** (TP1 EOID) **87 bpf** (TP2 EOID)	**75 bpf** (avg 17 piles) **96 bpf** (TP7 EOID) **120 bpf** (TP8 EOID)	**109 bpf** (avg 30 piles) **240 bpf** (TP3 EOID) **240 bpf** (TP4 EOID)	**92 bpf** (avg 24 piles) **136 bpf** (TP5 EOID) **136 bpf** (TP6 EOID)	-	-	-	
			Blows/inch (detail)	**8.33 bpi for 12 inches** (avg. 18 piles) **1.000 inch for 10 blows** (TP 1) **1.375 inches for 10 blows** (TP 2)	**6.25 bpi for 12 inches** (avg. 17 piles) **1.250 inches for 10 blows** (TP 7) **1.000 inches for 10 blows** (TP 8)	**9.09 bpi for 12 inches** (avg. 30 piles) **0.500 inches for 10 blows** (TP 3) **0.500 inches for 10 blows** (TP 4)	**7.69 bpi for 12 inches** (avg. 24 piles) **0.875 inches for 10 blows** (TP 5) **0.875 inches for 10 blows** (TP 6)	-	-	-	
		7.	Estimated field capacity (kips)	**18 Pile Avg. 128** (Mn/DOT formula) ------------ **TP 1 (EOID) 156** (Mn/DOT formula) ------------ **TP 2 (EOID) 136** (Mn/DOT formula)	**17 Pile Avg. 126** (Mn/DOT formula) ------------ **TP 7 (EOID) 136** (Mn/DOT formula) ------------ **TP 8 (EOID) 162** (Mn/DOT formula)	**30 Pile Avg. 124** (Mn/DOT formula) ------------ **TP 3 (EOID) 156** (Mn/DOT formula) ------------ **TP 4 (EOID) 172** (Mn/DOT formula)	**24 Pile Avg. 138** (Mn/DOT formula) ------------ **TP 5 (EOID) 186** (Mn/DOT formula) ------------ **TP 6 (EOID) 164** (Mn/DOT formula)	-	-	-	

Table A-11. Mn/DOT Foundation Construction Details of Bridge No. 34028

Case No.	Bridge No.	Details		Abutments S	Abutments N	Piers 1	Piers 2	Piers 3	Piers 4	Piers 5	Comments
11	34028	1.	Structure Type	**A6**	**A6**	-	-	-	-	-	
		2.	Design load total (kips)	**3364** (ASD)	**3364** (ASD)	-	-	-	-	-	
		3.	Design load per pile vert./horiz. (kips)	**116** (ASD)	**116** (ASD)	-	-	-	-	-	
		4.	Driving equipment	**DELMAG D19-32 D19-42**	**DELMAG D19-32 D19-42**	-	-	-	-	-	
		5.	Penetration criterion	**C**	**C**	-	-	-	-	-	
		6.	Final driving Resistance (typ.)	**0.18 in/blow** (avg 26 piles) **0.100 in/blow** (TP1 EOID) **0.100 in/blow** (TP2 EOID) **0.112 in/blow** (TP2A EOID)	**0.19 in/blow** (avg 27 piles) **0.225 in/blow** (TP3 EOID) **0.162 in/blow** (TP4 EOID)	-	-	-	-	-	
			Blows/ft (avg.)	**67 bpf** (avg 26 piles) **120 bpf** (TP1 EOID) **120 bpf** (TP2 EOID) **107 bpf** (TP2A EOID)	**63 bpf** (avg 27 piles) **53 bpf** (TP3 EOID) **74 bpf** (TP4 EOID)	-	-	-	-	-	
			Blows/inch (detail)	**5.56 bpi for 12 inches** (avg. 26 piles) **1.000 inch for 10 blows** (TP 1) **1.000 inch for 10 blows** (TP 2) **1.125 inches for 10 blows** (TP 2A)	**5.26 bpi for 12 inches** (avg. 27 piles) **2.250 inches for 10 blows** (TP 3) **1.625 inches for 10 blows** (TP 4)	-	-	-	-	-	
		7.	Estimated field capacity (kips)	**26 Pile Avg. 149** (Mn/DOT formula) ------------ **TP 1 (EOID) 188** (Mn/DOT formula) ------------ **TP 2 (EOID) 188**	**27 Pile Avg. 142** (Mn/DOT formula) ------------ **TP 3 (EOID) 136** (Mn/DOT formula) ------------ **TP 4 (EOID) 146**	-	-	-	-	-	

				(Mn/DOT formula) ------------ **TP 2A (EOID) 178** (Mn/DOT formula)	(Mn/DOT formula)						

Table A-12. Mn/DOT Foundation Construction Details of Bridge No. 34013

Case No.	Bridge No.	Details		Abutments S	Abutments N	Piers 1	Piers 2	Piers 3	Piers 4	Piers 5	Comments
12	34013	1.	Structure Type	**A6**	**A6**	**D2**	-	-	-	-	
		2.	Design load total (kips)	**4400** (ASD)	**4212** (ASD)	**6513** (ASD)	-	-	-	-	
		3.	Design load per pile vert./horiz. (kips)	**110** (ASD)	**108** (ASD)	**167** (ASD)	-	-	-	-	
		4.	Driving equipment	**DELMAG D19-32**	**DELMAG D19-32**	**DELMAG D19-32**	-	-	-	-	
		5.	Penetration criterion	**C**	**C**	**C**	-	-	-	-	
		6.	Final driving Resistance (typ.)	**0.18 in/blow** (avg 38 piles) **0.062 in/blow** (TP1 EOID) **0.075 in/blow** (TP2 EOID)	**0.17 in/blow** (avg 37 piles) **0.088 in/blow** (TP5 EOID) **0.100 in/blow** (TP6 EOID)	**0.075 in/blow** (avg 16 piles) **0.025 in/blow** (TP3 EOID) **0.025 in/blow** (TP4 EOID)	-	-	-	-	
			Blows/ft (avg.)	**67 bpf** (avg 38 piles) **194 bpf** (TP1 EOID) **160 bpf** (TP2 EOID)	**71 bpf** (avg 37 piles) **136 bpf** (TP5 EOID) **120 bpf** (TP6 EOID)	**160 bpf** (avg 16 piles) **480 bpf** (TP3 EOID) **480 bpf** (TP4 EOID)	-	-	-	-	
			Blows/inch (detail)	**5.56 bpi for 12 inches** (avg. 38 piles) **0.625 inch for 10 blows** (TP 1) **0.750 inches for 10 blows** (TP 2)	**5.88 bpi for 12 inches** (avg. 37 piles) **0.875 inches for 10 blows** (TP 5) **1.000 inches for 10 blows** (TP 6)	**13.3 bpi for 12 inches** (avg. 16 piles) **0.250 inches for 10 blows** (TP 3) **0.250 inches for 10 blows** (TP 4)	-	-	-	-	
		7.	Estimated field capacity (kips)	**38 Pile Avg. 167** (Mn/DOT formula) ------------ **TP 1 (EOID) 254** (Mn/DOT formula) ------------ **TP 2 (EOID) 200** (Mn/DOT formula)	**37 Pile Avg. 143** (Mn/DOT formula) ------------ **TP 5 (EOID) 170** (Mn/DOT formula) ------------ **TP 6 (EOID) 170** (Mn/DOT formula)	**16 Pile Avg. 196** (Mn/DOT formula) ------------ **TP 3 (EOID) 216** (Mn/DOT formula) ------------ **TP 4 (EOID) 236** (Mn/DOT formula)	-	-	-	-	

Table A-13. Mn/DOT Foundation Construction Details of Bridge No. 35010

Case No.	**Bridge No.**	**Details**		**Abutments W**	**Abutments E**	**Piers 1**	**Piers 2**	**Piers 3**	**Piers 4**	**Piers 5**	**Piers 6**
13	35010	1.	Structure Type	**A6**	**A6**	**D2**	**D2**	**D2**	**D2**	**D2**	**D2**
		2.	Design load total (kips)	**1420** (LRFD)	**1420** (LRFD)	**2064** (LRFD)	**2064** (LRFD)	**2064** (LRFD)	**2064** (LRFD)	**2064** (LRFD)	**2064** (LRFD)
		3.	Design load per pile vert./horiz. (kips)	**142** (LRFD)	**142** (LRFD)	**258** (LRFD)	**258** (LRFD)	**258** (LRFD)	**258** (LRFD)	**258** (LRFD)	**258** (LRFD)
		4.	Driving equipment	**DELMAG D30-32**	**DELMAG D30-32**	**DELMAG D30-32**	**DELMAG D30-32**	**DELMAG D30-32**	**DELMAG D30-32**	**DELMAG D30-32**	**DELMAG D30-32**
		5.	Penetration criterion	**C**	**C**	**C**	**C**	**C**	**C**	**C**	**C**
		6.	Final driving Resistance (typ.)	**0.11 in/blow** (avg 8 piles) **0.1333 in/blow** (TP1 EOID) **0.1464 in/blow** (TP2 EOID)	**0.12 in/blow** (avg 8 piles) **0.083 in/blow** (TP15 EOID) **0.200 in/blow** (TP16 EOID)	-	-	**0.10 in/blow** (avg 6 piles) **0.0556 in/blow** (TP1 EOID) **0.0423 in/blow** (TP2 EOID)	**0.06 in/blow** (avg 6 piles) **0.0300 in/blow** (TP1 EOID) **0.0938 in/blow** (TP2 EOID)	**0.10 in/blow** (avg 6 piles) **0.0522 in/blow** (TP11 EOID) **0.0615 in/blow** (TP12 EOID)	**0.06 in/blow** (avg 6 piles) **0.0545 in/blow** (TP13 EOID) **0.0500 in/blow** (TP14 EOID)
			Blows/ft (avg.)	**109 bpf** (avg 8 piles) **90 bpf** (TP1 EOID) **82 bpf** (TP2 EOID)	**100 bpf** (avg 8 piles) **144 bpf** (TP15 EOID) **60 bpf** (TP16 EOID)	-	-	**120 bpf** (avg 6 piles) **216 bpf** (TP7 EOID) **284 bpf** (TP8 EOID)	**200 bpf** (avg 6 piles) **400 bpf** (TP9 EOID) **128 bpf** (TP10 EOID)	**120 bpf** (avg 6 piles) **230 bpf** (TP11 EOID) **195 bpf** (TP12 EOID)	**200 bpf** (avg 6 piles) **220 bpf** (TP13 EOID) **240 bpf** (TP14 EOID)
			Blows/inch (detail)	**9.1 bpi for 12 inches** (avg. 8 piles) **7.5 bpi for 12 inches** (TP 1) **6.8 bpi for 12 inches** (TP 2)	**8.3 bpi for 12 inches** (avg. 8 piles) **1.2 bpi for 12 inches** (TP 15) **5.0 bpi for 12 inches** (TP 16)	-	-	**10.0 bpi for 12 inches** (avg. 6 piles) **18.0 bpi for 12 inches** (TP 7) **23.7 bpi for 12 inches** (TP 8)	**16.7 bpi for 12 inches** (avg. 6 piles) **33.3 bpi for 12 inches** (TP 9) **10.7 bpi for 12 inches** (TP 10)	**10.0 bpi for 12 inches** (avg.6 piles) **10.0 bpi for 12 inches** (TP 11) **16.2 bpi for 12 inches** (TP 12)	**16.7 bpi for 12 inches** (avg. 6 piles) **18.3 bpi for 12 inches** (TP 13) **20.0 bpi for 12 inches** (TP 14)
		7.	Estimated field capacity (kips)	**8 Pile Avg. 1212** (Mn/DOT formula) ------------ **TP 1 (EOID) 896** (Mn/DOT formula) ------------ **TP 2 (EOID) 822** (Mn/DOT formula)	**8 Pile Avg. 1218** (Mn/DOT formula) ------------ **TP 15 (EOID) 1090** (Mn/DOT formula) ------------ **TP 16 (EOID) 764** (Mn/DOT formula)	-	-	**6 Pile Avg. 982** (Mn/DOT formula) ------------ **TP 7 (EOID) 1060** (Mn/DOT formula) ------------ **TP 8 (EOID) 1146** (Mn/DOT formula)	**6 Pile Avg. 1084** (Mn/DOT formula) ------------ **TP 9 (EOID) 1206** (Mn/DOT formula) ------------ **TP 10 (EOID) 944** (Mn/DOT formula)	**6 Pile Avg. 978** (Mn/DOT formula) ------------ **TP 11 (EOID) 1100** (Mn/DOT formula) ------------ **TP 12 (EOID) 1060** (Mn/DOT formula)	**6 Pile Avg. 1166** (Mn/DOT formula) ------------ **TP 13 (EOID) 1140** (Mn/DOT formula) ------------ **TP 14 (EOID) 1218** (Mn/DOT formula)

Table A-14. Mn/DOT Foundation Construction Details of Bridge No. 35012

Case No.	Bridge No.	Details		Abutments S	Abutments N	Piers 1	Piers 2	Piers 3	Piers 4	Piers 5	Comments
14	35012	1.	Structure Type	**A6**	**A6**	**D2**	-	-	-	-	
		2.	Design load total (kips)	**1302** (LRFD)	**1302** (LRFD)	**1680** (LRFD)	-	-	-	-	
		3.	Design load per pile vert./horiz. (kips)	**186** (LRFD)	**186** (LRFD)	**240** (LRFD)	-	-	-	-	
		4.	Driving equipment	**DELMAG D30-32**	**DELMAG D30-32**	**DELMAG D30-32**	-	-	-	-	
		5.	Penetration criterion	**C**	**C**	**C**	-	-	-	-	
		6.	Final driving Resistance (typ.)	**0.09 in/blow** (avg 5 piles) **0.01875 in/blow** (TP1 EOID) **0.1765 in/blow** (TP2 EOID)	**0.10 in/blow** (avg 5 piles) **0.0600 in/blow** (TP5 EOID) **0.1165 in/blow** (TP6 EOID)	**0.115 in/blow** (avg 5 piles) **0.0960 in/blow** (TP3 EOID) **0.0088 in/blow** (TP4 EOID)	-	-	-	-	
			Blows/ft (avg.)	**133 bpf** (avg 5 piles) **640 bpf** (TP1 EOID) **68 bpf** (TP2 EOID)	**120 bpf** (avg 5 piles) **200 bpf** (TP5 EOID) **103 bpf** (TP6 EOID)	**104 bpf** (avg 5 piles) **125 bpf** (TP3 EOID) **136 bpf** (TP4 EOID)	-	-	-	-	
			Blows/inch (detail)	**0.1875 inches for 10 blows** **11.1 bpi for 12 inches** (avg. 5 piles) **53 bpi for 12 inches** (TP 1) **5.7 bpi for 12 inches** (TP 2)	**10.0 bpi for 12 inches** (avg. 5 piles) **16.7 bpi for 12 inches** (TP 5) **8.6 bpi for 12 inches** (TP 6)	**8.7 bpi for 12 inches** (avg. 5 piles) **10.4 bpi for 12 inches** (TP 3) **11.3 bpi for 12 inches** (TP 4)	-	-	-	-	
		7.	Estimated field capacity (kips)	**5 Pile Avg. 1140** (Mn/DOT formula) ------------ **TP 1 (EOID) 1540** (Mn/DOT formula) ------------ **TP 2 (EOID) 786** (Mn/DOT formula)	**5 Pile Avg. 1368** (Mn/DOT formula) ------------ **TP 5 (EOID) 1310** (Mn/DOT formula) ------------ **TP 6 (EOID) 1040** (Mn/DOT formula)	**5 Pile Avg. 868** (Mn/DOT formula) ------------ **TP 3 (EOID) 814** (Mn/DOT formula) ------------ **TP 4 (EOID) 1180** (Mn/DOT formula)	-	-	-	-	

Table A-15. Mn/DOT Foundation Construction Details of Bridge No. 43016

Case No.	Bridge No.	Details		Abutments		Piers					Comments
				S	N	1	2	3	4	5	
15	43016	1.	Structure Type	**A6**	**A6**	**D2**	**D2**	-	-	-	
		2.	Design load total (kips)	**3752** (LFD)	**3752** (LFD)	**3180** (LFD)	**3180** (LFD)	-	-	-	
		3.	Design load per pile vert./horiz. (kips)	**134** (LFD)	**134** (LFD)	**106** (LFD)	**106** (LFD)	-	-	-	
		4.	Driving equipment	**DELMAG D25-32**	**DELMAG D25-32**	**DELMAG D25-32**	**DELMAG D25-32**	-	-	-	
		5.	Penetration criterion	**C**	**C**	**C**	**C**	-	-	-	
		6.	Final driving Resistance (typ.)	**0.225 in/blow** (avg 26 piles) **0.088 in/blow** (TP1 EOID) **0.250 in/blow** (TP2 EOID)	**0.34 in/blow** (avg 26 piles) **0.175 in/blow** (TP7 EOID) **0.225 in/blow** (TP8 EOID)	**0.34 in/blow** (avg 28 piles) **0.262 in/blow** (TP3 EOID) **0.275 in/blow** (TP4 EOID)	**0.32 in/blow** (avg 28 piles) **0.238 in/blow** (TP5 EOID) **0.250 in/blow** (TP6 EOID)	-	-	-	
			Blows/ft (avg.)	**53 bpf** (avg 26 piles) **136 bpf** (TP1 EOID) **48 bpf** (TP2 EOID)	**35 bpf** (avg 26 piles) **69 bpf** (TP7 EOID) **53 bpf** (TP8 EOID)	**35 bpf** (avg 28 piles) **46 bpf** (TP3 EOID) **44 bpf** (TP4 EOID)	**37 bpf** (avg 28 piles) **50 bpf** (TP5 EOID) **48 bpf** (TP6 EOID)	-	-	-	
			Blows/inch (detail)	**4.4 bpi for 12 inches** (avg. 26 piles) **0.875 inches for 10 blows** (TP 1) **2.500 inches for 10 blows** (TP 2)	**2.9 bpi for 12 inches** (avg. 26 piles) **1.750 inches for 10 blows** (TP 7) **2.250 inches for 10 blows** (TP 8)	**2.9 bpi for 12 inches** (avg. 28 piles) **2.625 inches for 10 blows** (TP 3) **2.750 inches for 10 blows** (TP 4)	**3.1 bpi for 12 inches** (avg. 28 piles) **2.375 inches for 10 blows** (TP 5) **2.500 inches for 10 blows** (TP 6)	-	-	-	
		7.	Estimated field capacity (kips)	**26 Pile Avg. 215** (Mn/DOT formula) ------------ **TP 1 (EOID) 274** (Mn/DOT formula) ------------ **TP 2 (EOID) 198** (Mn/DOT formula)	**26 Pile Avg. 158** (Mn/DOT formula) ------------ **TP 7 (EOID) 206** (Mn/DOT formula) ------------ **TP 8 (EOID) 192** (Mn/DOT formula)	**28 Pile Avg. 182** (Mn/DOT formula) ------------ **TP 3 (EOID) 194** (Mn/DOT formula) ------------ **TP 4 (EOID) 186** (Mn/DOT formula)	**28 Pile Avg. 167** (Mn/DOT formula) ------------ **TP 5 (EOID) 194** (Mn/DOT formula) ------------ **TP 6 (EOID) 176** (Mn/DOT formula)	-	-	-	

Table A-16. Mn/DOT Foundation Construction Details of Bridge No. 49037

Case No.	Bridge No.	Details		Abutments S	Abutments N	Piers 1	Piers 2	Piers 3	Piers 4	Piers 5	Comments
16	49037	1.	Structure Type	**A6**	**A6**	**D2**	**D2**	-	-	-	
		2.	Design load total (kips)	**832** (LFD)	**832** (LFD)	**1686** (LFD)	**1686** (LFD)	-	-	-	
		3.	Design load per pile vert./horiz. (kips)	**104** (LFD)	**104** (LFD)	**105** (LFD)	**105** (LFD)	-	-	-	
		4.	Driving equipment	**DELMAG D25-32**	**DELMAG D25-32**	**DELMAG D25-32**	**DELMAG D25-32**	-	-	-	
		5.	Penetration criterion	**C**	**C**	**C**	**C**	-	-	-	
		6.	Final driving Resistance (typ.)	-	-	-	-	-	-	-	
			Blows/ft (avg.)	-	-	-	-	-	-	-	
			Blows/inch (detail)	-	-	-	-	-	-	-	
		7.	Estimated field capacity (kips)	**TP 1 (EOID)** **288** (Mn/DOT formula) ------------ **TP 2 (EOID)** **288** (Mn/DOT formula)	**TP 7 (EOID)** **252** (Mn/DOT formula) ------------ **TP 8 (EOID)** **312** (Mn/DOT formula)	**TP 3 (EOID)** **271** (Mn/DOT formula) ------------ **TP 4 (EOID)** **258** (Mn/DOT formula)	**TP 5 (EOID)** **304** (Mn/DOT formula) ------------ **TP 6 (EOID)** **346** (Mn/DOT formula)	-	-	-	

Table A-17. Mn/DOT Foundation Construction Details of Bridge No. 49038

Case No.	Bridge No.	Details		Abutments S	Abutments N	Piers 1	Piers 2	Piers 3	Piers 4	Piers 5	Comments
17	49038	1.	Structure Type	**A6**	**A6**	**D2**	**D2**	-	-	-	
		2.	Design load total (kips)	**832** (LFD)	**832** (LFD)	**1686** (LFD)	**1686** (LFD)	-	-	-	
		3.	Design load per pile vert./horiz. (kips)	**104** (LFD)	**104** (LFD)	**105** (LFD)	**105** (LFD)	-	-	-	
		4.	Driving equipment	**DELMAG D25-32**	**DELMAG D25-32**	**DELMAG D25-32**	**DELMAG D25-32**	-	-	-	
		5.	Penetration criterion	**C**	**C**	**C**	**C**	-	-	-	
		6.	Final driving Resistance (typ.)	-	-	-	-	-	-	-	
			Blows/ft (avg.)	-	-	-	-	-	-	-	
			Blows/inch (detail)	-	-	-	-	-	-	-	
		7.	Estimated field capacity (kips)	**TP 1 (EOID)** **171** (Mn/DOT formula)	**TP 7 (EOID)** **246** (Mn/DOT formula) ------------ **TP 8 (EOID)** **276** (Mn/DOT formula)	**TP 3 (EOID)** **286** (Mn/DOT formula) ------------ **TP 4 (EOID)** **258** (Mn/DOT formula)	**TP 5 (EOID)** **290** (Mn/DOT formula) ------------ **TP 6 (EOID)** **274** (Mn/DOT formula)	-	-	-	

Table A-18. Mn/DOT Foundation Construction Details of Bridge No. 49039

Case No.	Bridge No.		Details	Abutments S	Abutments N	Piers 1	Piers 2	Piers 3	Piers 4	Piers 5	Comments
18	49039	1.	Structure Type	**A6**	**A6**	**D2**	**D2**	-	-	-	
		2.	Design load total (kips)	**853** (LFD)	**853** (LFD)	**2886** (LFD)	**2886** (LFD)	-	-	-	
		3.	Design load per pile vert./horiz. (kips)	**107** (LFD)	**107** (LFD)	**131** (LFD)	**131** (LFD)	-	-	-	
		4.	Driving equipment	**DELMAG D25-32**	**DELMAG D25-32**	**DELMAG D25-32**	**DELMAG D25-32**	-	-	-	
		5.	Penetration criterion	**C**	**C**	**C**	**C**	-	-	-	
		6.	Final driving Resistance (typ.)	-	**0.2875 in/blow**	-	-	-	-	-	
			Blows/ft (avg.)	-	-	-	-	-	-	-	
			Blows/inch (detail)	-	-	-	**2.750 inches for 10 blows**	-	-	-	
		7.	Estimated field capacity (kips)	**TP 1 (EOID) 236** (Mn/DOT formula) ------------ **TP 2 (EOID) 225** (Mn/DOT formula)	**TP 7 (EOID) 215** (Mn/DOT formula) ------------ **TP 8 (EOID) 212** (Mn/DOT formula)	**TP 3 (EOID) 258** (Mn/DOT formula) ------------ **TP 4 (EOID) 244** (Mn/DOT formula)	**TP 5 (EOID) 231** (Mn/DOT formula) ------------ **TP 6 (EOID) 244** (Mn/DOT formula)	-	-	-	

Table A-19. Mn/DOT Foundation Construction Details of Bridge No. 49040

Case No.	Bridge No.	Details		Abutments S	Abutments N	Piers 1	Piers 2	Piers 3	Piers 4	Piers 5	Comments
1	49040	1.	Structure Type	**A6**	**A6**	**D2**	**D2**	-	-	-	
		2.	Design load total (kips)	**853** (LFD)	**853** (LFD)	**2886** (LFD)	**2886** (LFD)	-	-	-	
		3.	Design load per pile vert./horiz. (kips)	**107** (LFD)	**107** (LFD)	**131** (LFD)	**131** (LFD)	-	-	-	
		4.	Driving equipment	**DELMAG D25-32**	**DELMAG D25-32**	**DELMAG D25-32**	**DELMAG D25-32**	-	-	-	
		5.	Penetration criterion	**C**	**C**	**C**	**C**	-	-	-	
		6.	Final driving Resistance (typ.)	-	-	**0.100 in/blow** (TP 4 EOID)	**0.275 in/blow** (TP 5 EOID) **0.250 in/blow** (TP 6 EOID)	-	-	-	
			Blows/ft (avg.)	-	-	**48 bpf** (TP 3 EIOD)	-	-	-	-	
			Blows/inch (detail)	-	-	**1.000 inches for 10 blows** (TP 4 EOID)	-	-	-	-	
		7.	Estimated field capacity (kips)	**TP 1 (EOID) 212** (Mn/DOT formula) ------------ **TP 2 (EOID) 184** (Mn/DOT formula)	**TP 7 (EOID) 192** (Mn/DOT formula) ------------ **TP 8 (EOID) 188** (Mn/DOT formula)	**TP 3 (EOID) 244** (Mn/DOT formula) ------------ **TP 4 (EOID) 212** (Mn/DOT formula)	**TP 5 (EOID) 132** (Mn/DOT formula) ------------ **TP 6 (EOID) 244** (Mn/DOT formula)	-	-	-	

Table A-20. Mn/DOT Foundation Construction Details of Bridge No. 55068

Case No.	Bridge No.	Details		Abutments W	Abutments E	Piers 1	Piers 2	Piers 3	Piers 4	Piers 5	Comments
20	55068	1.	Structure Type	**A6**	**A6**	**D2**	-	-	-	-	
		2.	Design load total (kips)	**5931** (ASD)	**5931** (ASD)	**5256** (ASD)	-	-	-	-	
		3.	Design load per pile vert./horiz. (kips)	**135** (ASD)	**135** (ASD)	**131** (ASD)	-	-	-	-	
		4.	Driving equipment	**DELMAG D30-32 D19-42**	**DELMAG D30-32 D19-42**	**DELMAG D30-32 D19-42**	-	-	-	-	
		5.	Penetration criterion	**C**	**C**	**C**	-	-	-	-	
		6.	Final driving Resistance (typ.)	**0.35 in/blow** (avg 42 piles) **0.250 in/blow** (TP1 EOID) **0.080 in/blow** (TP2 EOID)	**0.16 in/blow** (avg 42 piles) **0.150 in/blow** (TP5 EOID) **0.080 in/blow** (TP6 EOID)	**0.17 in/blow** (avg 38 piles) **0.083 in/blow** (TP3 EOID) **0.063 in/blow** (TP4 EOID)	-	-	-	-	
			Blows/ft (avg.)	**34 bpf** (avg 42 piles) **48 bpf** (TP1 EOID) **150 bpf** (TP2 EOID)	**75 bpf** (avg 42 piles) **80 bpf** (TP5 EOID) **150 bpf** (TP6 EOID)	**71 bpf** (avg 38 piles) **145 bpf** (TP3 EOID) **190 bpf** (TP4 EOID)	-	-	-	-	
			Blows/inch (detail)	**2.9 bpi for 12 inches** (avg. 42 piles) **4.0 bpi for 12 inches** (TP 1) **12.5 bpi for 12 inches** (TP 2)	**6.2 bpi for 12 inches** (avg. 42 piles) **6.7 bpi for 12 inches** (TP 5) **12.5 bpi for 12 inches** (TP 6)	**5.9 bpi for 12 inches** (avg. 38 piles) **12.0 bpi for 12 inches** (TP 3) **15.9 bpi for 12 inches** (TP 4)	-	-	-	-	
		7.	Estimated field capacity (kips)	**42 Pile Avg. 280** (Mn/DOT formula) ------------ **TP 1 (EOID) 332** (Mn/DOT formula) ------------ **TP 2 (EOID) 534** (Mn/DOT formula)	**42 Pile Avg. 412** (Mn/DOT formula) ------------ **TP 5 (EOID) 428** (Mn/DOT formula) ------------ **TP 6 (EOID) 506** (Mn/DOT formula)	**38 Pile Avg. 172** (Mn/DOT formula) ------------ **TP 3 (EOID) 271** (Mn/DOT formula) ------------ **TP 4 (EOID) 292** (Mn/DOT formula)	-	-	-	-	

Table A-21. Mn/DOT Foundation Construction Details of Bridge No. 55073

Case No.	Bridge No.		Details	Abutments S	Abutments N	Piers 1	Piers 2	Piers 3	Piers 4	Piers 5	Comments
21	55073	1.	Structure Type	**A6**	**A6**	**D2**	**D2**	-	-	-	
		2.	Design load total (kips)	**1100** (ASD)	**1010** (ASD)	**1859** (ASD)	**1809** (ASD)	-	-	-	
		3.	Design load per pile vert./horiz. (kips)	**100** (ASD)	**101** (ASD)	**133** (ASD)	**129** (ASD)	-	-	-	
		4.	Driving equipment	**DELMAG D19-32**	**DELMAG D19-32**	**DELMAG D19-32**	**DELMAG D19-32**	-	-	-	
		5.	Penetration criterion	**C**	**C**	**C**	**C**	-	-	-	
		6.	Final driving Resistance (typ.)	**0.30 in/blow** (avg 9 piles) **0.15 in/blow** (TP1 EOID) **0.18 in/blow** (TP2 EOID)	**0.31 in/blow** (avg 8 piles) **0.18 in/blow** (TP7 EOID) **0.20 in/blow** (TP8 EOID)	**0.19 in/blow** (avg 12 piles) **0.11 in/blow** (TP3 EOID) **0.11 in/blow** (TP4 EOID)	**0.18 in/blow** (avg 12 piles) **0.10 in/blow** (TP5 EOID) **0.10 in/blow** (TP6 EOID)	-	-	-	
			Blows/ft (avg.)	**40 bpf** (avg 9 piles) **80 bpf** (TP1 EOID) **67 bpf** (TP2 EOID)	**39 bpf** (avg 8 piles) **67 bpf** (TP7 EOID) **60 bpf** (TP8 EOID)	**63 bpf** (avg 12 piles) **109 bpf** (TP3 EOID) **109 bpf** (TP4 EOID)	**67 bpf** (avg 12 piles) **120 bpf** (TP5 EOID) **120 bpf** (TP6 EOID)	-	-	-	
			Blows/inch (detail)	**3.3 bpi for 12 inches** (avg. 9 piles) **6.7 bpi for 12 inches** (TP 1) **5.6 bpi for 12 inches** (TP 2)	**3.2 bpi for 12 inches** (avg. 8 piles) **5.6 bpi for 12 inches** (TP 7) **5.0 bpi for 12 inches** (TP 8)	**5.3 bpi for 12 inches** (avg. 12 piles) **9.1 bpi for 12 inches** (TP 3) **9.1 bpi for 12 inches** (TP 4)	**5.6 bpi for 12 inches** (avg. 12 piles) **10.0 bpi for 12 inches** (TP 5) **10.0 bpi for 12 inches** (TP 6)	-	-	-	
		7.	Estimated field capacity (kips)	**9 Pile Avg. 122** (Mn/DOT formula) ------------ **TP 1 (EOID) 178** (Mn/DOT formula) ------------ **TP 2 (EOID) 166** (Mn/DOT formula)	**8 Pile Avg. 156** (Mn/DOT formula) ------------ **TP 7 (EOID) 166** (Mn/DOT formula) ------------ **TP 8 (EOID) 167** (Mn/DOT formula)	**12 Pile Avg. 158** (Mn/DOT formula) ------------ **TP 3 (EOID) 213** (Mn/DOT formula) ------------ **TP 4 (EOID) 213** (Mn/DOT formula)	**12 Pile Avg. 124** (Mn/DOT formula) ------------ **TP 5 (EOID) 208** (Mn/DOT formula) ------------ **TP 6 (EOID) 208** (Mn/DOT formula)	-	-	-	

Table A-22. Mn/DOT Foundation Construction Details of Bridge No. 55075

Case No.	Bridge No.	Details		Abutments S	Abutments N	Piers 1	Piers 2	Piers 3	Piers 4	Piers 5	Comments
22	55075	1.	Structure Type	**A6**	**A6**	**D2**	**D2**	-	-	-	
		2.	Design load total (kips)	**714** (ASD)	**714** (ASD)	**1370** (ASD)	**1370** (ASD)	-	-	-	
		3.	Design load per pile vert./horiz. (kips)	**102** (ASD)	**102** (ASD)	**137** (ASD)	**137** (ASD)	-	-	-	
		4.	Driving equipment	**DELMAG D19-32 D19-42**	**DELMAG D19-32 D19-42**	**DELMAG D19-32 D19-42**	**DELMAG D19-32 D19-42**	-	-	-	
		5.	Penetration criterion	**C**	**C**	**C**	**C**	-	-	-	
		6.	Final driving Resistance (typ.)	-	**0.17 in/blow** (avg 5 piles) **0.17 in/blow** (TP7 EOID) **0.125 in/blow** (TP8 EOID)	**0.20 in/blow** (avg 8 piles) **0.10 in/blow** (TP3 EOID) **0.07 in/blow** (TP4 EOID)	**0.14 in/blow** (avg 8 piles) **0.10 in/blow** (TP5 EOID) **0.11 in/blow** (TP6 EOID)	-	-	-	
			Blows/ft (avg.)	-	**71 bpf** (avg 5 piles) **71 bpf** (TP7 EOID) **96 bpf** (TP8 EOID)	**60 bpf** (avg 8 piles) **120 bpf** (TP3 EOID) **171 bpf** (TP4 EOID)	**86 bpf** (avg 8 piles) **120 bpf** (TP5 EOID) **109 bpf** (TP6 EOID)	-	-	-	
			Blows/inch (detail)	-	**5.9 bpi for 12 inches** (avg. 5 piles) **5.9 bpi for 12 inches** (TP 7) **8.0 bpi for 12 inches** (TP 8)	**5.0 bpi for 12 inches** (avg. 8 piles) **10.0 bpi for 12 inches** (TP 3) **14.3 bpi for 12 inches** (TP 4)	**7.1 bpi for 12 inches** (avg. 8 piles) **10.0 bpi for 12 inches** (TP 5) **9.1 bpi for 12 inches** (TP 6)	-	-	-	
		7.	Estimated field capacity (kips)	-	**5 Pile Avg. 174** (Mn/DOT formula) ------------ **TP 7 (EOID) 220** (Mn/DOT formula) ------------ **TP 8 (EOID) 182** (Mn/DOT formula)	**8 Pile Avg. 170** (Mn/DOT formula) ------------ **TP 3 (EOID) 232** (Mn/DOT formula) ------------ **TP 4 (EOID) 258** (Mn/DOT formula)	**8 Pile Avg. 200** (Mn/DOT formula) ------------ **TP 5 (EOID) 218** (Mn/DOT formula) ------------ **TP 6 (EOID) 224** (Mn/DOT formula)	-	-	-	

Table A-23. Mn/DOT Foundation Construction Details of Bridge No. 62902

Case No.	Bridge No.	Details		Abutments		Piers					Comments
				N	S	1 / 2	3 / 4	5 / 6	7 / 8		
23	62902	1.	Structure Type	**A6**	**A6**	**D1M**	**D1M**	**D1M**	**D1M**	-	
		2.	Design load total (kips)	**5586** (ASD)	**3248** (ASD)	**3475 / 5387** (ASD)	**6528 / 5760** (ASD)	**5824 / 5760** (ASD)	**5404 / 5978** (ASD)	-	
		3.	Design load per pile vert./horiz. (kips)	**114** (ASD)	**112** (ASD)	**145 / 192** (ASD)	**192 / 192** (ASD)	**182 / 192** (ASD)	**193 / 187** (ASD)	-	
		4.	Driving equipment	**DELMAG D25-32 D19-32**	**DELMAG D25-32 D19-32**	**DELMAG D25-32 D19-32**	**DELMAG D25-32 D19-32**	**DELMAG D25-32 D19-32**	**DELMAG D25-32 D19-32**	-	
		5.	Penetration criterion	**C**	**C**	**C**	**C**	**C**	**C**	-	
		6.	Final driving Resistance (typ.)	**0.26 in/blow** (avg 47 piles) **0.100 in/blow** (TP1 EOID) **0.100 in/blow** (TP2 EOID)	**0.33 in/blow** (avg 27 piles) **0.125 in/blow** (TP19 EOID) **0.350 in/blow** (TP20 EOID)	**0.10 in/blow** (avg 23 piles) **0.113 in/blow** (TP3 EOID) **0.075 in/blow** (TP4 EOID) **0.19 in/blow** (avg 27 piles) **0.075 in/blow** (TP5 EOID) **0.100 in/blow** (TP6 EOID)	**0.18 in/blow** (avg 25 piles) **0.250 in/blow** (TP7 EOID) **0.025 in/blow** (TP8 EOID) **0.16 in/blow** (avg 30 piles) **0.325 in/blow** (TP9 EOID) **0.125 in/blow** (TP10 EOID)	**0.26 in/blow** (avg 30 piles) **0.175 in/blow** (TP11 EOID) **0.100 in/blow** (TP12 EOID) **0.41 in/blow** (avg 28 piles) **0.100 in/blow** (TP13 EOID) **0.100 in/blow** (TP14 EOID)	**0.18 in/blow** (avg 26 piles) **0.100 in/blow** (TP15 EOID) **0.100 in/blow** (TP16 EOID) **17 in/blow** (avg 30 piles) **0.200 in/blow** (TP17 EOID) **0.250 in/blow** (TP18 EOID)	-	
			Blows/ft (avg.)	**46 bpf** (avg 47 piles) **120 bpf** (TP1 EOID) **120 bpf** (TP2 EOID)	**36 bpf** (avg 27 piles) **96 bpf** (TP19 EOID) **34 bpf** (TP20 EOID)	**120 bpf** (avg 23 piles) **63 bpf** (avg 27 piles)	**67 bpf** (avg 25 piles) **75 bpf** (avg 30 piles)	**46 bpf** (avg 30 piles) **29 bpf** (avg 28 piles)	**67 bpf** (avg 26 piles) **71 bpf** (avg 30 piles)	-	
			Blows/inch (detail)	**3.8 bpi for 12 inches** (avg. 47 piles) **10.0 bpi for 12 inches** (TP 1 EOID) **10.0 bpi for 12 inches** (TP 2 EOID)	**3.0 bpi for 12 inches** (avg. 27 piles) **8.0 bpi for 12 inches** (TP 19 EOID) **2.9 bpi for 12 inches** (TP 20 EOID)	**10.0 bpi for 12 inches** (avg. 23 piles) **5.3 bpi for 12 inches** (avg. 27 piles) **0.500 inches for 10 blows** (TP 6 Restrike)	**5.6 bpi for 12 inches** (avg. 25 piles) **0.250 inches for 10 blows** (TP 7 Restrike) **0.125 inches for 10 blows** (TP8 Restrike) **6.2 bpi for 12 inches** (avg. 30 piles) **1.250 inches for 10 blows** (TP 9 Restrike) **0.500 inches for 10 blows** (TP 10 Restrike)	**3.8 bpi for 12 inches** (avg. 30 piles) **1.000 inches for 10 blows** (TP 11 Restrike) **0.750 inches for 10 blows** (TP 12 Restrike) **2.4 bpi for 12 inches** (avg. 28 piles) **0.500 inches for 10 blows** (TP 14 Restrike)	**5.6 bpi for 12 inches** (avg. 26 piles) **2.500 inches for 10 blows** (TP 15 Restrike) **2.250 inches for 10 blows** (TP 16 Restrike) **5.9 bpi for 12 inches** (avg. 30 piles) **1.250 inches for 10 blows** (TP 17 Restrike) **1.500 inches for 10 blows** (TP 18 Restrike)	-	

		7.	Estimated field capacity (kips)	**47 Pile Avg.** **233** (Mn/DOT formula) ------------ **TP 1 (EOID)** **382** (Mn/DOT formula) ------------ **TP 2 (EOID)** **362** (Mn/DOT formula)	**27 Pile Avg.** **210** (Mn/DOT formula) ------------ **TP 19 (EOID)** **286** (Mn/DOT formula) ------------ **TP 20 (EOID)** **168** (Mn/DOT formula)	**23 Pile Avg.** **180** (Mn/DOT formula) ------------ **TP 3 (EOID)** **160** (Mn/DOT formula) ------------ **TP 4 (EOID)** **168** (Mn/DOT formula) ------------ **27 Pile Avg.** **320** (Mn/DOT formula) ------------ **TP 5 (EOID)** **480** (Mn/DOT formula) ------------ **TP 6 (EOID)** **440** (Mn/DOT formula)	**25 Pile Avg.** **340** (Mn/DOT formula) ------------ **TP 7 (EOID)** **260** (Mn/DOT formula) ------------ **TP 8 (EOID)** **390** (Mn/DOT formula) ------------ **30 Pile Avg.** **340** (Mn/DOT formula) ------------ **TP 9 (EOID)** **200** (Mn/DOT formula) ------------ **TP 10 (EOID)** **340** (Mn/DOT formula)	**30 Pile Avg.** **250** (Mn/DOT formula) ------------ **TP 11 (EOID)** **290** (Mn/DOT formula) ------------ **TP 12 (EOID)** **360** (Mn/DOT formula) ------------ **28 Pile Avg.** **220** (Mn/DOT formula) ------------ **TP 13 (EOID)** **390** (Mn/DOT formula) ------------ **TP 14 (EOID)** **370** (Mn/DOT formula)	**26 Pile Avg.** **330** (Mn/DOT formula) ------------ **TP 15 (EOID)** **390** (Mn/DOT formula) ------------ **TP 16 (EOID)** **415** (Mn/DOT formula) ------------ **30 Pile Avg.** **320** (Mn/DOT formula) ------------ **TP 17 (EOID)** **270** (Mn/DOT formula) ------------ **TP 18 (EOID)** **260** (Mn/DOT formula)	-	

Table A-24. Mn/DOT Foundation Construction Details of Bridge No. 73035

Case No.	Bridge No.		Details	Abutments S	Abutments N	Piers 1	Piers 2	Piers 3	Piers 4	Piers 5	Comments
24	73035	1.	Structure Type	**A6**	**A6**	**D2**	**D2**	**D2**	-	-	
		2.	Design load total (kips)	**784** (LFD)	**784** (LFD)	**987** (LFD)	**987** (LFD)	**987** (LFD)	-	-	
		3.	Design load per pile vert./horiz. (kips)	**131** (LFD)	**131** (LFD)	**197** (LFD)	**197** (LFD)	**197** (LFD)	-	-	
		4.	Driving equipment	**DELMAG DE50B D30-02**	**DELMAG DE50B D30-02**	**DELMAG DE50B D30-02**	**DELMAG DE50B D30-02**	**DELMAG DE50B D30-02**	-	-	
		5.	Penetration criterion	**C**	**C**	**C**	**C**	**C**	-	-	
		6.	Final driving Resistance (typ.)	**0.140 in/blow** (avg 4 piles) **0.100 in/blow** (TP1 EOID) **0.100 in/blow** (TP2 EOID)	**0.16 in/blow** (avg 4 piles) **0.100 in/blow** (TP9 EOID) **0.100 in/blow** (TP10 EOID)	**0.08 in/blow** (avg 3 piles) **0.100 in/blow** (TP3 EOID) **0.100 in/blow** (TP4 EOID)	**0.10 in/blow** (avg 3 piles) **0.162 in/blow** (TP5 EOID) **0.156 in/blow** (TP6 EOID)	**0.13 in/blow** (avg 3 piles) **0.150 in/blow** (TP7 EOID) **0.100 in/blow** (TP8 EOID)	-	-	
			Blows/ft (avg.)	**86 bpf** (avg 4 piles) **120 bpf** (TP1 EOID) **120 bpf** (TP2 EOID)	**75 bpf** (avg 4 piles) **120 bpf** (TP9 EOID) **120 bpf** (TP10 EOID)	**150 bpf** (avg 3 piles) **120 bpf** (TP3 EOID) **120 bpf** (TP4 EOID)	**120 bpf** (avg 3 piles) **74 bpf** (TP5 EOID) **77 bpf** (TP6 EOID)	**92 bpf** (avg 3 piles) **80 bpf** (TP7 EOID) **120 bpf** (TP8 EOID)	-	-	
			Blows/inch (detail)	**0.750 inches for 10 blows** ----------------- **2.000 inches for 10 blows** ----------------- **1.000 inches for 10 blows** (TP 1) ----------------- **1.000 inches for 10blows** (TP 2)	**4 Pile Avg. 6.25 bpi for 12 inches**	**0.875 inches for 10 blows** ----------------- **0.625 inches for 10 blows** ----------------- **1.000 inches for 10 blows** (TP 3) ----------------- **1.000 inches for 10blows** (TP 4)	**1.000 inches for 10 blows**	**0.750 inches for 10 blows** ----------------- **2.125 inches for 10 blows** ----------------- **1.500 inches for 10 blows** (TP 7)	-	-	
		7.	Estimated field capacity (kips)	**4 Pile Avg.** **240** (Mn/DOT formula) ------------ **TP 1 (EOID)** **240** (Mn/DOT formula) ------------ **TP 2 (EOID)** **226** (Mn/DOT formula)	**4 Pile Avg.** **240** (Mn/DOT formula) ------------ **TP 9 (EOID)** **234** (Mn/DOT formula) ------------ **TP 10 (EOID)** **280** (Mn/DOT formula)	**3 Pile Avg.** **320** (Mn/DOT formula) ------------ **TP 3 (EOID)** **288** (Mn/DOT formula) ------------ **TP 4 (EOID)** **288** (Mn/DOT formula)	**3 Pile Avg.** **280** (Mn/DOT formula) ------------ **TP 5 (EOID)** **234** (Mn/DOT formula) ------------ **TP 6 (EOID)** **244** (Mn/DOT formula)	**3 Pile Avg.** **260** (Mn/DOT formula) ------------ **TP 7 (EOID)** **246** (Mn/DOT formula) ------------ **TP 8 (EOID)** **282** (Mn/DOT formula)	-	-	

Table A-25. Mn/DOT Foundation Construction Details of Bridge No. 81003

Case No.	Bridge No.	Details		Abutments N	Abutments S	Piers 1	Piers 2	Piers 3	Piers 4	Piers 5	Comments
25	81003	1.	Structure Type	**A6**	**A6**	**D1M**	-	-	-	-	
		2.	Design load total (kips)	**5328** (LFD)	**4543** (LFD)	**4183** (LFD)	-	-	-	-	
		3.	Design load per pile vert./horiz. (kips)	**118** (LFD)	**111** (LFD)	**116** (LFD)	-	-	-	-	
		4.	Driving equipment	**DELMAG D19-32**	**DELMAG D19-32**	**DELMAG D19-32**	-	-	-	-	
		5.	Penetration criterion	**C**	**C**	**C**	-	-	-	-	
		6.	Final driving Resistance (typ.)	**0.19 in/blow** (avg 43 piles) **0.1125 in/blow** (TP1 EOID)	**0.22 in/blow** (avg 39 piles) **0.150 in/blow** (TP5 EOID) **0.150 in/blow** (TP6 EOID)	**0.19 in/blow** (avg 34 piles) **0.625 in/blow** (TP3 EOID) **0.1625 in/blow** (TP4 EOID)	-	-	-	-	
			Blows/ft (avg.)	**63 bpf** (avg 43 piles) **107 bpf** (TP1 EOID)	**55 bpf** (avg 39 piles) **80 bpf** (TP5 EOID) **80 bpf** (TP6 EOID)	**63 bpf** (avg 34 piles) **19 bpf** (TP3 EOID) **74 bpf** (TP4 EOID)	-	-	-	-	
			Blows/inch (detail)	**5.3 bpi for 12 inches** (avg. 43 piles)	**4.5 bpi for 12 inches** (avg. 39 piles)	**5.3 bpi for 12 inches** (avg. 34 piles)	-	-	-	-	
		7.	Estimated field capacity (kips)	**43 Pile Avg. 162** (Mn/DOT formula) ------------ **TP 1 (EOID) 202** (Mn/DOT formula)	**39 Pile Avg. 152** (Mn/DOT formula) ------------ **TP 5 (EOID) 180** (Mn/DOT formula) ------------ **TP 6 (EOID) 180** (Mn/DOT formula)	**34 Pile Avg. 162** (Mn/DOT formula) ------------ **TP 3 (EOID) 240** (Mn/DOT formula) ------------ **TP 4 (EOID) 174** (Mn/DOT formula)	-	-	-	-	

Table A-26. Mn/DOT Foundation Construction Details of Bridge No. 81004

Case No.	Bridge No.	Details		Abutments N	Abutments S	Piers 1	Piers 2	Piers 3	Piers 4	Piers 5	Comments
26	81004	1.	Structure Type	**A6**	**A6**	**D1M**	-	-	-	-	
		2.	Design load total (kips)	**4543** (LFD)	**?** (LFD)	**4183** (LFD)	-	-	-	-	
		3.	Design load per pile vert./horiz. (kips)	**111** (LFD)	**?** (LFD)	**116** (LFD)	-	-	-	-	
		4.	Driving equipment	**DELMAG D19-32**	**DELMAG D19-32**	**DELMAG D19-32**	-	-	-	-	
		5.	Penetration criterion	**C**	**C**	**C**	-	-	-	-	
		6.	Final driving Resistance (typ.)	**0.21 in/blow** (avg 39 piles) **0.0375 in/blow** (TP1 EOID) **0.1125 in/blow** (TP2 EOID)	**0.20 in/blow** (avg 39 piles) **0.100 in/blow** (TP5 EOID) **0.1125 in/blow** (TP6 EOID)	**0.22 in/blow** (avg 34 piles) **0.203 in/blow** (TP3 EOID) **0.113 in/blow** (TP4 EOID)	-	-	-	-	
			Blows/ft (avg.)	**57 bpf** (avg 39 piles) **320 bpf** (TP1 EOID) **107 bpf** (TP2 EOID)	**60 bpf** (avg 39 piles) **120 bpf** (TP5 EOID) **107 bpf** (TP6 EOID)	**55 bpf** (avg 34 piles) **59 bpf** (TP3 EOID) **106 bpf** (TP4 EOID)	-	-	-	-	
			Blows/inch (detail)	**4.8 bpi for 12 inches** (avg. 39 piles)	**5.0 bpi for 12 inches** (avg. 39 piles)	**4.5 bpi for 12 inches** (avg. 34 piles)	-	-	-	-	
		7.	Estimated field capacity (kips)	**39 Pile Avg. 152** (Mn/DOT formula) ------------ **TP 1 (EOID) 242** (Mn/DOT formula) ------------ **TP 2 (EOID) 202** (Mn/DOT formula)	**39 Pile Avg. 158** (Mn/DOT formula) ------------ **TP 5 (EOID) 210** (Mn/DOT formula) ------------ **TP 6 (EOID) 202** (Mn/DOT formula)	**34 Pile Avg. 156** (Mn/DOT formula) ------------ **TP 3 (EOID) 156** (Mn/DOT formula) ------------ **TP 4 (EOID) 178** (Mn/DOT formula)	-	-	-	-	

Table A-27. Mn/DOT Foundation Construction Details of Bridge No. 81005

Case No.	Bridge No.		Details	Abutments S	Abutments N	Piers 1	Piers 2	Piers 3	Piers 4	Piers 5	Comments
27	81005	1.	Structure Type	**A6**	**A6**	**D2**	-	-	-	-	
		2.	Design load total (kips)	**2974** (ASD)	**3006** (ASD)	**5500** (ASD)	-	-	-	-	
		3.	Design load per pile vert./horiz. (kips)	**114** (ASD)	**116** (ASD)	**115** (ASD)	-	-	-	-	
		4.	Driving equipment	**DELMAG D25-32**	**DELMAG D25-32**	**DELMAG D25-32**	-	-	-	-	
		5.	Penetration criterion	**C**	**C**	**C**	-	-	-	-	
		6.	Final driving Resistance (typ.)	**0.32 in/blow** (avg 24 piles) **0.25 in/blow** (TP1 EOID) **0.25 in/blow** (TP2 EOID)	**0.36 in/blow** (avg 24 piles) **0.2875 in/blow** (TP5 EOID) **0.35 in/blow** (TP6 EOID)	**0.27 in/blow** (avg 46 piles) **0.275 in/blow** (TP3 EOID) **0.2625 in/blow** (TP4 EOID)	-	-	-	-	
			Blows/ft (avg.)	**38 bpf** (avg 24 piles) **48 bpf** (TP1 EOID) **48 bpf** (TP2 EOID)	**33 bpf** (avg 24 piles) **42 bpf** (TP5 EOID) **34 bpf** (TP6 EOID)	**44 bpf** (avg 46 piles) **44 bpf** (TP3 EOID) **46 bpf** (TP4 EOID)	-	-	-	-	
			Blows/inch (detail)	**3.1 bpi for 12 inches** (avg. 24 piles)	**2.8 bpi for 12 inches** (avg. 24 piles)	**3.7 bpi for 12 inches** (avg. 46 piles)	-	-	-	-	
		7.	Estimated field capacity (kips)	**24 Pile Avg. 224** (Mn/DOT formula) ------------ **TP 1 (EOID) 242** (Mn/DOT formula) ------------ **TP 2 (EOID) 242** (Mn/DOT formula)	**24 Pile Avg. 198** (Mn/DOT formula) ------------ **TP 5 (EOID) 198** (Mn/DOT formula) ------------ **TP 6 (EOID) 224** (Mn/DOT formula)	**46 Pile Avg. 236** (Mn/DOT formula) ------------ **TP 3 (EOID) 230** (Mn/DOT formula) ------------ **TP 4 (EOID) 234** (Mn/DOT formula)	-	-	-	-	

Table A-28. Mn/DOT Foundation Construction Details of Bridge No. 85024

Case No.	Bridge No.	Details		Abutments W	Abutments E	Piers 1	Piers 2	Piers 3	Piers 4	Piers 5	Comments
28	85024	1.	Structure Type	**A6**	**A6**	**D2**	-	-	-	-	
		2.	Design load total (kips)	**1356** (LFD)	**1356** (LFD)	**1402** (LFD)	-	-	-	-	
		3.	Design load per pile vert./horiz. (kips)	**135.6** (LFD)	**135.6** (LFD)	**155.8** (LFD)	-	-	-	-	
		4.	Driving equipment	**DELMAG D19-32**	**DELMAG D19-32**	**DELMAG D19-32**	-	-	-	-	
		5.	Penetration criterion	**C**	**C**	**C**	-	-	-	-	
		6.	Final driving Resistance (typ.)	**0.21 in/blow** (avg 8 piles) **0.125 in/blow** (TP1 EOID) **0.125 in/blow** (TP2 EOID)	**0.22 in/blow** (avg 8 piles) **0.125 in/blow** (TP5 EOID) **0.125 in/blow** (TP6 EOID)	**0.13 in/blow** (avg 7 piles) **0.0875 in/blow** (TP3 EOID) **0.100 in/blow** (TP4 EOID)	-	-	-	-	
			Blows/ft (avg.)	**57 bpf** (avg 8 piles) **96 bpf** (TP1 EOID) **96 bpf** (TP2 EOID)	**55 bpf** (avg 8 piles) **96 bpf** (TP5 EOID) **96 bpf** (TP6 EOID)	**92 bpf** (avg 7 piles) **137 bpf** (TP3 EOID) **120 bpf** (TP4 EOID)	-	-	-	-	
			Blows/inch (detail)	**4.8 bpi for 12 inches** (avg. 8 piles)	**4.5 bpi for 12 inches** (avg. 8 piles)	**7.7 bpi for 12 inches** (avg. 7 piles)	-	-	-	-	
		7.	Estimated field capacity (kips)	**8 Pile Avg. 150** (Mn/DOT formula) ------------ **TP 1 (EOID) 192** (Mn/DOT formula) ------------ **TP 2 (EOID) 196** (Mn/DOT formula)	**8 Pile Avg. 144** (Mn/DOT formula) ------------ **TP 5 (EOID) 200** (Mn/DOT formula) ------------ **TP 6 (EOID) 200** (Mn/DOT formula)	**7 Pile Avg. 190** (Mn/DOT formula) ------------ **TP 3 (EOID) 220** (Mn/DOT formula) ------------ **TP 4 (EOID) 210** (Mn/DOT formula)	-	-	-	-	

APPENDIX B

PILE DRIVING CONTRACTORS MN/DOT STATE OF PRACTICE SURVEY

Minnesota Department of Transportation Research Project

Minnesota State University, Mankato
University of Massachusetts – Lowell

Pile Driving Contractors – Minnesota State of Practice Survey

PART 1 – Company/Contact Information

Company Name	Swingen Construction Company
Contact Name	Jason Odegard
Phone/Fax Number	701 775 5359 | 701 775 7631
E-mail Address	jason.odegard@swingenconstruction.com
Company Address	1437 N 83rd St PO Box 13456 Grand Forks, ND 58203

If you have any questions or require help in completing the forms, please contact Aaron Budge at MN State University, 507-389-3294 / Aaron.Budge@mnsu.edu or Sam Paikowsky at the University of Massachusetts Lowell, 978-934-2271 / Samuel_Paikowsky@uml.edu.

PART 2 - Details Regarding Pile Driving Equipment and Construction Methods

Please list the pile driving equipment your company uses on Mn/DOT (or similar) projects. List in order of the frequency of use; from the most common pile driving to the least common driving.

Equipment No.	Hammer						Typical Use			
	Type	Manufacturer	Model No.	Year	Stnd. Equip.		Pile			Hammer Setting
					Yes	No*	Type	Section	Max. Pen.	
	SA Diesel	Vulcan	Model 1		☒	☐	Sheet Pile and Timber			15,000 lbs rated energy 11-6 stroke
	SA Diesel	Delmag	D30-32		☒	☐	CIPC (Steel Pipe)	16 inch	40-220 ft	
	SA Diesel	MVE	M30		☒	☐	CIPC (Steel Pipe)	16 inch	40-220 ft	71,700 lbs rated energy

	SA Diesel	MKT	DE 42-35		☒	☐	CIPC (Steel Pipe)	12 inch	40-220 ft	42,000 lbs rated energy
					☐	☐				

*please use attached form if not using standard equipment. Please use the form to specify your hammer cushion, helmet and striking plates if used.

Does your company use vibratory hammers on Mn/DOT projects? If so, to what depth are vibratory hammers being used prior to the use of impact hammers? Are end bearing piles being driven with vibratory hammers only?

> We use vibratory hammers for driving sheet piling and cofferdam applications. We use a small air hammer to start piles prior to impact hammers, not vibratory hammers. The air hammer is used in cases where the top 30-50 feet of material is muck and doesn't provide enough resistance to fire the SA Diesel. No bearing piles are driven with vibratory hammers.

How frequently (if at all) do you use preboring on Mn/DOT projects? If preboring IS used for such projects, please provide additional details such as to what depth preboring would typically be performed relative to final tip penetration, etc. Additional comments relative to your experience with preboring would be helpful (e.g. hole diameter relative to pile size).

> We rarely use preboring. Preboring IS used for new embankment construction, where we bore through new material (which is still settling). So, the depth of preboring would be the thickness of the new fill material, up to a depth of about 25 ft.

How frequently (if at all) do you use jetting on Mn/DOT projects? If jetting IS used for such projects, please provide additional details such as to what depth jetting would be typically performed relative to final tip penetration, etc. Additional comments relative to your experience with jetting would be helpful.

> No jetting is used.

PART 3 - Details Regarding Preferred Pile Driving Practice

Assuming your company determines/proposes the piles and equipment used on a project (i.e. assuming value engineering is allowed and proposed by your company) provide details as to your preferred pile driving practice. Include preferred pile size and type, hammer type, range of loads, etc. Please list as many combinations as possible covering the range of projects your company dealt with.

> Preferred practice follows the information in the table above:
>
> For 16 inch CIPC piles (80-150 ton piles) use the Delmag D30-32 or the MVE M30.

For 12 inch CIPC piles (50-80 ton piles) use the MKT DE42-35.

Contract No.: ____________________
Project: ____________________
____
County: ____________________

Structure Name and/or No.: ____________________
____
Pile Driving contractor or Subcontractor: ____________
____

(Piles driven by)

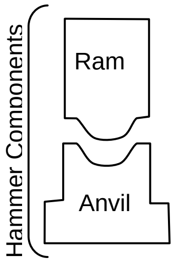

Hammer

Manufacturer: ____________ Model No.: ____________
Hammer Type: ____________ Serial No.: ____________
Manufacturers Maximum Rated Energy: ____________ (Joules)☐ (ft-k)☐
Stroke at Maximum Rated Energy: ____________ (meters)☐ (ft)☐
Range in Operating Energy: ____________ (Joules)☐ (ft-k)☐
Range in Operating Stroke: ____________ (meters)☐ (ft)☐
Ram Weight: ____________ (kN)☐ (kips)☐
Modification: ____________________
____
____

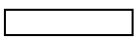

Striker Plate

Weight: ________ (kN)☐ (kips)☐ Diameter: ______ (mm)☐ (in)☐
Thickness: ________ (mm)☐ (in)☐

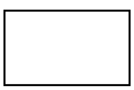

Hammer Cushion

Material #1	Material #2 (for Composite Cushion)
Name: ____________	Name: ____________
Area: ________ (cm^2)☐ (in^2)☐	Area: ________ (cm^2)☐ (in^2)☐
Thickness/Plate: _____ (mm)☐ (in)☐	Thickness/Plate: _____ (mm)☐ (in)☐
No. of Plates: ____________	No. of Plates: ____________

Total Thickness of Hammer Cushion: ____________________ (mm)☐ (in)☐

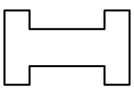

Helmet (Drive Head)

Weight: ____________ including inserts (kN)☐ (kips)☐

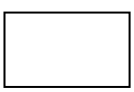

Pile Cushion

Material: ____________________
Area: ________ (cm^2)☐ (in^2)☐ Thickness/Sheet: ______ (mm)☐ (in)☐
No. of Sheets: ____________
Total Thickness of Pile Cushion: ____________ (mm)☐ (in)☐

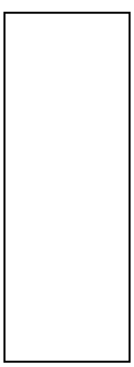

Pile

Pile Type: ____________________
Wall Thickness: ________ (mm)☐ (in)☐ Taper: ____________
Cross Sectional Area: ______ (cm^2)☐ (in^2)☐ Weight/Meter: ____________

Ordered Length: ____________ (m)☐ (ft)☐
Design Load: ____________ (kN)☐ (ft)☐
Ultimate Pile Capacity: ____________ (kN)☐ (kips)☐

Description of Splice: ____________________
____
Driving Shoe/Closure Plate Description: ____________________
____
Submitted By: ____________ Date: ____________
Telephone No.: ____________ Fax No.: ____________

Figure 16.24 Pile Driving and Equipment Data Form (Hannigan et al., 2006)

Reference:

Hannigan, P.J., Goble, G.G., Likins, G.E. and Rausche. (2006). Design and Construction of Driven Pile foundations – Volume II, FHWA report no. FHWA-NHI-05-043, 2006.

Minnesota Department of Transportation Research Project

Minnesota State University, Mankato
University of Massachusetts – Lowell

Pile Driving Contractors – Minnesota State of Practice Survey

PART 1 – Company/Contact Information

Company Name	Edward Kraemer & Sons, Inc.
Contact Name	Bob Beckel
Phone/Fax Number	952 890 2820 | 952 890 2996
E-mail Address	bbeckel@edkraemer.com
Company Address	1020 W. Cliff Road Burnsville, MN 55337

If you have any questions or require help in completing the forms, please contact Aaron Budge at MN State University, 507-389-3294 / Aaron.Budge@mnsu.edu or Sam Paikowsky at the University of Massachusetts Lowell, 978-934-2271 / Samuel_Paikowsky@uml.edu.

PART 2 - Details Regarding Pile Driving Equipment and Construction Methods

Please list the pile driving equipment your company uses on Mn/DOT (or similar) projects. List in order of the frequency of use; from the most common pile driving to the least common driving.

Equipment No.	Hammer				Stnd. Equip.		Typical Use			
	Type	Manufacturer	Model No.	Year	Yes	No*	Pile Type	Pile Section	Pile Max. Pen.	Hammer Setting
6587,6588	SA Diesel	Delmag	D-19	1992, 1993	☒	☐	H-pile & Pipe	12", 14x73, 12.75" Dia	120 ft	3-4
6589,6590	SA Diesel	Delmag	D-30		☒	☐	H-pile & Pipe	14", 16" Dia	180 ft	2-4
6580	SA Diesel	Delmag	D-25		☒	☐	H-pile	All 12" and 14"	150 ft	3-4
6584,6485,6486,6491	SA Diesel	Delmag	D-12		☒	☐	H-pile	12x53, 10"-	60 ft	2-4

							& Pipe	12" Dia		
6594	Vibro	MKT	V-17	1996	☒	☐	HP & Pipe	All	80 ft	N/A

*please use attached form if not using standard equipment. Please use the form to specify your hammer cushion, helmet and striking plates if used.

Does your company use vibratory hammers on Mn/DOT projects? If so, to what depth are vibratory hammers being used prior to the use of impact hammers? Are end bearing piles being driven with vibratory hammers only?

We only use the vibratory hammer in softer soils where we have spliced pile. The "base" pile is driven with a vibro and the added lengths are driven with impact.

How frequently (if at all) do you use preboring on Mn/DOT projects? If preboring IS used for such projects, please provide additional details such as to what depth preboring would typically be performed relative to final tip penetration, etc. Additional comments relative to your experience with preboring would be helpful (e.g. hole diameter relative to pile size).

Seldom. For areas with dragdown issues, anywhere from 15-30 ft. Usually used for utility or vibration concern areas. 16 ft auger for a 12 inch pipe or H-pile.

How frequently (if at all) do you use jetting on Mn/DOT projects? If jetting IS used for such projects, please provide additional details such as to what depth jetting would be typically performed relative to final tip penetration, etc. Additional comments relative to your experience with jetting would be helpful.

We have not used jetting on a Mn/DOT job. We have used it on Railroad work to get through soils next to an existing structure to eliminate settlement. We jetted 50 ft on a 70 ft pile.

PART 3 - Details Regarding Preferred Pile Driving Practice

Assuming your company determines/proposes the piles and equipment used on a project (i.e. assuming value engineering is allowed and proposed by your company) provide details as to your preferred pile driving practice. Include preferred pile size and type, hammer type, range of loads, etc. Please list as many combinations as possible covering the range of projects your company dealt with.

D19 ---- 12.75 inch pipe, HP 12x53, HP 12x74 ---- 50 ton - 100 ton

D30 ---- 16 inch pipe, HP 14x73, HP 14x89 ---- 100 ton - 200 ton

D25 ---- HP12x74, HP14x73, HP14x89 ---- 87 ton - 150 ton

Contract No.:______________________________ Structure Name and/or No.:______________________
Project:______________________________ ______________________
______________________________ Pile Driving contractor or Subcontractor: ______________________
County: ______________________________ ______________________

(Piles driven by)

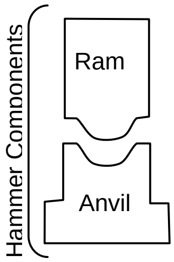

Hammer

Manufacturer: ______________ Model No.: ______________
Hammer Type: ______________ Serial No.: ______________
Manufacturers Maximum Rated Energy: ______________(Joules)☐ (ft-k)☐
Stroke at Maximum Rated Energy: ______________(meters)☐ (ft)☐
Range in Operating Energy: ______________(Joules)☐ (ft-k)☐
Range in Operating Stroke: ______________(meters)☐ (ft)☐
Ram Weight: ______________(kN)☐ (kips)☐
Modification: ______________________________
____
____

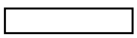

Striker Plate

Weight: ________ (kN)☐ (kips)☐ Diameter: ________(mm)☐ (in)☐
Thickness: ________ (mm)☐ (in)☐

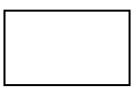

Hammer Cushion

Material #1
Name: ______________
Area: ________(cm^2)☐ (in^2)☐
Thickness/Plate: _____(mm)☐ (in)☐
No. of Plates:______________

Material #2
(for Composite Cushion)
Name: ______________
Area: ________(cm^2)☐ (in^2)☐
Thickness/Plate: _____(mm)☐ (in)☐
No. of Plates: ______________

Total Thickness of Hammer Cushion:______________________(mm)☐ (in)☐

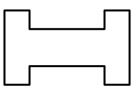

Helmet (Drive Head)

Weight: ______________ including inserts (kN)☐ (kips)☐

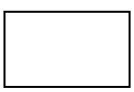

Pile Cushion

Material: ______________________________
Area: ________(cm^2)☐ (in^2)☐ Thickness/Sheet: ______(mm)☐ (in)☐
No. of Sheets: ______________
Total Thickness of Pile Cushion: ______________ (mm)☐ (in)☐

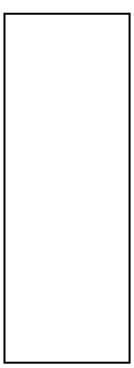

Pile

Pile Type: ______________________________
Wall Thickness: ________(mm)☐ (in)☐ Taper: ______________
Cross Sectional Area: ______(cm^2)☐ (in^2)☐ Weight/Meter: ______________

Ordered Length: ______________(m)☐ (ft)☐
Design Load: ______________ (kN)☐ (ft)☐
Ultimate Pile Capacity: ______________ (kN)☐ (kips)☐

Description of Splice: ______________________________
____
Driving Shoe/Closure Plate Description: ______________________________
____
Submitted By: ______________ Date: ______________
Telephone No.: ______________ Fax No.: ______________

Figure 16.24 Pile Driving and Equipment Data Form (Hannigan et al., 2006)

Reference:

Hannigan, P.J., Goble, G.G., Likins, G.E. and Rausche. (2006). Design and Construction of Driven Pile foundations – Volume II, FHWA report no. FHWA-NHI-05-043, 2006.

Minnesota Department of Transportation Research Project

Minnesota State University, Mankato
University of Massachusetts – Lowell

Pile Driving Contractors – Minnesota State of Practice Survey

PART 1 – Company/Contact Information

Company Name	C.S. McCrossan Construction, Inc.
Contact Name	Randy Reiner
Phone/Fax Number	763-425-4167 | 763-425-0520
E-mail Address	randyr@mccrossan.com
Company Address	P.O. Box 1240 Maple Grove, MN 55311

If you have any questions or require help in completing the forms, please contact Aaron Budge at MN State University, 507-389-3294 / Aaron.Budge@mnsu.edu or Sam Paikowsky at the University of Massachusetts Lowell, 978-934-2271 / Samuel_Paikowsky@uml.edu.

PART 2 - Details Regarding Pile Driving Equipment and Construction Methods

Please list the pile driving equipment your company uses on Mn/DOT (or similar) projects. List in order of the frequency of use; from the most common pile driving to the least common driving.

Equipment No.	Hammer						Typical Use			
	Type	Manufacturer	Model No.	Year	Stnd. Equip.		Pile			Hammer Setting
					Yes	No*	Type	Section	Max. Pen.	
M256	Impact	Delmag	D25-32	2006	☒	☐	Steel Tube	12" Dia. - 0.250" wall	Varies	58,248 ft-lbs
					☐	☐				
					☐	☐				
					☐	☐				
					☐	☐				

*please use attached form if not using standard equipment. Please use the form to specify your hammer cushion, helmet and striking plates if used.

Does your company use vibratory hammers on Mn/DOT projects? If so, to what depth are vibratory hammers being used prior to the use of impact hammers? Are end bearing piles being driven with vibratory hammers only?

We use a vibratory hammer to install steel sheetpiling, but not for bearing piles. If we were to use a vibratory hammer, we would use a Hercules Sonic Sidegrip 100T capacity backhoe-mounted vibratory hammer to start the base sections (up to 40' long), then add-on and drive home with a D25/32 for final bearing capacity.

How frequently (if at all) do you use preboring on Mn/DOT projects? If preboring IS used for such projects, please provide additional details such as to what depth preboring would typically be performed relative to final tip penetration, etc. Additional comments relative to your experience with preboring would be helpful (e.g. hole diameter relative to pile size).

Seldom used. Usually only used if trying to minimize vibration around existing utilities or foundations. Depth would vary to below the appurtenance that we want to avoid subjecting to vibration.

How frequently (if at all) do you use jetting on Mn/DOT projects? If jetting IS used for such projects, please provide additional details such as to what depth jetting would be typically performed relative to final tip penetration, etc. Additional comments relative to your experience with jetting would be helpful.

Never.

PART 3 - Details Regarding Preferred Pile Driving Practice

Assuming your company determines/proposes the piles and equipment used on a project (i.e. assuming value engineering is allowed and proposed by your company) provide details as to your preferred pile driving practice. Include preferred pile size and type, hammer type, range of loads, etc. Please list as many combinations as possible covering the range of projects your company dealt with.

12" or 16" diameter, 0.250" wall steel tube piling driven to bearing capacity and filled with concrete. Ideally, we would use a We would use a D25-32 impact hammer for all driving. HP12x53 pile driven to bearing capacity with a D25-32 impact hammer.

Contract No.:______________________________ Structure Name and/or No.:______________________
Project:______________________________ ______________________________
______________________________ Pile Driving contractor or Subcontractor: __________
County: ______________________________ ______________________________

(Piles driven by)

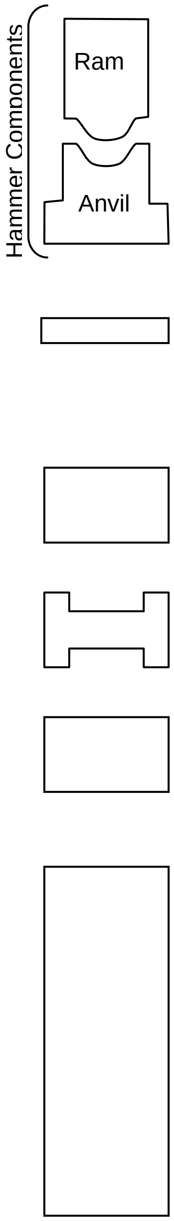

Hammer

Manufacturer:Delmag__________ Model No.:D25/32__________
Hammer Type:Diesel Impact__________ Serial No.: __________
Manufacturers Maximum Rated Energy:58.24__________(Joules)☐ (ft-k)☒
Stroke at Maximum Rated Energy:5__________(meters)☐ (ft)☒
Range in Operating Energy:29.486-58.248__________(Joules)☐ (ft-k)☒
Range in Operating Stroke:2.5-5__________(meters)☐ (ft)☒
Ram Weight:11.752__________(kN)☐ (kips)☒
Modification: ______________________________
____
____

Striker Plate

Weight:2.64__________ (kN)☐ (kips)☒ Diameter:12.5__________(mm)☐ (in)☒
Thickness:2__________ (mm)☐ (in)☒

Hammer Cushion

Material #1
Name: __________
Area: __________(cm^2)☐ (in^2)☐
Thickness/Plate: _____(mm)☐ (in)☐
No. of Plates:__________

Material #2
(for Composite Cushion)
Name: __________
Area: __________(cm^2)☐ (in^2)☐
Thickness/Plate: _____(mm)☐ (in)☐
No. of Plates: __________

Total Thickness of Hammer Cushion:__________(mm)☐ (in)☐

Helmet (Drive Head)

Weight: __________ including inserts (kN)☐ (kips)☐

Pile Cushion

Material: __________
Area: __________(cm^2)☐ (in^2)☐ Thickness/Sheet: ______(mm)☐ (in)☐
No. of Sheets: __________
Total Thickness of Pile Cushion: __________ (mm)☐ (in)☐

Pile

Pile Type: __________
Wall Thickness: __________(mm)☐ (in)☐ Taper: __________
Cross Sectional Area: ______(cm^2)☐ (in^2)☐ Weight/Meter: __________

Ordered Length: __________(m)☐ (ft)☐
Design Load: __________ (kN)☐ (ft)☐
Ultimate Pile Capacity: __________ (kN)☐ (kips)☐

Description of Splice: __________
____
Driving Shoe/Closure Plate Description: __________
____
Submitted By: __________ Date: __________
Telephone No.: __________ Fax No.: __________

Figure 16.24 Pile Driving and Equipment Data Form (Hannigan et al., 2006)

Reference:

Hannigan, P.J., Goble, G.G., Likins, G.E. and Rausche. (2006). Design and Construction of Driven Pile foundations – Volume II, FHWA report no. FHWA-NHI-05-043, 2006.

APPENDIX C

DATA REQUEST AND RESPONSE MN/DOT DATABASE

Mary Canniff

From: Paikowsky, Samuel [Samuel_Paikowsky@uml.edu]
Sent: Thursday, November 29, 2007 11:18 AM
Cc: Gary Person; Dave Dahlberg
Subject: STATE DOT ENGINEERS ASSISTANCE WITH PILE DATA

Dear DOT Engineer;
We are carrying out a research study for the Minnesota Department of Transportation addressing the needs of the state for field pile capacity evaluation examining the Mn/DOT pile driving formula and its adaptation to LRFD.

The design and construction practices of Minnesota are based on driven Pipe and H piles, and we are missing load test information on such piles; in particular, Closed-Ended Pipe piles 12 and 16 inch in diameter, and H piles H12x53, 10x42 and 14x73. Ideally the cases should include dynamic measurements and static load test results but every other partial information (e.g. field observations and static load test or just dynamic measurements when driven with diesel hammers) will be greatly appreciated.

If the information is available in a report, we will be glad to make copies and send you back the originals.

Please send the information to me at:

Samuel G. Paikowsky
Geotechnical Engineering Research Laboratory
University of Massachusetts Lowell
1 University Ave.
Lowell, MA 01854

We realize how busy you are and, therefore, sincerely appreciate your efforts in sharing your personal and departmental experience with others. Your response determines our ability to incorporate your practices in the Mn/DOT pile driving formula and, hence, the quality of our work.

Sincerely Yours,

Samuel G. Paikowsky

==

Samuel G. Paikowsky, ScD, Professor
Geotechnical Engineering Research Lab
Dept. of Civil & Environmental Engineering
University of Massachusetts
1 University Ave., Lowell MA. 01854

Tel. (978) 934-2277 Fax. (978) 934-3046
Email: Samuel_Paikowsky@uml.edu
web: http://civil.caeds.eng.uml.edu/Faculty/Paikowsky/Paikowsky.html
Geotechnical Engineering Research Lab:
http://geores.caeds.eng.uml.edu

==

Summary of States Response Mn/DOT Database

State	Contact	Contact Info		Reports
Illinois	William Kramer	State Foundations and Soils Engineer Bureau of Bridges and Structures Illinois Department of Transportation Phone: (217) 782-7773 Fax: (217) 782-7960 e-mail: WILLIAM.KRAMER@ILLINOIS.GOV	Website: 1	Friction Bearing Design of Steel H-Piles Final Project Report for IDOT ITRC 1-5-38911 J.H. Long and M. Maniaci, CE Dept., University of Illinois at Urbana-Champaign, Dec, 2000
			2	Final Report on Drilled Shaft Load Testing (Osterberg Method) Rt 6265 over Illinois River, LaSalle, County, IL LoadTest, Inc., Project No. LT-8276, Sept. 1996
			3	Results of Pile Load Tests Conducted for IDOT, Peoria, IL J.H. Long, compiled October 2001
			4	Foundation Selection and Construction Performance – Clark Bridge Replacement Alton, Illinois D.E. Daniels, V.A. Modeer, and M.C. Lamie
Iowa	Kenneth Dunker	Office of Bridges and Structures Iowa Dept. of Transportation 800 Lincoln Way Ames, IA 50010 Phone: 515-233-7920 Fax: 515-239-1978 E-mail: kenneth.dunker@dot.iowa.gov	Database to be completed by Feb 2008	The Iowa State research team is being led by Sri Sritharan (PI) and Muhannad Suleiman (Co-PI)
Tennessee	Houston Walker	Civil Engineering Manager 2 TDOT Structures Division 1100 James K. Polk Bldg. Nashville, TN 37243-0339 (615) 741-5335 Houston.Walker@state.tn.us	email attachments	Load Test Data from Tennessee DOT on 3 projects Spanning from 2002 thru 2005 Mclemore Dynamic Load Test Heathcott Load Tests Garland Load Tests
Connecticut	Leo Fontaine		mail	Connecticut DOT Results of Static Load Tests from 13 Projects 1966-1999
West Virginia	Jim Fisher	WVDOT	email attachments	Driven Pile Foundations, US35 Flyover Ramp 5, Putnam County, West Virginia. H.C. Nutting Company, Report May 10, 2006 compiled by Joe Carte - geotechnical eng. on project
Missouri	David Straatmann	Senior Structural Engineer MoDOT Bridge Division Ph: 573.526.4855 e-mail: David.Straatmann@modot.mo.gov	email attachments	Pile Dynamic Analysis, Bridge A7077, US 136, Mercer County Missouri Geotechnology, Inc. Report No. 0941901.71KS, July 31, 2007

APPENDIX D

S-PLUS PROGRAM OUTPUT

DEVELOPMENT OF THE GENERAL AND DETAILED MN/DOT NEW DYNAMIC PILE CAPACITY EQUATION

Table D-1. S-PLUS Linear Regression Analysis – General Equation

Pile Type	Condition	No. of Cases	Searched Coefficient[1]	Coefficient of Determination r^2	Detailed Output Location
H	All Cases	135	35.814	0.880	pg. D-2 & Figure D-1
H	All excluding Cook's Outliers	132	35.170	0.896	pg. D-3 & Figure D-2
H	EOD Only	125	35.660	0.896	pg. D-5 & Figure D-3
H	EOD excluding Cook Outlier's	123	34.550	0.914	pg. D-6 & Figure D-4
Pipe	All Cases	128	35.866	0.861	pg. D-8 & Figure D-5
Pipe	All excluding Cook's Outliers	125	34.875	0.877	pg. D-9 & Figure D-6
Pipe	EOD Only	102	37.142	0.851	pg. D-11 & Figure D-7
Pipe	EOD excluding Cook Outlier's	99	35.866	0.868	pg. D-12 & Figure D-8

Notes:
1. See section 4.9 for details
2. The following output files and Cook's outlier analysis charts present in progressive order the cases summarized in the above table.

Table D-2. S-PLUS Linear Regression Analysis – Detailed Equation

Pile Type	Condition	No. of Cases	Searched Coefficient[1]	Coefficient of Determination r^2	Detailed Output Location
H	EOD Only	125	35.637	0.896	pg. D-14, Fig. D-9
H	EOD Only excluding Cook's Outliers	122	34.151	0.925	pg. D-15, Fig. D-10
H	EOD, Diesel Hammer, B.C. ≥4 BPI	39	33.527	0.907	pg. D-16, Fig. D-11
H	EOD, Diesel Hammer, B.C. ≥4 BPI excluding Cook's Outliers	38	32.126	0.935	pg. D-17, Fig. D-12
H	EOD, Diesel Hammer, MnDOT Energy[2], B.C. ≥4 BPI	13	34.401	0.870	pg. D-18, Fig. D-13
H	EOD, Diesel Hammer, MnDOT Energy[2], B.C. ≥4 BPI excluding Cook's Outliers	12	31.181	0.924	pg. D-19, Fig. D-14
Pipe	EOD Only	99	36.746	0.850	pg. D-20, Fig. D-15
Pipe	EOD Only excluding Cook's Outliers	97	35.839	0.859	pg. D-21, Fig. D-16
Pipe	EOD, Diesel Hammer, B.C. ≥4 BPI	41	30.532	0.918	pg. D-22, Fig. D17
Pipe	EOD, Diesel Hammer, B.C. ≥4 BPI excluding Cook's Outliers	38	29.983	0.946	pg. D-23, Fig. D-18
Pipe	EOD, Diesel Hammer, MnDOT Energy[2], B.C. ≥4 BPI	16	33.294	0.974	pg. D-24, Fig. D-19
Pipe	EOD, Diesel Hammer, MnDOT Energy[2], B.C. ≥4 BPI excluding Cook's Outliers	14	33.146	0.989	pg. D-25, Fig. D-20

Notes:
[1]Searched Coefficient for the equation $R_u = Coeff.\sqrt{E_h} \cdot \log(10N)$
[2]MnDOT energy range contains hammers with rated energies between 42.4 and 75.4 k-ft

H-Piles All Cases

```
       *** Linear Model ***
Call:
lm(formula = Static ~ Gates + (-1), data = HPILESALL, na.action = na.exclude)

Coefficients:
    Gates
 35.81346

Degrees of freedom: 135 total; 134 residual
Residual standard error: 158.5005

Call: lm(formula = Static ~ Gates + (-1), data = HPILESALL, na.action = na.exclude)
Residuals:
  Min     1Q Median    3Q   Max
 -429 -86.36 -21.32 49.68 779.8

Coefficients:
        Value Std. Error t value Pr(>|t|)
Gates 35.8135  1.1412    31.3814  0.0000

Residual standard error: 158.5 on 134 degrees of freedom
Multiple R-Squared: 0.8802
F-statistic: 984.8 on 1 and 134 degrees of freedom, the p-value is 0
```


```
       *** Linear Model ***
Call:
lm(formula = Static ~ Gates + (-1), data = HPILESALL, na.action = na.exclude)

Coefficients:
    Gates
 35.81346

Degrees of freedom: 135 total; 134 residual
Residual standard error: 158.5005

Call: lm(formula = Static ~ Gates + (-1), data = HPILESALL, na.action = na.exclude)
Residuals:
  Min     1Q Median    3Q   Max
 -429 -86.36 -21.32 49.68 779.8

Coefficients:
        Value Std. Error t value Pr(>|t|)
Gates 35.8135  1.1412    31.3814  0.0000

Residual standard error: 158.5 on 134 degrees of freedom
Multiple R-Squared: 0.8802
F-statistic: 984.8 on 1 and 134 degrees of freedom, the p-value is 0
```

H-Piles 132 Cases – Cook's Outliers Removed

```
       *** Linear Model ***
Call:
lm(formula = Static ~ Gates + (-1), data = HPILESALL, na.action = na.exclude)

Coefficients:
    Gates
 35.16964

Degrees of freedom: 132 total; 131 residual
Residual standard error: 143.7643

Call: lm(formula = Static ~ Gates + (-1), data = HPILESALL, na.action = na.exclude)
Residuals:
    Min    1Q Median    3Q   Max
 -410.2 -78.6 -17.01 53.57 585.8

Coefficients:
        Value Std. Error t value Pr(>|t|)
Gates 35.1696  1.0464    33.6091  0.0000

Residual standard error: 143.8 on 131 degrees of freedom
Multiple R-Squared: 0.8961
F-statistic: 1130 on 1 and 131 degrees of freedom, the p-value is 0
```



```
       *** Linear Model ***
Call:
lm(formula = Static ~ Gates + (-1), data = HPILESALL, na.action = na.exclude)

Coefficients:
    Gates
 35.16964

Degrees of freedom: 132 total; 131 residual
Residual standard error: 143.7643

Call: lm(formula = Static ~ Gates + (-1), data = HPILESALL, na.action = na.exclude)
Residuals:
    Min    1Q Median    3Q   Max
 -410.2 -78.6 -17.01 53.57 585.8

Coefficients:
        Value Std. Error t value Pr(>|t|)
Gates 35.1696  1.0464    33.6091  0.0000

Residual standard error: 143.8 on 131 degrees of freedom
Multiple R-Squared: 0.8961
F-statistic: 1130 on 1 and 131 degrees of freedom, the p-value is 0
```

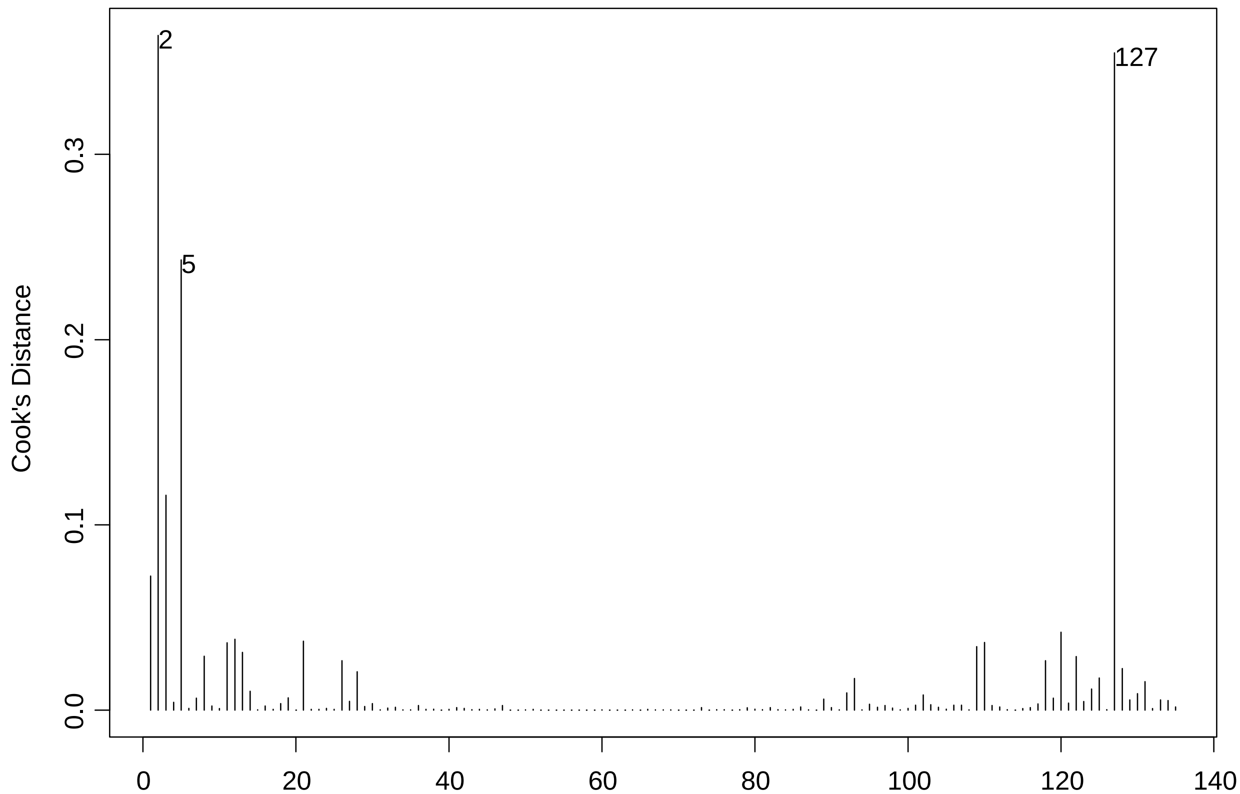

Figure D-1. H-Piles All Cases

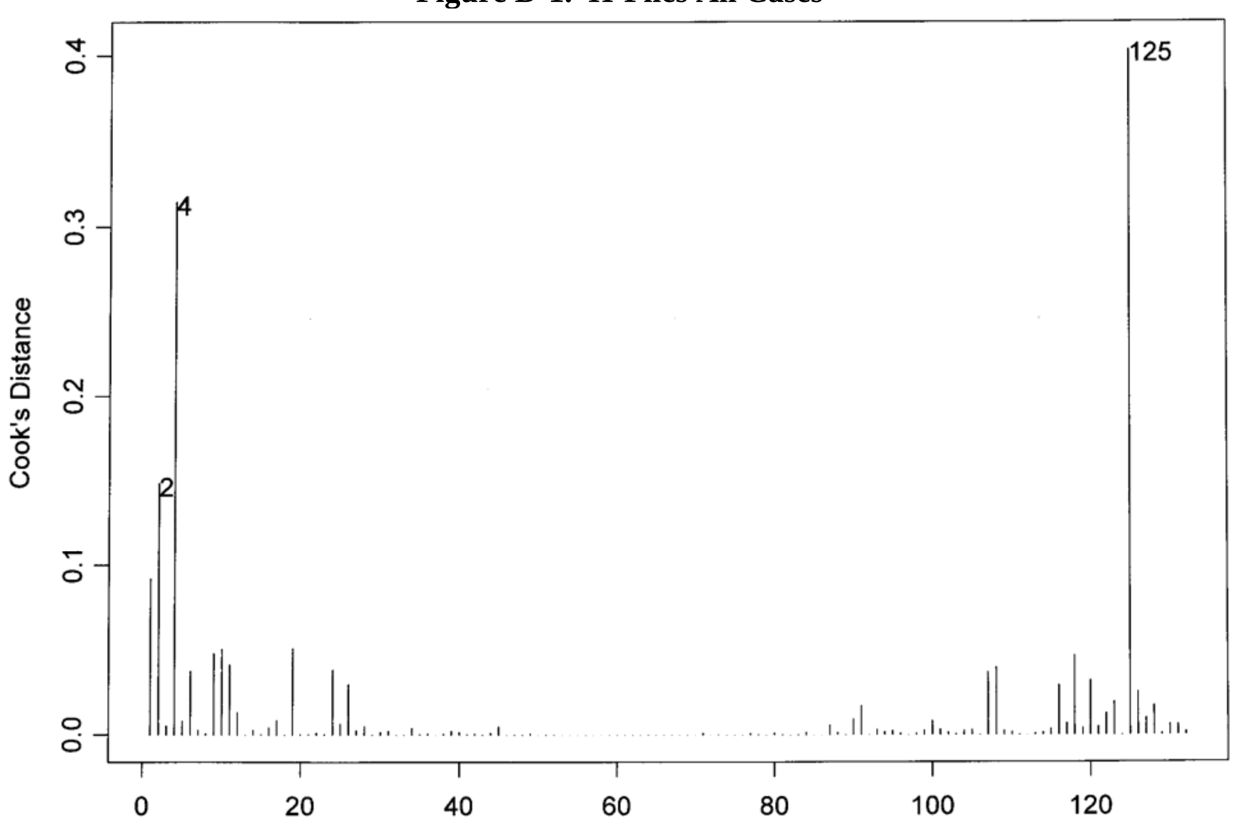

Figure D-2. H-Piles All Cases – Cook's Outliers Removed

H-Piles EOD

```
       *** Linear Model ***
Call:
lm(formula = Static ~ Gates.Param + (-1), data = HPILESEOD, na.action =
       na.exclude)

Coefficients:
 Gates.Param
    35.65916

Degrees of freedom: 125 total; 124 residual
Residual standard error: 141.7361

Call: lm(formula = Static ~ Gates.Param + (-1), data = HPILESEOD, na.action =
       na.exclude)
Residuals:
    Min     1Q Median    3Q   Max
 -226.8 -81.13 -23.69 46.36 576.7

Coefficients:
              Value Std. Error t value Pr(>|t|)
Gates.Param 35.6592  1.0924    32.6424  0.0000

Residual standard error: 141.7 on 124 degrees of freedom
Multiple R-Squared: 0.8958
F-statistic: 1066 on 1 and 124 degrees of freedom, the p-value is 0


       *** Linear Model ***
Call:
lm(formula = Static ~ Gates.Param + (-1), data = HPILESEOD, na.action =
       na.exclude)

Coefficients:
 Gates.Param
    35.65916

Degrees of freedom: 125 total; 124 residual
Residual standard error: 141.7361

Call: lm(formula = Static ~ Gates.Param + (-1), data = HPILESEOD, na.action =
       na.exclude)
Residuals:
    Min     1Q Median    3Q   Max
 -226.8 -81.13 -23.69 46.36 576.7

Coefficients:
              Value Std. Error t value Pr(>|t|)
Gates.Param 35.6592  1.0924    32.6424  0.0000

Residual standard error: 141.7 on 124 degrees of freedom
Multiple R-Squared: 0.8958
F-statistic: 1066 on 1 and 124 degrees of freedom, the p-value is 0
```

H-Piles EOD – Cook's Outliers Removed

```
       *** Linear Model ***
Call:
lm(formula = Static ~ Gates.Param + (-1), data = HPILESEOD, na.action =
       na.exclude)

Coefficients:
 Gates.Param
    34.54525

Degrees of freedom: 123 total; 122 residual
Residual standard error: 122.4812

Call: lm(formula = Static ~ Gates.Param + (-1), data = HPILESEOD, na.action =
       na.exclude)
Residuals:
    Min     1Q Median    3Q   Max
 -205.4 -73.69 -10.65 55.92 552.6

Coefficients:
              Value Std. Error t value Pr(>|t|)
Gates.Param 34.5453  0.9591    36.0184  0.0000

Residual standard error: 122.5 on 122 degrees of freedom
Multiple R-Squared: 0.914
F-statistic: 1297 on 1 and 122 degrees of freedom, the p-value is 0
```


```
       *** Linear Model ***
Call:
lm(formula = Static ~ Gates.Param + (-1), data = HPILESEOD, na.action =
       na.exclude)

Coefficients:
 Gates.Param
    34.54525

Degrees of freedom: 123 total; 122 residual
Residual standard error: 122.4812

Call: lm(formula = Static ~ Gates.Param + (-1), data = HPILESEOD, na.action =
       na.exclude)
Residuals:
    Min     1Q Median    3Q   Max
 -205.4 -73.69 -10.65 55.92 552.6

Coefficients:
              Value Std. Error t value Pr(>|t|)
Gates.Param 34.5453  0.9591    36.0184  0.0000

Residual standard error: 122.5 on 122 degrees of freedom
Multiple R-Squared: 0.914
F-statistic: 1297 on 1 and 122 degrees of freedom, the p-value is 0
```

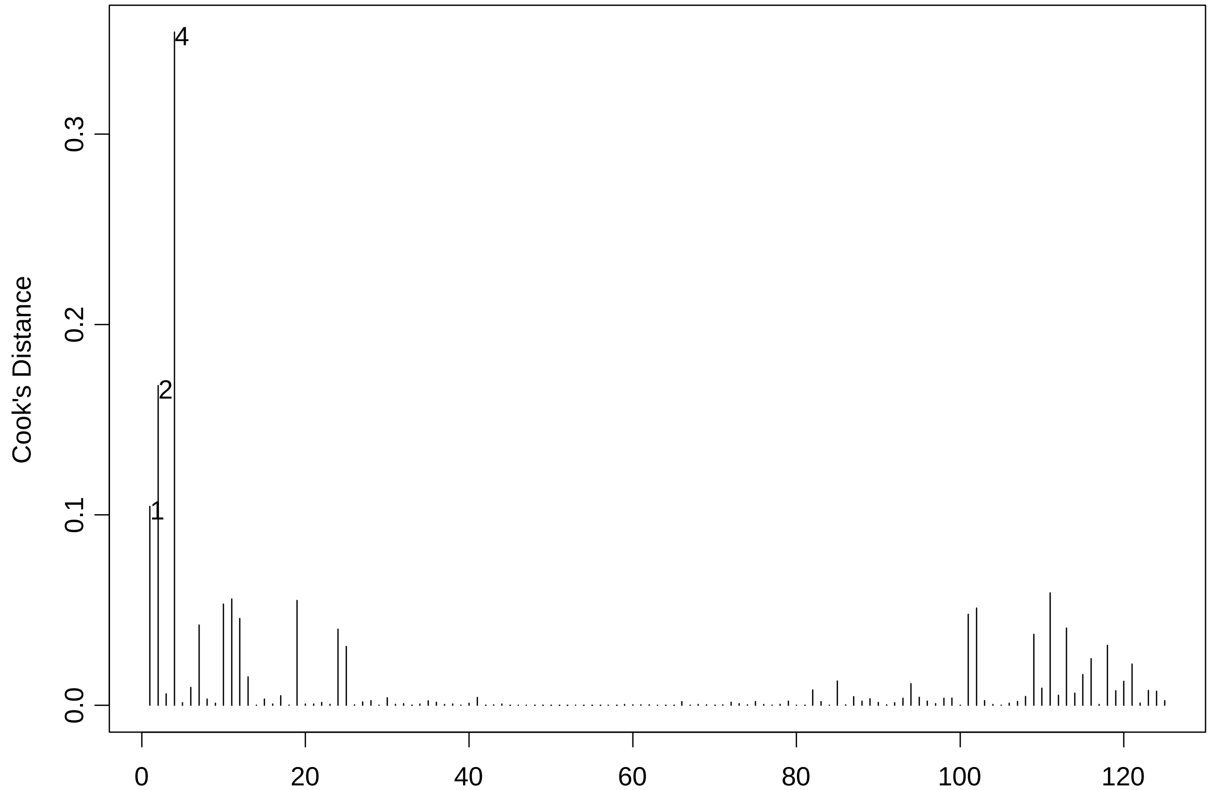

Figure D-3. H Piles EOD Data only

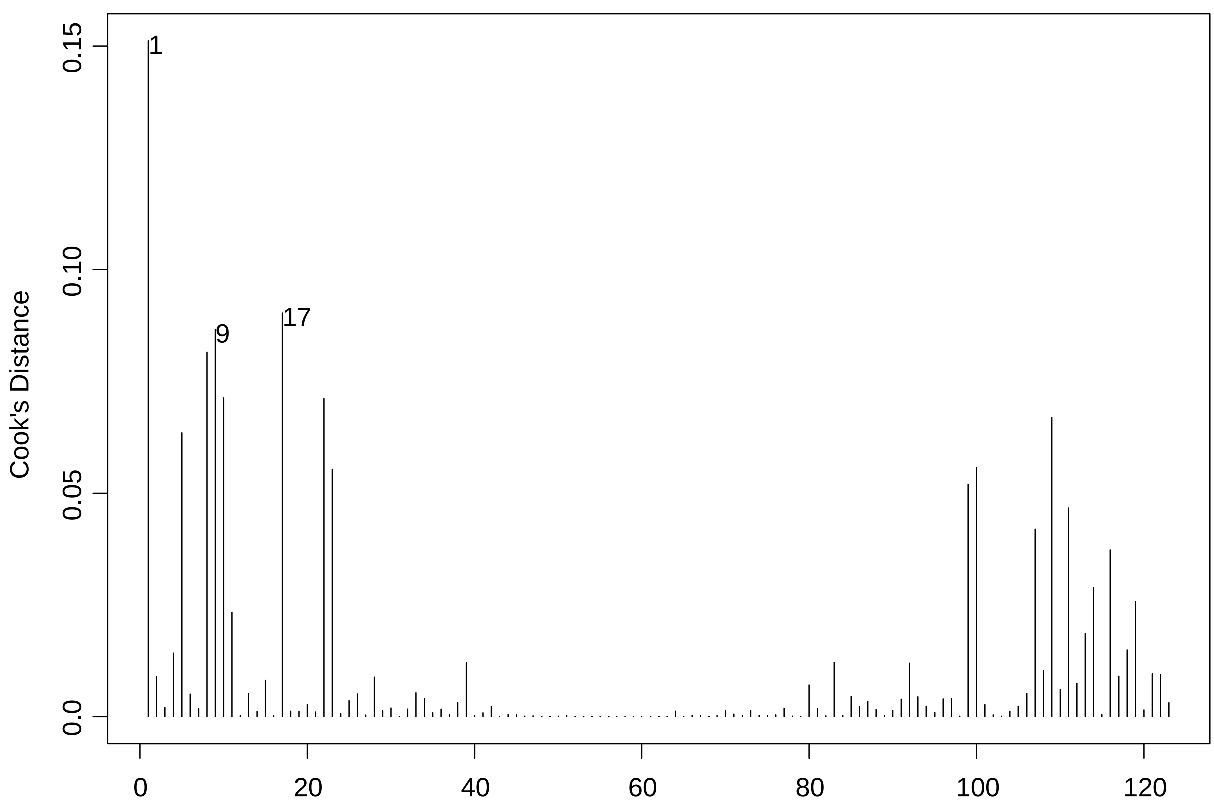

Figure D-4. H Piles EOD Data only – Cook's Outliers Removed

Pipe Piles All Cases

```
       *** Linear Model ***
Call:
lm(formula = Static ~ Gates.Parameters + (-1), data = PIPEPILESALL, na.action
        = na.exclude)

Coefficients:
 Gates.Parameters
         35.86644

Degrees of freedom: 128 total; 127 residual
Residual standard error: 174.9289

Call: lm(formula = Static ~ Gates.Parameters + (-1), data = PIPEPILESALL, na.action
        = na.exclude)
Residuals:
    Min     1Q Median    3Q   Max
 -293.8 -105.2 -36.11 63.76 548.6

Coefficients:
                   Value Std. Error t value Pr(>|t|)
Gates.Parameters 35.8664  1.2802    28.0170  0.0000

Residual standard error: 174.9 on 127 degrees of freedom
Multiple R-Squared: 0.8607
F-statistic: 785 on 1 and 127 degrees of freedom, the p-value is 0
```


```
       *** Linear Model ***
Call:
lm(formula = Static ~ Gates.Parameters + (-1), data = PIPEPILESALL, na.action
        = na.exclude)

Coefficients:
 Gates.Parameters
         35.86644

Degrees of freedom: 128 total; 127 residual
Residual standard error: 174.9289

Call: lm(formula = Static ~ Gates.Parameters + (-1), data = PIPEPILESALL, na.action
        = na.exclude)
Residuals:
    Min     1Q Median    3Q   Max
 -293.8 -105.2 -36.11 63.76 548.6

Coefficients:
                   Value Std. Error t value Pr(>|t|)
Gates.Parameters 35.8664  1.2802    28.0170  0.0000

Residual standard error: 174.9 on 127 degrees of freedom
Multiple R-Squared: 0.8607
F-statistic: 785 on 1 and 127 degrees of freedom, the p-value is 0
```

Pipe Piles All Cases – Cook's Outliers Removed

```
       *** Linear Model ***
Call:
lm(formula = Static ~ Gates.Parameters + (-1), data = PIPEPILESALL, na.action
        = na.exclude)

Coefficients:
 Gates.Parameters
         34.87463

Degrees of freedom: 125 total; 124 residual
Residual standard error: 158.0164

Call: lm(formula = Static ~ Gates.Parameters + (-1), data = PIPEPILESALL, na.action
        = na.exclude)
Residuals:
    Min    1Q Median    3Q   Max
 -280.7 -96.2 -24.78 59.88 473.3

Coefficients:
                   Value Std. Error t value Pr(>|t|)
Gates.Parameters 34.8746  1.1706    29.7913  0.0000

Residual standard error: 158 on 124 degrees of freedom
Multiple R-Squared: 0.8774
F-statistic: 887.5 on 1 and 124 degrees of freedom, the p-value is 0
```


```
       *** Linear Model ***
Call:
lm(formula = Static ~ Gates.Parameters + (-1), data = PIPEPILESALL, na.action
        = na.exclude)

Coefficients:
 Gates.Parameters
         34.87463

Degrees of freedom: 125 total; 124 residual
Residual standard error: 158.0164

Call: lm(formula = Static ~ Gates.Parameters + (-1), data = PIPEPILESALL, na.action
        = na.exclude)
Residuals:
    Min    1Q Median    3Q   Max
 -280.7 -96.2 -24.78 59.88 473.3

Coefficients:
                   Value Std. Error t value Pr(>|t|)
Gates.Parameters 34.8746  1.1706    29.7913  0.0000

Residual standard error: 158 on 124 degrees of freedom
Multiple R-Squared: 0.8774
F-statistic: 887.5 on 1 and 124 degrees of freedom, the p-value is 0
```

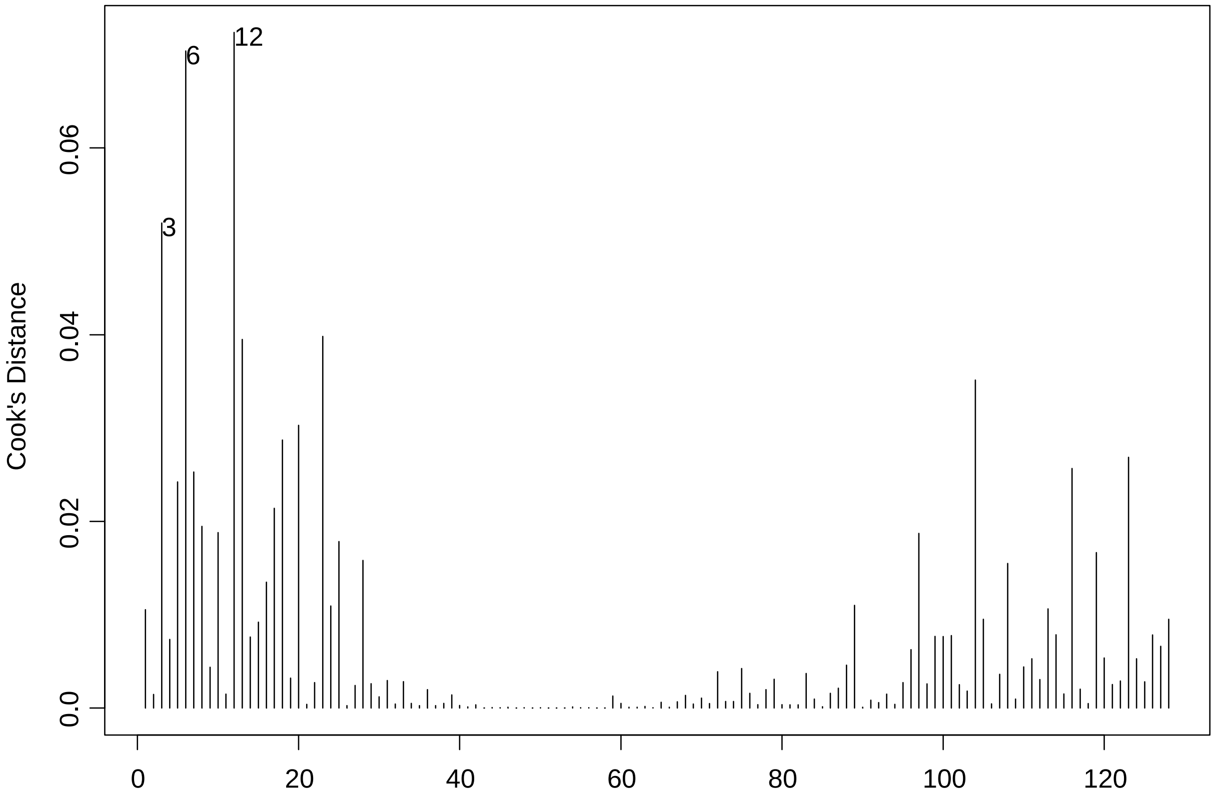

Figure D-5. Pipe Piles All Cases

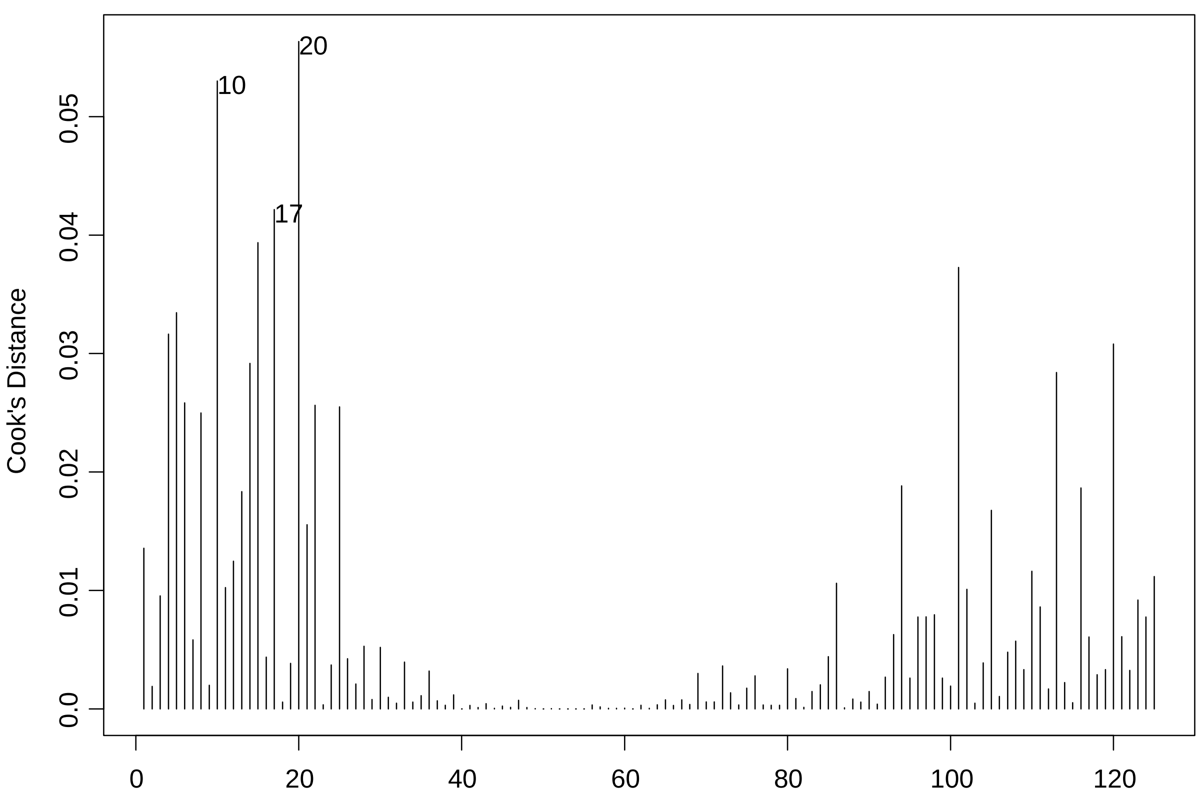

Figure D-6. Pipe Piles All Cases – Cooks Outliers Removed

Pipe Piles EOD

```
       *** Linear Model ***
Call:
lm(formula = Static ~ Gates.Parameters + (-1), data = PIPEPILESEOD, na.action
        = na.exclude)

Coefficients:
 Gates.Parameters
         37.14222

Degrees of freedom: 102 total; 101 residual
Residual standard error: 184.3219

Call: lm(formula = Static ~ Gates.Parameters + (-1), data = PIPEPILESEOD, na.action
        = na.exclude)
Residuals:
    Min   1Q Median    3Q Max
 -310.7 -102 -36.67 72.97 536

Coefficients:
                   Value Std. Error t value Pr(>|t|)
Gates.Parameters 37.1422  1.5487    23.9822  0.0000

Residual standard error: 184.3 on 101 degrees of freedom
Multiple R-Squared: 0.8506
F-statistic: 575.1 on 1 and 101 degrees of freedom, the p-value is 0
```


```
       *** Linear Model ***
Call:
lm(formula = Static ~ Gates.Parameters + (-1), data = PIPEPILESEOD, na.action
        = na.exclude)

Coefficients:
 Gates.Parameters
         37.14222

Degrees of freedom: 102 total; 101 residual
Residual standard error: 184.3219

Call: lm(formula = Static ~ Gates.Parameters + (-1), data = PIPEPILESEOD, na.action
        = na.exclude)
Residuals:
    Min   1Q Median    3Q Max
 -310.7 -102 -36.67 72.97 536

Coefficients:
                   Value Std. Error t value Pr(>|t|)
Gates.Parameters 37.1422  1.5487    23.9822  0.0000

Residual standard error: 184.3 on 101 degrees of freedom
Multiple R-Squared: 0.8506
F-statistic: 575.1 on 1 and 101 degrees of freedom, the p-value is 0
```

Pipe Piles EOD – Cook's Outliers Removed

```
       *** Linear Model ***
Call:
lm(formula = Static ~ Gates.Parameters + (-1), data = PIPEPILESEOD, na.action
        = na.exclude)

Coefficients:
 Gates.Parameters
         35.86638

Degrees of freedom: 99 total; 98 residual
Residual standard error: 165.4422

Call: lm(formula = Static ~ Gates.Parameters + (-1), data = PIPEPILESEOD, na.action
        = na.exclude)
Residuals:
    Min    1Q Median    3Q   Max
 -293.8 -90.5 -25.07 68.45 468.1

Coefficients:
                   Value Std. Error t value Pr(>|t|)
Gates.Parameters 35.8664  1.4128    25.3868  0.0000

Residual standard error: 165.4 on 98 degrees of freedom
Multiple R-Squared: 0.868
F-statistic: 644.5 on 1 and 98 degrees of freedom, the p-value is 0
```


```
       *** Linear Model ***
Call:
lm(formula = Static ~ Gates.Parameters + (-1), data = PIPEPILESEOD, na.action
        = na.exclude)

Coefficients:
 Gates.Parameters
         35.86638

Degrees of freedom: 99 total; 98 residual
Residual standard error: 165.4422

Call: lm(formula = Static ~ Gates.Parameters + (-1), data = PIPEPILESEOD, na.action
        = na.exclude)
Residuals:
    Min    1Q Median    3Q   Max
 -293.8 -90.5 -25.07 68.45 468.1

Coefficients:
                   Value Std. Error t value Pr(>|t|)
Gates.Parameters 35.8664  1.4128    25.3868  0.0000

Residual standard error: 165.4 on 98 degrees of freedom
Multiple R-Squared: 0.868
F-statistic: 644.5 on 1 and 98 degrees of freedom, the p-value is 0
```

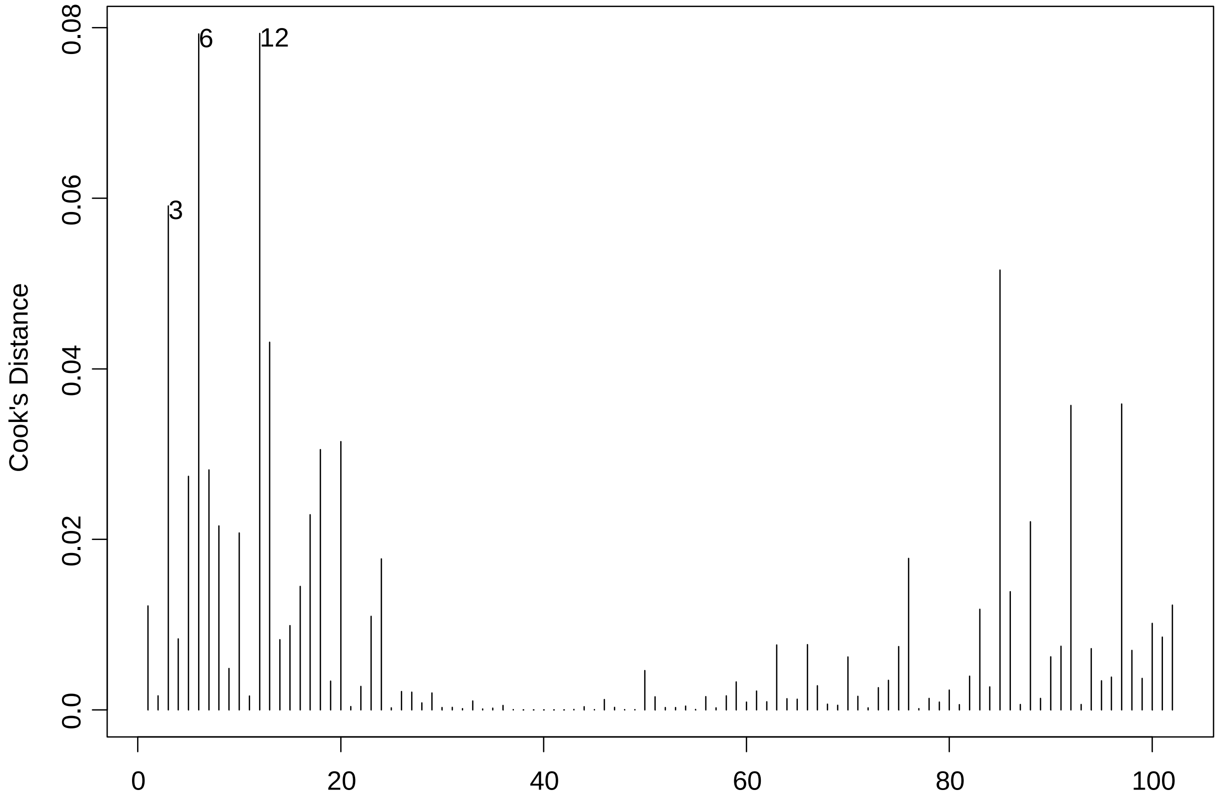

Figure D-7. Pipe Piles EOD Data only

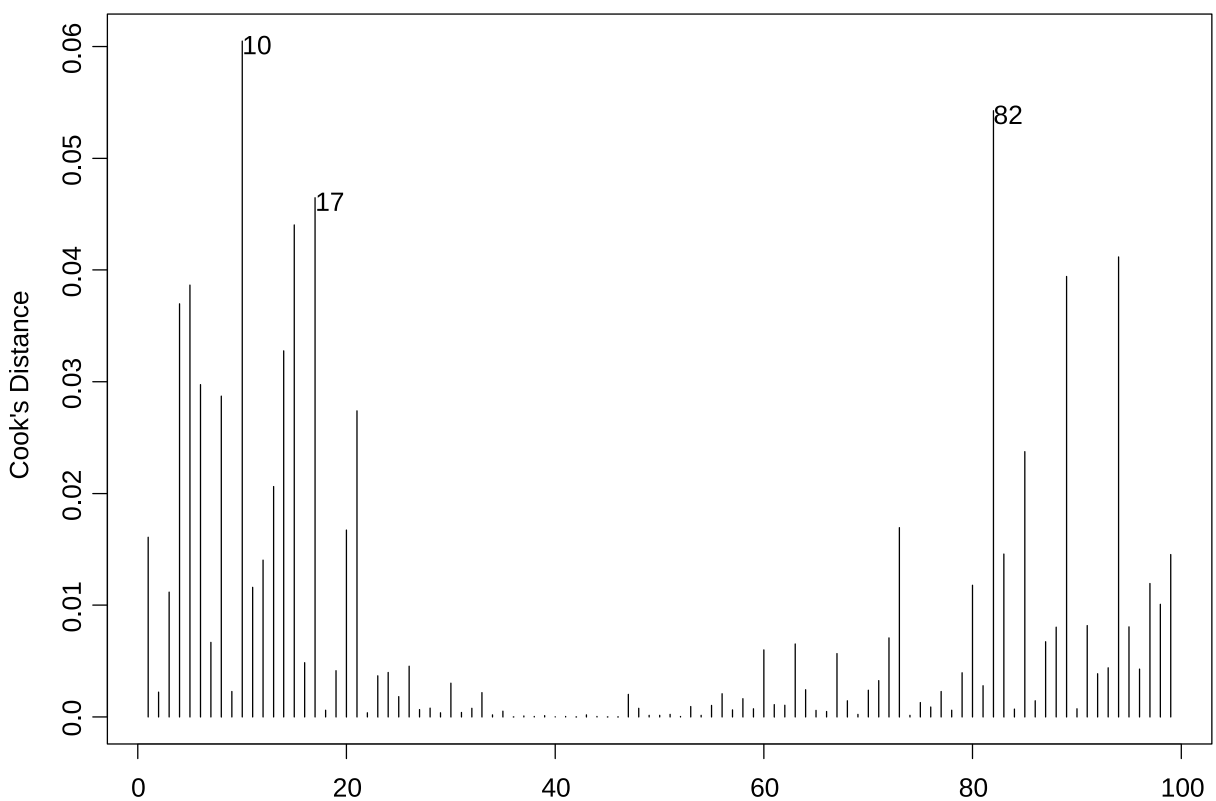

Figure D-8. Pipe Piles EOD Data only Cooks Outliers Removed

H-Piles EOD Data Only

```
       *** Linear Model ***

Call: lm(formula = static ~ xaxis + (-1), data = HPileB, na.action = na.exclude)
Residuals:
    Min     1Q Median    3Q   Max
 -226.4 -88.21 -23.44 46.61 577.1

Coefficients:
        Value Std. Error t value Pr(>|t|)
xaxis 35.6374  1.0930    32.6049  0.0000

Residual standard error: 141.9 on 124 degrees of freedom
Multiple R-Squared: 0.8955
F-statistic: 1063 on 1 and 124 degrees of freedom, the p-value is 0
```

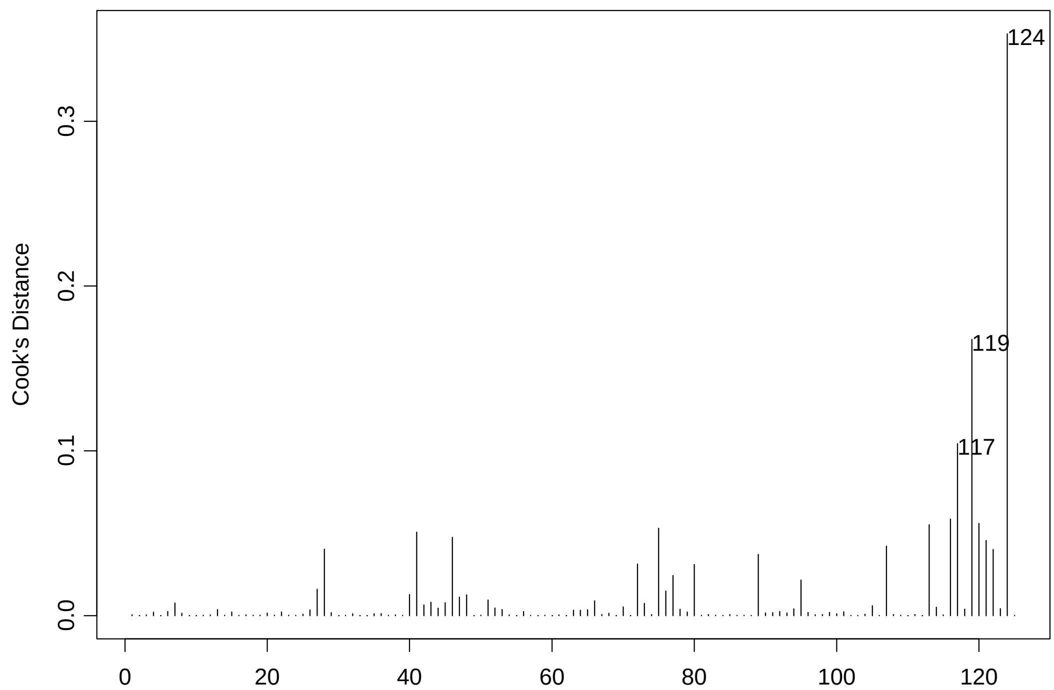

Figure D-9. H-Piles EOD Data Only

H-Piles EOD Data only Cooks Outliers Removed

```
*** Linear Model ***

Call: lm(formula = static ~ xaxis + (-1), data = HPileBoutlier, na.action =
      na.exclude)
Residuals:
    Min     1Q Median    3Q Max
 -197.8 -72.03  -8.06 58.74 331

Coefficients:
        Value Std. Error t value Pr(>|t|)
xaxis 34.1512  0.8824    38.7036  0.0000

Residual standard error: 112.3 on 121 degrees of freedom
Multiple R-Squared: 0.9253
F-statistic: 1498 on 1 and 121 degrees of freedom, the p-value is 0
```

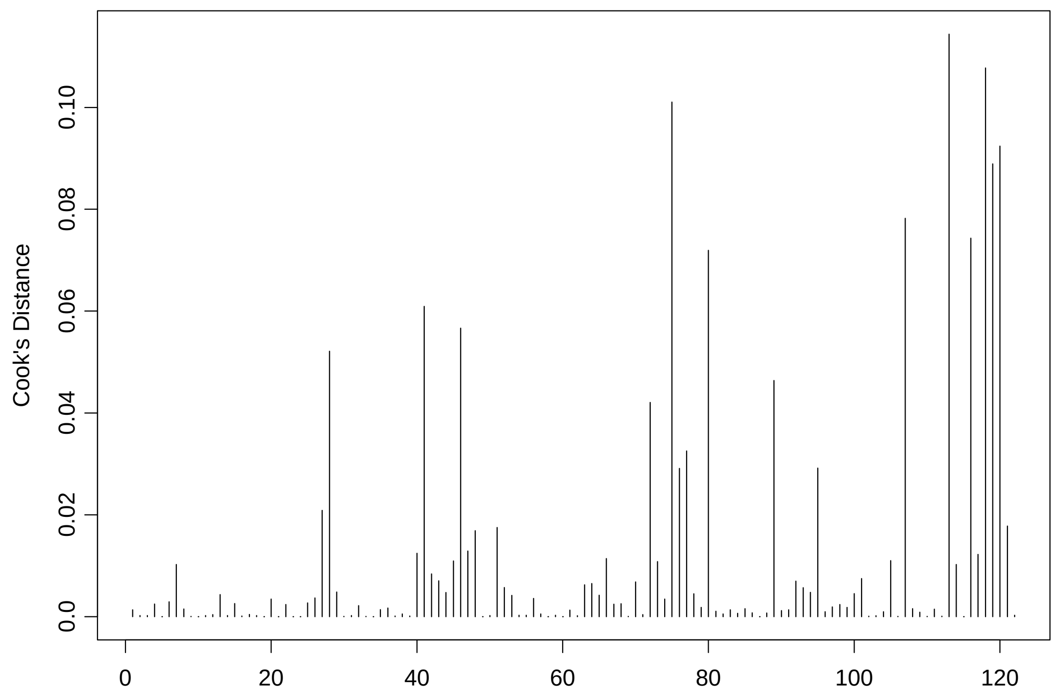

Figure D-10. H-Piles EOD Data only Cooks Outliers Removed

H- Piles EOD, Diesel Hammer, and B.C. ≥ 4BPI Data Only

```
       *** Linear Model ***

Call: lm(formula = Static ~ x.axis + (-1), data = HPileB6, na.action = na.exclude)
Residuals:
    Min     1Q Median    3Q   Max
 -185.8 -102.7 -43.94 64.35 616.3

Coefficients:
         Value Std. Error t value Pr(>|t|)
x.axis 33.5265  1.7397    19.2714  0.0000

Residual standard error: 160.6 on 38 degrees of freedom
Multiple R-Squared: 0.9072
          F-statistic: 371.4 on 1 and 38 degrees of freedom, the p-value is 0
```

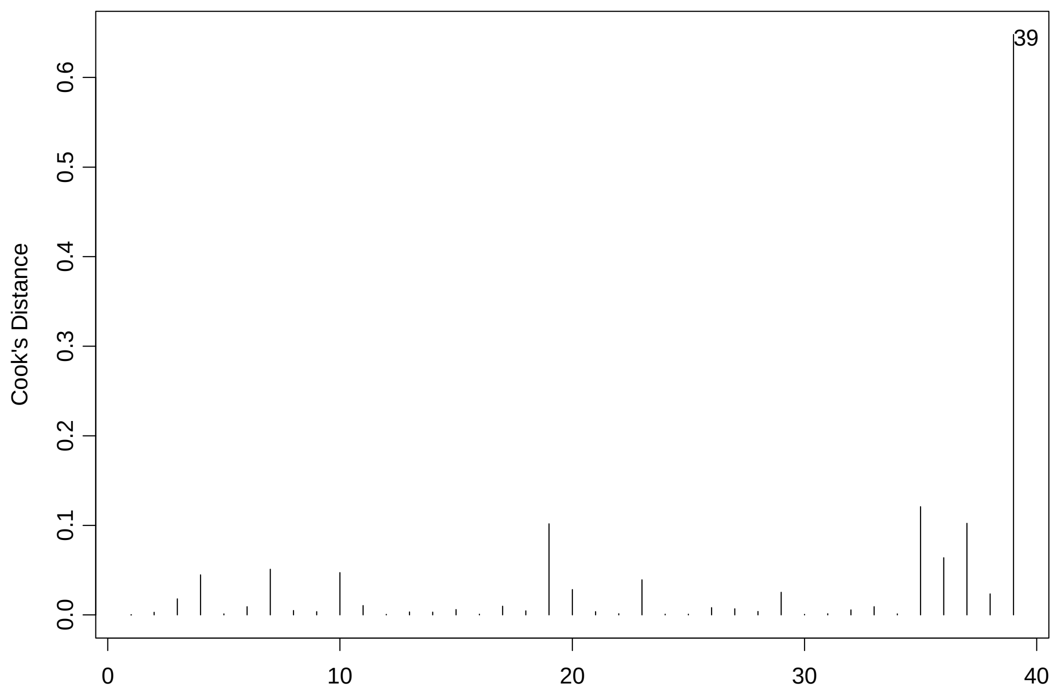

Figure D-11. H- Piles EOD, Diesel Hammer, and B.C. ≥ 4BPI Data Only

H- Piles EOD, Diesel Hammer, and B.C. ≥ 4BPI Data only Cooks Outliers Removed

```
       *** Linear Model ***

Call: lm(formula = Static ~ x.axis + (-1), data = HPileB6outlier, na.action =
       na.exclude)
Residuals:
    Min    1Q Median    3Q Max
 -163.8 -88.7 -30.51 79.12 347

Coefficients:
         Value Std. Error t value Pr(>|t|)
x.axis 32.1261  1.3895    23.1204  0.0000

Residual standard error: 125.6 on 37 degrees of freedom
Multiple R-Squared: 0.9353
F-statistic: 534.6 on 1 and 37 degrees of freedom, the p-value is 0
```

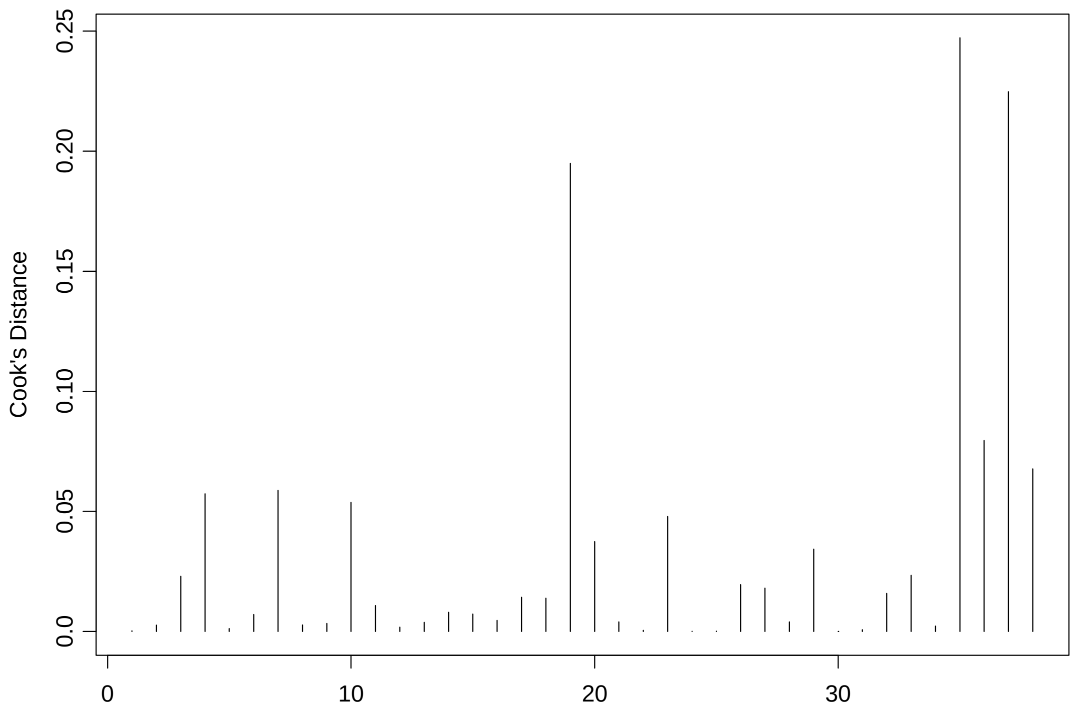

Figure D-12. H- Piles EOD, Diesel Hammer, and B.C. ≥ 4BPI Data only Cooks Outliers Removed

H- Piles EOD, Diesel Hammer, Mn/DOT Energy Range, and B.C. ≥ 4BPI Data Only

```
       *** Linear Model ***

Call: lm(formula = Static ~ x.axis + (-1), data = HPileB8, na.action = na.exclude)
Residuals:
    Min     1Q Median    3Q Max
 -202.6 -170.4 -90.56 50.62 600

Coefficients:
         Value Std. Error t value Pr(>|t|)
x.axis 34.4015  3.8412     8.9560  0.0000

Residual standard error: 237 on 12 degrees of freedom
Multiple R-Squared: 0.8699
F-statistic: 80.21 on 1 and 12 degrees of freedom, the p-value is 1.163e-006
```

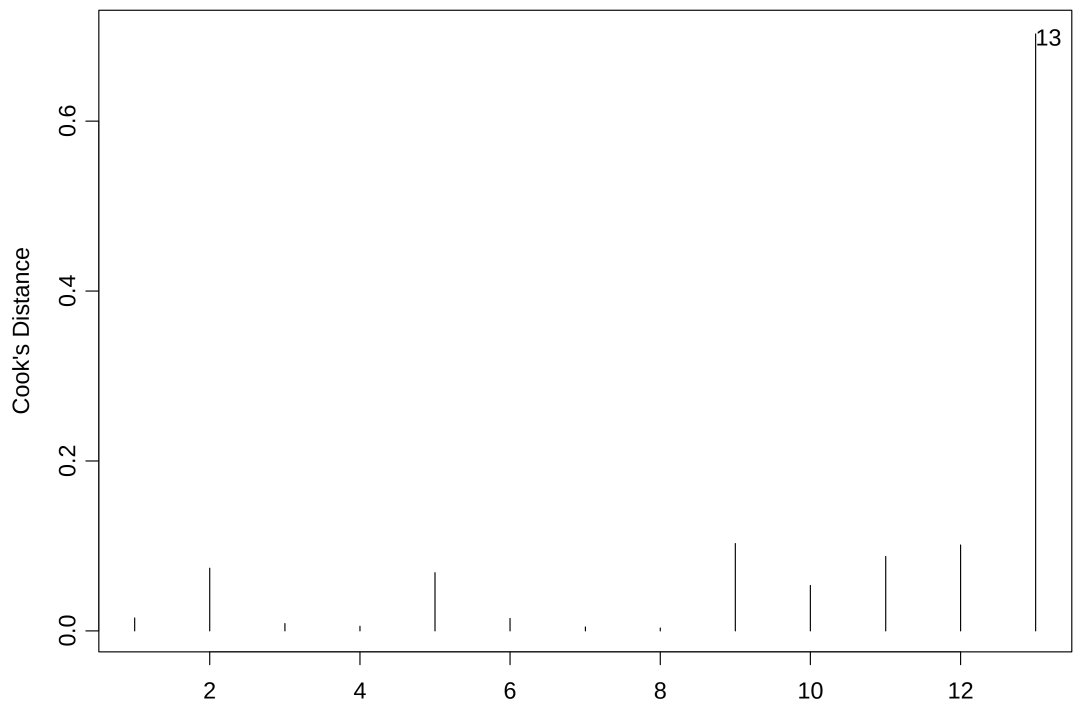

Figure D-13. H- Piles EOD, Diesel Hammer, Mn/DOT Energy Range, and B.C. ≥ 4BPI Data Only

H- Piles EOD, Diesel Hammer, Mn/DOT Energy Range, and B.C. ≥ 4BPI Data only Cooks Outliers Removed

```
       *** Linear Model ***

Call: lm(formula = Static ~ x.axis + (-1), data = HPileB8outlier, na.action =
      na.exclude)
Residuals:
    Min     1Q Median    3Q   Max
 -140.6 -106.9 -47.61 11.98 360.3

Coefficients:
         Value Std. Error t value Pr(>|t|)
x.axis 31.1813  2.7020    11.5402  0.0000

Residual standard error: 159 on 11 degrees of freedom
Multiple R-Squared: 0.9237
F-statistic: 133.2 on 1 and 11 degrees of freedom, the p-value is 1.736e-007
```

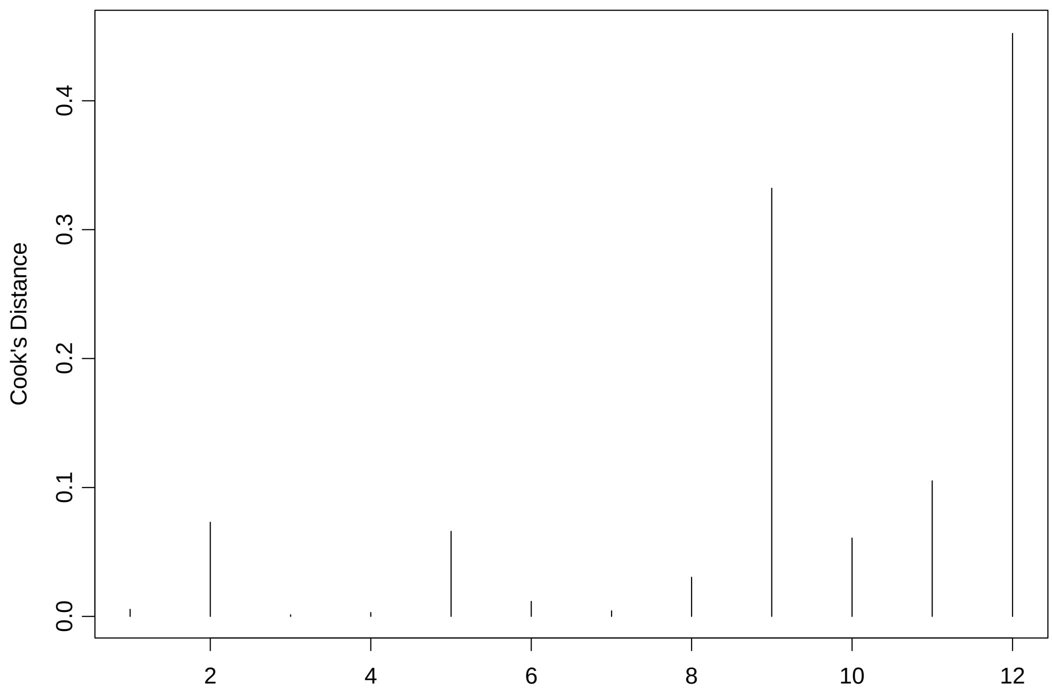

Figure D-14. H- Piles EOD, Diesel Hammer, Mn/DOT Energy Range, and B.C. ≥ 4BPI Data only Cooks Outliers Removed

Pipe Piles EOD Data Only

```
       *** Linear Model ***

Call: lm(formula = Static ~ x.axis + (-1), data = PipePileC, na.action = na.exclude)
Residuals:
    Min    1Q Median   3Q   Max
 -305.4 -98.6 -33.28 66.5 539.9

Coefficients:
         Value Std. Error t value Pr(>|t|)
x.axis 36.7454  1.5601    23.5533  0.0000

Residual standard error: 184.3 on 98 degrees of freedom
Multiple R-Squared: 0.8499
F-statistic: 554.8 on 1 and 98 degrees of freedom, the p-value is 0
```

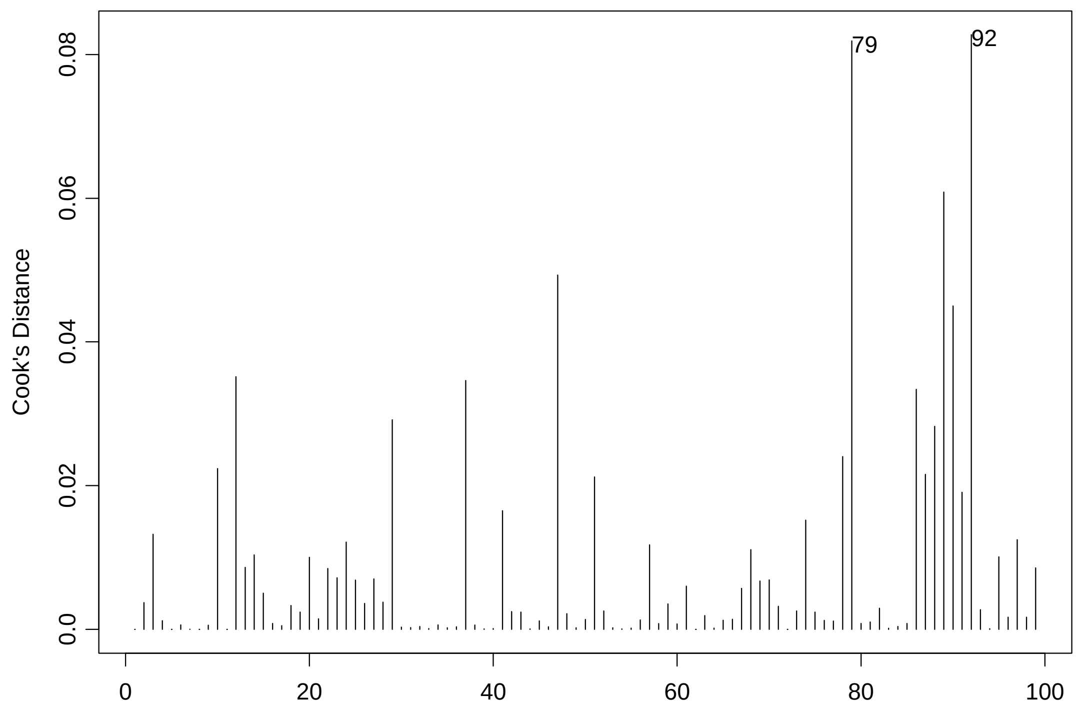

Figure D-15. Pipe Piles EOD Data Only

Pipe Piles EOD Data only Cooks Outliers Removed

```
*** Linear Model ***

Call: lm(formula = Static ~ x.axis + (-1), data = PipePileCoutlier, na.action =
      na.exclude)
Residuals:
    Min     1Q Median    3Q   Max
 -293.4 -91.55 -26.43 67.04 548.9

Coefficients:
         Value Std. Error t value Pr(>|t|)
x.axis 35.8385  1.4821    24.1801  0.0000

Residual standard error: 172.9 on 96 degrees of freedom
Multiple R-Squared: 0.859
F-statistic: 584.7 on 1 and 96 degrees of freedom, the p-value is 0
```

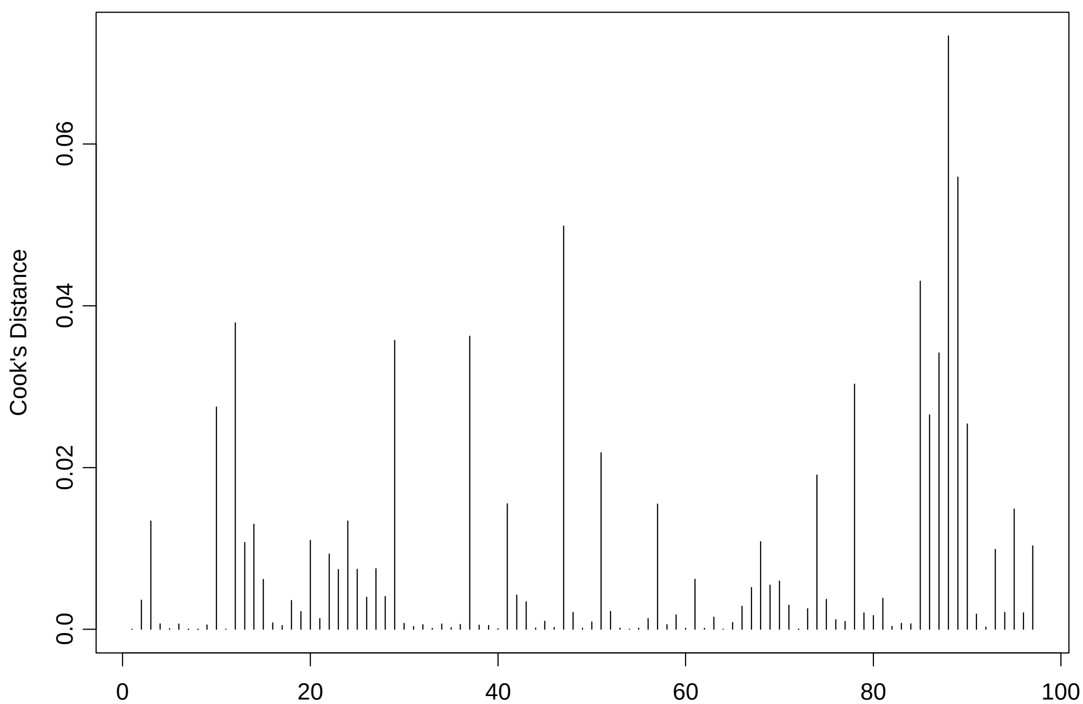

Figure D-16. Pipe Piles EOD Data only Cooks Outliers Removed

Pipe Piles EOD, Diesel Hammer, and B.C. ≥ 4BPI Data Only

```
*** Linear Model ***

Call: lm(formula = Static ~ x.axis + (-1), data = PipePileC6, na.action = na.exclude
       )
Residuals:
    Min     1Q Median    3Q   Max
 -223.3 -114.9 -4.687 67.63 396.9

Coefficients:
         Value Std. Error t value Pr(>|t|)
x.axis 30.5316  1.4448    21.1319  0.0000

Residual standard error: 129.8 on 40 degrees of freedom
Multiple R-Squared: 0.9178
F-statistic: 446.6 on 1 and 40 degrees of freedom, the p-value is 0
```

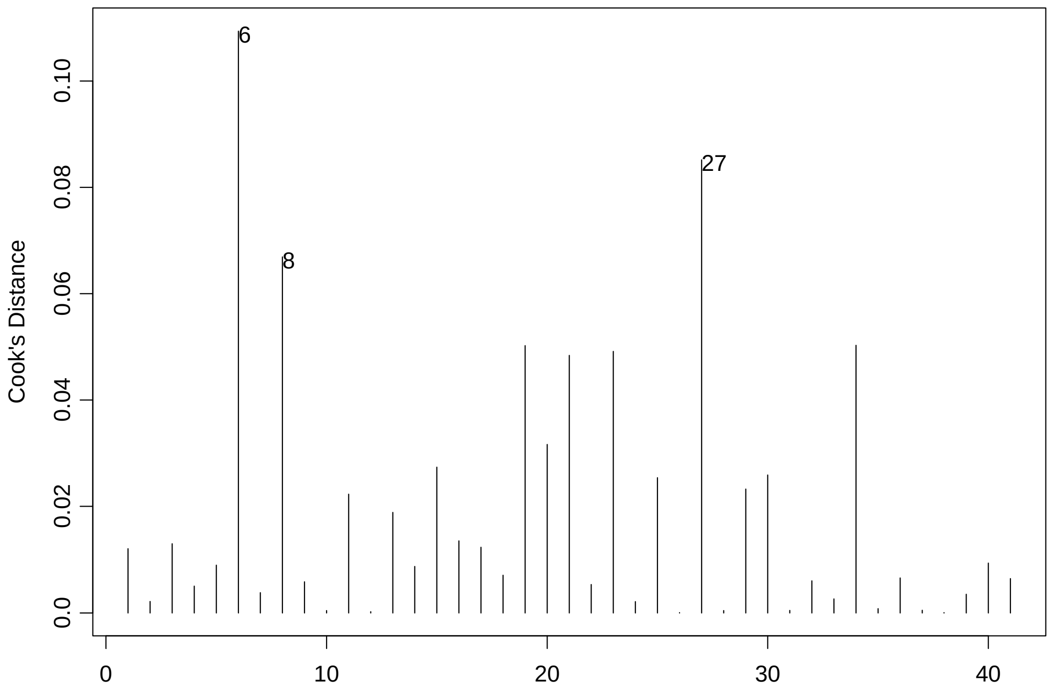

Figure D-17. Pipe Piles EOD, Diesel Hammer, and B.C. ≥ 4BPI Data Only

Pipe Piles EOD, Diesel Hammer, and B.C. ≥ 4BPI Data only Cooks Outliers Removed

```
*** Linear Model ***

Call: lm(formula = Static ~ x.axis + (-1), data = PipePileC6outlier, na.action =
      na.exclude)
Residuals:
  Min     1Q Median    3Q   Max
 -213 -105.8 -3.668 68.33 160.8

Coefficients:
         Value Std. Error t value Pr(>|t|)
x.axis 29.9826  1.1816    25.3746  0.0000

Residual standard error: 103.3 on 37 degrees of freedom
Multiple R-Squared: 0.9457
F-statistic: 643.9 on 1 and 37 degrees of freedom, the p-value is 0
```

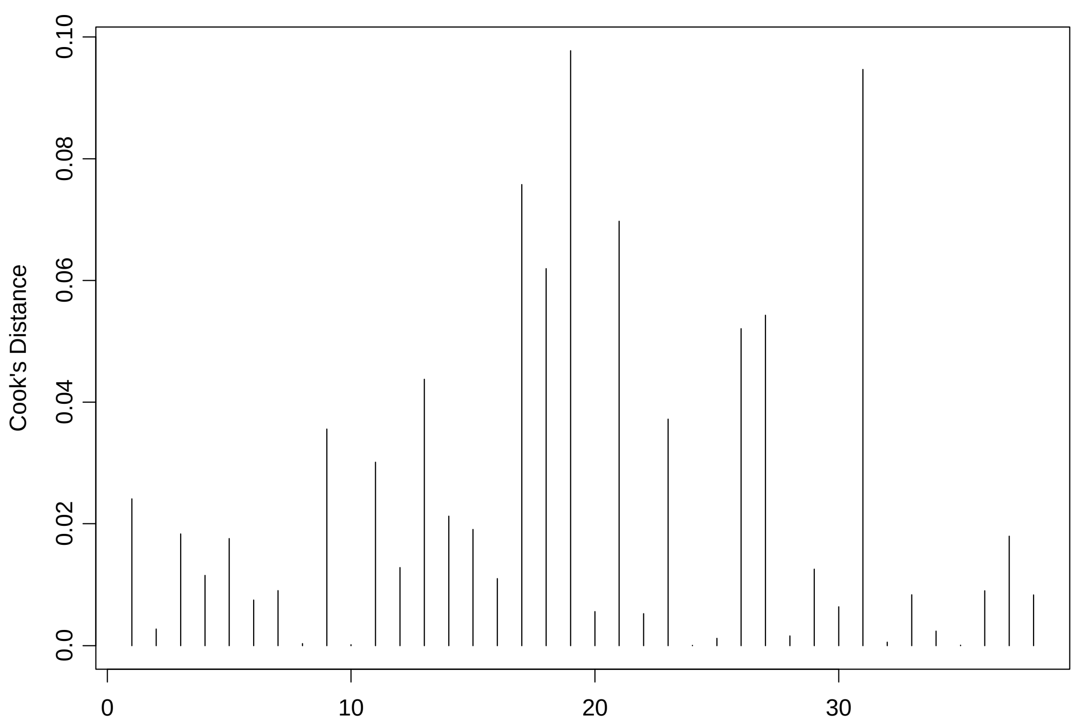

Figure D-18. Pipe Piles EOD, Diesel Hammer, and B.C. ≥ 4BPI Data only Cooks Outliers Removed

Pipe Piles EOD, Diesel Hammer, Mn/DOT Energy Range, and B.C. ≥ 4BPI Data Only

```
*** Linear Model ***

Call: lm(formula = Static ~ x.axis + (-1), data = PipePileC8, na.action = na.exclude
       )
Residuals:
    Min     1Q Median    3Q   Max
 -135.1 -42.37  2.814 40.02 228.1

Coefficients:
         Value Std. Error t value Pr(>|t|)
x.axis 33.2942  1.3926    23.9087  0.0000

Residual standard error: 87.54 on 15 degrees of freedom
Multiple R-Squared: 0.9744
F-statistic: 571.6 on 1 and 15 degrees of freedom, the p-value is 2.343e-013
```

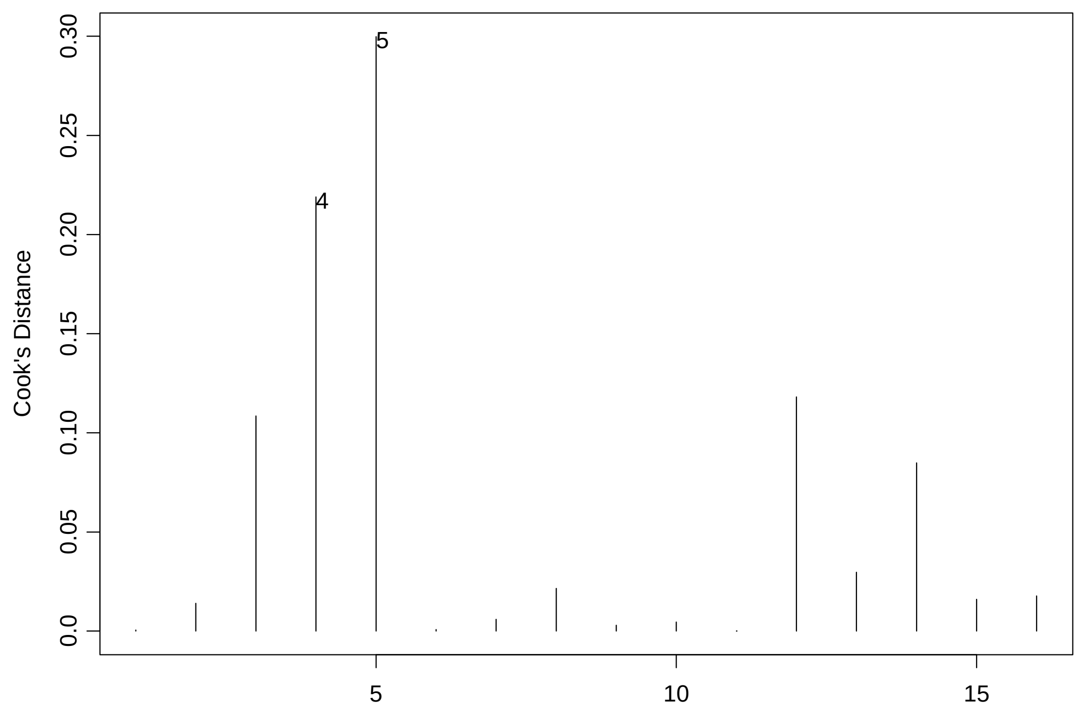

Figure D-19. Pipe Piles EOD, Diesel Hammer, Mn/DOT Energy Range, and B.C. ≥ 4BPI Data Only

Pipe Piles EOD, Diesel Hammer, Mn/DOT Energy Range, and B.C. ≥ 4BPI Data only Cooks Outliers Removed

```
*** Linear Model ***

Call: lm(formula = Static ~ x.axis + (-1), data = PipePileC8outlier, na.action =
      na.exclude)
Residuals:
  Min     1Q Median    3Q   Max
 -101 -29.49  5.082 36.99 108.1

Coefficients:
         Value Std. Error t value Pr(>|t|)
x.axis 33.1458  0.9924    33.3990  0.0000

Residual standard error: 58.57 on 13 degrees of freedom
Multiple R-Squared: 0.9885
F-statistic: 1115 on 1 and 13 degrees of freedom, the p-value is 5.473e-014
```

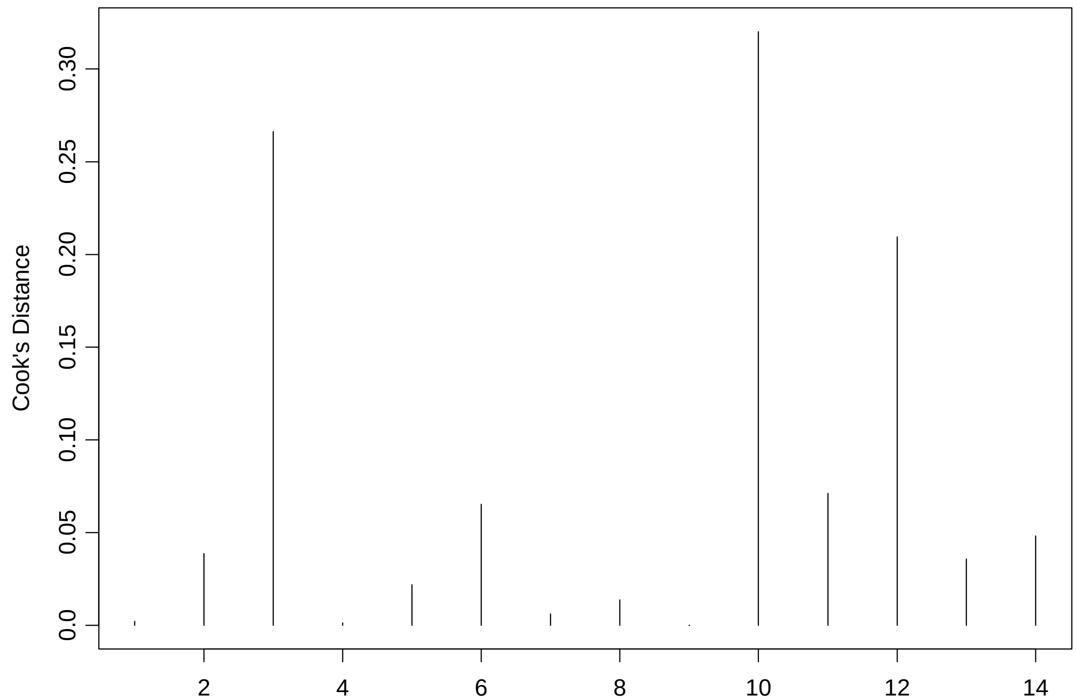

Figure D-20. Pipe Piles EOD, Diesel Hammer, Mn/DOT Energy Range, and B.C. ≥ 4BPI Data only Cooks Outliers Removed